THE SYNTHESIS, NMR, AND CONFORMATIONAL STUDIES OF PURINOPHANES AND APPROACHES TOWARDS THE SYNTHESIS OF PYRIMIDINOPHANES

By

ALFREDO CAPRETTA, B.Sc.

A Thesis

Submitted to the School of Graduate Studies

in Partial Fulfilment of the Requirements

for the Degree of

Doctor of Philosophy

McMaster University

October, 1992

THE SYNTHESIS, NMR, AND CONFORMATIONAL STUDIES OF PURINOPHANES AND APPROACHES TOWARDS THE SYNTHESIS OF PYRIMIDINOPHANES

DOCTOR OF PHILOSOPHY (1992) McMASTER UNIVERSITY

(Chemistry) Hamilton, Ontario

TITLE: The Synthesis, NMR and Conformational Studies of Purinophanes and Approaches Towards the Synthesis of Pyrimidinophanes

AUTHOR: Alfredo Capretta, B.Sc. (McMaster University)

SUPERVISOR: Professor Russell A. Bell

NUMBER OF PAGES: xxvii, 250

ABSTRACT

In an effort to investigate the magnetic effects exerted by the heterobases found in ribo- and deoxyribonucleic acids, work has been directed towards the synthesis of purine and pyrimidine cyclophanes. The bridging methylene protons act as "reporter" groups of the magnetic environment of these systems furnishing values for the spatial definition of the diamagnetic susceptibility anisotropy and supplying a viable means of appraising the existing theoretical models.

[8]-(N6,9)-6-Aminopurinophane (**1**) (an adenine based cyclophane) was the first to be prepared in our laboratory. Its nonamethylene (**2**) and decamethylene (**3**) homologs have also been synthesized using nucleophilic aromatic substitution for bridge attachment at the 6-position and the Mitsunobu reaction for alkylation at the 9-site. Both the C9 and C10 cyclophanes have been investigated using NMR spectroscopy while the structure of [9]-(N6,9)-6-Aminopurinophane has been determined using X-ray crystallography. Many of the interesting fluxional properties of the purinophane series result from restricted rotation about the N6-C6 bond and manifest themselves in the variable temperature NMR. UV spectroscopy has been used to provide further insight into the conformational properties of these molecules.

The "Intact Bridge Attachment" and "Bridge Formation via Coupling" approaches to cyclophane formation have been applied towards the synthesis of the pyrimidinophane, [9]-(1,N4)-4-amino-2-one-pyrimidinophane (**4**) (a cytosine based cyclophane). Unfortunately, repeated attempts failed to produce the desired target molecule. The problems associated with each approach will be discussed.

A semi-empirical model developed for calculation of the chemical shifts of the bridge protons in the [n]-(N6,9)-6-aminopurinophane series proved to be an effective tool for anisotropy mapping.

Acknowledgements

I wish to express my thanks to the following individuals for their unique contributions to this work:

My family for their support and understanding (despite the fact they often didn't understand what it was they were supporting);

Professor Russell A. Bell for his words of wisdom, his encouragement and his friendship. The insightful chats in his office and his gentle steering in the relevant direction were much appreciated;

Professor A. D. Bain's advice in dealing with issues pertaining to NMR spectroscopy ("No one ever really understands NMR... It just stops bothering them after a while."); Professor B. E. McCarry's proficiency in synthesis and his uncanny ability to see the "Big Picture (Pitcher)"; Professor M. J. McGlinchey for discussions dealing with the development of chemical shift calculations, his consultations into the mechanisms of the organometallic reactions and his sabbatical time which he generously offered;

The technical assistance supplied by B. Sayer, Dr. R. W. Smith and F. A. Ramelan and especially the insight provided by Dr. D. W. Hughes dealing with the experimental aspects of NMR spectroscopy; Dr. H. N. Hunter's indispensable dialogues concerning the purinophanes; Dr. C. S. Frampton for his crystallographic expertise (Ock, Jimmy!); Dr. T. Hemscheidt for his advice concerning the synthesis of the pyrimidinophanes (Aloha!); Mike Mallot for sanity sessions (Built for Tweed).

RFC Research and Recreational Facility for the discussions over "coffee" and "ingredients" and the WJL group for their lunchtime diatribes; Rob Maharajh and Charlie

Younger for their companionship, assistance in the lab and their sympathy during my "ranting and raving" sessions.

My better-half, Julie, who not only acted as typist, proof-reader and graphic artist but who also provided the encouragement and support that helped to see the project to its conclusion.

Finally, I wish to express my gratitude to N.S.E.R.C. and J.A.C. for their financial support.

TABLE OF CONTENTS

LIST OF FIGURES

LIST OF TABLES

"If one believes in nothing, if nothing makes sense, if we can assert no value whatsoever, everything is permissible and nothing is important ... One is free to stoke the crematory fires or to give one's life to the care of lepers."

Albert Camus, *L'Homme Révolté* (The Rebel), 1953

"How is it possible to find meaning in a finite world? This is a very difficult question when we realize that science has failed us... After all, can the human soul be glimpsed through a microscope? Maybe - but you'd definitely need one of those very good ones with two eyepieces."

Woody Allen, *Side Effects*, 1975

Chapter 1

Introduction

1.1. Nuclear Magnetic Resonance Spectroscopy

Many of the recent strides made in nucleic acid research can be attributed, in part, to the development of new synthetic methods for the preparation of oligonucleotides and, perhaps to a larger extent, the application of new nuclear magnetic resonance (NMR) spectroscopy techniques. One-dimensional multi-nuclear NMR, as well as the myriad of two-dimensional techniques available, have allowed the researcher to probe the solution state structure of oligonucleotides, study the dynamics of these molecules, observe their interaction with other biomolecules, and study the effects of base pairing and base stacking.[1]

Numerous books and reviews exist[2] that discuss in detail the theory of NMR spectroscopy. As the name implies, understanding nuclear magnetic resonance spectroscopy requires some knowledge of the magnetic properties of nuclei. All nuclei carry charge, and in some nuclei this charge "spins" about the nuclear axis. This circulation or spinning of nuclear charge results in a small magnetic moment, μ, along the

---

[1] Majumdar, A. and Hosur, R. V. *Prog. NMR Spec.* **24**, 109 (1992); Wemmer, D. E. *Curr. Opin. Struct. Bio.* **1**, 452 (1991); Hosur, R.V., Govil, G., and Miles, H.T. *Magn. Res. Chem.* **26**, 927-944 (1988); Van de Ven, F.J., and Hilbers, C.W. *Eur. J. Biochem.* **178**, 1-38 (1988)

[2] Bovey, F.A. Nuclear Magnetic Resonance Spectroscopy. (New York: Academic Press, 1988); Harris, R. K. Nuclear Magnetic Resonance Spectroscopy. (Essex: Longman Scientific and Technical, 1986); Gunther, H. NMR Spectroscopy. (New York: John Wiley and Sons, 1980)

axis of spin. In the presence of an external magnetic field, B_o, the nuclear magnetic moment will orient itself with respect to the applied field. With each of these orientations, there exists an energy proportional to the nuclear moment and the applied field. The difference between these energy levels or spin states is dependent on the field strength of the magnet and is given by:

$$\Delta E = \frac{\gamma h}{2\pi} B_o \qquad (1)$$

where h is Planck's constant and γ is the magnetogyric ratio. Each nucleus has its own particular γ constant.

Nuclear magnetic resonance spectroscopy detects the transitions from one spin state to another. When a correct amount of energy, $\Delta E = h\nu$, is applied to a nucleus in a magnetic field, transitions between spin states occur and the fundamental resonance condition can be written:

$$\nu = \frac{\gamma}{2\pi} B_o \qquad (2)$$

That is, when a nucleus is placed in a magnetic field B_o, the resonant condition is satisfied when the frequency of applied radiation ν is provided. In a nuclear magnetic rHxonance spectrometer, the energy required to induce these transitions between energy levels is supplied by electromagnetic radiation in the radio frequency region. Transitions between energy levels generate a small electric current in the receiver coils of the spectrometer surrounding the sample and, after it is amplified, this current is displayed as a signal in the spectrum.

The sophistication of the NMR experiment was greatly advanced with the advent

of Fourier Transform NMR (FT-NMR). A strong, single radiofrequency pulse is applied at the start of the NMR experiment exciting all the nuclei. As these nuclei return to their equilibrium state, each re-emits its own characteristic frequency. These frequencies are collected as a decay signal over time (free induction decay) and Fourier transformed to yield a spectrum.

If the character of NMR spectra was determined solely by nuclear properties, then at any particular frequency v all the nuclei of a given species would resonate at the same value of B_o. Fortunately, this is not the case. One does not observe bare nuclei, but rather nuclei surrounded by a cloud of electrons as part of a molecule. When a molecule is placed in an external magnetic field B_o, orbital currents are induced in the electron clouds and these give rise to small, local magnetic fields. As a consequence, the nucleus is exposed to an effective field that is somewhat smaller (or larger in some cases) than the external field. The magnitude of the field developed internally is directly proportional to the applied external field. This can be expressed as:

$$B_{loc}=B_o-\sigma B_o=B_o(1-\sigma) \qquad (3)$$

where B_{loc} is the actual local field experienced by the nucleus and σ is the screening constant or shielding parameter.

Since electron density depends upon the structure of a compound, nuclei of the same species may be found in different chemical environments (hence magnetic environments). As a consequence, different frequencies are required to induce the resonance condition in chemically different nuclei. This effect is called the chemical shift. The various shielding constants reflect the different environments within a molecule and

the resulting chemical shifts (in conjunction with spin-spin splitting effects[3] make NMR spectroscopy a powerful analytical tool for the determination of structures.

Classically, the total shielding σ_{total} can be thought of as the summation of contributions from local electronic shielding effects as well as contributions from more distant influences:

$$\sigma_{total}=\sigma_{d(local)}+\sigma_{p(local)}+\sigma_m+\sigma_r+\sigma_a+\sigma_s \qquad (4)$$

where σ_d=diamagnetic effects

σ_p=paramagnetic effects

σ_m=neighbour anisotropy effects

σ_r=effects of ring currents

σ_a=electric field effects

σ_s=solvent (or medium) effects

The σ_d and σ_p terms arise from electrons proximate to the magnetic nucleus and usually exert the greatest influence on the screening; however, electron currents generated in neighbouring parts of the molecule also contribute significantly.

Electric field shieldings, σ_a, are through space effects caused by molecules containing strongly polar groups. By generating electric dipoles or point charges, these polar groups will, effectively, distort the electron density in the molecule and thereby affect the screening constant. Solvents with strong magnetic anisotropy or polar character may also contribute a significant σ_s to the total nuclear screening. Dipole-dipole attractions with solvent molecules lead to some perturbations. By changing solvent, the nuclei may

---

3 Carrington, A. and McLachlan, A. D. Introduction to Magnetic Resonance. (New York: Harper and Row, 1967)]

resonate at different frequencies and these solvent induced shifts may be useful in assigning spectra.

Neighbouring anisotropy, σ_m, often exerts a marked effect on the character of an NMR spectrum. Recalling that the magnetic field B_o will induce magnetic moments in all the electrons of a molecule and that each electron is generally associated with an atom or a bond, one can easily envision the induced moments in a distant chemical bond or in neighbouring atoms affecting the observed nucleus.

Electrons delocalized in the π-framework of aromatic systems can be made to circulate by application of an external magnetic field. This induced electron circulation, known as the "ring current" is analogous to a current in a loop of wire and results in the generation of a secondary field that acts in opposition to the applied field. The net results are the so-called shielding and deshielding zones illustrated in Figure 1. Protons above and below the ring experience not only the applied field but the opposing secondary field as well. The cumulative result is a shielding zone which causes protons within this volume to absorb at lower frequency. Conversely, protons in the molecular plane experience a field greater than the applied field. The net effect is deshielding causing a proton to resonate at a higher frequency. These ring current effects, σ_r, can have a strong influence on the chemical shift of a proton.

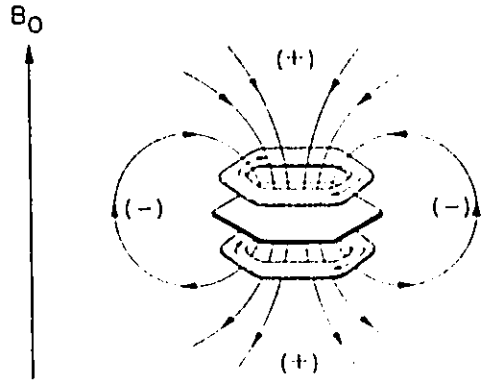

Figure 1: Ring Currents

The neighbouring anisotropy and ring current effects are believed to be largely responsible for a curious phenomenon which manifests itself in the ^{1}H-NMR spectra of nucleic acids and is the subject of the present thesis.

1.2. Magnetic Anisotropy of Nucleic Acid Heterobases

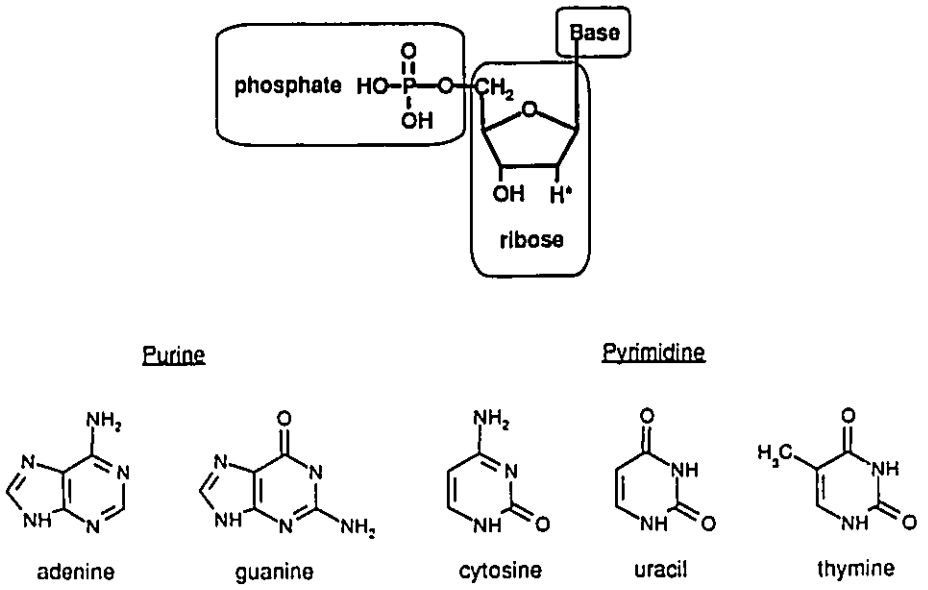

Figure 2: Nucleotide Structure

The unique properties of nucleic acids can be shown to result from their three-dimensional structure. Essentially, these biomolecules may be regarded as long, linear polymers composed of a number of nucleotide monomeric units. As seen in Figure 2, each nucleotide consists of a carbohydrate fragment; a nitrogenous base; and a phosphate. The carbohydrate or sugar portion of the nucleotide is either a D-ribose (found in RNA) or 2-deoxy-D-ribose (found in DNA). The heterobases are either the

bicyclic purine-type (adenine or guanine) or the monocyclic pyrimidine-type (thymine, uracil or cytosine) and are connected to the ribose by a β-glycosyl linkage. The nucleotides are connected by phosphate ester linkages from the 3′ position of one sugar to the 5′ position of the adjacent ribose to form a nucleic acid chain.

Both the base and ribose units of each of the nucleoside monomers (adenosine, guanosine, cytidine, uridine and thymidine) show characteristic chemical shifts and coupling patterns in the ^{1}H-NMR. In an oligonucleotide strand, however, the addition of neighbouring bases changes the magnetic environment experienced by these protons. For example, NMR investigations by Lee *et al.*[4] noted an upfield change in the chemical shifts of the H2 and H8 protons on adenine in proceeding from the monomer to the adenine-adenine dinucleoside. Other studies show similar trends for oligonucleotides of various lengths.[5]

The NMR phenomenon is a result of the preferred conformation adopted by nucleic acids wherein the bases tend to align themselves in stacks. Not surprisingly, the aggregation is known as base stacking.[6] Originally observed in the X-ray crystallographic structures of oligonucleotides, polar substituents like NH_2, =N- and =O often superimpose themselves over the aromatic system of the adjacent base. Dipoles, π-electron systems interactions from hydrophobic binding, London dispersion forces and dipole-induced dipole

---

4 Lee, C.-H., Ezra, F.S., Kondo, N.S., Sarma, R. H. and Danyluk, S. S. *Biochemistry.* **15**, 3627 (1976)

5 Ezra, F.S., Lee, C.-H., Kondo, N.S., Danyluk, S.S., and Sarma, R. H.. *Biochemistry.* **16**, 1977 (1977); Bell, R.A., Everett, J.R., Hughes, D.W., Coddington, J.M., Alkema, D., Hader, P.A. and Neilson, T. *J. Biomol. Struct. and Dynamics.* **2**, 693-707 (1985)

6 Basic Principles in Nucleic Acid Chemistry, P.O.P. Ts'O, editor. (New York: Academic Press, 1974). Volume I, pp.453-584.

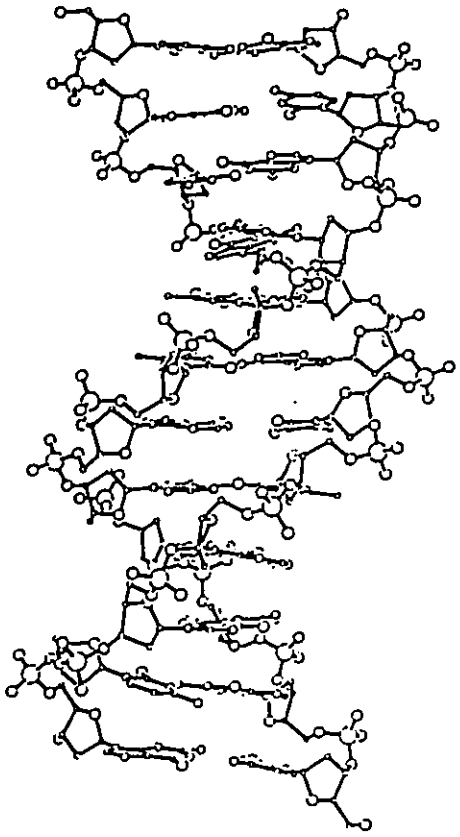

Figure 3: Base Stacking in DNA

moments appear to be the important forces stabilizing vertical base stacking.[7] The effect is seen in both doubly-stranded DNA (see Figure 3) and single strands of RNA. While base stacking is independent of sequence length (ie. the effect seen in dimers and long sequences), the largest effects are seen when the nucleic acids are dissolved in aqueous solutions of high ionic strength.

The upfield shift of the heterobase protons in an oligonulceotide is a result of this

---

[7] Saenger, W. Principles of Nucleic Acid Structure (New York: Springer-Verlag, 1984), Chapter 6, pp. 116-158.

stacking of aromatic bases. Adjacent bases are separated by as little as 3.4 Å and, at this proximity, can exert pronounced diamagnetic shielding on their neighbours; that is, the protons of a heterobase can find themselves in the shielding cone of the neighbouring purine or pyrimidine (see Figure 4). A detailed knowledge of the spatial distribution of the total diamagnetic shielding anisotropy about these aromatic systems could aid in the assignment of the heterobase protons in the ^{1}H-NMR spectra of large oligomers. Furthermore, this information could prove invaluable in the study of the conformational properties of specific sequences.

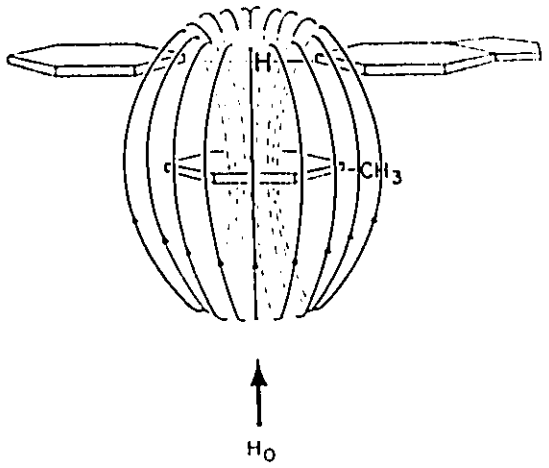

Figure 4: Stacked Bases and Induced Local Magnetic Fields

Traditionally, experimental investigations of heterobase anisotropy have looked at the difference in chemical shift between aromatic protons in the monomer and those in an oligomer; these oligomer shifts were ascribed to ring current and local anisotropy effects.[4,5] Alternatively, Robillard and Reid[a] used the crystal structure coordinates of t-RNA sequences to relate proton chemical shifts to ring current shieldings. Overall, the experimental approaches to anisotropy investigation have left much to be desired.

Theoretical models used for predicting the magnetic anisotropy of these systems

---

[a] Robillard, G. T. and Reid, B. R. in Biological Applications of Magnetic Resonance, R. G. Shulman, editor. (New York: Academic Press, 1979)

have been developed, adopting either a semi-empirical or quantum mechanical approach. Originally, the semi-empirical investigations concentrated on calculating the contributions to the total shielding from ring currents[9], local magnetic anisotropy[10] and polarization effects caused by protonation or hydrogen bonding.[11] Giessner-Prettre *et al.*[12] have used this procedure to calculate the shielding experienced by the protons of a nucleotide as a result of the different units of a single or double stranded helix. The magnetic isoshielding diagrams generated using this methodology have been published.[13]

A slightly different approach has been provided by a quantum mechanical study of the total shielding. Giessner-Prettre and Pullman developed a procedure which utilized the self-consistent perturbation method developed for gauge invariant atomic orbitals (GIAO) using a minimum basis set.[14] Schindler chose an individual gauge for localized molecular orbitals (IGLO) approach to calculate the chemical shift tensors and magnetic susceptibilities for purine and pyrimidine bases.[15] While both these *ab initio* methods calculate the total shielding experienced by a nucleus, the computational effort required does not allow for the determination of values for large molecules.

Despite the level of sophistication of these two theoretical approaches, a method

---

[9] Giessner-Prettre, C., Pullman, B., Borer, P.N., Kan, L-S, and Ts'o, P.O.P. *Biolpolymers.* 15, 2277-2286 (1976)

[10] Giessner-Prettre, C. and Pullman, B. *Biochem. Biophys. Res. Comms.* 70, 578-581 (1976)

[11] Giessner-Prettre, C., Pullman, B. and Caillet, J. *Nuc. Acids Res.* 4, 99-116 (1977)

[12] Giessner-Prettre, C. and Pullman, B. *J. Theor. Biol.* 65, 171-188 and 189-201 (1977)

[13] Giessner-Prettre, C. and Pullman, B.. *J. Theor. Biol.* 27, 87-95 (1970)

[14] Giessner-Prettre, C. and Pullman, B. *Quarterly Rev. of Biophys.* 20, 113-172 (1987)

[15] Schindler, M. *J. Amer. Chem. Soc.* 110, 6623-6630 (1988)

of experimentally determining the diamagnetic shielding anisotropy is needed. One such approach to the study of these magnetic phenomenon involves the use of cyclophanes. The distinctive proton NMR spectra of these bridged aromatic species illustrates the potential use of cyclophanes as probes of magnetic anisotropy.

1.3. Cyclophanes and Their Use as Probes of Magnetic Anisotropy

Since the first appearance of cyclophanes in the literature in 1951[16], numerous papers, reviews and books have been published detailing their unusual chemical and spectroscopic properties.[17] These bridged aromatic compounds have provided insight into a variety of areas including the nature of aromaticity, the effects of strain on reactivity, conformational dynamics, nuclear magnetic resonance spectroscopy, ultraviolet spectroscopy and host-guest chemistry. More recently, cyclophanes are being used as synthetic analogues of enzymes and receptors. The preparation of simple, singly-bridged aromatic systems, as well as the more complex, multibridged and multilayered cyclophanes has required the development of new synthetic methodologies.

Early cyclophane chemistry dealt most often with bridged systems of benzene.[18] Since then, virtually every aromatic system seems to have been girded by an aliphatic chain. Examples of cyclophanes based upon pyridine, pyrrole, anthracene, naphthalene, furan, substituted-benzenes and thiophene are plentiful[17] while such biologically important

---

[16] Cram, D.J., and Steinberg, H. *J. Amer. Chem. Soc.*. **73**, 5691 (1951)

[17] Cyclophanes, Vol. I and II, Keehn, P. M. and Rosenfeld, S. M., eds. (New York, Academic Press, 1983); F. Diederich, Cyclophanes (Cambridge: Royal Society of Chemistry, 1991)

[18] Bickelhaupt, F. *Pure & Appl. Chem.* 62, 373-382 (1990)

aromatic systems as flavins[19] and porphyrins[20] are now also being investigated. Newest trends in the field include mixed cyclophanes, metal containing cyclophanes, and catenanes ("linked cyclophanes").[17]

The syntheses of cyclophanes based on the purine and pyrimidine ring systems have also been reported. Acetylenic coupling followed by hydrogenation allowed for the preparation of [10]-(4,6)- 2-methyl-pyrimidinophane (i) (see Figure 5).[21] The 3,4-dithiapyrimidinophane (ii) was produced by

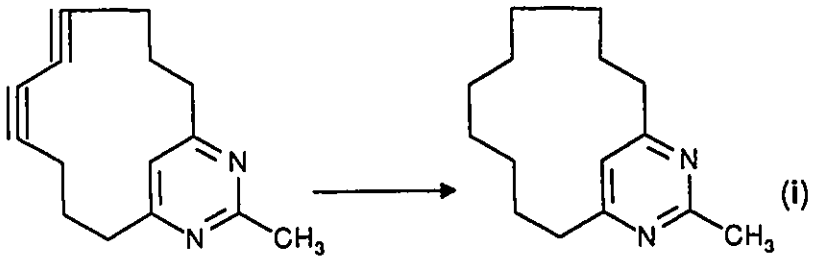

(i)

Figure 5: [10]-(4,6)-2-Methyl-pyrimidinophane

Kinoshita, Tanaka and Furukawa to be used as a potential complexing agent for metals (see Figure 6).[22] This rather lengthy synthesis involves the *de novo* generation of the pyrimidine rings. The isomeric compound (iii) has also been prepared.[23]

The Dimroth rearrangement has proved its synthetic utility in the production of a

---

19 Zipplies, M.F., and Staab, H.A. *Tet. Lett.* **25**, 1035 (1984) and Zipplies, M.F., Krieger, C., and Staab, H.A. *Tet. Lett.* **24**, 1925 (1983)

20 Baldwin, J.E., and Perlmutter, P. *Top. Curr. Chem.* **121**, 181 (1984)

21 Sakamoto, T., Nishimura, S., Kondo, Y. and Yamanaka, H. *Heterocycles.* **27**, 475-478 (1988)

22 Kinoshita, T., Tanaka, H., and Furukawa, S. *Chem. Pharm. Bull.* **34**, 1809-1813 (1986)

23 Kinoshita, T., Odawara, S., Fukumura, K., and Furukawa, S. *J. Heterocyclic Chem.* **22**, 1573-1576 (1985)

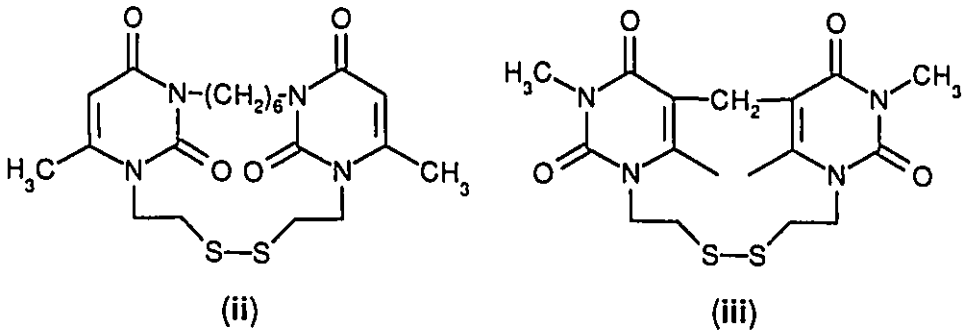

Figure 6: Dithiapyrimidinophanes

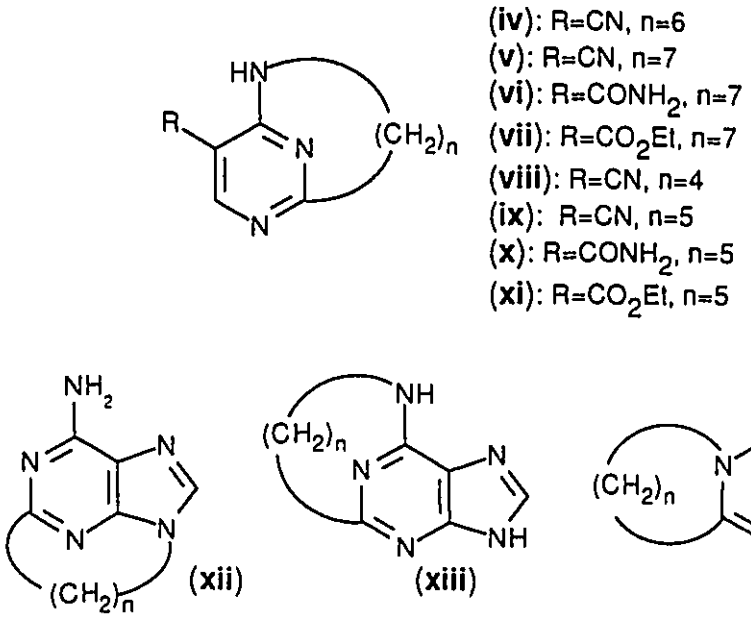

Figure 7: Purinophanes and Pyrimidinophanes via the Dimroth Rearrangement

number of purino- and pyrimidinophanes (**iv-xi**) (see Figure 7). Brown and Ienaga used

this reaction to prepare a number of 5-substituted-[n]-(2,N4)-pyrimidinophanes.[24] More recently, Ienaga has used this rearrangement in the preparation of (2,9)-, (2,N6)-, and (1,2)-polymethylene-adenines (**xii**, **xiii**, **xiv**).

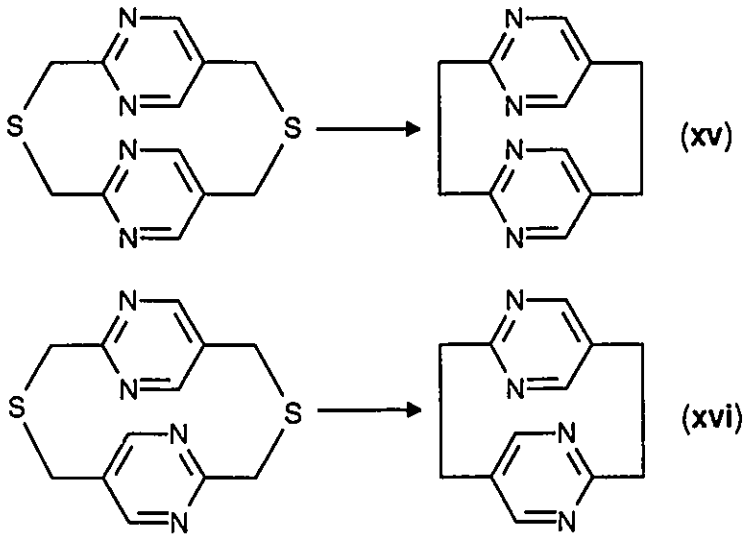

Figure 8: [2,2]-(2,5)-Pyrimidinophanes

Eiermann, Krieger and Neugebauer prepared two isomeric [2,2]-(2,5)-pyrimidinophanes (**xv** and **xvi**) by photolytic sulphur extrusion of 2,11-dithia [3,3]-(2,5)-pyrimidinophane (see Figure 8).[25]

In their study of base stacking and its relationship to ultraviolet-hypochromism, Seyama *et al.* prepared twelve purinophanes (**xvii-xxviii**) (Figure 9) in which two purines

---

[24] Brown, D.J., and Ienaga, K. *J. Chem. Soc., Perkins I*, 2182-2185 (1975) and Brown, D.J., and Ienaga, K.. *Aust. J. Chem.* **28**, 119-127 (1975)

[25] Eiermann, U., Krieger, C., and Neugebauer, F.A. *Chem. Ber.* **123**, 1885-1889 (1990)

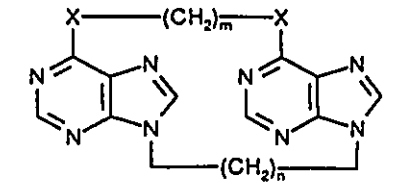

(xvii): X=NH, m=2, n=3
(xviii): X=NH, m=2, n=4
(xix): X=S, m=2, n=3
(xx): X=S, m=2, n=4
(xxi): X=S, m=3, n=3

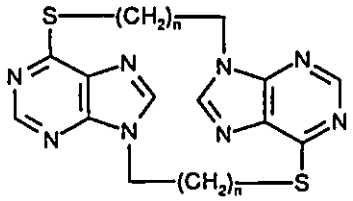

(xxii): n=2
(xxiii): n=3

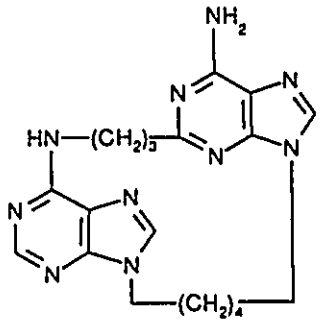

(xxiv)

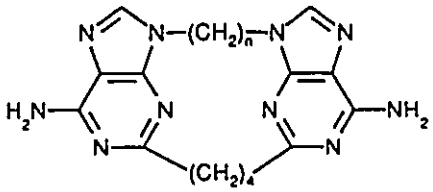

(xxv): n=3
(xxvi): n=4

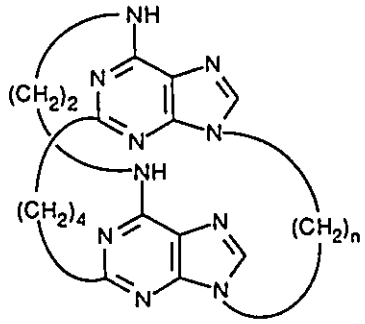

(xxvii): n=3
(xxviii): n=4

Figure 9: Stacked Purinophanes

are fixed in different geometries by short methylene chains.[26] Sakata *et al.* noted

---

[26] Seyama, F., Akahori, K., Sakata, Y., Misumi, S., Aida, M. and Nagata, C. *J. Amer. Chem. Soc.* 110, 2192-2201 (1988)

unusual reactivity in a series of mixed purino-pyrimidinophanes (**xxix-xxxii**) (see Figure 10) which they ascribed to the stereoelectronic effect.[27]

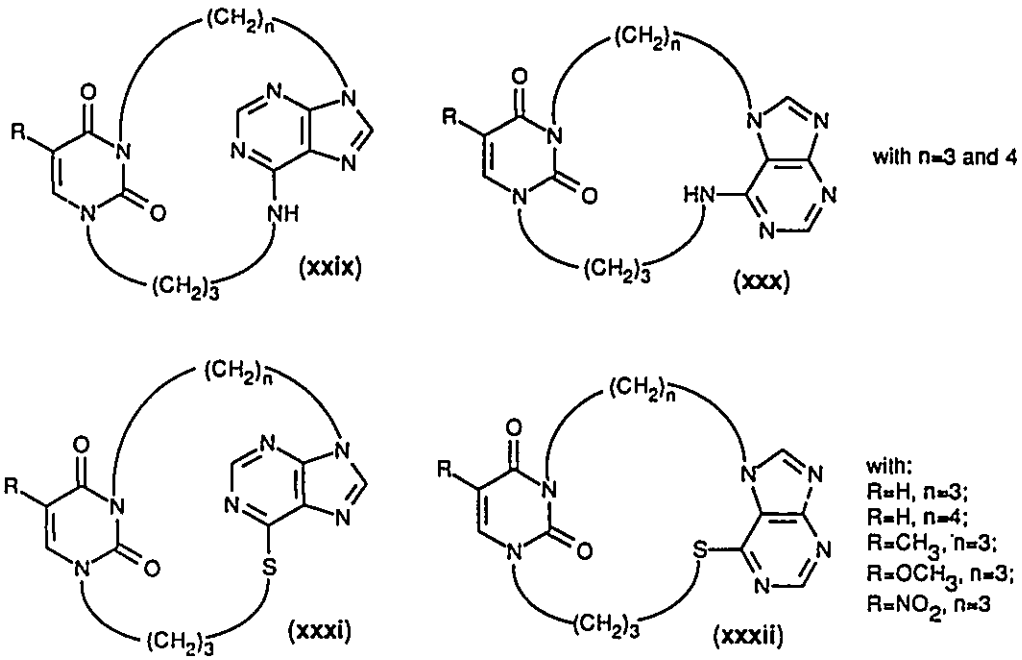

Figure 10: Mixed purino-pyrimidinophanes

Huguchi *et al.* also noted this unusual reactivity in [n]-(6,9)-purinophanes of 6-

---

27 Sakata, Y., Higuchi, H., Doyama, K., Higashii, T., Mitsuoka, M., and Misumi, S.. *Bull. Chem. Soc. Jpn.* **62**, 3155-3160 (1989)

thiopurine (**xxxiii**) (see Figure 11).[28]

[n]-Cyclophanes provide an unusual perspective of the diamagnetic shielding about aromatic systems. Unlike the methylene protons of an ordinary aliphatic chain (typically having chemical shifts around 1.3 ppm), the signals from the bridge protons of a cyclophane can assume a wide range of values (often between 3 and -1 ppm). For example, the chemical shifts of the bridge protons in [10]-paracyclophane (Figure 12, **xxxiv**) ranged from 2.62 to 0.51 ppm.[29] Work carried out by Nozaki *et al.* demonstrated that such heteroaromatic systems as [8]-(2,5)-pyrrolophane, [8]-(2,5)-furanophane, and [8]-(2,5)-thiophenophane

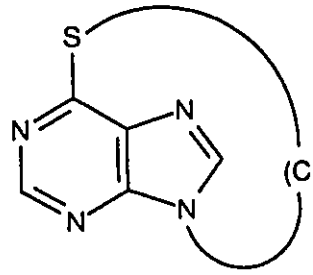

(xxxiii)

Figure 11: [n]-(6,9)-6-Thio-purinophane

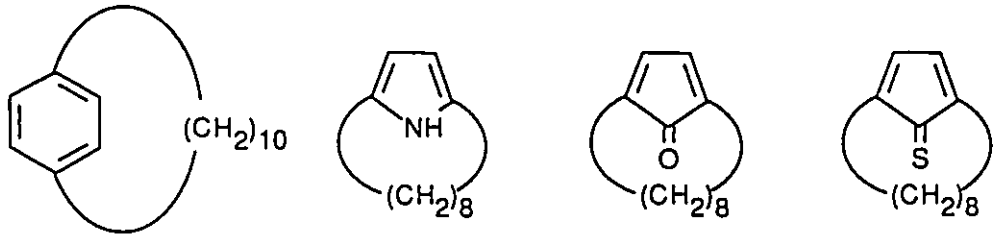

(xxxiv) **(xxxv)** **(xxxvi)** **(xxxvii)**

Figure 12: [10]-Paracyclophane, [8]-(2,5)-Pyrrolophane, [8]-(2,5)-Furanophane, and [8]-(2,5)-Thiophenophane

---

[28] Higuchi, H., Mitsuoka, M., Sakata, Y., and Misumi, S.. *Tet. Lett.*. **26**, 3849 (1985)

[29] Agarwal, A., Barnes, J.A., Fletcher, J.L., McGlinchey, M.J. and Sayer, B.G. *Can J. Chem.* **55**, 2575-2581 (1977)

(Figure 12, **xxxv**, **xxxvi**, and **xxxvii** respectively) also show similar dispersion of signals from the aliphatic chain protons.[30] Once again, ring currents and local magnetic anisotropy have been implicated in the curious spectra.

Rather than dismiss these spectra as curiosities, they may be exploited in the study of purine and pyrimidine anisotropy. Allowing an aliphatic chain to pass over the aromatic plane of a heterobase enables the methylene protons to act as "reporter" groups of the magnetic environment of the system. Ultimately, the proton chemical shifts can furnish values for the spatial definition of the diamagnetic susceptibility anisotropy around these aromatic systems and supply a viable means of appraising the theoretical calculations.

Previous work involving the examination of the proton chemical shifts of [10]-paracyclophane provided a method of complementing and assessing the calculated shielding anisotropy of benzene.[29] Calculated proton chemical shifts for the cyclophane were a composite of a standard methylene shift, and a contribution to the total shielding from ring currents and local anisotropic contributions. With the geometry of the cyclophane provided by a molecular model, estimates of the ring current effect were made using the "free electron" model of Waugh and Fessenden[31] while the local atomic contributions to the diamagnetic anisotropy were evaluated using the method developed by Barfield *et al.*[32] The success of the [10]-paracyclophane study provided the inspiration for the investigation of the diamagnetic anisotropy of the purine and pyrimidine

---

[30] Nozaki, H., Koyama, T. and Mori, T. *Tetrahedron.* 25, 5357 (1969)

[31] Waugh, J. S., and Fessenden, R. W. *J. Amer. Chem. Soc.* 79, 846 (1957)

[32] Barfield, M., Grant, D.M., and Ikenberry, D. *J. Amer. Chem. Soc.* 97, 6956-6961 (1975)

heterobases using a cyclophane approach.

1.4. Synthetic Considerations and Strategies

If the cyclophanes of purine and pyrimidine bases are to provide any information about the diamagnetic shielding anisotropy about these ring systems, certain prerequisites must be incorporated into their design. Firstly, the sites of attachment of the methylene bridge must be chosen such that the chain traverses over the centre of the aromatic plane. Such a geometry ensures a wide variety of magnetic environments for the bridge protons. Secondly, the length of the methylene chain must be short enough to allow for a minimum amount of flexibility, yet long enough to avoid "puckering" of the aromatic system. Conformational rigidity will allow for precise determination of each proton's position above the heterobase and, thus, provide precise spatial conformation about the diamagnetic shielding anisotropy. The use of computer generated models has proven to be of great benefit and the considerations listed above can be resolved, to a large extent, by programs such as Macromodel[33] or PC-Model.[34]

Having decided upon an appropriate chain length and the sites for attachment, two synthetic considerations must be addressed. First of all, one must determine whether it is synthetically feasible to fasten the methylene bridge at the locations desired. Obviously, certain positions in the purine and pyrimidine rings are not amenable for such a task. A review of the literature allows one to determine the best site of attachment from a

---

[33] Macromodel Computer Program. Version 1.5. W. C. Still (1987), Columbia University

[34] PC-Model. Version 4.0. Serena Software, (1991)

synthetic point of view.

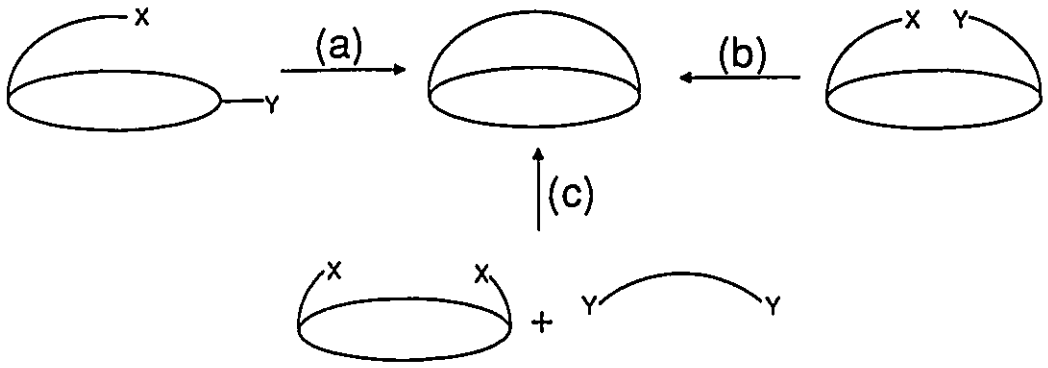

Figure 13: Approaches to Bridge Formation

Secondly, one must decide on the best way to fashion the methylene bridge. Figure 13 gives three possibilities: Intact Bridge Attachment, Bridge Formation by Coupling or Bimolecular Bridge Formation. The Intact Bridge Attachment method, (a), perhaps the most straightforward, involves connecting the entire chain at one end of the ring, then bonding at the other terminus. Another intramolecular route, Bridge Formation by Coupling, (b), envisions two shorter chains, each attached at opposite ends of the aromatic system and appropriately functionalized for the final ring closure. Finally, an intermolecular option, Bimolecular Bridge Formation, (c), has short chains connected to the ring and requires an additional piece to complete the methylene bridge.

Each of the routes has its own advantages and disadvantages. Method (a) is the most direct, but the final ring closure requires very demanding geometrical constraints. More freedom is allowed by cyclization route (b). Furthermore, this pathway allows for more synthetic flexibility. Here, ring closure is achieved by coupling two alkyl chains. There are a number of synthetic methodologies that allow for such a connection. Routes

which involved the incorporation of some heteroatom or functionality into the methylene bridge were avoided since such an inclusion would affect the magnetic environment of the chain protons and give a distorted picture of the actual diamagnetic shielding anisotropy about the aromatic system. Extrusion of the heteroatom or functional group can be difficult and add to the length of the synthetic pathway. Intermolecular route (c) has been employed in the synthesis of cyclophanes in the past, but suffers from both the heteroatom incorporation in the bridge and the greater degree of cross reactions. In all cases, high dilution conditions were employed to avoid unwanted intermolecular products. While other routes are possible, including certain *de novo* syntheses, these tend to be longer and are often more involved.

Each of these items was considered in the development of the preparative routes for the purinophanes and pyrimidinophanes and are addressed at the beginning of the relevant chapters.

1.5. Objectives

The main objective of this thesis has been to prepare cyclophanes centred around the purine and pyrimidine bases found in ribo- and deoxyribonucleic acids. Conformational and NMR studies will then serve to give an experimental accounting of the magnetic environments of these heterobases. Ultimately, this information will be compared to that derived from theoretical models.

The preparation, X-ray crystal structure and nuclear magnetic resonance spectroscopy of [8]-(N6,9)-6-aminopurinophane (Figure 14, 1) have already been

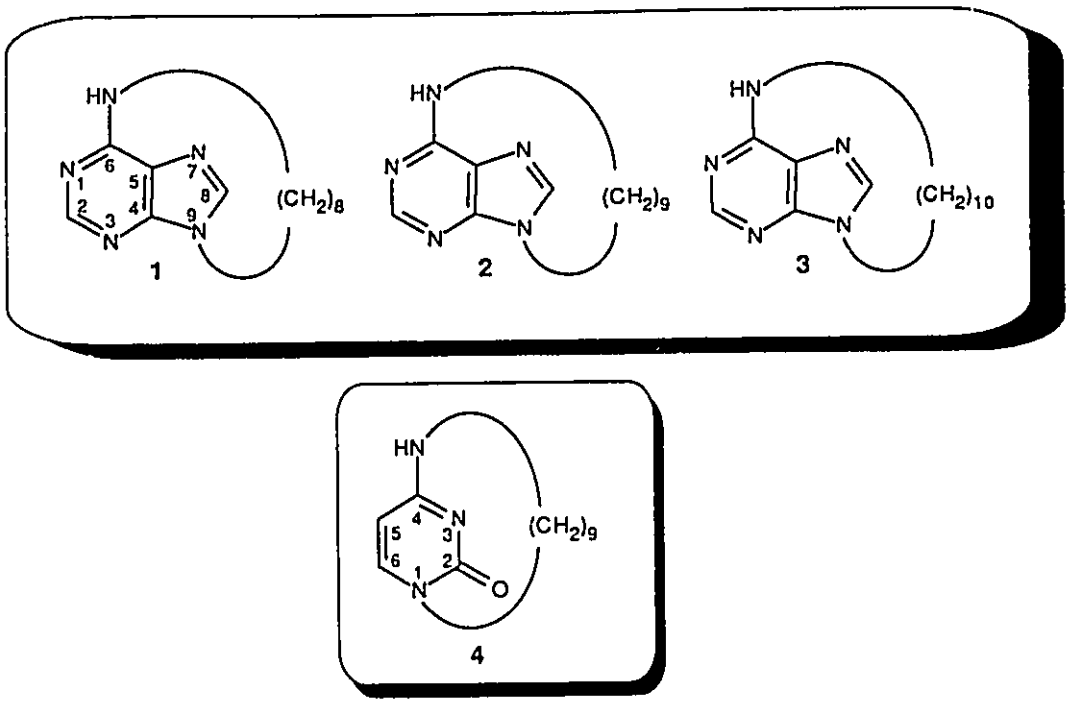

Figure 14: [n]-(N6,9)-6-amino-purinophane and [9]-(1,N4)-2-one-4-amino-pyrimidinophane

described by Bell *et al.*[35,36] Additionally, samples of N6,N9-nonamethylenepurine cyclophane have been prepared by Hunter.[37] In an effort to continue this work, [9]- and [10]-(N6,9)-6-aminopurinophane (see Figure 14, **2** and **3** respectively) have been

---

35 Bell, R. A., Hunter, H. N., Lock, C. J. L. and Fagiani, R. *Can. J. Chem.*. **70**, 186 (1992)

36 Bell, R.A. and Hunter, H.N. *Tetrahedron Lett.* **28**, 147-150 (1987)

37 Hunter, H.N.. PhD. Thesis. McMaster University, 1988

synthesized (Chapter 2) and investigated using nuclear magnetic resonance spectroscopy (Chapter 5). Crystallographic work involving the nonamethylene purinophane will be presented as will an ultraviolet spectroscopy study of the entire adenine cyclophane series (Chapter 5).

Approaches towards the preparation of [9]-(1,N4)-2-one-4-amino-pyrimidinophane (a cytosine cyclophane) (Figure 14, 4) will be described including attempts using the "Intact Bridge Attachment" route (Chapter 3) and the "Bridge Formation by Coupling" strategy (Chapter 4).

Following an approach similar to that undertaken in the [10]-paracyclophane investigation[29], the diamagnetic anisotropy experienced by the methylene bridge protons will be correlated to the effects exerted by the local magnetic anisotropies and ring currents of adenine (Chapter 6).

Chapter 2

Syntheses of [n]-(N6,9)-6-Aminopurinophanes

2.1. Synthesis of [8]-(N6,9)-6-Aminopurinophane

Studies involving the preparation and nuclear magnetic resonance spectroscopy of [8]-(N6,9)-6-aminopurinophane have already been reported by Bell and Hunter.[35,36,37] Some of the features of that previous work deserve consideration since many aspects have been carried on in the present investigation of homologous adenine cyclophanes.

In keeping with the synthetic prerequisites and strategies outlined in the Introduction, a number of options were considered in choosing the bonding positions for the methylene bridge to adenine. Ideally, the chain should traverse as much of the plane of the aromatic system as possible in order to provide the maximum information about the diamagnetic anisotropy. A survey of the relevant literature indicated that the most suitable sites for attachment would be N9 and N6.

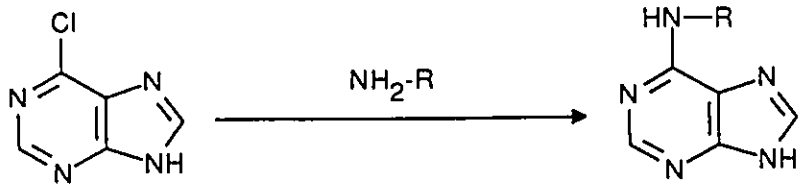

Figure 15: Nucleophilic Aromatic Substitution at the 6-Position

In their study of 6-substituted purines, Sutherland and Christensen prepared a

number of 6-alkylamino-purines by treating 6-chloropurine with a series of primary amines (see Figure 15).[38] The nitrogen of the attacking amine becomes the N6 of adenine.

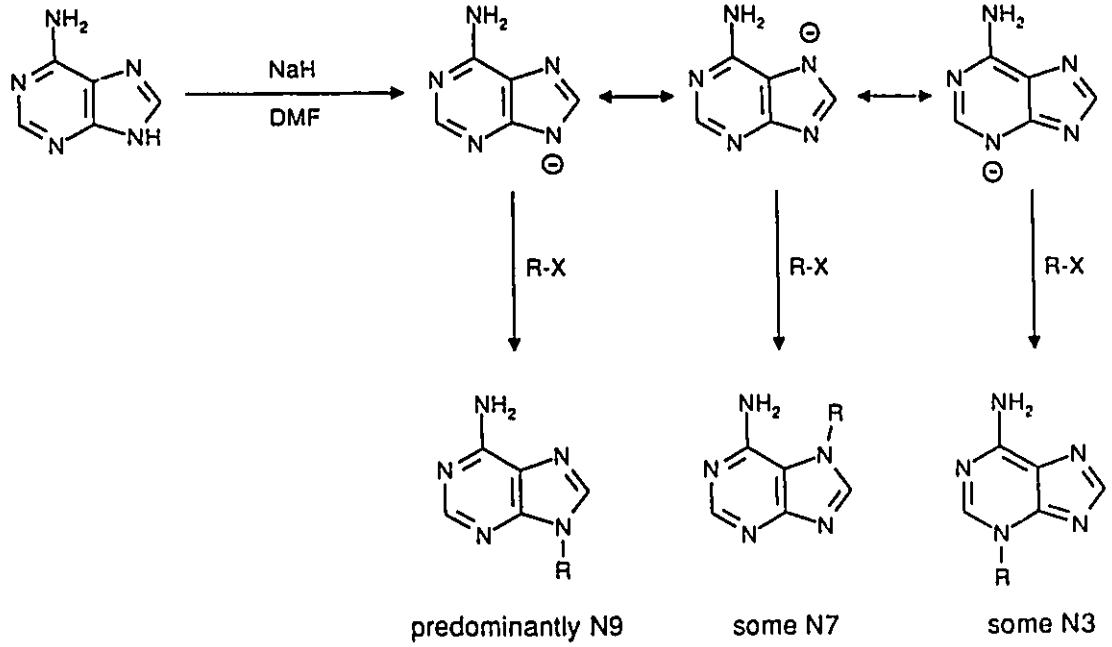

Figure 16: Alkylation Using Sodium Hydride and Alkyl Halides

Many of the reactions involving alkylation at N9 also result in appreciable amounts of N7 and N3 alkylated products.[39] As seen in Figure 16, treatment of adenine with sodium hydride in dimethylformamide generates the sodium salt of adenine. Introduction of an alkyl halide results in alkylation predominantly at N9 (yields: 27-38%); but, because of the delocalization of charge about the purine ring, appreciable amounts of N3 and N7

---

38 Sutherland, M. and Christensen, B.E. *J. Amer. Chem. Soc.* 79, 2251-2252 (1957)

39 Osterman, R. M., McKittrick, B. A., and Chan, T.-M. *Tet. Lett.* 33, 4867 (1992) and Carraway, K.L., Haung, P.C., and Scott, T.G. in Synthetic Procedures in Nucleic Acid Chemistry, Zorbach, W.W. and Tipson, R.S., eds. (New York: John Wiley and Sons, Inc., 1968). Vol. I, pp. 3-5

alkylation occurs.

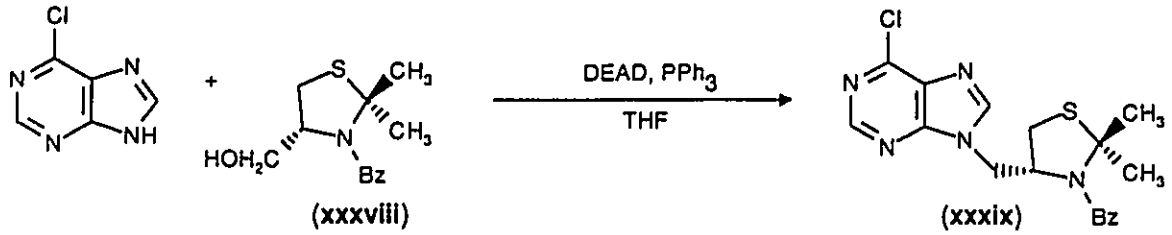

Figure 17: Mitsunobu Reaction at the 9-Position

Fortunately, use of the Mitsunobu reaction permits reaction only at N9.[40] Iwakawa *et al.*[41], for example, were able to prepare 6-chloro-9[(3-benzoyl-2,2-dimethylthiazolidin-4(R)-yl)methyl]-9H-purine (**xxxix**) in 62% yield by treating the alcohol (**xxxviii**) with 6-chloropurine, triphenylphosphine (PPh_3) and diethyl azodicarboxylate (DEAD) in tetrahydrofuran (THF) at room temperature (see Figure 17).

The mechanism of the Mitsunobu reaction is presented in Figure 18. Attack of triphenylphosphine on the carbonyl oxygen of diethyl azodicarboxylate results in the species, (**xl**), which quickly rearranges upon migration of the phosphorus to the nitrogen to give (**xli**). Evidence in support of betaine intermediates (**xl**) and (**xli**) have been provided by ^{31}P NMR.[42] Protonation of the quaternary phosphonium salt by N9 results in intermediate (**xlii**). Subsequent addition of an alcohol leads to an alkoxy-phosphonium

---

40 Mitsunobu, O. *Synthesis*, 1-28 (1981)

41 Iwakawa, M., Pinto, B.M. and Szarek, W.A. *Can. J. Chem.* 56, 326-335 (1978)

42 Mitsunobu, O. and Iguchi, M. *Bull. Chem. Soc. Jpn.* 44, 2327 (1971)

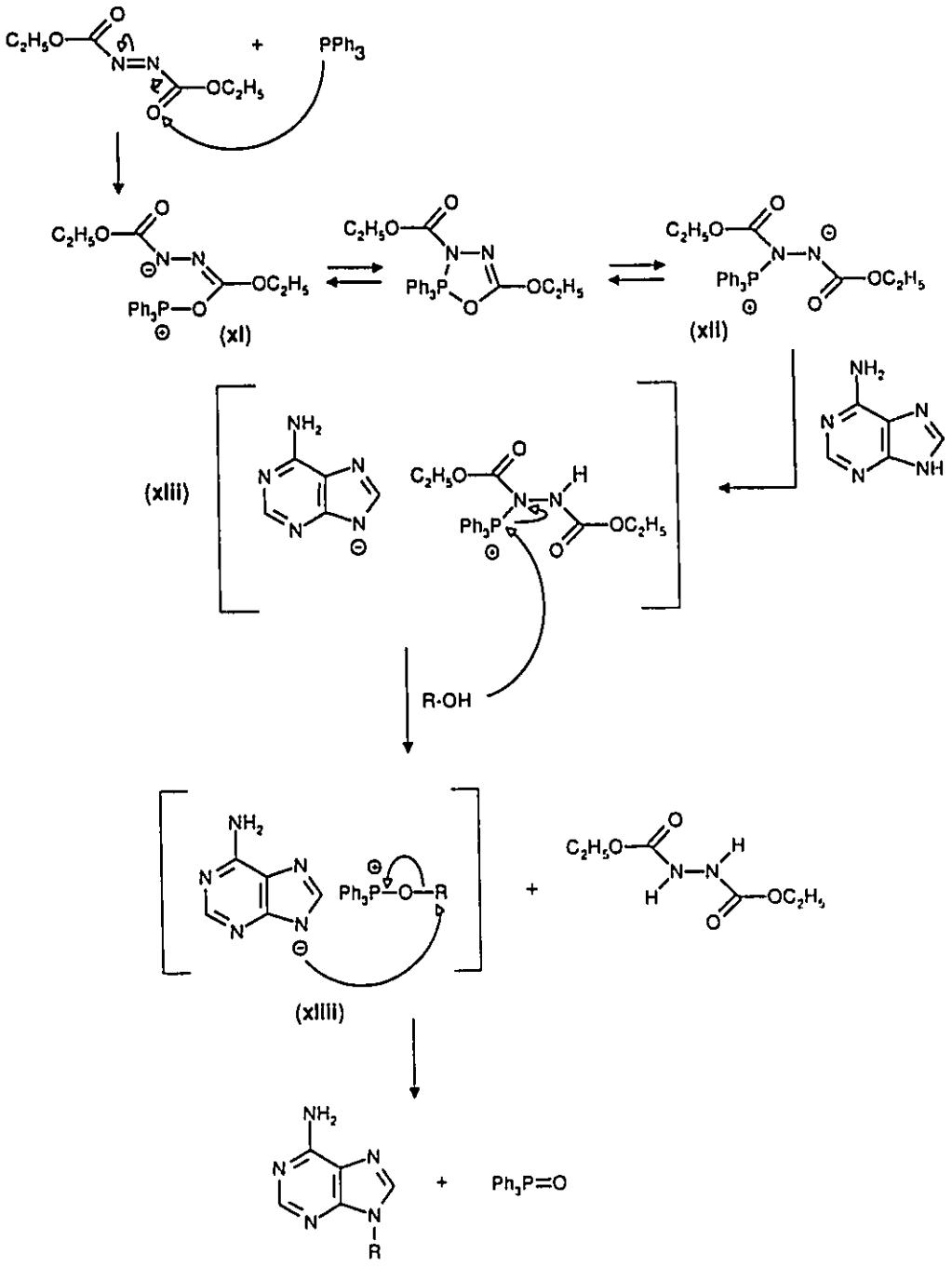

Figure 18: Mechanism of the Mitsunobu Reaction

salt (**xiiii**) which then undergoes an S_N2 type of displacement leading to the substituted adenine. The importance of this key reaction in the [8]-(N6,9)-6-aminopurinophane

synthesis has warranted a theoretical discussion of the Mitsunobu reaction and its selectivity, which may be found further within the chapter.

With the alkylation reactions in hand, an appropriate length for the aliphatic bridge of the cyclophane was then considered. Bearing in mind that a suitable chain had to be sufficiently taut so as to restrict movement of the methylene protons relative to the purine system while not distorting the aromatic plane, a molecular modelling study was undertaken to determine a suitable candidate and an eight-carbon chain was shown to best satisfy the requirements.

The synthetic route developed by Bell and Hunter is depicted in Figure 19.[35] Poor yields of the required 8-aminooctanol from direct reduction of the 8-amino octanoic acid (**xliv**) were due, in part, to the insolubility of the amino acid in suitable aprotic solvents. Treatment of the acid with thionyl chloride and ethanol resulted in the more soluble ethyl ester. Protection of the amine was then deemed necessary. Blocking of the amino end with a methoxytrityl group not only prevented the formation of insoluble poly(N-alkyliminoalanes) in the lithium aluminum hydride reduction step[43], but also averted the reaction of the amine with the diethyl azidocarboxylate (DEAD) used in the Mitsunobu step to form mono and diamides. The N-trityl ester (**xlv**) was subsequently reduced smoothly to the corresponding alcohol (**xlvi**) in high yield.

The subsequent Mitsunobu reaction saw the treatment of the N-methoxytrityl aminooctanol with 6-chloropurine, triphenylphosphine and DEAD in tetrahydrofuran to afford the N9-alkylated product (**xlvii**). Trifluoroacetic acid in methylene chloride followed

---

[43] Cucinella, S., Dozzi, G., Mazzei, A. and Salvatori, T. *J. Organomet. Chem.* **90**, 257 (1975); Cucinella, S., Salvatori, T., Busetto, G., Perego, G. and Mazzei, A. *J. Organomet. Chem.* **78**, 185 (1974)

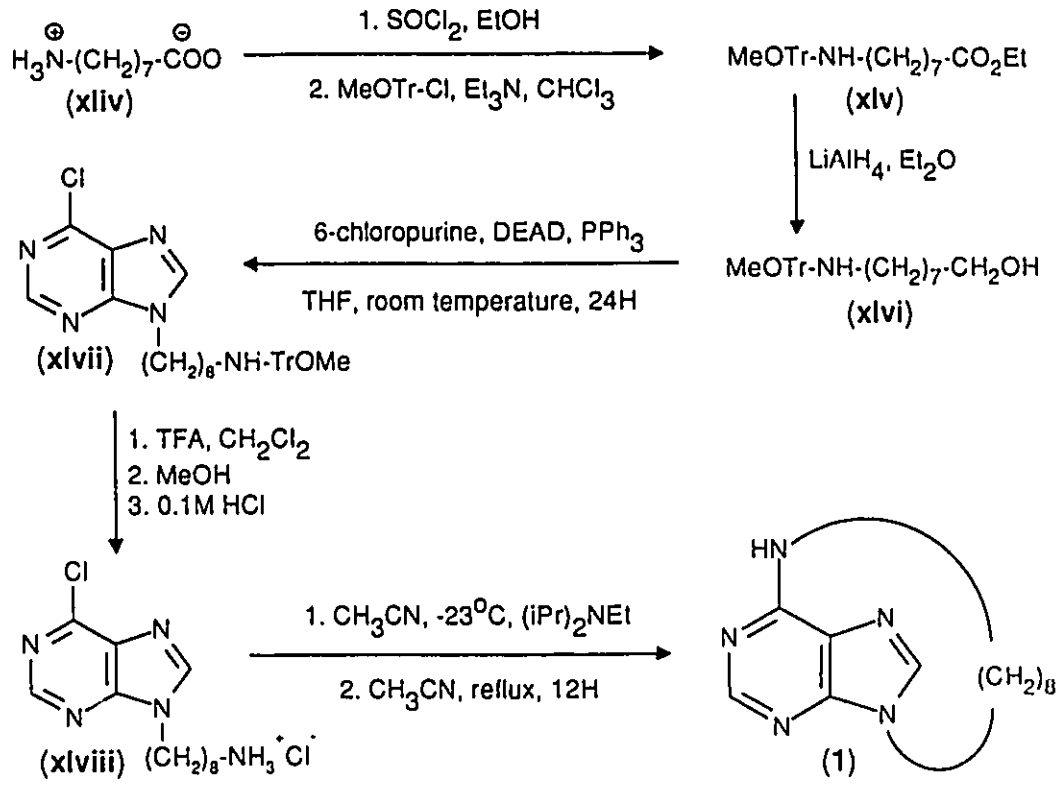

Figure 19: Synthesis of [8]-(N6,9)-6-Aminopurinophane

by a methanol quench successfully cleaved the methoxytrityl group yielding the amino-purine which was isolated as the hydrochloride salt (**xlviii**). The free amine was best generated *in situ* and by combining N,N-diisopropylethylamine (a hindered non-nucieophilic base) with the amine (**xlviii**) at -23°C. The mixture was then diluted to 10^{-3}M with dry acetonitrile and heated. High dilution conditions were applied in order to prevent intermolecular reaction and allow for only the desired intramolecular cyclization. Ultimately, the octamethylenepurine cyclophane (1) was produced in 30% yield after chromatographic purification.

The proton NMR spectrum of the [8]-(N6,9)-6-aminopurinophane clearly showed all eight pairs of diastereotopic methylene protons ranging in chemical shift from -0.6 ppm to 4.8 ppm (see Chapter 5, Figure 56). Assignments were made initially from a two-dimensional COSY spectrum in conjunction with energy minimized, computer generated molecular models. Further confirmation came from two-dimensional ^{13}C-^{1}H heteronuclear shift correlated spectra together with the solid state conformation of the molecule demonstrated by the X-ray crystallography. Aspects of the NMR spectroscopy and conformational analysis will be presented in Chapter 5.

2.2. Modelling Studies of the Mitsunobu Reaction

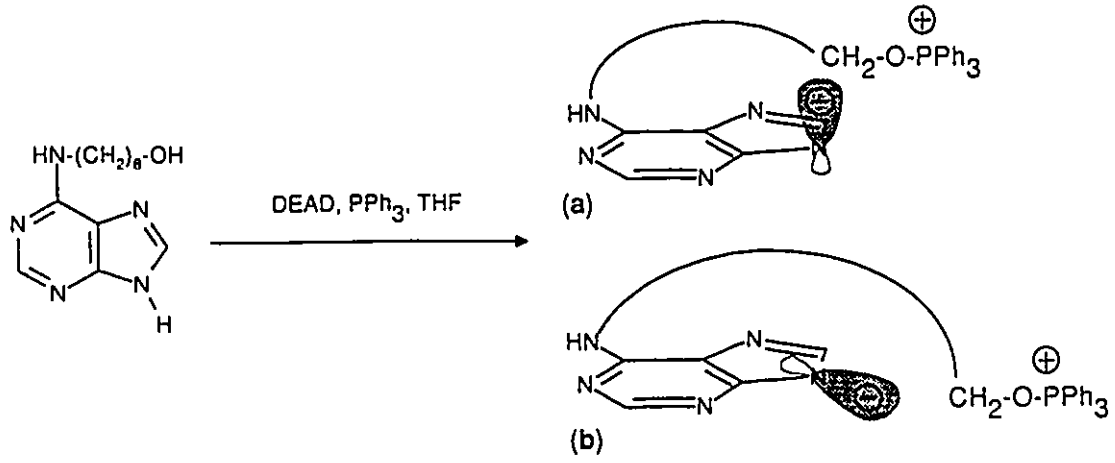

Figure 20: Transition State Geometry of the Mitsunobu Intramolecular Cyclization Intermediate

Preliminary experimental work on the [8]-(N6,9)-6-aminopurinophane indicated that alkylation at N9 should precede bonding at the 6 position. In fact, attempts at first forming the C6-N6 bond by intermolecular nucleophilic substitution and then using the Mitsunobu

reaction to carry out the intramolecular cyclization failed. As seen in Figure 20, the course of the reaction should have eventually led to the formation of the zwitterion intermediate pictured. One would expect the electrostatic attraction present in this Mitsunobu zwitterion to assist in the ring closure. Bell and Hunter have offered an explanation for these failed cyclizations based upon the orientation of the electron density in the highest occupied molecular orbital (HOMO) on N9.[35] It is argued that if the HOMO at N9 is *perpendicular* to the ring (see Figure 20, intermediate **a**) then there would be minimal steric strain in the approach of the end $CH_2OP^+(Ph)_3$ unit, and an S_N2 transition state should be attainable with a normal activation barrier. If, however the HOMO at N9 is *in the plane* of the purine ring (see Figure 20, intermediate **b**), then to attain an S_N2 transition state would require severe stretching of the end methylene beyond N9 and in the plane of the ring. Molecular models suggested that such a transition state would be very difficult to attain without excessive strain on the alkyl chain and bending of the purine. Such an orientation of the HOMO, effectively, makes the intramolecular reaction inaccessible.

In an effort to evaluate the mechanistic proposal of Bell and Hunter, an AMPAC[44] study of some substituted adenines was undertaken in order to model the intermediates in the Mitsunobu reaction and determine the orientation of the HOMO at N9. Calculations using the AM1 Hamiltonian on the anions of 6-chloropurine, N6-aminomethylpurine and adenine were undertaken and allowed for the determination of the vector eigenvalues, charge distributions and relative heats of formation for each system.

Molecular orbitals may be looked upon as the linear combination of atomic orbitals.

---

[44] Dewar Research Group and J. J. P. Stewart. *QCPE Bull.* 6, 2 (1986)

AMPAC delineates the individual atomic orbital (AO) contributions to the molecular orbital (MO) by assigning a weighing factor or coefficient to each atomic orbital (s, p_x, p_y, p_z) making up the MO. If one regards the atoms within the purine ring system as roughly sp^2 hybridized, then by aligning the purines in the x-y plane prior to the calculations, the computed value for the p_z coefficient can be thought of as a measure of electron density in that p-orbital perpendicular to the x-y plane. (Actually, the square of these coefficients provides the probability of finding an electron in the orbital.) Since the geometry of that p-orbital has been fixed, the orientation of the molecular orbital on N9 (as well as the other atoms) could be established. That is, if the HOMO at N9 is *in the plane* of the purine ring, then the value of the coefficient should be low. Conversely, a large coefficient value of the p_z orbital would be indicative of a HOMO at N9 *perpendicular* to the ring.

The AM1 calculations for the modelled adenine anion show that the negative charge is relatively well delocalized throughout the π-system. As seen in Table 1 of Appendix A, the coefficient of the p_z atomic orbital on N9 within the HOMO is 0.20526 while the contributions from the s, p_x and p_y orbitals are effectively zero. The remaining atoms in the purine also seem to have large p_z contribution with relatively small contributions for the corresponding s, p_x and p_y orbitals. According to the modelling, therefore, the HOMO at N9 adopts the orientation required for successful displacement as dictated by Bell and Hunter.

Perhaps a better model for the Mitsunobu intermediate being examined is 6-aminomethyl adenine. Its geometry was lifted from the crystal structure of [8]-(N6,9)-6-aminopurinophane with the octamethylene chain cleaved and N6 capped with a methyl group. The 6-aminomethyl adenine borrows two important structural features from the

cyclophane. In the cyclophane, the alkyl chain imparts a severe twist to N6, bending it above the purine plane. This twisting also bends the lone pair of electrons on N6 out of conjugation with the remainder of the purine ring. These factors are likely to be mirrored in the twisted intermediate of the Mitsunobu reaction and should, therefore, reflect themselves in the molecular orbital calculations of 6-aminomethyl adenine. But as in the adenine anion, atoms in the purine also seem to have large p_z contributions with relatively small contributions for the corresponding s, p_x and p_y orbitals. Noticeably larger is the p_z coefficient value (0.45450) obtained for the N9 of 6-aminomethylpurine when compared to that of adenine. Table 2 of Appendix A shows AMPAC's calculation of the net atomic charges within the models studied. Note the charge of the N9 atom in the adenine anion (-0.2318) in comparison to that found in 6-aminomethylpurine (-0.2905). These effects are likely due to the twisting about the N6-C6 bond forcing the lone pair of electrons out of conjugation with the purine ring resulting in an inability to further delocalize the charge out to N6. One can see this effect manifested in the charge on N6 in 6-aminomethyleadenine (-.2917) as compared to that of adenine (-.3112).

6-Chloropurine was modelled in order to provide a basis of comparison between the other anion molecules. It is, in many ways, like the adenine anion modelled (see Tables 1 and 2 of Appendix A). Overall, the picture painted by the AMPAC calculations showed that the HOMO at N9 can be considered to be perpendicular to the plane as required by the Bell and Hunter proposal. Furthermore, the charge is clearly delocalized throughout the purine system. In light of these semi-empirical calculations, the failure of the intramolecular Mitsunobu is more likely a result of the stringent geometry required for the S_N2 step. The linearity required of the nucleophile, the substituting carbon and the

leaving group may be too energetically demanding in the intramolecular case where the aliphatic chain is constrained at one end. The conformational freedom of the reagents in the intermolecular Mitsunobu reaction allow for relatively unimpeded reaction.

The AM1 calculations may also be used to rationalize the preponderance of N9 alkylated adenines over N3 and N7 substituted material. As seen in Table 2 of Appendix A, the atomic charge at N9 is generally higher than at N3 or N7 making it the more reactive site. Additionally, the relative heats of formation of N3-methyladenine, N7-methyladenine and N9-methyladenine calculated by AMPAC showed that the product of N3 alkylation is roughly 4 kcal mol^{-1} higher in energy than the energetically similar N7 and N9 materials. This thermodynamic advantage is not surprising since N3 alkylation alters the aromaticity within the 6 member ring of the purine. Finally, in contrast to N3 and N9, the amino group at N6 may obstruct reaction at the N7 site. In fact, the bulky leaving group in the Mitsunobu reaction most likely precludes alkylation at the sterically hindered N7 position.

The higher degree of N9 alkylation in the Mitsunobu reaction in comparison to that of the reaction involving the sodium salt of adenine may be explained on the basis of the "Hard and Soft Acids and Bases Principle".[45] In the reaction of adenine with sodium hydride (see Figure 16), the resultant sodium salt brings together a soft base (the adenine anion) and a hard acid (the sodium cation). In the Mitsunobu reaction, the adenine is paired with a rather soft phosphorous-based acid. With soft acids preferring to associate themselves with soft bases, the higher degree of N9 alkylation may result from the nature

---

[45] Ho, T.-L. *Tetrahedron*. 41, 1 (1985)

of the intermediate ion pair.

One must avoid reading too much into the numbers generated by the AMPAC program. AM1 calculations assume the molecules studied are in the gas phase while, in solution, solvents exert a great influence. Our exercise also suffers from the fact that only one partner in the intermediate could be modelled. Undoubtedly, the counter cation should not be ignored. But, in defense of AMPAC, the numbers are consistent with the interpretation presented and are offered as a useful guide.

2.3. Synthesis of [9]-(N6,9)-6-Aminopurinophane

The diffraction studies revealed that the adenine moiety of the [8]-(N6,9)-6-aminopurinophane was slightly non-planar as evidenced by the torsional angles C6-C5-C4-N9 (169.2°) and N7-C5-C4-N3 (176.3°).[35] This provided the impetus for the preparation of the nonamethylene cyclophane homolog. The strain imparted to the purine ring by a C8 methylene chain should be relieved by a C9 bridge. Furthermore, a longer chain would undoubtedly assume different conformations, allowing the aliphatic protons to reside in different regions of space, and thus provide different chemical shifts and more shielding values for adenine.

Exploratory experiments into the synthesis of [9]-(N6,9)-6-aminopurinophane were conducted by Hunter and resulted in small amounts of product.[37] This work has been modified and has produced purer samples as evidenced by NMR spectroscopy and chromatography. The strategy employed for the synthesis of [9](N6,9)-6-aminopurinophane is outlined in the Figure 21. Following the general methodology developed for the construction of [8](N6,9)-6-aminopurinophane, the approach illustrated

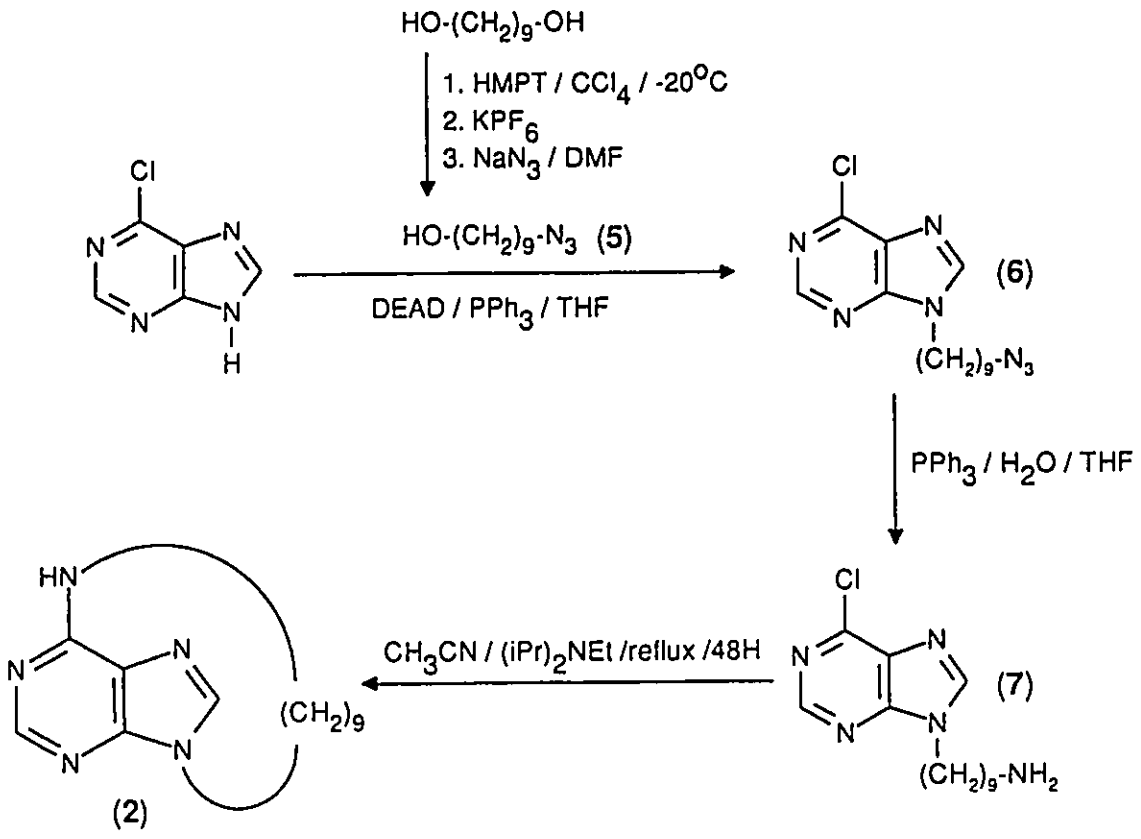

Figure 21: Synthesis of [9]-(N6,9)-6-Aminopurinophane

was more direct. While the alkylation of N9 via the Mitsunobu reaction and the final ring closure step remain, a different synthon for the aliphatic bridge was chosen.

Conversion of 1,9-nonanediol into the azido-alcohol (5) was realized using the method described by Castro *et al.*[46] As illustrated in Figure 22, reaction of hexamethylphosphorous triamide (HMPT) with carbon tetrachloride in THF at -20°C rapidly generated an trichloromethylphosphonium salt (a). The high nucleophilicity of the

---

[46] Boigegrain, R., Castro, B., and Selve, C. *Tetrahedron Lett.* No. 30, 2529-2530 (1975) and Castro, B. *Organic Reactions*. Vol.29, Chpt.1.; Castro, B., and Selve, C. *Bull. Soc. Chim. France*. 12, 3009-3014 (1974)

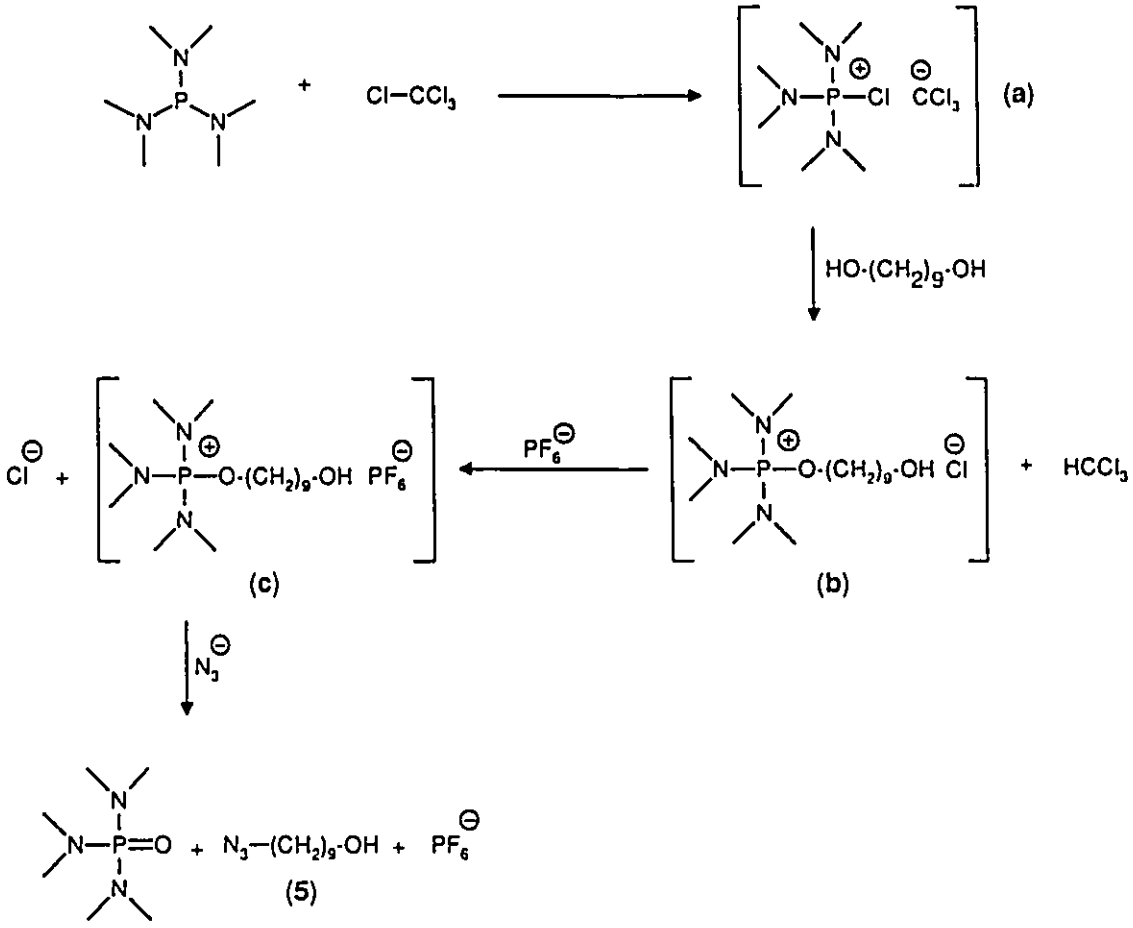

Figure 22: Mechanism of 9-Azidononanol Formation

aminophosphine allowed for abstraction of Cl^- and complete charge transfer to the trichloromethyl anion whose existence has been demonstrated by trapping experiments. In the next step, the mono-oxyphosphonium salt (**b**) produced upon the addition of the diol precipitates from solution, thereby making bifunctionalization impossible. Care must be taken so as not to allow the reaction to warm above 0°C at which temperature the alkoxyphosphonium chloride is known to break down to the alkyl chloride. Treatment with potassium hexafluorophospate (KPF_6) produced the stable and more organophilic PF_6 salt (**c**) which can then be displaced by the N_3^- nucleophile, affording only the ω-substituted

alcohol (5).

Once reduced, the azido group (effectively a protected amine) provided the nitrogen atom at the 6 position of the cyclophane. Note that the use of the azido-alcohol intermediate avoided the cumbersome protection, deprotection and functionalization steps involved in the octamethylene cyclophane synthesis.

The Mitsunobu reaction was once again planned as the procedure for coupling 9-azidononanol to 6-chloropurine (Figure 21). However, the reaction was approached with some caution as one of the reagents, triphenylphosphine, is known to be an efficient reductant of azides (*vide infra*). By carrying out the reaction with prior mixing of the triphenylphosphine, diethylazodicarboxylate (DEAD), and 6-chloropurine and then adding of 9-azidononanol, a modest yield of 23% of purified 6-chloro-9-(1-azidononyl)purine (6) could be obtained. Clearly the lower than normal yield (normal range 65-80%) was a result of unwanted triphenylphosphine reductive processes. No attempt was made to isolate these additional products.

Reduction of the azido group to the amine (7) was then readily accomplished with a further 1 mole-equivalent of triphenylphosphine and 1.5 equivalents of water in tetrahydrofuran (THF) (Figure 21). While Vaultier, Knouzi and Carrie[47] have demonstrated the synthetic utility of this reaction, its origin can be traced back to 1919 and the work of Staudinger.[48] Presumably, as illustrated in Figure 23, attack of the azide by triphenylphosphine results in a phosphotriazene intermediate (a) which quickly loses

---

[47] Knouzi, N., Vaultier, M. and Carrie, R. *Bulletin de la Société Chimique de France.* No. 5, 815-819 (1985); Vaultier, M., Knouzi, N. and Carrie, R. *Tetrahedron Lett.* 24, 763-764 (1983)

[48] Staudinger, H and Meyer, J. *Helv. Chim. Acta.* 2, 635 (1919)

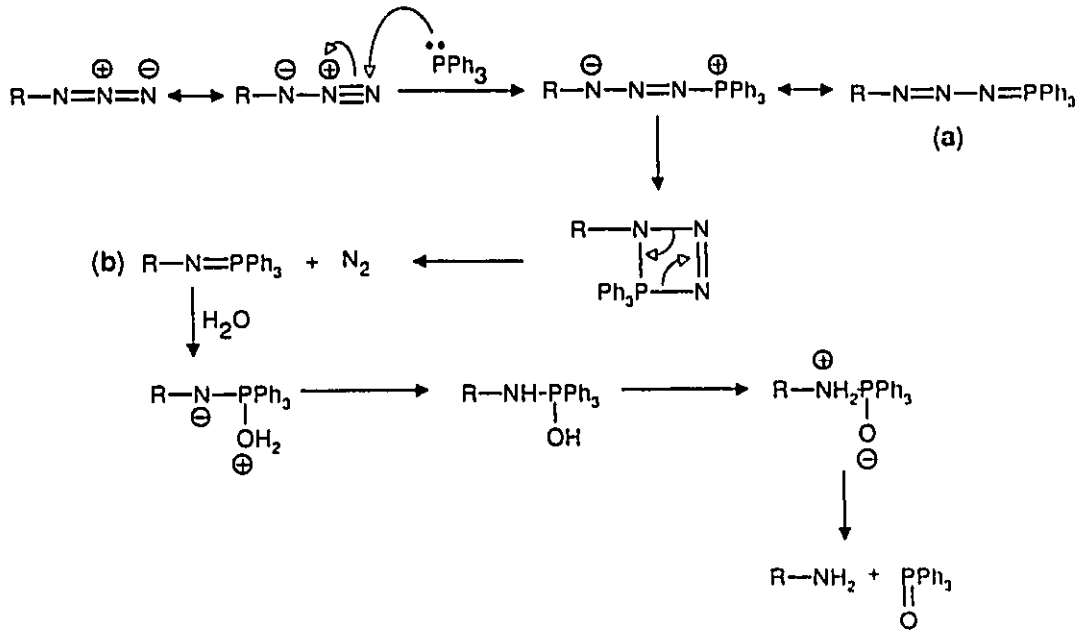

Figure 23: Mechanism of Azide Reduction

nitrogen to yield the isolable iminophosphorane (**b**). In the presence of water, this ylid hydrolyzes to give an amine and triphenylphosphine oxide. Curiously this reduction proceeds in high yields only if the concentration of the azide is of the order of one molar or greater. The reasons for this behaviour are not entirely clear, but reactions conducted at concentrations of 10-100 mmolar afforded distinctly poorer yields of amine product.

The final, and crucial, cyclization step in the synthesis was the intramolecular nucleophilic aromatic substitution (Figure 21). While the nonamethylene chain permitted ready access of the amine nitrogen to carbon-6 of the 6-chloropurine it was anticipated that the reaction rate would be slower than that recorded for the octamethylene chain because of the additional degrees of freedom present with the extra methylene group.

After refluxing for 48 hours in acetonitrile all of the chloro-amine (**7**) had reacted, as judged by thin layer chromatography (TLC) but chromatographic purification of the products yielded only 26% of the desired cyclophane (**2**). Much of the starting **7** appeared to have degraded, presumably by the presence over the long time period of adventitious water and/or oxygen.

High resolution mass spectroscopy (HRMS) together with proton and carbon-13 NMR spectroscopy further confirmed the homogeneity of the [9](N6,9)-6-aminopurinophane. Crystallization of a sample of **2** from chloroform-toluene (1:3) yielded large acicular crystals that were found to be suitable for X-ray crystallographic analysis (see Chapter 5).

2.4. Synthesis of [10]-(N6,9)-6-Aminopurinophane

The clearly superior synthetic scheme developed in the preparation of the nonamethylene cyclophane was employed in the formation of the decamethylene counterpart. While Castro's method for preparing azido-alcohols worked well, the price of HMPT coupled with the diminished yields upon the "scaling-up" of the reaction prompted the search for a new preparative course for 10-azido-1-decanol (see Figure 24, **9** with n=10). Kang, Kim and Moon describe a simple method for the

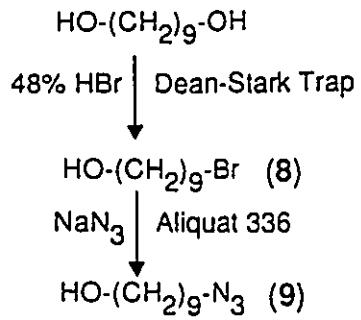

Figure 24: Alternate Route to Azido-alcohols

preparation of ω-bromoalcohols (8) from α,ω-diols.[49] Refluxing a mixture of an aliphatic diol with an equivalent of aqueous hydrogen bromide (48%) in benzene using a Dean-Stark apparatus provided high yields of the monobrominated alcohols. Under such conditions one might expect a statistical mixture of mono- and di-brominated material as well as unreacted starting diol; but the preponderance of the singly functionalized material leads one to believe that the reaction must proceed micellularly. Water was being continually azeotroped from the reaction leaving behind the HBr in the benzene. Once brominated, the bromo-alcohol molecules arrange themselves in a micellar fashion such that the bromo ends are exposed to the benzene while polar hydroxyl ends of the material aggregate themselves, pointing inwards and effectively preventing further reaction.

In the next step (Figure 24), the bromo-alcohol (8) was treated with aqueous sodium azide in the presence of Aliquat 336 (primarily tricaprylmethylammonium chloride) to yield the ω-azidoalcohol (9) as described by Reeves and Bahr.[50] Traditionally, chemists have been burdened with the exercise of finding a solvent in which all the reagents for a reaction are soluble. In this case, the bromo-alcohol is quite hydrophobic, only dissolving in non-polar solvents while the ionic nucleophile, sodium azide, can only be taken up by polar solvents. The inherent poor solubility of azide in organic solvents can be over come through the use of these phase transfer reactions.[51] The phase-transfer salt, in this case a quaternary ammonium salt, is somewhat soluble in both the

---

[49] Kang, S.-K., Kim, W.-S., and Moon, B.-H. *Synthesis.* 1161-1162 (Dec. 1985)

[50] Reeves, W. P. and Bahr, M. L. *Synthesis.* 823 (1976)

[51] Readers interested in the phase transfer catalysis should see *Top. Curr. Chem.* **102**, 147 (1982)

aqueous and organic phase. The Aliquat 336 forms an ion pair with the anion and the large alkyl groups in the ammonium ion permit migration into the organic phase. Once in the organic phase, the ion pair reacts with the water insoluble reagent. Stripped of its solvating water molecules, the azide ion is actually more reactive in the organic phase. Ultimately, the implementation of these two procedures allowed efficient access to large quantities of pure, low-cost azidoalcohols.

The remaining steps in the decamethylene adenine cyclophane were the same as those of the nonamethylene homolog. Alkylation at N9 takes place via a Mitsunobu reaction involving 6-chloropurine and 10-azido-1-decanol. Following the reduction of the azide (**10**) to the amine (**11**), nucleophilic attack at C6 resulted in the formation of the cyclophane. As expected, the ^{1}H-NMR spectrum of [10]-(N6,9)-6-aminopurinophane (**3**) was comparable to those of the other purine cyclophanes, although complicated to a greater extent by the presence of the additional methylene proton resonances and exchange processes.

2.5. Synthetic Approaches to [7]-(N6,9)-6-Aminopurinophane

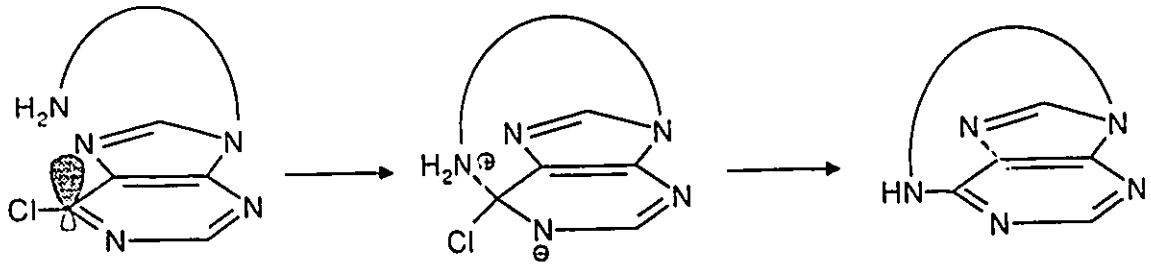

Figure 25: Transition State of Nucleophilic Aromatic Substitution Step

Attempts to prepare the heptamethylenepurine cyclophane were also undertaken using the route successfully implemented in the synthesis of the C9 homolog. While the first steps were successful, the final ring closure did not proceed despite a variety of solvents and reaction times. The outcome was disappointing, although not surprising. The mechanism for this reaction is illustrated in Figure 25. Attack by the primary amine at the p-orbital on C6 (perpendicular to the plane of the purine), results in a tetrahedral, charge separated intermediate. Subsequent loss of Cl^- and regeneration of sp^2 hybridization at C6 results in cyclization of the cyclophane. The heptamethylene chain may, simply, not be long enough. The significant bending of the adenine system required to make the ends meet is, most likely, too energetically demanding.

In an effort to alleviate the problems that plagued this final step, cyclization attempts were made in the presence of a silver salt. Ideally, the silver should have enhanced the leaving ability of the chloride (probably stripping it from the 6-chloropurine) and provided the driving force for ring closure.[52] An equivalent of silver tetrafluoroborate (one of the few silver salts soluble in organic solvents) was added to a solution of 6-chloro-9-(7-aminoheptyl) purine in acetonitrile. The solution darkened immediately and the reaction allowed to stand for an additional 24 hours before work-up. Failure to isolate any cyclophane material from the reaction mixture may have be due to the fact that no cyclophane was produced or because of an inherent instability of the cyclophane making its isolation difficult. Studies by Higuchi *et al.*[28] showed that various 6,9-thiopurinophanes possessed enhanced reactivity towards nucleophiles at the C6 position which they

---

[52] Long, J. R. *Aldrich Chimica Acta.* **14**, 63 (1981)

explained on the basis of a stereoelectronic effect. Although no testing was done on our (6,9)-aminopurinophanes to establish their reactivity toward nucleophilic aromatic substitution, the Higuchi *et al.* precedence makes one wonder about the stability of heptamethylene cyclophane. Severe bending of the N6-C6 bond out of the plane of the purine would be predicted for the heptamethylene cyclophane. This twisting would not only further expose C6 to attack from nucleophiles but gives the cyclophane a geometry well on its way to the tetrahedral intermediate transition state like the one shown in Figure 25.

Access to a [7]-(N6,9)-6-aminopurinophane may be possible via a synthetic approach employing a ring contraction. In his synthesis of [7]-paracyclophane, Allinger used an α-diazoketone ring contraction of an appropriately functionalized [8]-paracyclophane.[53] In order for this series of reactions to find use in the [7]-(N6,9)-6-aminopurinophane synthesis, an octamethylene analogue with the requisite carbonyl in the bridge must be prepared. Although such a synthesis was conceivably not difficult, consideration of the potential length discouraged an attempt.

2.6. Synthesis of N6-aminononyl-purine, 9-nonyladenine and N6-aminononyl-9-nonyl-purine

A number of standard compounds to be used in the UV and NMR spectroscopy studies were also prepared and provided samples of alkylated adenines to compare with their cyclized counterparts. Dissolving 6-chloropurine in a solution of excess *n*-nonyl

---

[53] Allinger, N.L., Walter, T.J. and Newton, M.G. *J. Amer. Chem. Soc.* 96, 4588-4597 (1974)

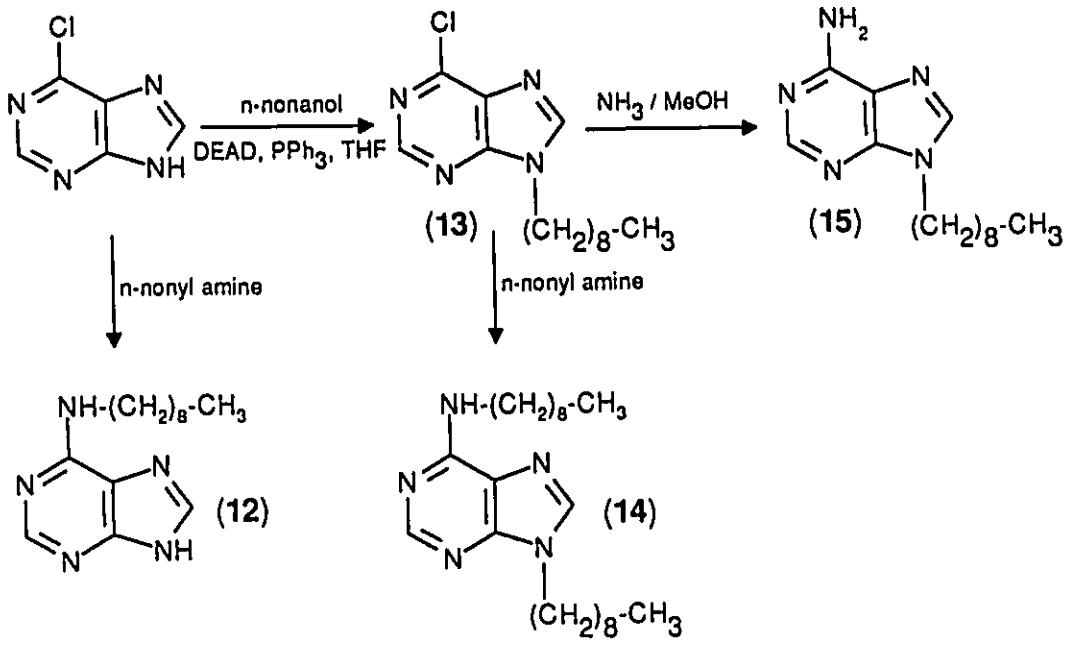

Figure 26: Alkylated Adenines

amine in acetonitrile readily provided N6-aminononyl-purine (**12**) in good yield. The indispensable Mitsunobu reaction lead to the synthesis of 6-chloro-9-nonyl purine (**13**) which could then either be treated with *n*-nonyl amine to yield the N6,N9-dialkylated purine (**14**) or dissolved in methanolic ammonia to prepare 9-nonyladenine (**15**).

Chapter 3

Approaches to Pyrimidinophanes: "Intact Bridge Attachment"

3.1. The "Intact Bridge Attachment" Approach

Attempts to construct a pyrimidinophane did not meet with the success encountered in the purinophane preparation. As a result, the present and subsequent chapters will deal with the approaches taken towards the synthesis of a cytosine cyclophane and a commentary on the limitations of these pathways. Discussions dealing with potential modifications as well as other alternative schemes will also be presented.

There are a number of options open to a synthetic chemist interested in preparing a pyrimidinophane. As with the purinophane, the selection of a representative pyrimidine, the choice of suitable sites for bonding and aspects involving chain length are all of concern. Furthermore, as seen in the Synthetic Considerations and Strategies section of the Introduction (Figure 13), the manner in which the aliphatic bridge is to be constructed and attached to the aromatic system (ie. intact bridge attachment, bridge formation by coupling or bimolecular bridge formation) will ultimately determine the synthetic route developed. Finally, appropriate synthetic methodologies must exist or must be developed in order to bring together all these aspects.

From the outset, it was decided that a methylene chain should be attached in the *para* positions of the aromatic system since this would provide the maximum information about the magnetic environment (see Figure 27). A survey of the pertinent literature

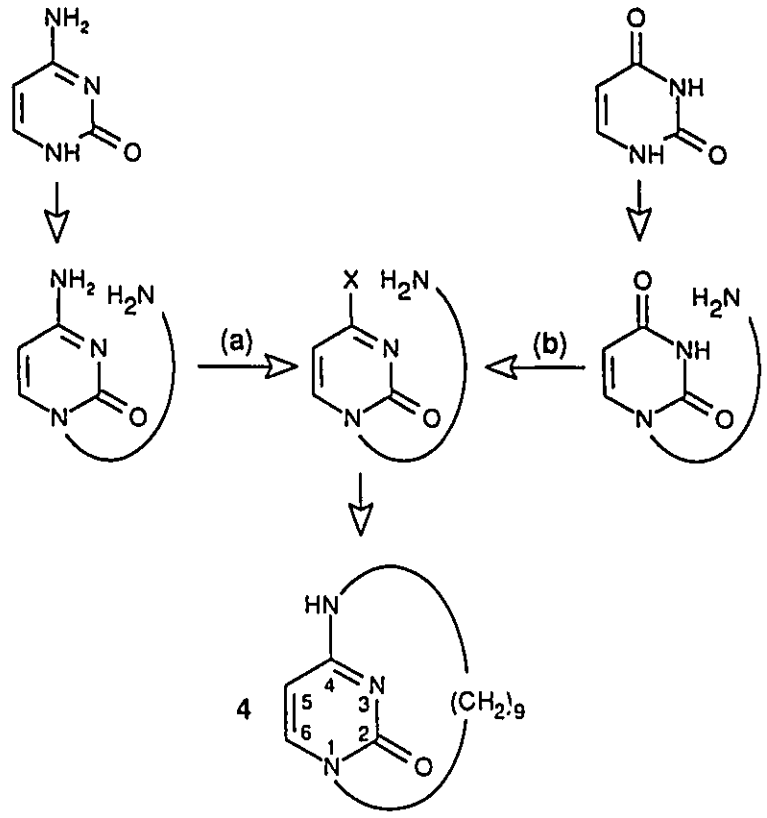

Figure 27: Pyrimidinophane Bridge Attachment

showed a variety of methods had been developed for the alkylation of N1 and for the amination of C4 of the pyrimidine system. The amination at C4 could be accomplished in one of two ways. Transformation of the amino group at the 4 position of cytosine into a good leaving group could then be followed by treatment with an aliphatic amine to give C4 substitution. Alternatively, a uracil type of precursor can be modified at the 4-position to permit amination at this location. In either case, a nitrogen will be bonded at the 4-position so that cytosine will be the heterobase at the heart of the cyclophane.

Once again, computer modelling was used to ascertain the optimum chain length. Structures of cytosine with a C9 methylene bridge connected at N1 and N4 were minimized using PC-Model[34] and a conformation with an energy of -78.97 kJ/mol was

found. The aromatic plane was shown to be flat and relatively free from "pucker". The conformers generated, however, converged on a wide variety of local energy minima with only a few values seen repeatedly. With the additional flexibility in the bridge comes a greater number of chain conformations and, consequently, a greater number of possible local energy minima. This seems to imply that the methylene chain is somewhat longer than necessary and able to adopt a number of different geometries. These additional orientations might complicate NMR assignment and conformational analysis.

Despite these potential complications, the preliminary synthetic work involved the use of a nonamethylene chain. There were two reasons for this choice. Firstly, previous work attempting to account for the diamagnetic shielding anisotropy displayed by the methylene protons of [10]-paracyclophane had met with great success.[29] The [10]-paracyclophane structurally parallels the target [9](1,N4)-4-amino-2-one-pyrimidinophane (4) in that both are 6-membered aromatic rings with a 10-atom long bridge connected at the *para* positions. Secondly, it was expected that the use of a slightly longer chain would alleviate the potential difficulties associated with the final intramolecular ring closure. A nonamethylene chain would allow some leeway and certainly not impose any strain on the aromatic ring. Once a suitable synthetic methodology had been optimized, substrates with shorter chains could then be prepared.

Initially, strategies were developed that involved the connection of an aliphatic bridge at one end of a cytosine moiety followed by bonding at the other end. These "intact bridge attachment" approaches (see Introduction) were considered to be the simplest and most straightforward in practical terms.

3.2. Cytosine Cyclophane via Tosamides

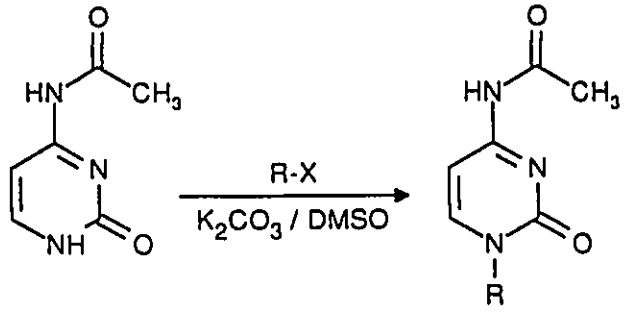

Figure 28: Alkylation at N1 of Cytosine

Browne and co-workers developed a relatively modest method for the alkylation of cytosine at N1 (Figure 28).[54] N4-acetylcytosine was added to a suspension of potassium carbonate in dimethylsulphoxide and the resultant anion could then be treated with an alkyl halide to yield the substituted cytosine. It was necessary to use N4-acetylcytosine for this reaction because of the insolubility of cytosine in most solvents and to preclude any reaction at N4. The yields were typically 25-30%.

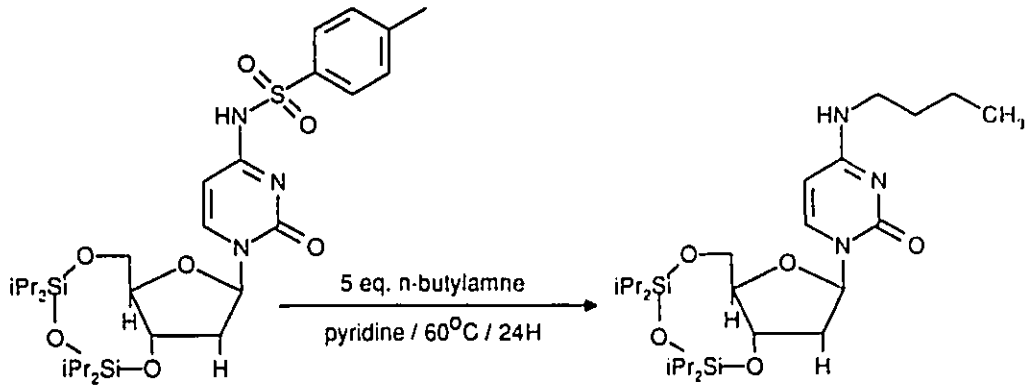

Figure 29: Amination at C4 of Cytosine via a Tosamide Intermediate

Inspiration for the final ring closure step came from work done by Markiewicz.

---

54 Browne, D.T., Eisinger, J. and Leonard, N.J. *J. Amer. Chem. Soc.* 90, 7302-7323 (1968)

Kierzek and Hernes.[55] N4-Toluenesulphonyl cytosine nucleosides were prepared and converted to the N4-alkyl derivatives by treatment with a primary amine in pyridine. As seen in Figure 29, for example, reaction of the cytosine tosamide nucleoside with 5 equivalents of *n*-butyl amine in pyridine at 60°C for 24 hours gave 100% of the N4-alkylated material.

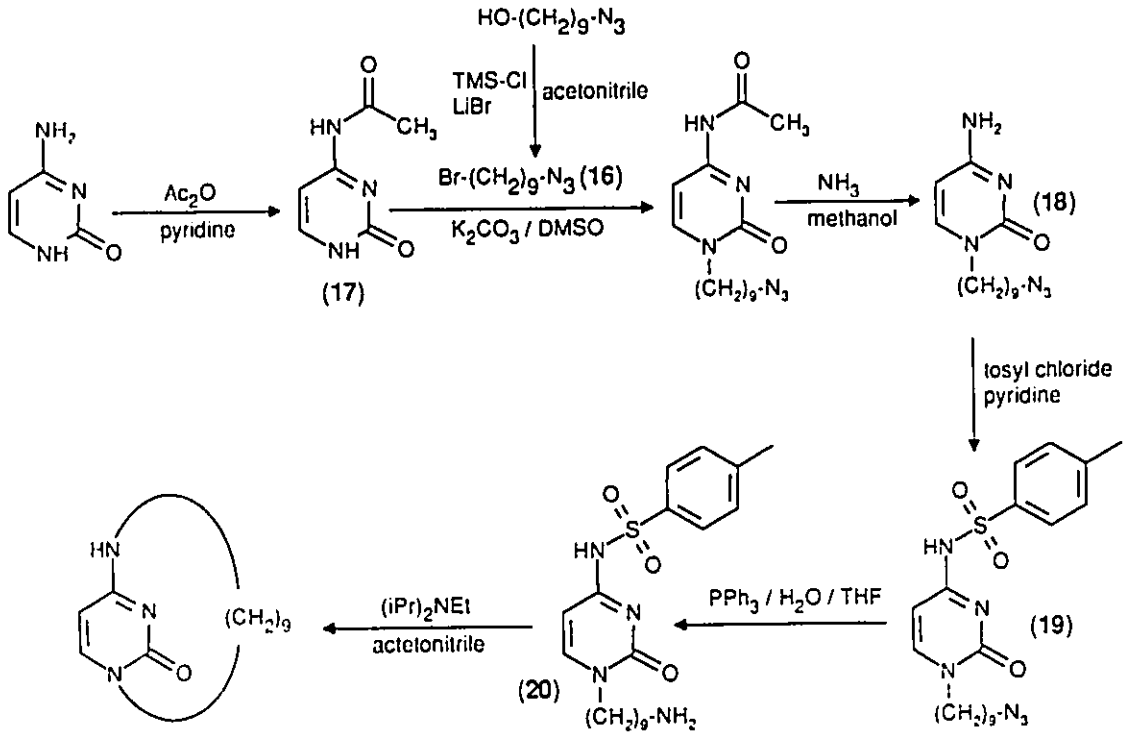

Figure 30: Pyrimidinophane via Tosamide Intermediate

A synthetic pathway for the preparation of [9](1,N4)-4-amino-2-one-pyrimidinophane was developed based on these reactions and is shown in Figure 30. Note that many of the successful elements of the nonamethylenepurine cyclophane synthesis are used here.

---

55 Markiewicz, W.T., Kierzek, R. and Hernes, B. *Nucleosides and Nucleotides*. 6, 269-272 (1987)

9-Azidononanol (**5**), derived again from 1,9-nonanediol, was converted to the bromo-azide (**16**). The procedure used for this transformation was that of Olah and co-workers and proceeds via silylation of the hydroxyl using chlorotrimethylsilane followed by nucleophilic displacement of hexamethyldisiloxane by Br^- to give the corresponding alkyl-bromide (see Figure 31).[56] ^{1}H-NMR readily confirmed the transformation by showing the signal of the methylene next to the bromide at 3.37 ppm compared to 3.51 ppm in the alcohol precursor. Loss of the broad hydroxyl stretch in the IR further characterized the bromo-azide. Olah's conditions were chosen from the plethora of methods for bromine atom introduction because of their tolerance towards the azide functionality. The method described by Browne *et al.*[54] was then used for alkylation at N1 (see Figure 30). Deprotonation at N1 of **17** was followed by nucleophilic displacement of the bromide of 1,9-azidobromononane (**16**). The methylene group adjacent to N1 showed a proton chemical shift of 3.58 ppm confirming that reaction had taken place. The acetyl group at N4 was removed via ammoniolysis and resulted in the desired 1-(9-azidononyl)cytosine (**18**). Low yields were due mostly to concentration factors (large amounts of DMSO were needed to dissolve the acetylcytosine) and the loss of material to side reactions (some O-alkylated cytosine).

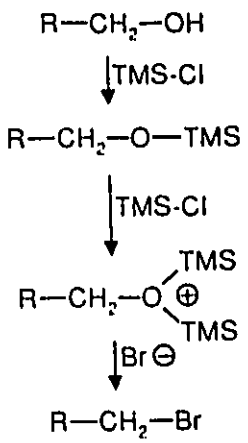

Figure 31: Mechanism of Bromination Reaction

Treatment of the substituted heterobase (**18**) with tosyl chloride in pyridine yielded the tosamide of 1-(9-azidononyl) cytosine (**19**) which was then reduced to the amine (**20**)

---

56 Olah, G.A., Balaram Gupta, B.G., Malhorta, R., Narang, S.C. *J. Org. Chem.* **45**, 1638-1639 (1980)

using the triphenylphosphine/water methodology developed earlier (see Chapter 2). Unfortunately, heating a 0.005 M solution of the 1-(9-aminononyl)-4-tosyl cytosine in pyridine at 60°C for five days did not produce any cyclophane. Careful work-up, chromatography and analysis of the reaction mixture yielded mostly starting material along with apparent degradation products of the cytosine ring system.

Failure to cyclize may be due to a number of reasons. Perhaps, the entropy demands on the reaction may be too great. This seems unlikely though, for molecular models indicate that the C9 chain is long and mobile enough to allow for the amine to react at C1. Although the original work by Markiewicz used 5 equivalents of amine for each equivalent of tosamide, it was felt that this might be compensated for by the fact that the cytosine cyclophane cyclization was an intramolelcular process. Most likely, the failure of the reaction may be due to the fact that the p-toluenesulfonamide is not sufficiently labile and so a search began for a better leaving group.

3.3. Alkylation at N1 of Uracil

Uracil type precursors can be modified at the 4-position to permit amination at C4 (see Figure 27). Looking forward to the cytosine cyclophane, the obvious synthetic precursor to these C4-activated pyrimidines is 1-(9-azidononyl)-uracil. One can envision the azide end of the aliphatic chain being reduced to an amine and then used to displace a leaving group at C4, permitting cyclization to a pyrimidinophane. The synthesis of such a substituted uracil could proceed in much the same way as the 1-(9-azidononyl)-cytosine preparation. Application of Brown's method[54] would involve deprotonation at N1 of uracil with potassium carbonate, followed by nucleophilic displacement of the bromide of 1-

azido-9-bromononane resulting in the desired 1-(9-azidononyl)-uracil.

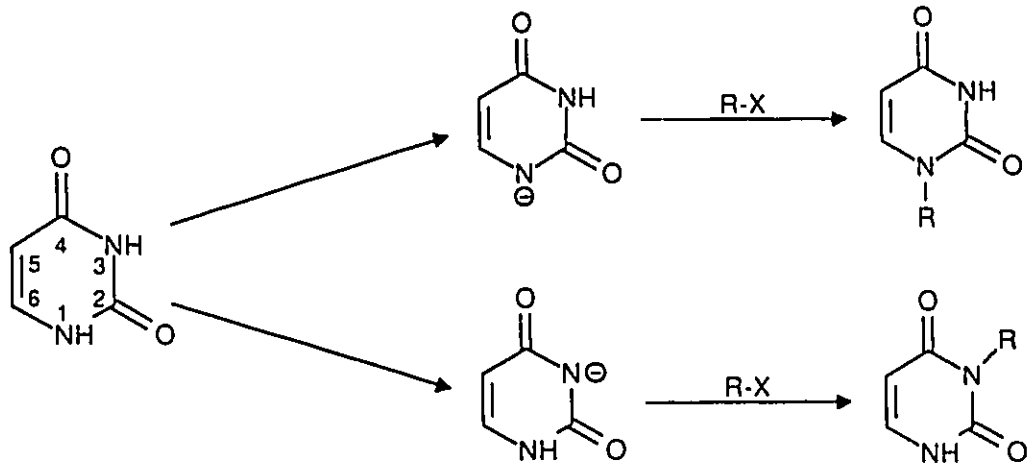

Figure 32: Regioselectivity Problems

Possible regioselectivity problems were anticipated since deprotonation might occur at N3 rather than the desired N1 position (see Figure 32). Information concerning the pK_a of uracils has appeared in the literature[57], but is somewhat ambiguous since only the various pK_a values are given and not the sites to which they correspond. With N3 sandwiched between two carbonyl units, one might intuitively expect the resonance stabilization provided by an adjacent carbonyl to give the N3 anion a distinct advantage over the anion at N1. But the AMPAC calculations showed the N1 anion to be roughly 16 kcal mol^{-1} more stable than the corresponding N3 anion.[44] Granted, AM1 calculates gas phase heats of formation and not those found in solution; nevertheless, it is interesting that it should predict correctly that N1 is the location of deprotonation. One can rationalize

---

57 Handbook of Biochemistry and Molecular Biology, Third Edition. G.E. Fasman, ed. (Cleveland: Chemical Rubber Company Press, Inc., 1976)

that the N1 anion is favoured over the one at N3 by drawing out the various resonance structures and noting that the N1 species has an additional contributor (see Figure 33). Treatment of the uracil with potassium carbonate will result in exclusive formation of the N1 anion and, consequently, substitution at this position. Furthermore, the steric hindrance provided by the two carbonyls surrounding N3 should effectively minimize any reaction at this location.

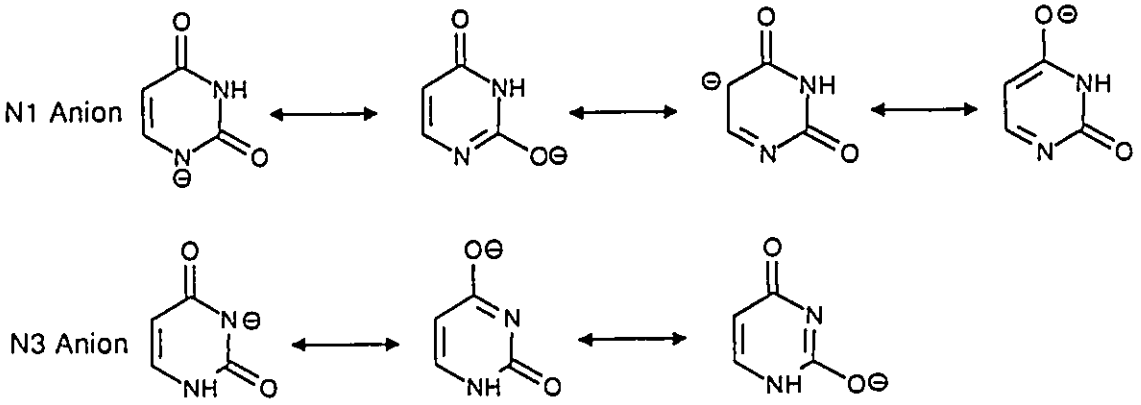

Figure 33: Resonance Structures for Possible Uracil Anions

Although the yields were modest (30-34%), the chromatography of the reaction mixtures allowed for isolation of the N1 alkylated material (see Figure 34). The regiochemistry was confirmed by taking advantage of the nuclear Overhauser effect (NOE) in the ^{1}H-NMR.[2] Routinely used in structure determination, an NOE experiment involves the irradiation of a particular spin system followed by observation of an enhancement in the signal of another spatially proximate system. A nuclear Overhauser effect can only be observed if the nuclei under consideration are in close proximity, since only then does the dipole-dipole interaction represent a significant relaxation mechanism. The magnitude of the effect is inversely related to the distance between the nuclei, r, falling off as $1/r^6$.

In our system, irradiation of the H6 proton on the uracil resulted in an

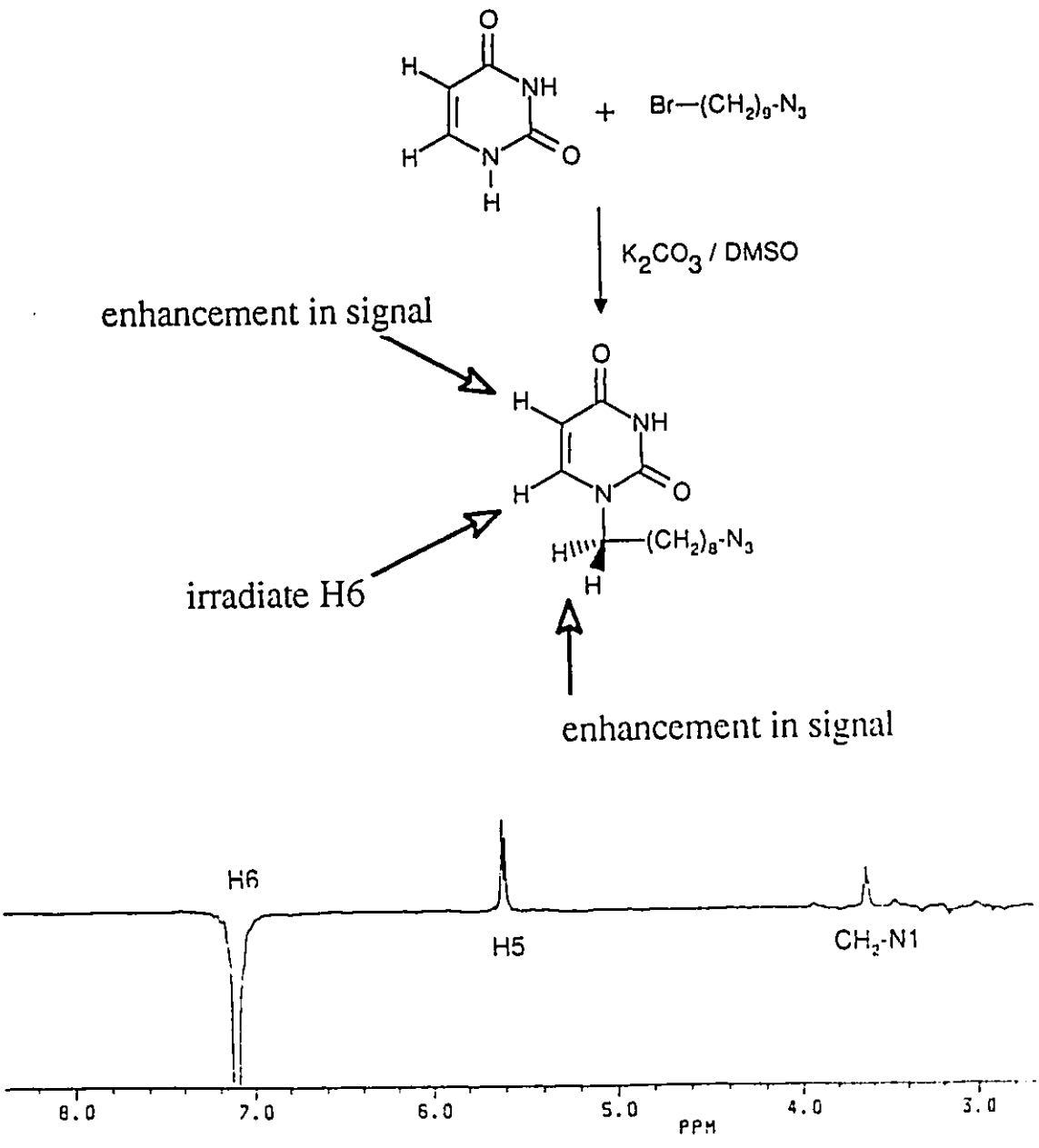

Figure 34: N1 Alkylation of Uracil and NOE Spectrum

enhancement in the signal of the methylene protons bonded at N1 (see Figure 34). Note that, if the alkylation had taken place at N3, the distance between the studied nuclei

would preclude the observation of such an enhancement.

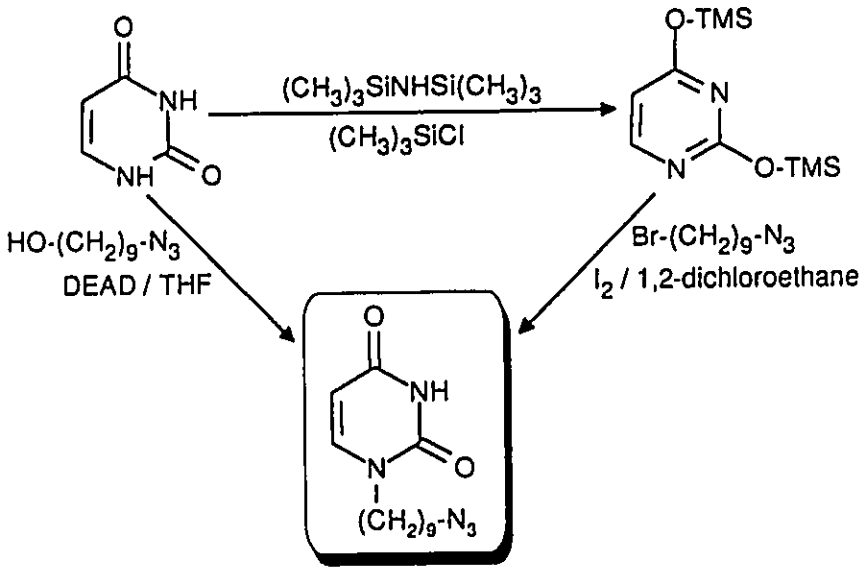

Figure 35: Alternate Methods for Alkylation of Uracil at N1

Due to the rather low yields of Brown's method to generate 1-(9-azidononyl)-uracil, other preparations were sought out (Figure 35). Uracil and 9-azido-1-nonanol were reacted under Mitsunobu conditions but afforded very small amounts of the desired product (less than 7%)[40,41]. The reasons for the rather abysmal yield are not clearly understood and the reaction was not optimized.

Singh, Aggarwal and Kumar found that heating 2,4-bis(trimethylsiloxy)pyrimidine with functionalized alkyl halides in 1,2-dichloroethane in the presence of iodine affords exclusively the N1-substituted uracils.[58] Many of the examples given were quite high-yielding. The 2,4-bis(trimethylsiloxy)pyrimidine was generated by the action of

---

[58] Singh, H., Aggarwal, P., and Kumar, S. *Synthesis.*, 520-522 (June 1990)

hexamethyldisilazane on uracil in the presence of chlorotrimethylsilane under reflux.[59] Alkylation at N1 occurred via silyl enol-ether type chemistry with the N3 sterically inhibited from reaction. Catalytic amounts of iodine were added to provide a source of iodide. By displacing the bromide on the alkyl chain, the iodide served as a better leaving group and helped to expedite the substitution reaction. Treatment of the 2,4-bis(trimethylsiloxy)pyrimidine with 1-azido-9-bromononane under the conditions described produced 29% of the desired alkylated uracil (Figure 35) a yield comparable to that attained using Brown's methodology but markedly lower than examples offered by Singh, Aggarwal and Kumar.

3.4. Cytosine Cyclophane via Chloropyrimidines

With the procedures for the alkylation of uracil at N1 developed, attention was then focused on the activation of the 4-position of 1-(9-azidononyl)-uracil with a labile leaving group. Chloropyrimidines are known to be highly reactive and allow for amination at C4.[60] Generated by the action of Vilsmeier's reagent (chloromethylenedimethylammonium chloride)[61] on uracils blocked at the 1 position, these 4-chloropyrimidines can then be treated with aliphatic amines to give substituted cytosines. Preliminary work was carried out on the model compound 1-octyl-uracil.

Literature examples have shown that the chlorination reaction may be performed

---

[59] Aoyama, H. *Bull. Chem. Soc. Jap.* **60**, 2076 (1987)

[60] Hrebabecky, H. and Beranek, J. *Coll. Czech. Chem. Comm.* **49**, 2689-2697 (1984) and Zemlicka, J. and Sorm, F. *Coll. Czech. Chem. Comm.* **30**, 2052-2066 (1965)

[61] Hepburn, D. R. and Hudson, H. R. *J. Chem. Soc., Perkins I.* 754-757 (1976)

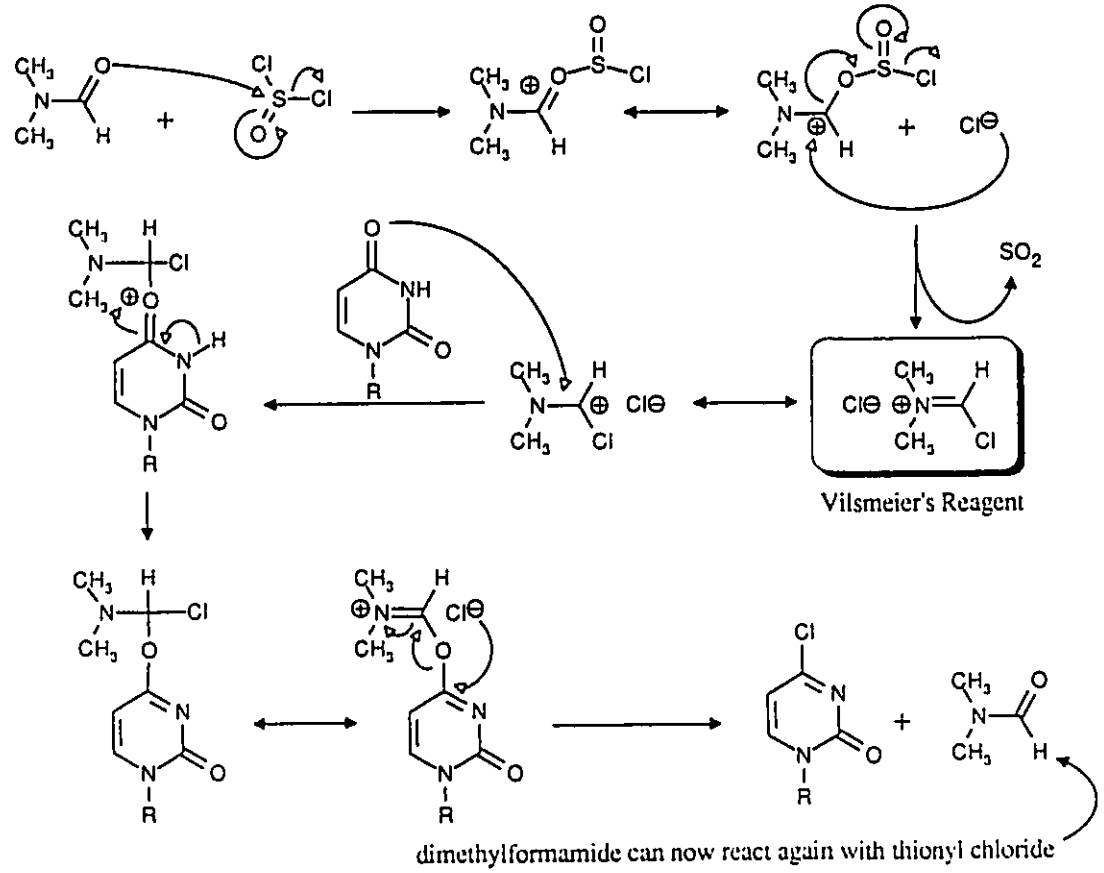

Figure 36: Catalytic Chlorination of Uracil using Vilsmeier's Reagent

via catalytic generation of Vilsmeier's reagent *in situ* or via the addition of one equivalent of pre-prepared Vilsmeier's reagent. With the *in situ* process (shown in Figure 36), thionyl chloride and a catalytic amount of dimethylformamide react to generate the active chlorinating species, chloromethylenedimethylammonium chloride. Addition of the 1-substituted-uracil results in the desired 4-chloropyrimidine and a molecule of

dimethylformamide which can react once again with the thionyl chloride. If the chlorination is performed in deuterated chloroform, the progress of the reaction can be followed in the ^{1}H-NMR by monitoring the change in chemical shift of the H5 and H6 protons. Complete conversion could usually be affected in about 3 hours.

Alternatively, the Vilsmeier reagent could be prepared beforehand by simply dissolving phosphorous pentachloride in dimethylformamide, refluxing for a short time, then cooling the reaction to allow for precipitation of the desired salt. This extremely hygroscopic crystalline material can then be collected under nitrogen and refrigerated for months without any loss of effectiveness. By adding one equivalent of the chlorinating agent, it was possible to avoid any side reactions that could be incurred with the catalytic procedure (ie. over longer periods of time, chlorination at C2 can take place).

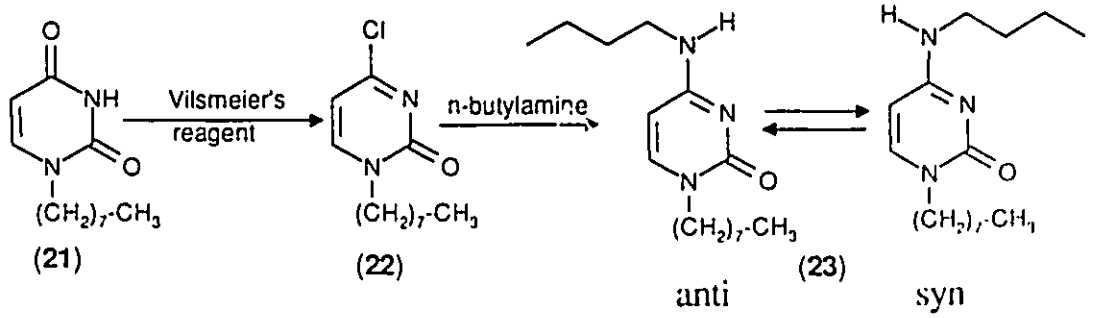

Figure 37: Chlorination and Amination of 1-Octyl-uracil

Conversion of 1-octyl-uracil (**21**) to its corresponding chloro derivative (**22**) using one equivalent of Vilsmeier's reagent was completed in about 3 hours with slightly diminished yields (see Figure 37). Treated with *n*-butyl amine, the 1-octyl-4-chloro-pyrimidin-2-one was cleanly converted to 1-octyl-4-N-butyl-pyrimidin-2-one (**23**) as evidenced by the molecular ion at 279 amu at in the mass spectrum. The proton NMR

spectrum showed a shift of the methylene protons adjacent to the amino nitrogen from a sharp triplet at 2.70 ppm in butylamine to a broadened peak at 3.35 ppm for the product. Restriction rotation about the N4-C4 bond results in two conformations, the *anti* and *syn* conformations (see Figure 37), that are slowly exchanging at room temperature and result in the overall broadening in the NMR.[62] Despite the adverse impact on the appearance of the spectrum, the effect was taken as further verification of successful substitution.

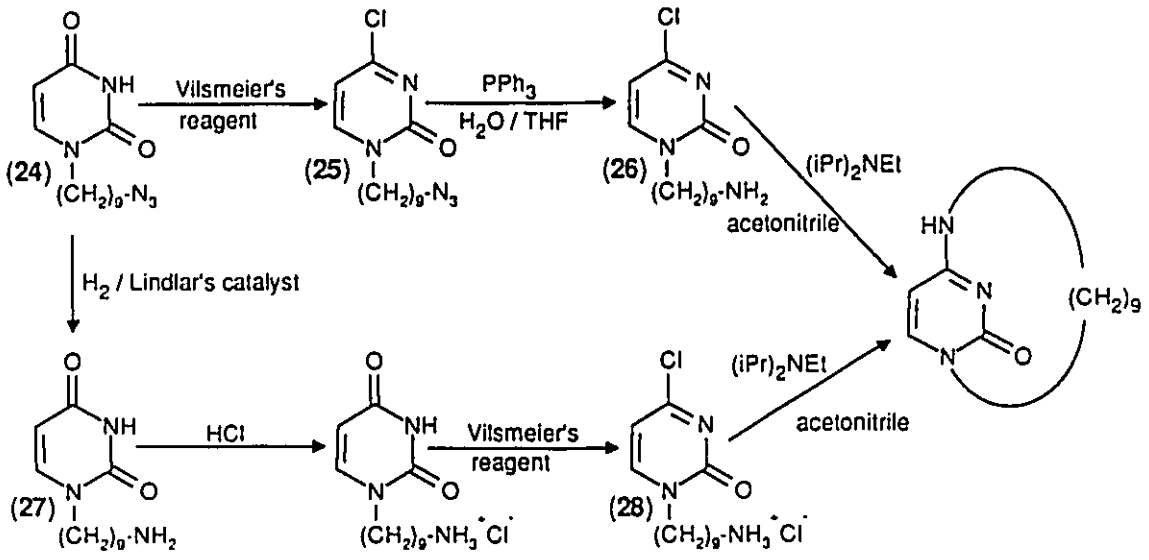

Figure 38: Pyrimidinophanes via Chloropyrimidines

Having proven the effectiveness of the Vilsmeier reaction for the activation of the model compounds, attention was then turned to its application in the synthesis of the cytosine cyclophane. The preparation may proceed along two slightly different routes differing in the order in which activation and reduction are carried out before the final

---

62 Reitz, A.B., Graden, D.W., Jordan, A.D., and Maryanoff, B.E., *J. Org. Chem.* 55, 5761-5766 (1990)

cyclization. One could chlorinate the uracil, reduce the azide to the amine, then proceed to cyclize. Alternatively, the reduction could be performed first, followed by the activation of the uracil moiety before the cyclization (see Figure 38).

Initial work concentrated on the first option. 1-(9-Azidononyl)-uracil (**24**) was treated with Vilsmeier's reagent to give 1-(9-azidononyl)-4-chloro-pyrimidin-2-one (**25**). Unfortunately, it was determined that the chloro-substituent (**26**) did not withstand the Vaultier *et al.* reduction protocol.[47] The water necessary for the hydrolysis of the iminophosphorane intermediate hydrolyzed the chloropyrimidine to a mixture of compounds, mostly 1-(9-aminononyl)-uracil. Other reduction methods (catalytic hydrogenation and lithium aluminium hydride) were also found to be incompatible with the chloro-pyrimidine due to the extreme lability of the leaving group.

The synthetic pathway involving reduction of the azide prior to the activation was then undertaken. While the Vaultier reduction protocol had been considered for the reduction, the triphenylphosphine needed for the reaction was suspected to be responsible, in part, for the degradation of the pyrimidine ring. The inability to account for all the mass in the reductions and the appearance of by-products on TLC after using the triphenylphosphine/water reduction prompted the use of catalytic hydrogenation. Hydrogenation in the presence of Lindlar's catalyst (palladium on calcium carbonate, poisoned with lead) resulted in the clean production of 1-(9-aminononyl)-uracil (**27**).[63]

Since the amine nitrogen is more nucleophilic than the C4 carbonyl oxygen of uracil, one could anticipate reaction of the amino end of the substituted uracil with the

---

[63] Corey, E.J., Nicolaou, K.C., Balanson, R.D., and Machida, Y. *Synthesis*. 590-591 (Sept. 1975)

Vilsmeier reagent to give formamidine-type byproducts. In order to avoid this, the 1-(9-aminononyl)-uracil would be converted to its hydrochloride salt by treatment with dry HCl gas. Additional *in situ* protection of the amine as the protonated, non-nucleophilic cation would be provided in solution by the acidic nature of the Vilsmeier reagent. Since the subsequent cyclization reaction would be carried out in acetonitrile, it would have been ideal if the chlorination reaction could have been performed in the same solvent. Unfortunately, the hydrochloride salt of the amine was completely insoluble in acetonitrile and the chlorination was carried out in dimethylformamide instead.

The Vilsmeier chlorination protocol was applied and the reaction mixture containing the 1-(9-aminononyl)-4-chloro-pyrimidin-2-one hydrochloride salt (**28**) was added to a solution of diisopropylethylamine in acetonitrile to allow for cyclization (see Figure 38). The crude reaction mixture as well as the fractions isolated by flash chromatography were analyzed by ^{1}H-NMR, mass spectrometry and thin layer chromatography and failed to show any evidence for cyclophane formation. The numerous components isolated were difficult to fully characterize since many of the collected fractions were quite small and not completely pure. Detailed structure assignment of the various components would require implementation of high performance liquid chromatography (HPLC) techniques and were not carried out. Some degradation of the pyrimidine did take place as evidenced by the lack of the H5-H6 uracil A-B splitting pattern in the ^{1}H-NMR of some of the fractions. Roughly 25% of the crude reaction mixture was found to be the hydrolyzed precursor, 1-(9-aminononyl)-uracil.

The Vilsmeier reaction was repeated in deuterated DMF using 1-octyl-uracil and the progress of the reaction followed by ^{1}H-NMR. After adding one equivalent of the

chlorinating reagent to the alkyl-uracil, the NMR tube was heated to 60°C and the progress of the reaction checked periodically by NMR. As mentioned above, the H6 and H5 resonances on the uracil normally at 7.11 and 5.61 ppm respectively, showed a dramatic shift upon chlorination moving to 7.59 and 6.30 ppm. After roughly three hours, resonances of the chloro-pyrimidine had reached maximum intensity; but, surprisingly, the chlorinated species began to disappear over time and revert back to its uracil precursor. It would seem that traces of water or oxygen were making their way into the NMR tube and hydrolyzing the activated pyrimidine. After an additional 18 hours at 60°C, the ^{1}H-NMR spectrum indicated that some degradation had occurred as evidence by the appearance of numerous, small additional signals. In light of this experiment, it would seem that failure of the cyclization reaction was due to the fact that the competitive processes of reversion to the starting material or decomposition were proceeding at a rate faster than the cyclization reaction. Most likely, small amounts of water hydrolyzed the 4-chloro compound pre-empting the cyclization reaction. Although preliminary drying of the solvents was performed, the quantity of acetonitrile used in this "high dilution" reaction may have contained sufficient water to result in the failure of the reaction. The small amount of water needed for hydrolysis may have also been introduced through syringes, needles, glassware or via the stream of nitrogen used to blanket the reaction. Despite repeated attempts at the experiment, no cyclophane was recovered.

Although the chloropyrimidines were too reactive to survive the cyclization conditions, their high reactivity towards nucleophiles opened up other avenues of approach. Perhaps substitution of the chloro with another group better able to withstand the reduction and cyclization protocols could be found. Indeed, the sulphoxide and

sulphone groups, to be described below, seemed to be ideal candidates.

3.5. Cytosine Cyclophanes Via Pyrimidinyl Sulphones and Sulphoxides

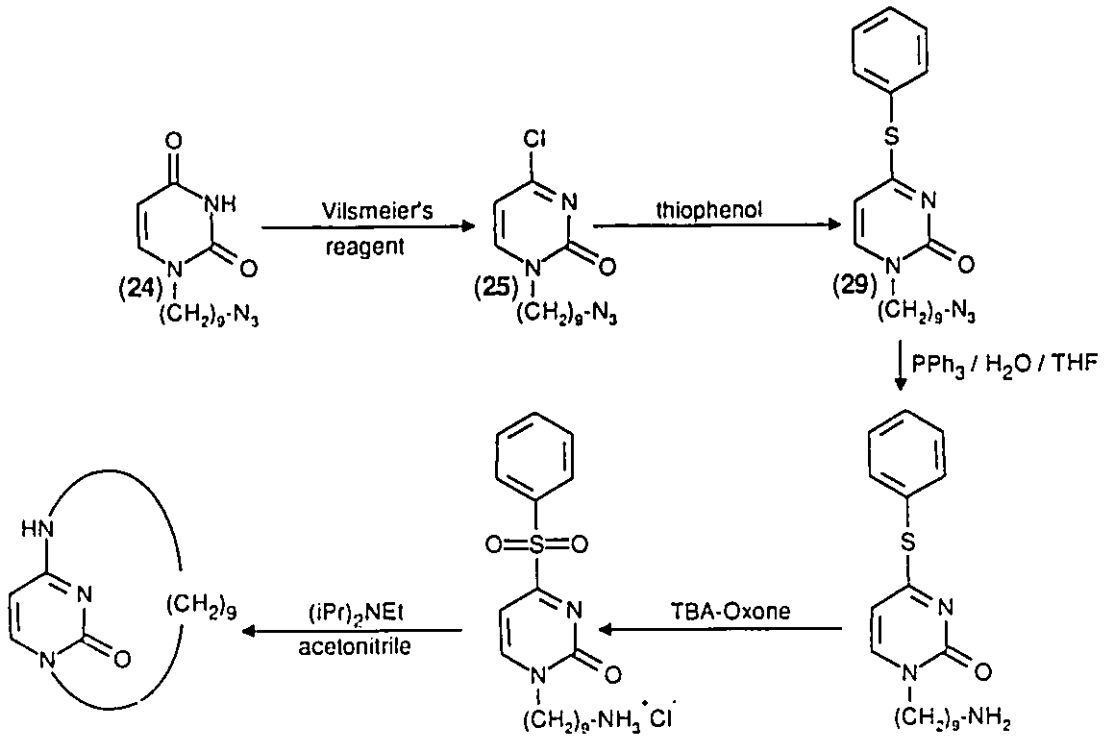

Figure 39: Pyrimidinophanes via Pyrimidinyl Sulphones and Sulphoxides

In their study of pyrimidinyl derivatives, Brown and Ford determined that 4-pyrimidinyl sulphone and sulphoxides were slightly more reactive towards nucleophilic substitution than the corresponding chloropyrimidines and roughly 10,000 times as reactive as the thio-ethers from which they were derived.[64] This information led to the modified synthesis shown in Figure 39. 1-(9-Azidononyl)-4-chloro-pyrimidin-2-one (**25**)

---

[64] Brown, D.J. and Ford, P.W. *J. Chem. Soc. (C)*. 568-572 (1967)

could be treated with thiophenol to give the 4-thiophenyl-pyrimidin-2-one (**29**) which was anticipated to be stable towards the conditions required to reduce the azide to the amine. The thio-ether could then be oxidized to the more highly reactive sulphone or sulphoxide, and subsequently cyclized.

The protocol to be used in the oxidation should be effective under anhydrous conditions (to preclude any sulphone or sulphoxide hydrolysis) and should not affect the amine. Trost's tetra-*n*-butylammonium oxone (TBA-OX) was considered to be the perfect reagent.[65] The ternary mixture of potassium hydrogen persulphate ($KHSO_5$), potassium bisulphate ($KHSO_4$) and potassium sulphate (K_2SO_4), sold commercially as Oxone, has been shown to be an excellent reagent for the oxidation of sulphides to sulphones.[66] Although generally employed under aqueous conditions, coupling of Oxone with a quaternary ammonium salt allows the oxidizing agent to become soluble in many organic solvents. Oxidations can be performed in the absence of water while the acidity of TBA-OX provides *in situ* protection of the basic nitrogen which could also be oxidized.

The rather odiferous model compound for the oxidation was 1-octyl-4-thiophenyl-pyrimidin-2-one (**30**), prepared by treating 1-octyl-4-chloro-pyrimidin-2-one with thiophenol. This substitution reaction worked well yielding 83% of the thio-ether as confirmed by NMR and MS. The oxidizing agent was prepared according to the literature procedure. Surprisingly, when tested (Figure 40), the TBA-OX failed to oxidize the pyrimidine-sulphide to the sulphone (**31**). Closer screening of the Trost paper[65] uncovered a footnote which

---

[65] Trost, B.M., and Braslau, R. *J. Org. Chem.* **53**, 532-537 (1988)

[66] Trost, B.M., and Curran, D.P. *Tetrahedron. Lett.* **22**, 1287-1290 (1981)

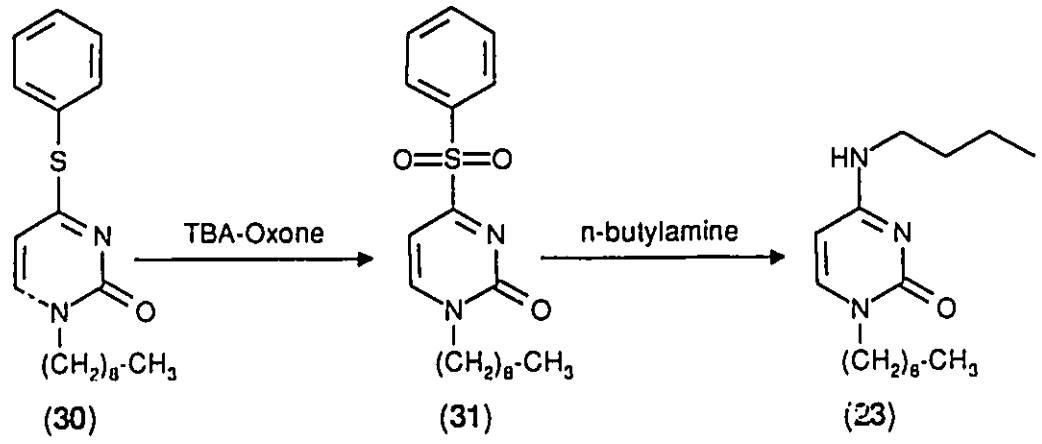

Figure 40: TBA-Oxone Oxidation of 1-Octyl-4-thiophenyl-pyrimidin-2-one

claimed that "the tetra-*n*-butylammonium bisulphate [a reagent required for the preparation of TBA-OX] purchased from Aldrich gave a far less potent TBA-OX than use of the ammonium salt obtained from Kodak."

A supply of tetra-*n*-butylammonium bisulphate was purchased from Kodak and the reaction repeated. An excess of the TBA-OX was used and the reaction monitored by TLC. After 2 days, an aliquot of the reaction mixture was removed and treated with iodine establishing that not all the oxidizing agent had not been spent. Treatment of the remainder of the reaction mixture with *n*-butylamine resulted in very small amounts (less than 5%) of the 1-(octyl)-4N-butyl-cytosine (**23**) as determined by NMR.

It would seem that the either the TBA-Oxone was not oxidizing as claimed or that the activate pyrimidine was reverting rapidly back to the uracil precursor. In either case, the approach would have been useless for cyclophane synthesis application. Other oxidation methods which could perform the reaction under anhydrous conditions and not oxidize the amine could not be found.

3.6. Cytosine Cyclophanes via 4-O-Triisopropylphenylsulphonyl Pyrimidines

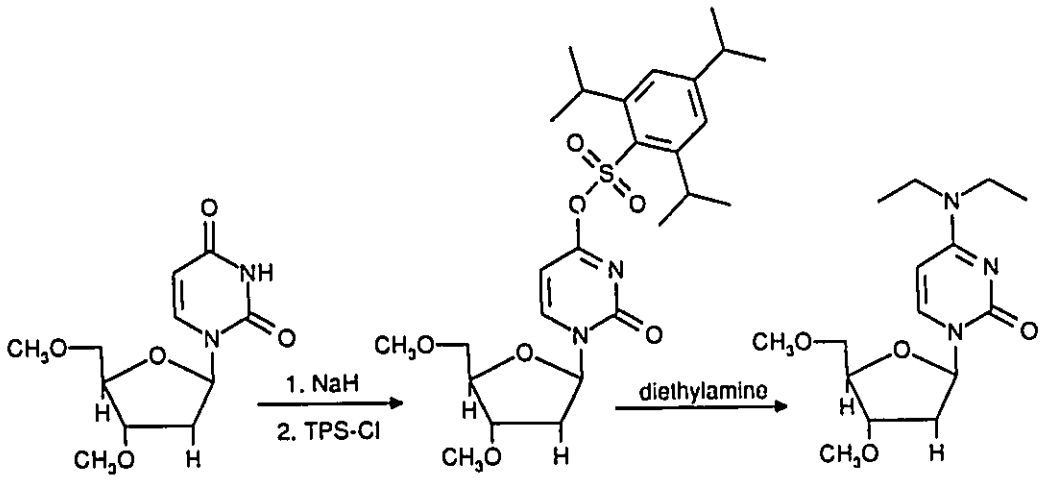

Figure 41: Amination of Pyrimidine using Triisopropylphenylsulphonyl Derivatives

Work published by Bischofberger in 1987 showed that 4-O-triisopropylphenylsulphonyl pyrimidines were simple to prepare, easily chromatographed and quite reactive with a variety of nucleophiles.[67] For example, sugar-protected uridines were converted to their 4-O-triisopropylphenylsulphonyl (TPS) derivatives by reacting with sodium hydride (NaH) and TPS-Cl in THF, followed by aqueous work-up. Once chromatographed, the sulphonate reacted readily with diethylamine to give the 4-N-aminodiethyl-uridine in 95% yield (see Figure 41).

Model experiments with 1-octyl-uracil also demonstrated the potential of the TPS-derivatives. Treatment of 1-octyl-uracil with NaH allowed for deprotonation at N3 and subsequent sulphonation at O4 with triisopropylphenylsulphonyl chloride. Introduction of *n*-butylamine enabled conversion of 1-octyl-4-O-TPS-pyrimidin-2-one (**32**) cleanly to 1-

---

67 Bischofberger, N. *Tetrahedron Lett.* **28**, 2821-2824 (1987)

octyl-4-N-butyl cytosine (23).

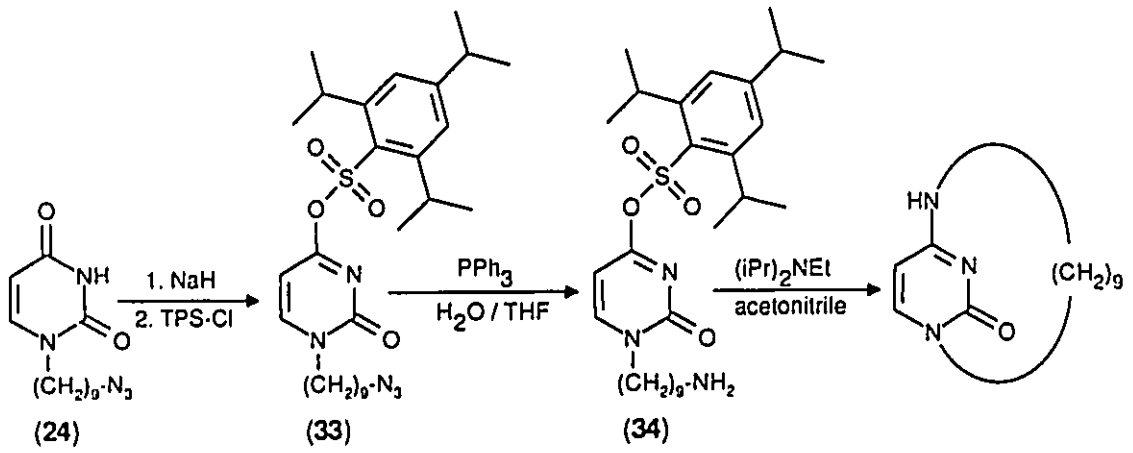

Figure 42: Pyrimidinophanes via Triisopropylphenylsulphonates

Encouraged by the success of the exploratory experiments, the synthesis of 1-(9-azidononyl)-4-O-(triisopropylphenylsulphonyl)-pyrimidin-2-one (Figure 42) was undertaken (see Figure 42). Employing the methodology outlined above, the C4 position of 1-(9-azidononononyl)-uracil (**24**) was activated as the TPS-ester (**33**). Reduction of the azide to the amine (**34**) followed. Once again, the procedure developed by Vaultier *et al.* (triphenylphosphine/water in THF) was implemented.[47] Suspicions about efficiency of this method or reduction of the pyrimidin-2-one azides were confirmed during this reaction. While some of the azide was converted to the amine, ^{1}H-NMR showed the presence of small amounts of decomposition products. Nonetheless, a greater part of this reaction mixture (in excess of 95%) was determined to be the desired 1-(9-aminononyl)-4-O-TPS-pyrimidin-2-one which was subjected to cyclization conditions in acetonitrile. Analysis of the reaction mixture by ^{1}H-NMR and mass spectrometry showed no evidence of

cyclophane formation; instead, mostly the starting TPS-ester amine and some hydrolyzed uracil-amine were recovered.

Additional 1-(9-azidononyl)-4-O-(triisopropylphenylsulphonyl)-pyrimidin-2-one was prepared, reduced and the cyclization repeated under more forceful conditions. Stirring the amine in refluxing xylenes (bp. 137-144°C) for 7 days gave essentially the same result as the acetonitrile cyclization attempt; namely, recovered starting material, some uracil derivative and some ring degradation products (loss of the H5-H6 coupling pattern).

3.7. Problems with the "Intact Bridge Attachment" Approach

In reviewing the "intact bridge attachment" attempts at the synthesis of a cytosine cyclophane, all the avenues explored seem to fail at the final cyclization. There are a number of rationalizations that may be offered to explain the shortcomings of this crucial step.

One might argue that the chain length of the bridge is too short. Work done by Galli, Illuminati and Mandolini[68] on the kinetics of ring closure reactions provided interesting insight into the effect of chain length on these macrocyclizations. In their study of the intramolecular acylation of thiophene (see Figure 43), they noted that rate of macrocyclization decreased as the chain length decreased due to obvious steric impositions. But the relief of strain in the larger rings causes the reactivity to become essentially independent of chain length. Consequently, macrocyclization occurred at relatively the same rate for substrates with chain lengths longer than 11 members.

---

[68] Galli, C., Illuminati, G. and Mandolini, L. *J. Org. Chem.* **45**, 311 (1980)

Naturally, the rate of cyclization depends heavily upon the type of reaction used, but the trends in behaviour do appear to be general. Similar tendencies are seen in the ring formation reactions of *para*- and *meta*-bromoalkoxy phenoxides.[69]

When set against this study, the length of the C-9 chain used for the attempted cytosine cyclophane preparations may seem inadequate. Including the amino nitrogen, the pyrimidine substrates prepared should have cyclized to

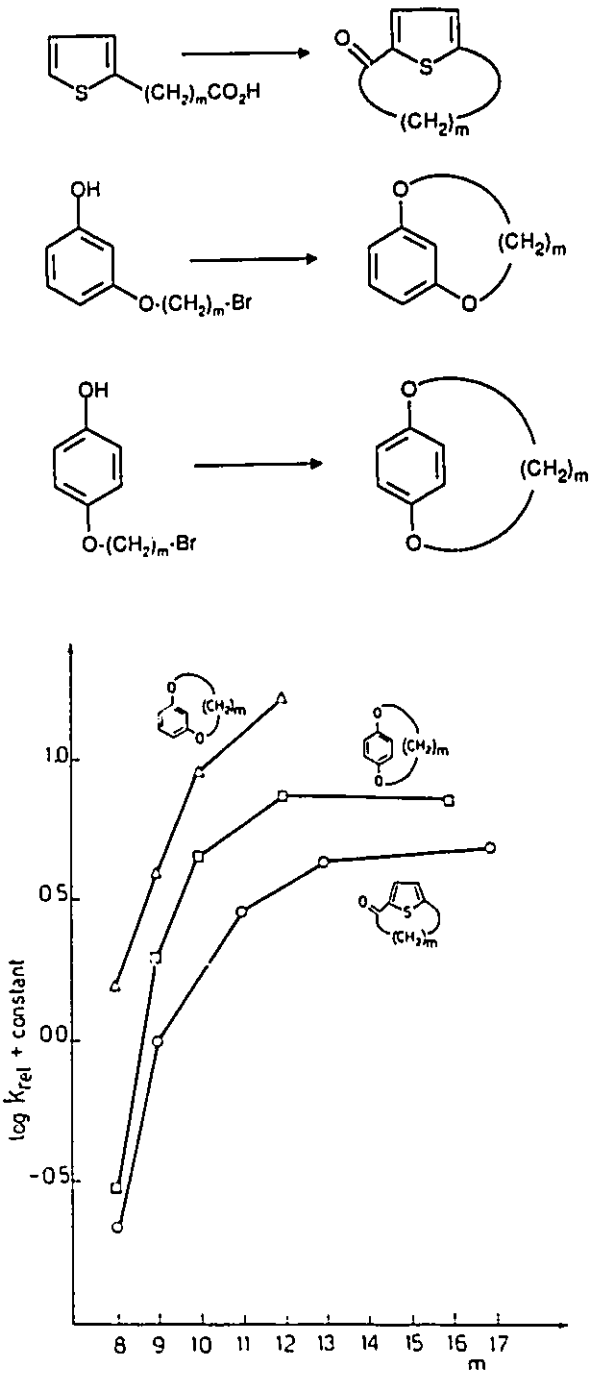

Figure 43: Kinetic Studies of Macrocyclization

[69] Illuminati, G., Mandolini, L. and Galli, C., *J. Amer. Chem. Soc.* **99**, 6308 (1977)

cyclophanes with 10-membered bridges. Looking at Figure 43, the rate curves begin to level off when 11 and 12 membered rings are used. This would seem to indicate that the rate of cyclization for a nonamethylene chain is less than optimal. But if the reaction did in fact proceed, albeit slowly, one would still expect to see at least **some** cyclization taking place. The inability to produce any cyclophane (despite additional attempts with increased reaction times) indicated that the final cyclization suffers from some additional complications.

Generally, chromatographic and spectroscopic analyses revealed the cyclization reaction mixtures to be complex mixtures composed of starting material, uracil-type compounds formed as a result of the hydrolysis the leaving group or byproducts derived from apparent degradative processes of the ring system. Clearly, the competing processes responsible for these products are operating at a rate faster than the cyclization and these side reactions must be considered in conjunction with the nature of the leaving group. In the reactions involving the chloro and the sulphone/sulphoxide derivatives, the leaving groups were sufficiently labile that traces of water transformed these activated pyrimidines back to their uracil-based precursors. With the TPS and tosamide cyclization substrates, the relatively poorer leaving groups hindered cyclization and, under the conditions employed, degradation of the pyrimidine prevailed. A leaving group of intermediate lability to the ones used would be more appropriate.

Perhaps the chain was too short to allow the amine to reach the reaction site? This is doubtful since molecular models clearly showed the nonamethylene chain to be sufficiently long to allow for nucleophilic aromatic substitution. Furthermore, it is unlikely that the transition state geometry required of intramolecular attack is inaccessible. As in

the purinophane synthesis, the final cyclization should begin with the attack of the primary amine at the p-orbital on C4 which is perpendicular to the plane of the pyrimidine. While the transition state geometry required for such an attack can be easily adopted by the substrate, the energetics associated with this geometry may be too demanding. The effects of bond angle deformations and transannular interactions manifest themselves in the enthalpy ($\Delta H^{\ddagger}$) and entropy ($\Delta S^{\ddagger}$) of activation and ultimately in the free energy of activation ($\Delta G^{\ddagger}$). These activation parameters are difficult to quantify especially in a reaction that does not appear to work, but stringent energetic impositions can thwart a reaction. Comparison of our particular cyclization to the [10]-paracyclophane synthesis, though, leads one to believe that the energetics are not insurmountable.

The difficulties encountered in the "intact bridge attachment" approach prompted the use of a strategy which would see the bridge constructed by a coupling reaction. Aspects of this approach are discussed in Chapter 4.

Chapter 4

Approaches to Pyrimidinophanes: "Bridge Formation by Coupling"

4.1. The "Bridge Formation by Coupling" Approach

The inability to produce a cytosine cyclophane via an "intact bridge attachment" approach prompted the development of syntheses based on "bridge formation via coupling" (see Introduction, Figure 13). It was hoped that many of the limitations of the first approach might be overcome by the latter. A "bridge formation by coupling" strategy requires that two shorter chains, each attached at opposite ends of the aromatic system, are appropriately functionalized for the final ring closure. As seen in the previous chapter, the reactions necessary for the preliminary alkylations of the pyrimidine have already been developed.

With a wide variety of coupling reactions to choose from, one is no longer limited solely to nucleophilic aromatic substitution for the crucial cyclization step. The synthetic freedom granted by this approach opens up new avenues for the design of routes to previously inaccessible cyclophanes with bridges attached at other positions on the pyrimidine. Provided the initial alkylation of the aromatic system at the desired sites is possible, the final coupling reaction will see to the bridge formation.

In choosing a reaction for the final coupling, the field of potential candidates was narrowed down by considering only those protocols that involved metal catalysis and techniques that would not introduce heteroatoms into the girding chain. The first

prerequisite would help deal with the energy requirements of the final cyclization reaction. With all the coupling chemistry taking place on the surface of a metal, the entropy demands of a particular reaction can be greatly reduced. This type of metal templating has been used before in catenane-type syntheses with great success.[70] The second characteristic desired of the coupling reaction would avoid the presence of a heteroatom in the bridge and, in turn, avoid complications with the anisotropy calculations. A search of the literature was initiated and two coupling reactions involving copper and palladium appeared to be suitable.

4.2. Copper Coupling of Bis-Alkynes

The Glaser coupling of two terminal acetylenes has been utilized by chemists since its discovery in 1869.[71] The modifications made by Eglinton and co-workers have further increased its synthetic utility.[72] Although a number of modifications exist[73,74,75], the reaction is generally carried out by treating an alkyne with an appropriate copper (II) salt, usually in the presence of a base.

Some controversy still surrounds the reaction although the generally accepted

---

[70] Dietrich-Buchecker, C.O. and Sauvage, J-P. *Chem. Rev.* **87**, 795 (1987)

[71] Glaser, C. *Ann.* **154**, 137 (1870) and Glaser, C. *Ber.* **2**, 422 (1869)

[72] Eglinton, G. and McCrae, W. in Advances in Organic Chemistry: Methods and Results, Volume 4. (New York: John Wiley and Sons, Inc.) p.225 (1963)

[73] Ojima, J., Shiroishi, Y., Wada, K., and Sondheimer, F. *J. Org. Chem.* **45**, 3564-3570 (1980)

[74] O'Krongly, D., Denmead, S.R., Chiang, M.Y., and Breslow, R. *J. Amer. Chem. Soc.* **107**, 5544-5545 (1985)

[75] Dietrich-Buchecker, C.O., Khemiss, A., and Sauvage, J.P. *J. Chem. Soc., Chem. Commun.*, 1376-1378 (1986)

mechanism is shown in Figure 44.[76] Deprotonation of the acetylene proceeds oxidation by Cu^{2+} of the resultant acetylide to an acetylenic radical. The radical is likely associated with the copper and is probably not a free radical in solution. Coupling of two such radicals leads to the generation of the bis-alkyne. The Cu^{2+} species is then regenerated by the action of air on the Cu^{+}. Obviously, reactions involving the preparation of symmetrical diynes are the most efficient since the unwanted cross coupling byproducts formed in the unsymmetrical case are difficult to minimize.

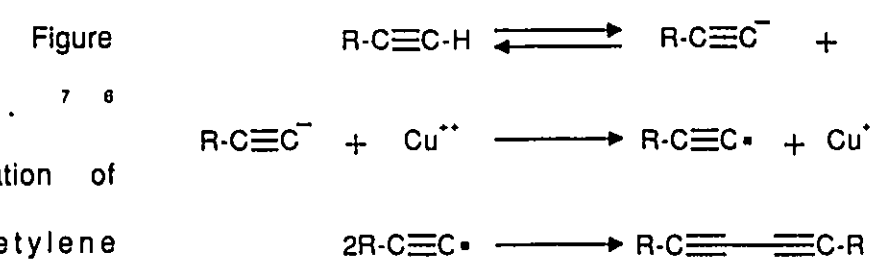

Figure 44: Mechanism of Copper Coupling of Alkynes

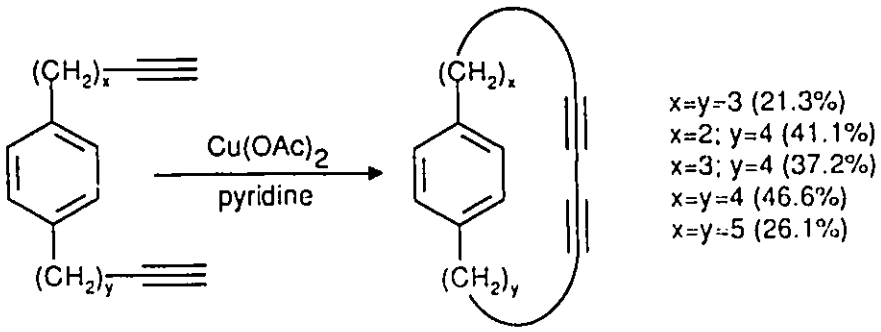

Figure 45: Benzene Cyclophanes via Alkyne Coupling

There are a number of examples in the literature where the coupling of two

---

[76] Kleblansky, A. L., Grachev, I. V., and Kuznetsova, J. *J. Gen. Chem. U.S.S.R.* **27**, 3008 (1957)

terminal acetylenes has been used to form cyclophanes. Matsuoka *et al.* prepared a number of [m,n]-paracyclophadiynes using copper acetate in pyridine (see Figure 45).[77] Sakamoto *et al.* were also reasonably successful in their synthesis of the pyrimidinophane illustrated in Figure 46.[21] Strangely, cyclization of the isomeric compound shown could not be affected under the same conditions. No explanation for this peculiar selectivity was given. Reduction of the diynes to their corresponding alkanes was realized using catalytic hydrogenation.

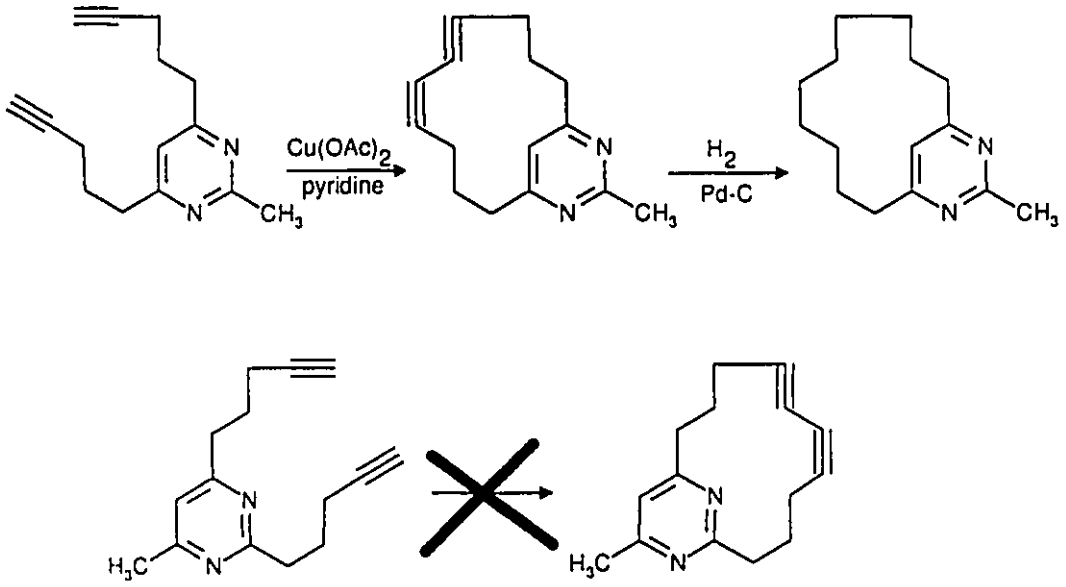

Figure 46: Pyrimidine Cyclophanes via Alkyne Coupling

Prior to its use in cytosine cyclophane synthesis, a number of standard compounds

---

[77] Matsuoka, T., Negi, T., Oysubo, T., Sakata, Y. and Misumi, S. *Bulletin of the Chemical Society of Japan*, 45, 1825-1833 (1972)

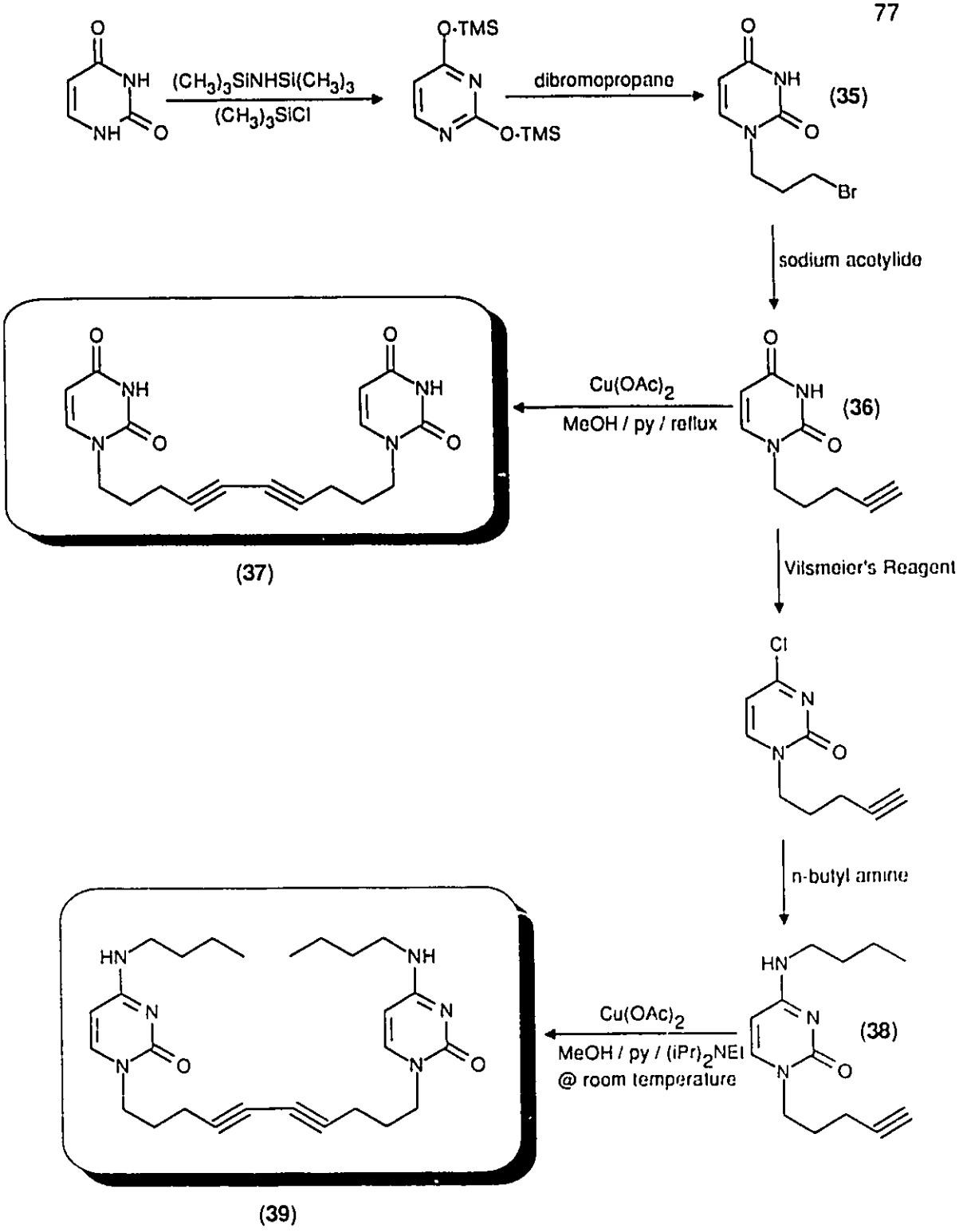

Figure 47: Copper Coupling of Model Compounds

were prepared to test the effectiveness of the copper coupling for pyrimidine-type molecules. Figure 47 illustrates the preparation and coupling of two such substrate. 2,4-Bis(trimethylsiloxy)pyrimidine (*vide supra*)[59] was treated with 1,3-dibromopropane under the conditions described by Browne *et al.*[54] to give 1-(3-bromopropyl)-uracil (**35**). Subsequent displacement of the bromide using sodium acetylide gave 1-(4-pentynyl)-uracil (**36**) in good yield. The acetylene prepared showed the expected ^{1}H-NMR spectrum with the terminal alkyne hydrogen coupled to the methylene protons four bonds away. The chemical shifts of the triply bonded carbons in the ^{13}C-NMR at 70.12 and 82.24 ppm are also characteristic of an acetylene. Additional confirmation came from the molecular ion in the mass spectrum at 178 amu.

The uracil-alkyne was then subjected to the coupling conditions described by Eglinton.[72] Refluxing 1-(4-pentyl)-uracil with copper acetate in a mixture of methanol and pyridine for 4 hours yielded 83% of the coupled product (**37**) although repeated chromatography was required to separate the diyne from the copper catalyst. High resolution mass spectrometry showed the molecular ion of the product at 354.1311 amu while the ^{1}H-NMR spectrum of the dimer showed loss the terminal acetylenic proton.

To further establish the applicability of the Glaser-Eglinton procedure, a cytosine-based standard compound was coupled. As illustrated in Figure 47, 1-(5-pentynyl)-uracil (**36**) was treated with Vilsmeier's reagent and transformed to the 1-(5-pentynyl)-4-chloro-pyrimidin-2-one. Addition of the chloro-pyrimidine to *n*-butylamine readily produced 1-(4-pentyl)-4-N-butyl-cytosine (**38**) in excellent yield. Coupling of this compound was achieved using copper acetate in methanol, pyridine and diisopropylethylamine at room temperature for 2 days. The hindered base was added to increase the preliminary deprotonation step

of the acetylene. The coupled compound generated (**39**) was characterized using mass spectrometry as well as proton and carbon-13 NMR. The yield (40%) was not quite as impressive as in the 1-(4-pentyl)-uracil coupling experiments but, nonetheless, showed that the reaction does proceed at lower temperatures.

The coupling of 1-(4-pentyl)-4-N-butyl-cytosine (**38**) was repeated under a variety of conditions with substantially the same results. The reaction was amazingly tolerant to a variety of temperatures (reflux or room temperature), reaction times (generally 2-6 hours when heated or 1-2 days at room temperature), solvents, or the quality of the copper acetate used (hydrated or anhydrous).

Encouraged by the results of the intermolecular studies, a synthetic plan was devised to prepare a synthon to be used in intramolecular copper coupling to the cytosine cyclophane. The choice of proper chain lengths was based on an examination of the substrates used in the Matsuoka *et al.* studies.[77] The review indicated that 1-(4-pentynyl)-4-N-(4-pentynyl)-cytosine would be a suitable cyclization candidate. The synthesis route is outlined in Figure 48. Note that the alkyl fragment to be connected at the 1-position is derived from 5-chloro-1-pentyne. Following the procedure developed by Lindgren *et al.*[78], treatment of the chloride with an excess of sodium azide in dimethylformamide gave the azido species shown. Subsequent reduction to the amine using lithium aluminum hydride afforded 5-amino-1-pentyne (**40**). Meanwhile, the 1-(5-pentynyl)-uracil (**36**) (prepared as described above) was treated with Vilsmeier's reagent and transformed to the 1-(4-pentynyl)-4-chloro-pyrimidin-2-one. The desired bis-acetylene product (**41**) was

---

[78] Lindgren, S., Svensson, U., and Dahlbom, R. *Acta Pharm. Suec.* **12**, 503-506 (1975)

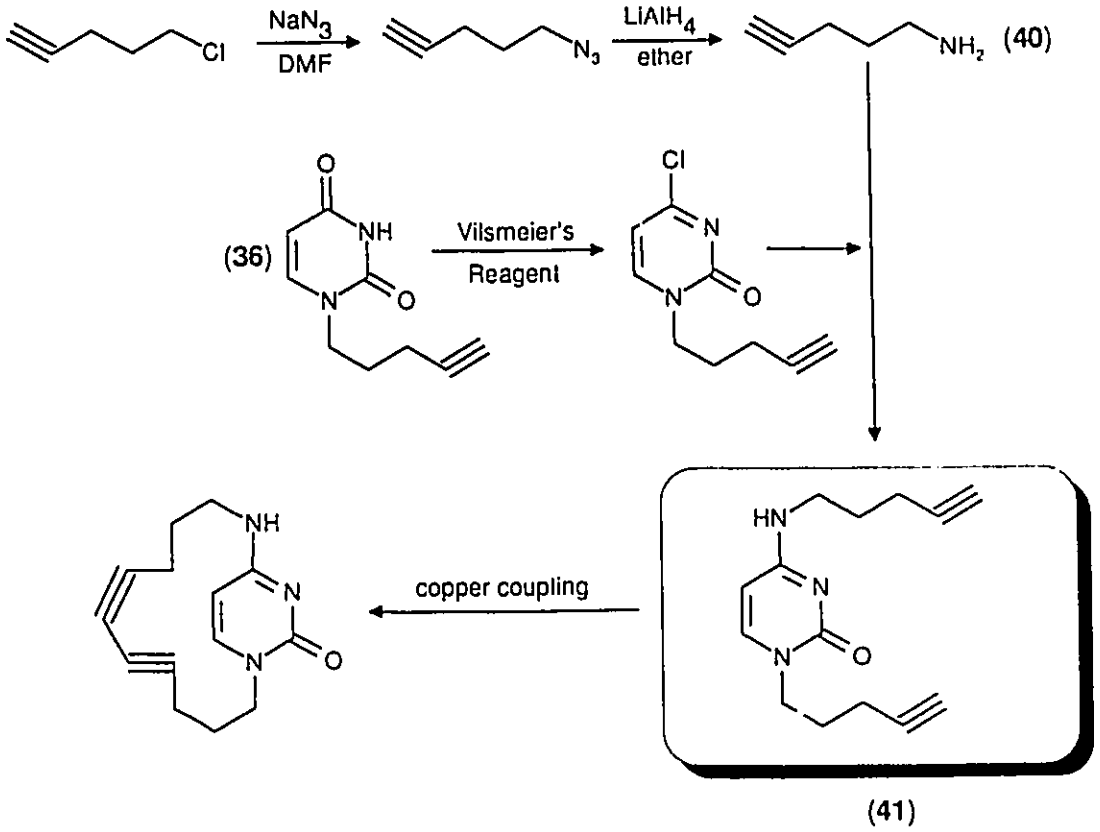

Figure 48: Synthesis of 1-(4-Pentynyl)-4N-(4-pentynyl)-cytosine

prepared by adding the chloro-pyrimidine to the amino-alkyne to give 1-(4-pentynyl)-4-N-(4-pentynyl)-cytosine as evidenced by the molecular ion at 242 amu in the mass spectrum. Both ^{1}H and ^{13}C-NMR further helped to characterize the product. It should be pointed out that all the reactions described above proceeded smoothly in moderate to excellent yields.

A variety of reaction conditions were applied in an effort to induce intramolecular coupling of the substrate. A "high dilution" version of the protocol applied in the coupling of 1-(4-pentynyl)-uracil was the first implemented. A solution of 1-(4-pentynyl)-4-N-(4-pentynyl)-cytosine (41) in pyridine was added dropwise to a refluxing suspension of

copper acetate in methanol and pyridine. The reaction was stopped after 2 days when TLC of a concentrated aliquot established the complete disappearance of the starting material.

Some of the aspects of the "high dilution" technique deserve comment. The volume of solvent in the reaction vessel was such that the concentration of the bis-alkyne was of the order of 10^{-4} to 10^{-3} M in order to minimize the competing intermolecular reactions possible. The large volumes of solvent required by a high dilution experiment meant that, in order to achieve a local concentration of copper similar to that seen in the standard experiments, large amounts of copper acetate were used for the intramolecular coupling. Ultimately, though, this excess of copper acetate seems to have been detrimental to the reaction. With the reaction being carried out using small amounts of bis-acetylene and considerable quantities of copper acetate, the propensity for side reactions increased and isolation of the reaction products became difficult.

The crude reaction mixture from this first coupling attempt was assayed by TLC, NMR and MS. Flash chromatography permitted isolation of several fractions each of which was, in turn, also analyzed by using the above techniques. The repeated chromatography required to separate the copper acetate from the reaction products resulted in some loss of material. Chromatographic fractions were numerous, generally quite small and often not pure (containing traces of other products and copper salts as demonstrated by TLC). No starting material was isolated. The presence of paramagnetic copper in the NMR samples resulted in severe line broadening and made interpretation exceedingly difficult. The proton spectra generally contained aliphatic moieties as evidenced by the large peaks at around 1.28-1.30 ppm. Several spectra were missing the

characteristic A-B splitting pattern expected of the H5 and H6 of the uracil and the region between 3.25 and 4.00 ppm, usually populated by signals from methylenes adjacent to heteroatoms, was often crowded with several broadened resonances making assignments impossible. Mass spectrometry also failed to provide any evidence for cyclophane formation.

It would seem that the conditions employed in this intramolecular cyclization attempt resulted in numerous unwanted side reactions. Destruction of the pyrimidine was apparent although it was impossible to tell whether this was a result of prolonged reaction times at elevated temperatures, or due to the large amounts of copper acetate present. Consequently, the final step was repeated using the conditions employed in the coupling of 1-(4-pentyl)-4-N-butyl-cytosine (**38**). Recall that this intermolecular reaction involved treatment of the alkyne with the copper salt in methanol, pyridine and diisopropylethylamine at room temperature. A high dilution modification of the reaction conditions was applied to 1-(4-pentynyl)-4-N-(4-pentynyl)-cytosine (**41**). Maintaining the same amount of copper acetate and similar solvent volumes used in the previous attempt, analysis of the reaction mixture after 2 days showed the reaction mixture to be composed of roughly 50% starting bis-alkyne and 50% degraded material with no clear evidence of cyclophane formation. Increasing the reaction times only served to increase the amount of side reaction products.

Other protocols were tried. The success encountered by Sondheimer and co-workers[73] with the application of copper coupling chemistry in the preparation of [n]-annulenones, prompted use of their reaction conditions on the bis-acetylene-pyrimidine. The substrate was introduced dropwise into a reaction vessel containing a ten-fold excess

of copper acetate suspended in pyridine at 50°C. Reaction times of 3 hours, 24 hours and 3 days were tried. Analysis of the crude mixtures and the chromatographed fractions by NMR, MS and TLC failed to provide any evidence for the presence of the desired product. Rather, the products of apparent degradative processes and some small traces of starting material were to be found.

Breslow *et al.*[74] have claimed that treatment of a bis-alkyne with a mixture of copper (I) chloride and copper (II) chloride in "O_2-free" pyridine at 0°C results in excellent yields of the coupled product. Unfortunately, utilization of this procedure with our substrate did not elicit the desired result with mostly starting material being isolated. Doubts about the efficacy of this technique were raised when a paper by Dietrich-Buchecker, Khemiss and Sauvage was uncovered.[75] They reported that direct use of Breslow's methodology in their synthesis of catenanes had failed. It was only when they attempted to perform the reaction aerobically in dimethylformamide that the coupling took place. Implementation of this new set of reaction conditions on 1-(4-pentynyl)-4-N-(4-pentynyl)-cytosine lead to results similar

to those obtained in the previous coupling attempts.

The inability to prepare any cyclophane, especially in light of the success had by Matsuoka and co-workers with similar substrates, was quite disturbing. What if the molecule could not achieve the required transition state geometry because of insufficient chain lengths? In the hope of ameliorating the final cyclization step, a substrate with a longer chain length was prepared. The synthesis of 1-(4-pentynyl)-4-N-(6-heptynyl)-cytosine is shown in Figure 49. Unlike 1-(4-pentynyl)-4-N-(4-pentynyl)-cytosine, the alkyl fragment used to aminate C1 was derived from 1,5-pentanediol. The diol was mono-

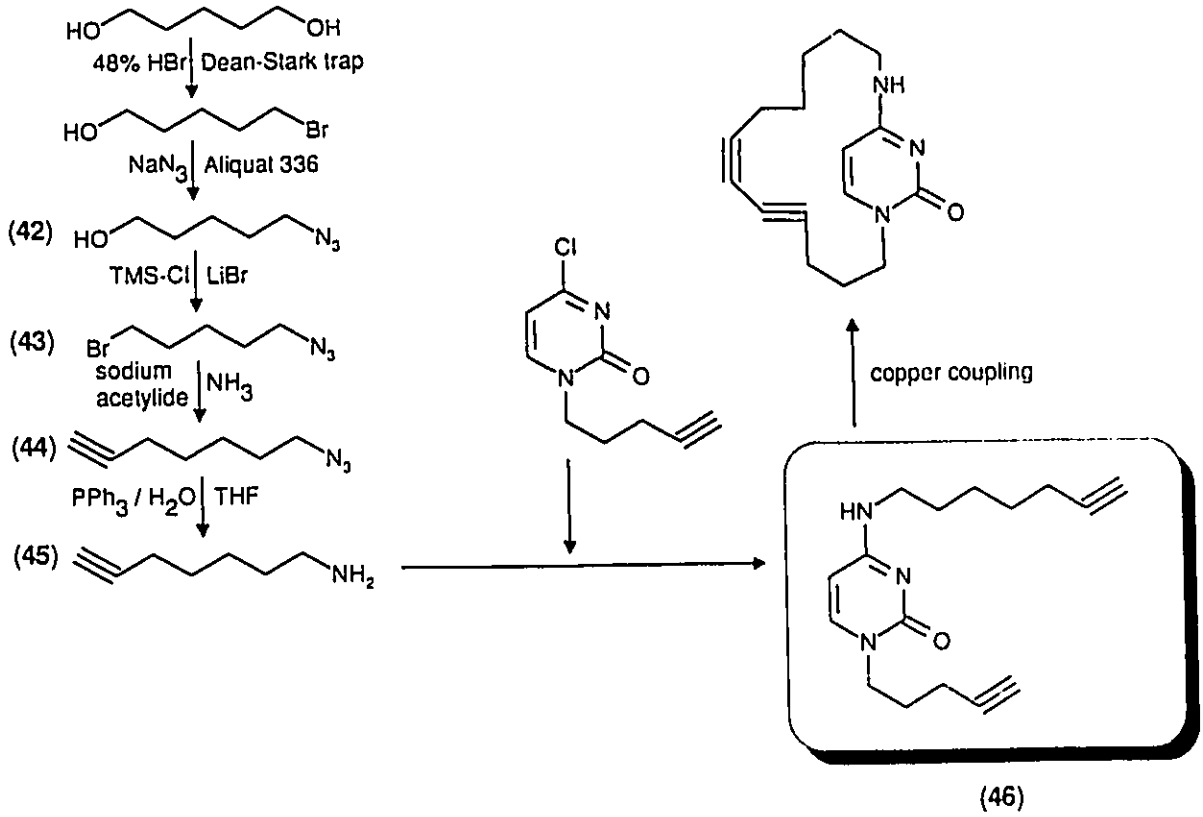

Figure 49: Synthesis of 1-(4-Pentynyl)-4-N-(6-heptynyl)-cytosine

brominated using the procedure of Kang *et al.*[49], converted to the azido-alcohol (**42**) as described by Reeves *et al.*[50], and transformed to 1-bromo-5-azido-pentane (**43**) using the method of Olah *et al.*[56] Acetylide displacement of the bromide to give (**44**) was followed by reduction of the azido end to yield the desired 7-amino-1-heptyne (**45**). This amino-yne was then treated with 1-(4-pentynyl)-4-chloro-pyrimidin-2-one (prepared as above) to give 1-(4-pentynyl)-4-N-(6-heptynyl)-cytosine (**46**) which was fully characterized. Unfortunately, despite the application of the copper coupling protocols of Eglinton[72], Sondheimer[73], Breslow[74], and Sauvage[75] no cyclophane material was realized. The reaction mixtures of the longer chain bis-alkyne were virtually identical to those of the short chain analog.

Once again, the cytosine cyclophane synthesis appeared to have fallen victim to a problem of relative reaction rates. The attempts reported above seemed to indicate that coupling required for cyclization was slower than the degradative processes responsible for the byproducts. Short reaction times did not permit cyclization, while prolonged exposure to the copper acetate resulted in numerous side reactions while increasing the temperature only served to increase the rate of degradation of the pyrimidine ring. Some insight into the nature of this degradation was offered by Eglinton and McCrae[72] who report that the "cupric acetate coupling procedure normally works well..however, the reagent is known to effect the oxidation of.. aromatic amines". Although details concerning this oxidation process are not elaborated upon, it would seem that these kinds of side reactions are not uncommon. A complete and thorough analysis of the reaction mixtures would have required a great deal of time and the use of high performance liquid chromatography (HPLC) for adequate resolution of the components without making any useful contribution to the fundamental problem, namely the low rate of cyclization. It was, therefore, decided to devote effort to the development of a alternate cyclization reaction.

4.3. Palladium Coupling of Alkynes and Vinyl Halides

Numerous reports have appeared in the literature involving the coupling of vinyl halides with acetylenes using palladium catalysis.[79] Nicolaou and co-workers[80] have used the reaction in their synthesis of lipoxin A. The Trost group has demonstrated the

---

[79] Tsuji, J. Organic Synthesis with Palladium Compounds. (New York: Springer-Verlag, 1980)

[80] Nicolaou, K.C., Veale, C.A., Webber, S.E. and Katerinopoulos, H. *J. Amer. Chem. Soc.* **107**, 7515-7518 (1985)

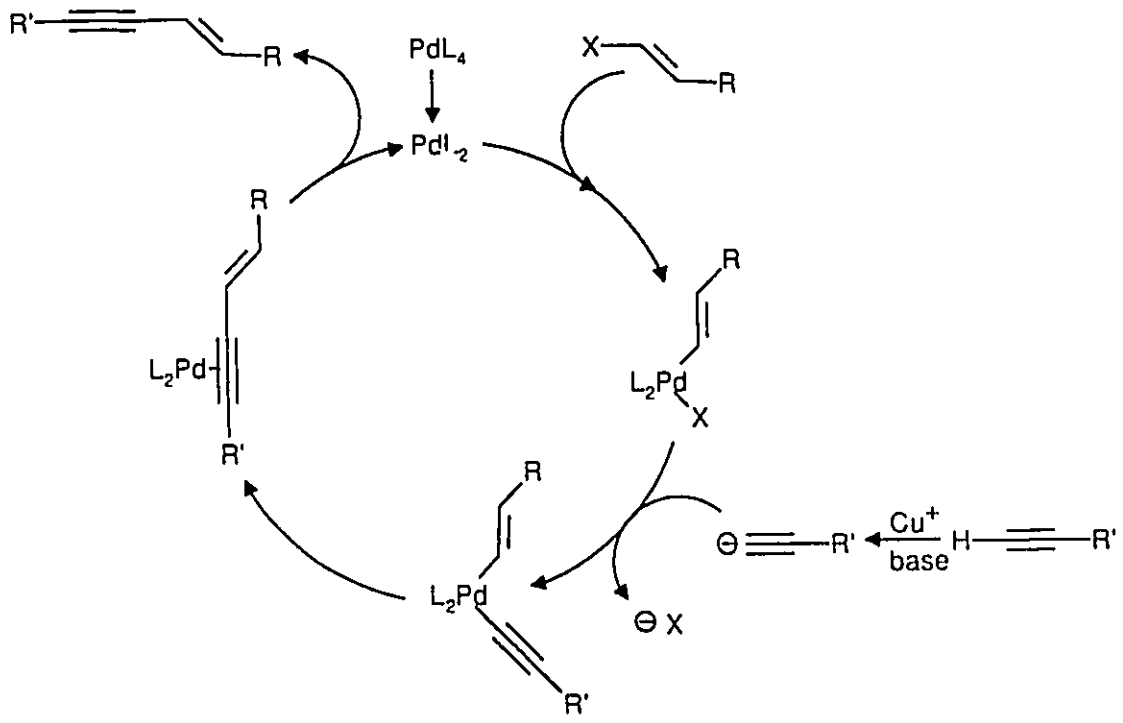

Figure 50: Mechanism of Palladium Coupling

synthetic utility of this approach in the preparation of cyclopentane enynes.[81] Tetrakis(triphenylphosphine) palladium is the catalyst of choice and the use of a copper co-catalyst has proven beneficial although not absolutely necessary.[82]

---

81 Trost, B.M., Chan, C., and Ruhter, G. *J. Amer. Chem. Soc.* **109**, 3486-3487 (1987)

82 Takahashi, S., Kuroyama, Y., Sonogashira, K., and Hagihara, N. *Synthesis*, 627 (1980)

The catalytic cycle is believed to proceed as illustrated in Figure 50.[83] Loss of two triphenylphosphine ligands liberates two co-ordination sites on the palladium to which the vinyl halide oxidatively adds. Meanwhile, deprotonation of the acetylene by the base (likely facilitated by the copper (I) catalyst) results in the acetylide, which displaces the halogen on the palladium to give the intermediate shown. Reductive elimination of the enyne permits the palladium to continue the catalytic cycle.

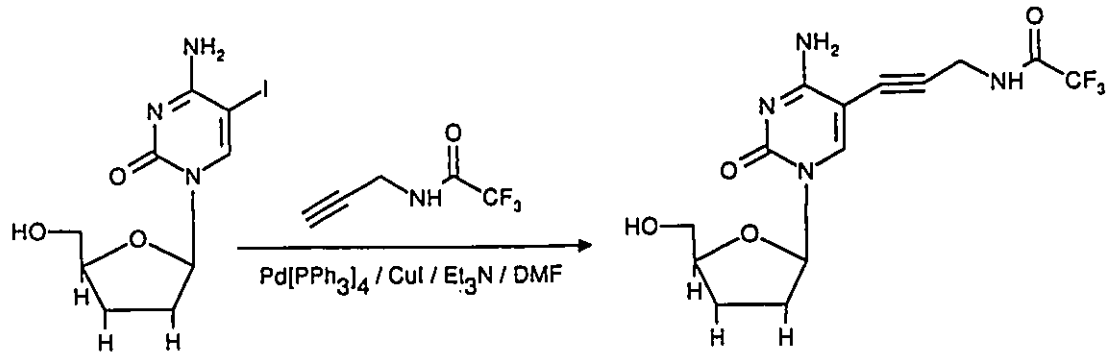

Figure 51: Nucleoside Enynes Via Palladium Coupling

Although this reaction has not, as yet, been applied to cyclophane synthesis, Hobbs has used a modification of this system to generate alkynylamino nucleosides as seen in Figure 51.[84] The iodonucleosides were treated with the alkyne, 10 mol% of the palladium catalyst, 5 mol% of copper iodide and triethylamine in dimethylformamide. Reaction times were generally a few hours with yields ranging from 64% to 92%.

A few standard intermolecular reactions were carried out in order to establish the efficiency of the coupling reaction. The synthesis of dodec-5-en-7-yne (47) (shown in

---

[83] Heck, R. F. Palladium Reagents in Organic Syntheses. (London: Academic Press, Inc., 1985) p. 299

[84] Hobbs, F.W. *J. Org. Chem.* 54, 3420-3422 (1989)

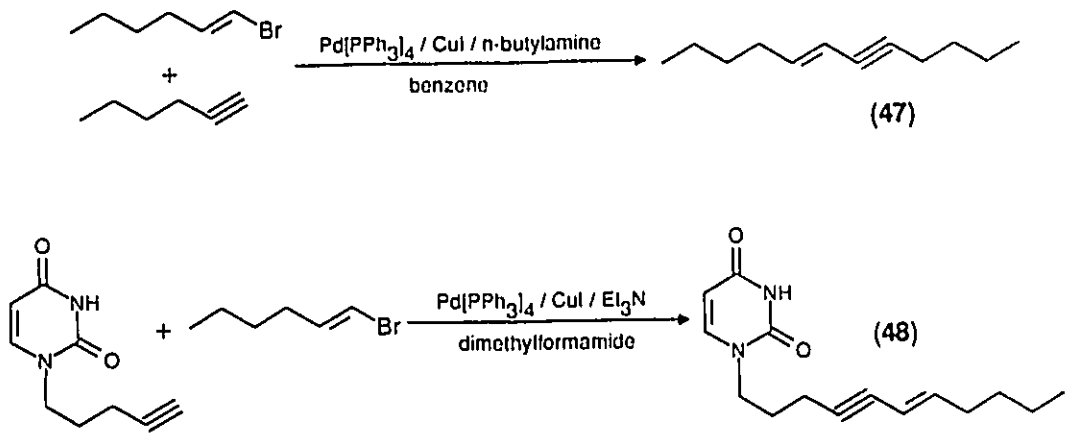

Figure 52: Palladium Coupling of Model Compounds

Figure 52) followed the procedure described by Ratovelomana and Linstrumelle.[85] 1-Bromo-1-hexene was reacted with 1-hexyne in the presence of tetrakis(triphenylphosphine) palladium, copper iodide and *n*-butyl amine in benzene to form the desired enyne in 70% yield. Measurement of the coupling constants of the alkene protons (J= 15.7 Hz) found in the ^{1}H-NMR spectrum of the product indicated that the reaction proceeded to give exclusively the *trans* isomer despite the fact that a mixture of *cis* and *trans* 1-bromo-1-hexene was used.

Although the Ratovelomana and Linstrumelle method worked well, the likely insolubility of a pyrimidine-based cyclization substrate in benzene prompted the testing of Hobbs' protocol which employs dimethylformamide. Synthesis of 1-(undec-4-yn-6-enyl)-uracil (46) (Figure 52) was achieved by treating 1-bromo-1-hexene with 1-(4-pentynyl)-uracil in the presence of the palladium and copper catalysts. Once again, ^{1}H-NMR

---

[85] Ratovelomana, V., and Linstrumelle, G. *Synthetic Comm.* **11**, 917-923 (1981)

demonstrated that the reaction only yielded *trans* product. The product was further characterized by ^{13}C-NMR and HRMS. It was also determined that as little as 1 mol% of the palladium catalyst with 0.5 mol% of copper iodide could be used although completion of the reaction took 18 hours.

Work with the standard compounds also established that the order of addition of the reagents is important. Prior mixing of the palladium and copper catalyst resulted in a black, heterogeneous suspension. If the correct order was applied (ie. vinyl halide first followed by the palladium catalyst, the alkyne, the base and finally the copper catalyst) the reaction mixture would remain clear and amber in colour. Additionally, increasing the ratio of copper catalyst to palladium catalyst beyond 2:1 resulted in the solution turning black and, according to Hobbs, consumption of his iodonucleoside.

An appropriate substrate for intramolecular coupling to a cytosine cyclophane is 1-(4-Pentynyl)-4-N-(5-bromo-4-pentenyl)-cytosine; its synthesis is outlined in Figure 53. The amino-vinyl bromide to be affixed at the 1-position is derived from 4-pentyn-1-ol. The hydroxyl end of the starting material is protected as the *tert*-butyldimethylsilyl (TBDMS) ether (**49**) using a procedure developed by Corey *et al.*[86] Conversion of the alkyne to the vinyl bromide was achieved by Nicolaou's method[80] which involved refluxing the 4-pentynyl-TBDMS ether in tributyltin hydride to give an intermediate vinyl stannane species. Addition of bromine to this intermediate to gave the vinyl halide, which was then treated with ammonium fluoride to allow for cleavage of the silyl protecting group.[87] The 1-

---

[86] Corey, E.J., Cho, H., Rucker, C., and Hua, D.H. *Tetrahedron. Lett.* **22**, 3455-3458 (1981)

[87] Zhang, W., and Robins, M.J. *Tetrahedron. Lett.* **33**, 1177-1180 (1992)

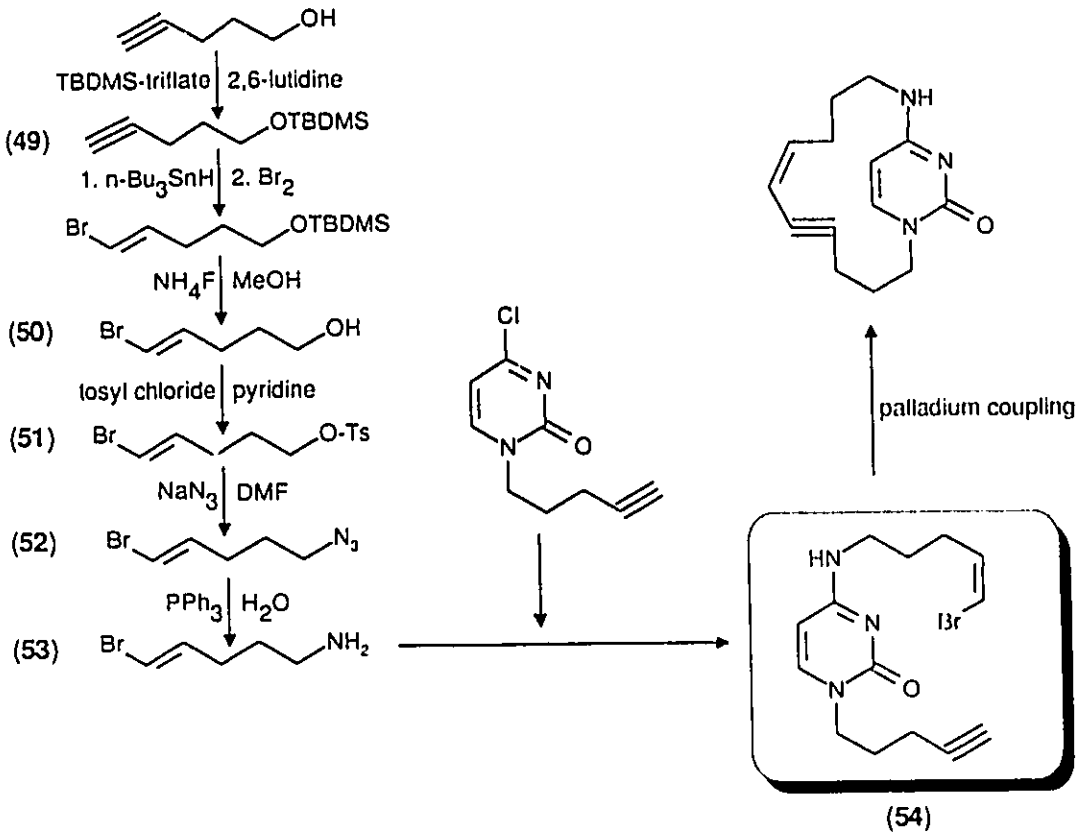

Figure 53: Synthesis of 1-(4-Pentynyl)-4-N-(5-bromo-4-pentenyl)-cytosine

bromo-1-penten-5-ol (**50**) was a mixture of both the *cis* and *trans* isomers as evidenced by ^{1}H-NMR. Tosylation of the hydroxyl (**51**) and treatment with sodium azide resulted in 1-bromo-5-azido-1-pentene (**52**) which was then cleanly reduced using the triphenylphosphine / water method.[47] The 1-bromo-5-amino-1-pentene (**53**) was then added to 1-(5-pentynyl)-4-chloro-pyrimidin-2-one to produce the desired 1-(4-pentynyl)-4-N-(5-bromo-4-pentenyl)-cytosine (**54**). The crystalline product was fully characterized by NMR and HRMS.

With the cyclization substrate in hand, an intramolecular palladium coupling reaction was performed. Based on Hobbs' procedure, the vinyl-bromide-alkyne was

treated with an equivalent of the tetrakis(triphenylphosphine)palladium in a small volume of dimethylformamide. The solution was stirred for an hour to permit the initial oxidative addition of the vinyl halide to the palladium. Dilution of the reaction mixture with additional DMF was followed by the addition of triethylamine and copper iodide. The reaction mixture darkened immediately. After 2 days, analysis by TLC, NMR and MS of the crude reaction mixture and the fractions isolated by chromatography failed to provide any evidence of cyclophane product. Most of the material collected was shown to be starting material although some degradation had occurred. Attempts involving reaction times of 7 and 30 days met with similar results.

The dark reaction mixtures were taken as an indication that the course of the reaction was not proceeding as it should have. It was decided that smaller amounts of palladium and copper reagents should be employed. As seen in the synthesis of 1-(undec-4-yn-6-enyl)-uracil standard, the reaction can be run with as little as 1 mol% of the palladium catalyst and 0.5 mol% of copper iodide. Maintaining the same volume of dimethylformamide as was used in the previous attempt, the intramolecular reaction was repeated using these lower levels of catalysts. Unfortunately, the reaction mixture proceeded to become dark as it had in the former effort (although not nearly as intense). Analysis after 10 days showed the presence of mostly starting material.

Attempts were made to follow the course of the reaction by ^{1}H-NMR. 1-(4-Pentynyl)-4-N-(5-bromo-4-pentenyl)-cytosine was dissolved in deuterated DMF and treated with 10% mol of tetrakis(triphenylphosphine)palladium. The proton NMR showed some broadening but, remarkably, did not show any evidence of oxidative addition. The vinyl region of the spectrum remained unchanged despite heating of the sample. When the 5%

mol of the copper iodide and triethylamine were added, severe broadening of the spectrum due to the paramagnetic copper was seen. Heating the sample for 1 hour at 60°C resulted in polymerization and the precipitation of product. The inability to see the oxidative addition of the vinyl halide to the palladium prompted another NMR experiment wherein 1-bromo-1-hexene was treated with the palladium catalyst in deuterated benzene. Again, the vinyl region remained virtually unchanged for hours. Severe broadening was seen after 18 hours. While these results call into question the validity of the proposed mechanism, they do little to help remedy the failed cyclization attempts.

4.4. Problems with the "Bridge Formation by Coupling" Approach

Failure of the intramolecular palladium coupling procedure may be due, in part, to the stringent geometric requirements of the reaction's transition state. In order for coupling to occur, both alkyl chains must extend above the plane of the pyrimidine. With two triphenylphosphine ligands already coordinated to the palladium, the reaction takes place on a rather crowded metal surface. In the intermolecular case, the conformational freedom of the incoming vinyl halide and acetylene allow for proper positioning on the palladium surface. Restrained at one end, the alkyl chains in the intramolecular case are limited in geometric latitude, making correct arrangement for reaction more difficult. Additionally, palladium (II) complexes are generally square planar[88] and, as a result, the two alkyl pieces might find themselves in either a *cis* or *trans* arrangement about the metal. If only the *cis* arrangement leads to coupling and the ligands find themselves in

---

[88] Cotton, F.A. and Wilkinson, G. Advanced Inorganic Chemistry. (New York: John Wiley and Sons, 1980). pp. 950-966

trans orientation, then the energetic or geometric requirements for isomerization may be too demanding for the reaction to proceed.

Modelling studies have also helped to reveal another source of potential problems for both the copper and the palladium intramolecular coupling. The two lowest energy conformations of 1-methyl-4-N-butyl-cytosine are those wherein the N4 lone pair of electrons are aligned with the π-system of the pyrimidine (see Figure 54). Amino heterocycles typically display added stabilization for the in-plane conformers due to enhanced delocalization of the nitrogen lone pair into the π-deficient ring.[62] As seen previously, this alignment results in restricted rotation about the N4-C4 bond and the *anti* and *syn* conformations (based on the relative orientation of the N4 substituent with N3). In both the *syn* and *anti* conformations, the butyl chain extends away from the aromatic ring in the plane of the pyrimidine. With the coupling reactions, the side chain at N4 has to be brought back up above the plane of the cytosine. This would require twisting the N4-C4 bond out of the stable *syn* or *anti* conformation. Once more, the energetic requirements of such an orientation may be so imposing that the chain at N4 is rarely in a proper geometry for reaction to occur.

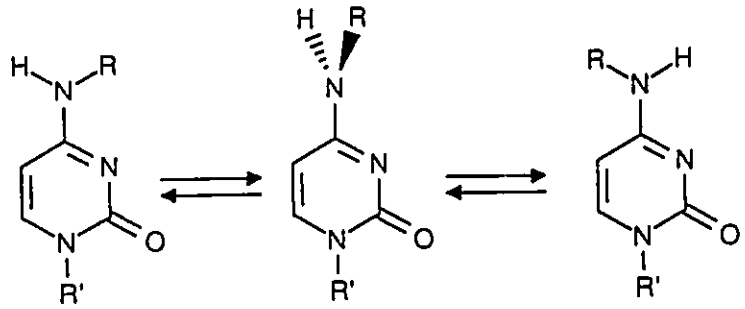

Figure 54: *Anti* and *Syn* Geometries in N4-Alkylated Cytosines

Finally, in both the palladium and copper intramolecular coupling reactions, the rate of degradation is clearly faster than that of any cyclization. Any modification of these "bridge formation via coupling" techniques must address this fundamental issue.

4.5. The "Bimolecular Bridge Formation" Approach

The final approach to cyclophane synthesis described in the Introduction is the "bimolecular bridge formation" method (Figure 13) and should be considered as a future proposal for the synthesis of a pyrimidinophane. The reaction of a dithiol with a dihalide is an excellent example of this type of strategy. In 1978, Otsubo and Misumi reported the preparation of [8]-, [9]-, [10]-, [11]-, [12]- and [14]-paracyclophanes by intermolecular coupling dihalides and dithiols (see Figure 55).[89] Subsequent oxidation of the disulphides to disulphones followed by pyrolysis yielded the desired compounds in 30 to 46% overall yield.

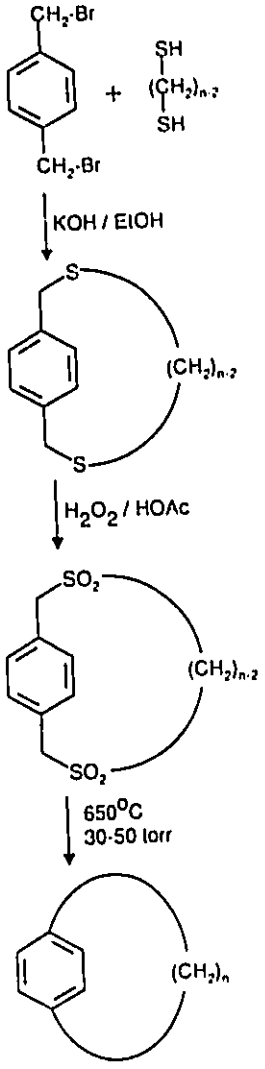

Figure 55: Paracyclophanes by Intermolecular Coupling Dihalides and Dithiols

[89] Otsubo, T. and Misumi, S. *Synth. Commun.* 8, 285 (1978)

For our purposes, though, this type of reaction is not very practical nor is it likely to produce a cyclophane suitable for the study of its magnetic anisotropy. Remember that while the first step of this approach is intermolecular, the final cyclization step involves an intramolecular process. The same problems that plagued the "intact bridge attachment" and the "bridge formation via coupling" type strategies may creep up in the final cyclization step of a "bimolecular bridge formation" approach.

Secondly, once the dihalide and dithiol are snapped together, the two sulphur atoms will become part of the aliphatic bridge. Since the presence of these heteroatoms would complicate anisotropy mapping, the sulphurs would have to be removed from the aliphatic bridge. In the paracyclophane case, the sulphur was first oxidized then extruded by pyrolysis. These pyrolytic reactions generally involve heating the compounds to 300-700°C to allow for loss of SO_2 and ring contraction.[90] It is likely, though, that the pyrimidine ring would decompose at the temperatures required for the pyrolysis.

---

[90] Vogtle, F. and Rossa, L. *Angew. Chem. Int. Ed. Eng.*, 18 515 (1979)

Chapter 5

NMR Spectroscopy and Conformational Properties of the Purine Cyclophanes

5.1. Mapping the Magnetic Anisotropy of Adenine

Figure 56 presents the room temperature NMR spectra of [8]-, [9]-, and [10]-(N6,9)-6-aminopurinophane (spectrum (a), (b) and (c), respectively). Contained within each of these spectra is information describing the magnetic environment about adenine with each bridging methylene proton providing a measurement of the magnetic field it experiences.

There are three steps involved in extracting anisotropy information from these spectra. Firstly, a complete, unambiguous assignment of the proton NMR is needed. Since the chemical shifts will ultimately furnish values for the diamagnetic susceptibility anisotropy of the heterobase, it must determined which methylene proton is giving rise to which resonance. A number of one and two-dimensional NMR techniques exist allowing for such an assignment.[91] Secondly, the spatial distribution of the protons in the bridge and their relationship to the purine system must be resolved. A measurement of the magnetic environment experienced by a proton is useless unless we know the exact region in space above the aromatic system where the proton resides. Ideally, this type of conformational information is provided by an X-ray crystal structure but in situations where crystallographic analysis is not possible, computer generated molecular models

---

[91] Derome, A. E. Modern NMR Techniques for Chemistry Research. (Oxford: Pergamon Press, 1988) and Sanders J. K. M. and Hunter, B. K. Modern NMR Spectroscopy: A Guide for Chemists. (Oxford: Oxford University Press, 1988)

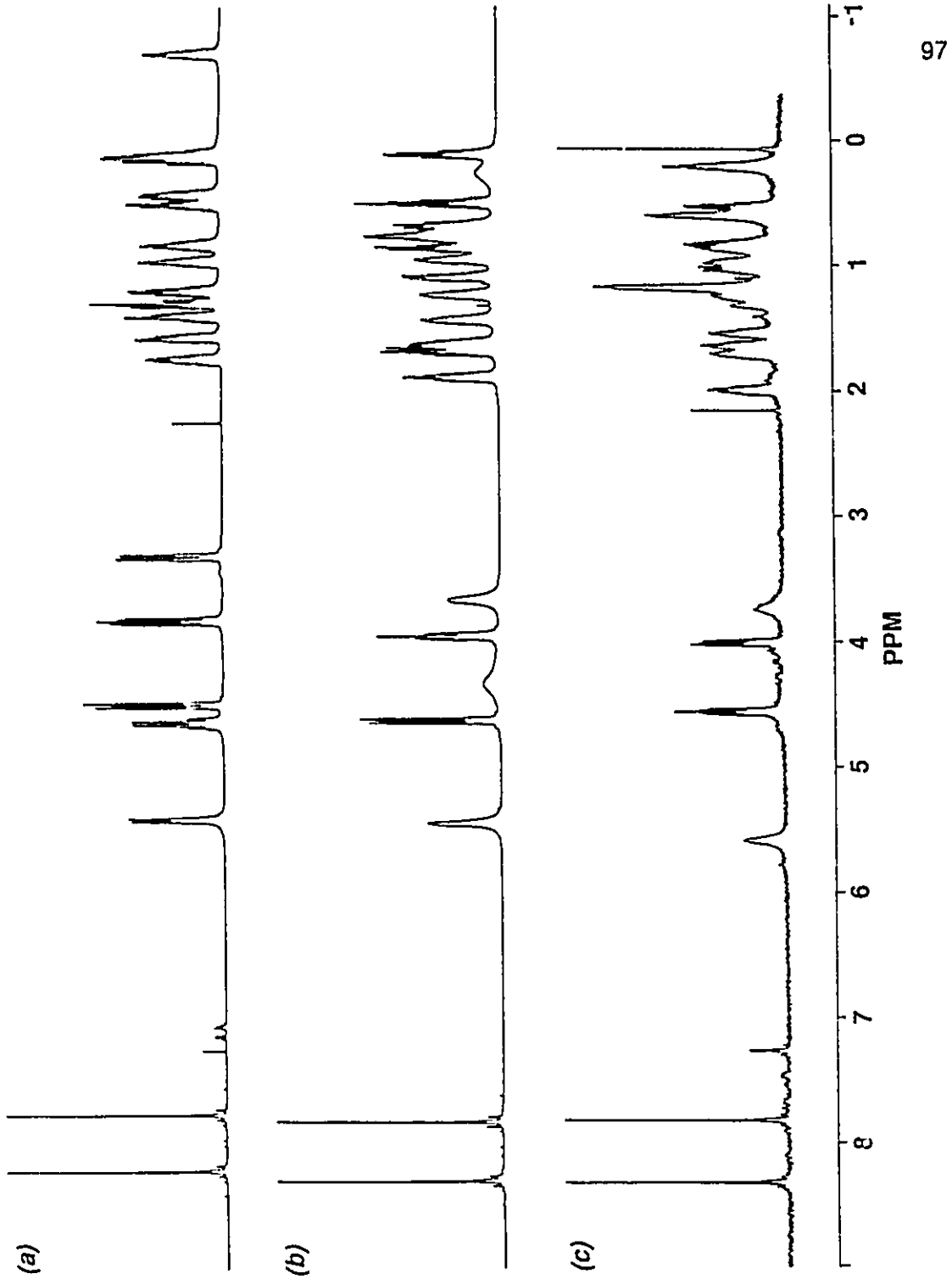

Figure 56: ^{1}H-NMR Spectra of [8]-, [9]-, and [10]-(N6,9)-6-Aminopurinophane

may be used as a "next best" approach. Finally, a link must be established between the first two steps. The geometry adopted in solution, as recorded by the NMR spectrum, must be shown to be the same as that determined in the solid state or by conformational computation. Solid state NMR is often used as a bridge between the solution and solid state. Alternatively, if the coupling constants of the various spin systems can be sorted out, the dihedral angles calculated using Karplus' equation (*vide infra)* can be compared with those acquired from the X-ray structure or the computer model. Once all this information has been assimilated, one can provide an experimentally determined description of the diamagnetic shielding anisotropy of adenine.

The present chapter will deal mainly with the NMR spectroscopy and structural characteristics of the adenine cyclophane series. Some of the interesting dynamic properties of the molecules displayed in the NMR will be also presented. Finally, the ultraviolet spectroscopy of the purinophanes will be discussed.

5.2. NMR Spectroscopy and Conformational Properties of [8]-(N6,9)-6-Aminopurinophane

Studies by Bell and Hunter involving structural determination and NMR spectroscopy of the octamethylene adenine cyclophane provide us with an excellent example of how the methodology described above can be successfully applied. While the specific details concerning their investigations may be found elsewhere[35,36,37], use of their results in this and the subsequent chapter warrants a summary of their findings. What follows is an overview of the steps involved in unravelling the NMR and crystal structure of [8](N6,9)-6-aminopurinophane which will serve as an introduction to the techniques

applied.

The diffraction studies and conformational analysis of [8]-(N6,9)-6-aminopurinophane have been published[35] and provide the spatial distribution information needed for anisotropy mapping. A SNOOPI plot of the molecule appears in Figure 57 along with its atomic numbering. Note that the bridging carbons are denoted by the prime symbol (') and are numbered sequentially beginning at N6. Comparisons performed by Hunter[37] demonstrated that the lowest energy minimized computer model of the cyclophane was virtually identical to the crystallographic conformation. This exercise seems to validate molecular modelling as a useful tool for the conformational analysis of these adenophanes. The cartesian coordinates of the X-ray structure appear in Table 1 of Appendix B.

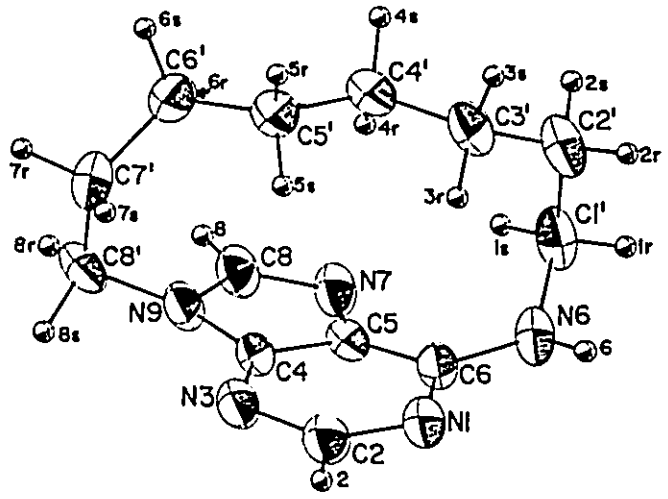

Figure 57: SNOOPI Plot of [8]-(N6,9)-6-Aminopurinophane

As seen in Figure 56, the proton NMR spectrum of the C8-cyclophane clearly shows all eight geminal pairs of diastereotopic methylene protons ranging in chemical shift from -0.6 ppm to 4.8 ppm. Compared to the C9 and C10 analogues, the proton resonances of octamethylene cyclophane were adequately separated with well defined

splitting patterns and, consequently, a few assignments could be made upon inspection of the [8](N6,9)-6-aminopurinophane spectrum. The H8 and H2 protons of the adenine moiety appeared at 8.21 and 7.76 ppm respectively while the broad doublet at 5.40 ppm was due to the amino proton bonded to N6. The inductive character of nitrogens at the 6 and 9 positions shifted the resonances of the protons attached to C1′ and C8′ downfield to between 3 and 5 ppm separating them from the other methylene bridge signals. Based on splitting patterns resulting from coupling to the nitrogen H6 proton, the chemical shifts at 3.35 and 4.49 ppm were assigned as the C1′ methylene protons, leaving the C8′ protons at 4.55 and 3.92 ppm. Note that these assignments were in keeping with those of the standard compounds studied. The remaining signals between 1.80 and -0.69 ppm could not be assigned quite so easily and had to be sorted out using two-dimensional (2D) NMR techniques.

The 2D heteronuclear chemical shift correlated experiment (HETCORR), most often used for ^{1}H and ^{13}C, is a popular technique among NMR spectroscopists for structure elucidation.[91] Exploiting the one bond ^{1}H-^{13}C couplings, this experiment directly shows which protons are attached to which carbon atoms. The results are generally presented as a contour map with a 1D ^{13}C spectrum along the horizontal axis (the F2 frequency domain) and a 1D ^{1}H spectrum along the vertical (the F1 frequency domain) (for an example of a HETCORR spectrum, please see Figure 59). Correlations appear as cross peaks in the spectrum at the intersections of the proton F1 frequency and the F2 frequency of the bonded carbon. Geminal pairs can be easily picked out since both protons show correlation to the same carbon. The pulse sequence used in the experiment incorporates broadband proton decoupling (ie. proton-proton coupling is removed) and

allows for ^{13}C-^{1}H decoupling (ie. carbon-proton coupling is not seen). As a result, reasonably good values for the proton chemical shifts can be obtained (depending on the amount of digital resolution employed in the acquisition of the spectrum) uncluttered by the superimposed coupling seen in the regular proton spectrum. The HETCORR experiment was carried out on the octamethylene adenine cyclophane and the results examined in order to obtain the chemical shifts of the bridge protons and identity of the geminal proton pairs.[92]

The COSY (COrrelated SpectroscopY) experiment is one of the most commonly used homonuclear shift correlated two dimensional NMR techniques.[93,91] An indispensable tool for structure analysis, this technique provides information about directly coupled spin systems effectively showing which nucleus is coupled to which. Once processed, the experiment can be presented as a two dimensional contour map with correlations between spin systems appearing as off-diagonal "cross peaks" (for an example of a COSY spectrum, please see Figure 60).

The COSY experiment was performed on a sample of [8](N6,9)-6-aminopurinophane. The information obtained from the HETCORR (the proton chemical shifts and geminal pair data) was first marked out on the COSY spectrum and then, beginning at either end of the aliphatic bridge (the C1′ or C8′ protons), the coupling correlations displayed in the spectrum allowed for the determination of neighbouring protons. Proceeding sequentially along the bridge, all the proton signals could be

---

[92] The curious artifacts found in the HETCORR spectra of [8]-(N6,9)-6-aminopurinophane have been studied. Interested readers are referred to Bain, A.D., Hughes, D.W. and Hunter, H.N. *Mag. Res. Chem.* 26, 1058-1061 (1988).

[93] Bax, A. and Freeman, R. *J. Mag. Res.*, 44 542 (1981)

assigned with respect to their position along the chain. Returning to the HETCORR with this "neighbouring proton" information allowed for complete assignment of the carbon spectrum.

Finally, assigning each methylene proton as either *pro*-R or *pro*-S[94] involved the extraction of the coupling constants buried in the individual proton spin systems and the application of modified Karplus equation[95]:

$$^3J_{HH}=7-\cos\phi+5\cos 2\phi \qquad (5)$$

As seen in the equation above, the vicinal proton coupling, $^3J_{HH}$, is dependant on the dihedral angle, ϕ. Initial estimates of the values for the various coupling constants were refined through the use of spectral simulations.[96] The $^3J_{HH}$ values were then substituted in the above equation and the value of the dihedral angle calculated. A comparison of the dihedral angles derived from Karplus' equation with those seen in the crystallographic studies not only established that the solution state and solid state conformations were identical but also permitted assignment of the chemical shifts to either the *pro*-R or *pro*-S proton. The assignments and chemical shifts for the bridge protons of [8](N6,9)-6-aminopurinophane appear in the Table 1 of Appendix B.

A few additional observations about the NMR spectroscopy of [8]-(N6,9)-6-aminopurinophane are worth noting. Attempts at bridging the solution and solid state

---

[94] Lowry, T. H. and Richardson, K. S. Mechanism and Theory in Organic Chemistry. (New York: Harper and Row, 1987). p.133

[95] Bothner-By, A. A. *Adv. Magn. Res.*, 1 195 (1965); Karplus, M. *J. Amer. Chem. Soc.* **85**, 2870 (1963) and Karplus, M. *J. Chem. Phys.* **30**, 11 (1959)

[96] Parameter Adjustment in NMR by Iterative Calculation (PANIC.81) Program. Bruker Spectrospin, 1981.

geometry of the octamethylene cyclophane by solid state NMR were unsuccessful. The quadrupolar moments of the ^{14}N atom found in the purine system gave rise to an electric field gradient at the nuclei and provided a highly efficient relaxation mechanism for the ^{13}C carbons found in the methylene bridge. Although of minimal influence in solution NMR, the effect broadened the solid state spectrum of [8]-(N6,9)-6-aminopurinophane to such an extent that assignments became impossible.

A variable temperature NMR (VT-NMR) study demonstrated that the chain of [8]-(N6,9)-6-aminopurinophane assumed only one conformation over a wide range of temperatures. None of the *anti / syn* isomerization seen in the C9 and C10 homolog VT-NMR (*vide infra*) was witnessed in the octamethylene case. It would seem that the octamethylene chain was sufficiently taut so as to assume only one conformation.

5.3. NMR Spectroscopy and Conformational Properties of [9]-(N6,9)-6-Aminopurinophane

The ^1H-NMR spectrum of the nonamethylene adenine cyclophane recorded in $CDCl_3$ at 25°C is illustrated in Figure 58 (spectrum (b)). With chemical shifts ranging from δ 4.53 to -0.01, many of the 9 diastereotopic bridge proton pairs appeared as well resolved multiplets while others were broadened to various degrees. In contrast to its C8 homolog, much of the fine structure of the [9]-(N6,9)-6-aminopurinophane spin systems had been lost. The splitting of the C1′ protons by H6 as seen in the octamethylene purinophane spectrum (Figure 56, spectrum (a), 3.35 and 4.49 ppm), for example, disappeared in the [9]-(N6,9)-6-aminopurinophane NMR (3.65 and 4.35 ppm). Such behaviour is characteristic of an exchange process operating in an intermediate rate

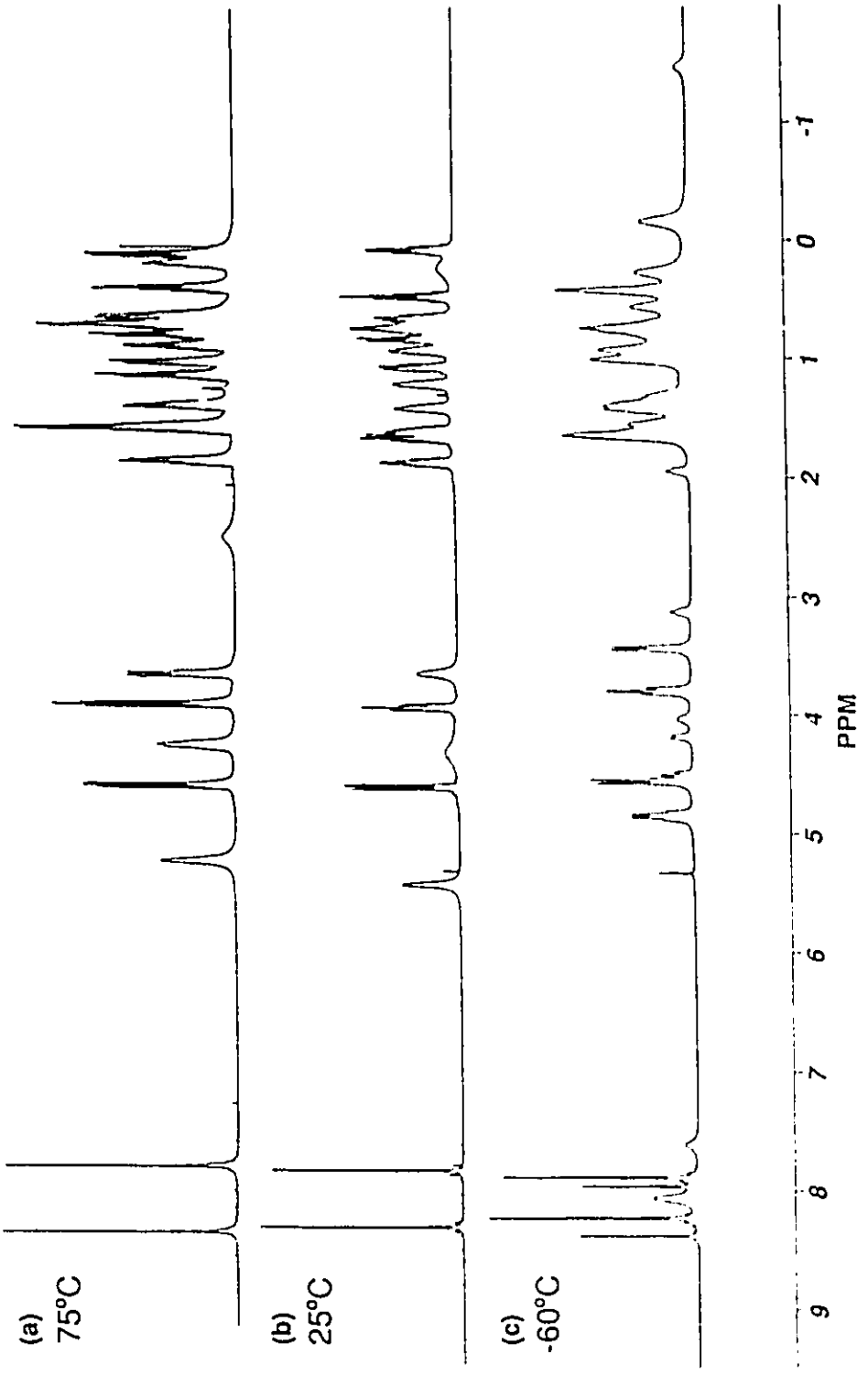

Figure 58: ^{1}H-NMR Spectra of [9]-(N6,9)-6-Aminopurinophane

region and indicated that the methylene chain was undergoing interconversion between two or more conformers. Although some assignments were made based on comparisons to N6-aminononyl-purine, 9-nonyladenine and N6-aminononyl-9-nonyl-purine, failure to observe some of the expected correlations in the 2D NMR experiments (a result of the conformational exchange) prevented complete spectral assignment at this temperature.

When [9]-(N6,9)-6-aminopurinophane was heated to 75°C and its spectrum recorded ($CDCl_3$, sealed tube; see Figure 58, spectrum (a)), the majority of the signals became sharp, demonstrating that the fast exchange limit had been reached. Employing the methodology developed for [8]-(N6,9)-6-aminopurinophane, assignments were made using the 2D NMR techniques described above. Figure 59 shows the ^{13}C-^{1}H heteronuclear shift correlated spectrum of [9]-(N6,9)-6-aminopurinophane at the elevated temperature. Note that all the protons clearly show correlations to the carbons to which they are bonded while the geminal pairing is apparent. Applying this information to the COSY spectrum (Figure 60) allowed for assignment with respect to position in the aliphatic bridge. The assignments appear in Table I.

Table I: ^{1}H and ^{13}C-NMR Assignments of [9]-(N6,9)-6-Aminopurinophane at 75°C (ppm)

	^{13}C	^{1}H	
C1′	42.87	4.24	3.63
C2′	30.28	1.59	1.38
C3′	24.30	1.02	0.68
C4′	26.96	0.72	0.62
C5′	27.35	0.79	0.11
C6′	27.74	0.39	0.18
C7′	24.54	1.14	0.88
C8′	27.90	1.86	1.56
C9′	44.97	4.58	3.88

Although important for NMR assignments and characterization, the high

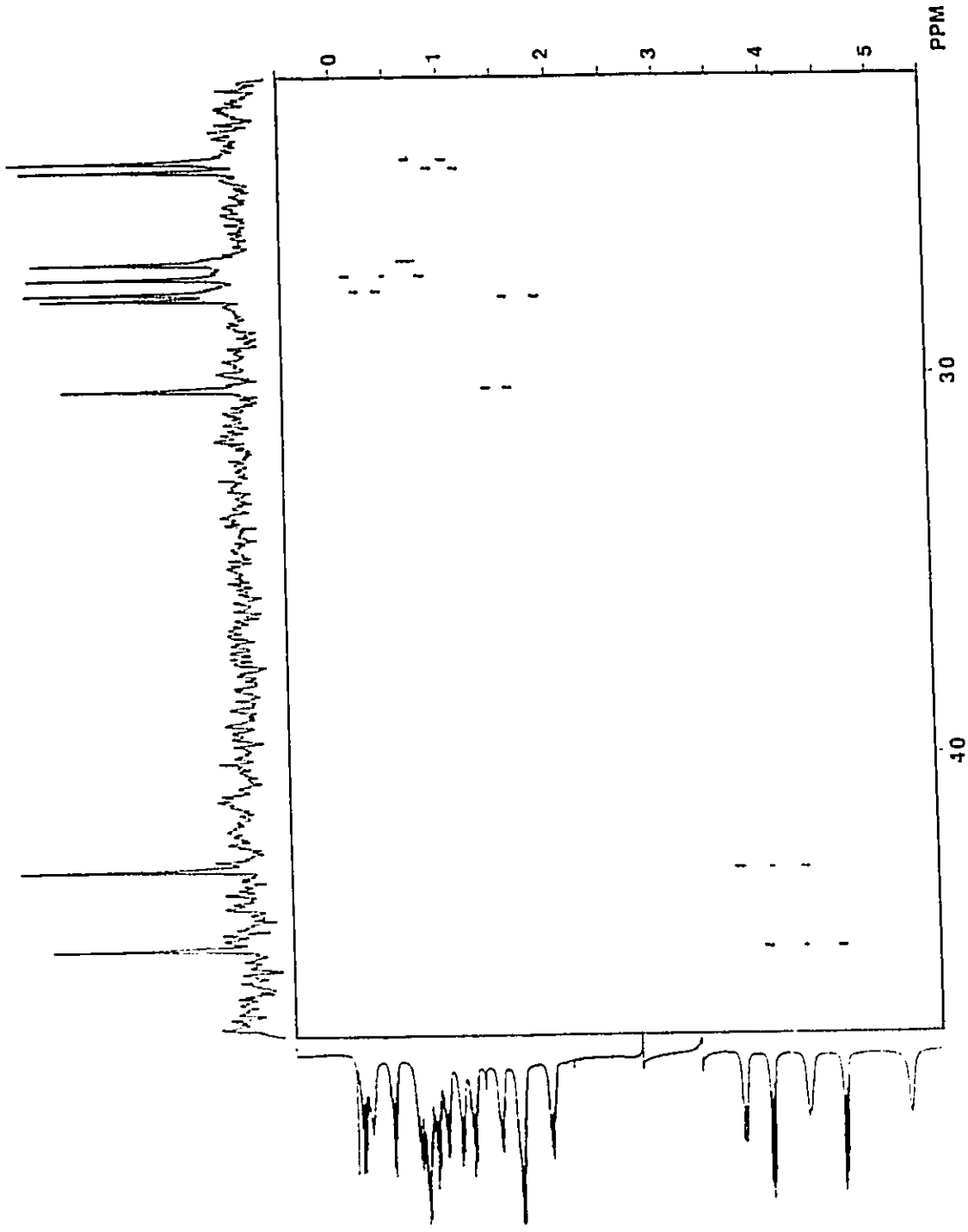

Figure 59: ^{1}H-^{13}C Shift Correlated Spectrum of [9]-(N6,9)-6-Aminopurinophane at 75°C

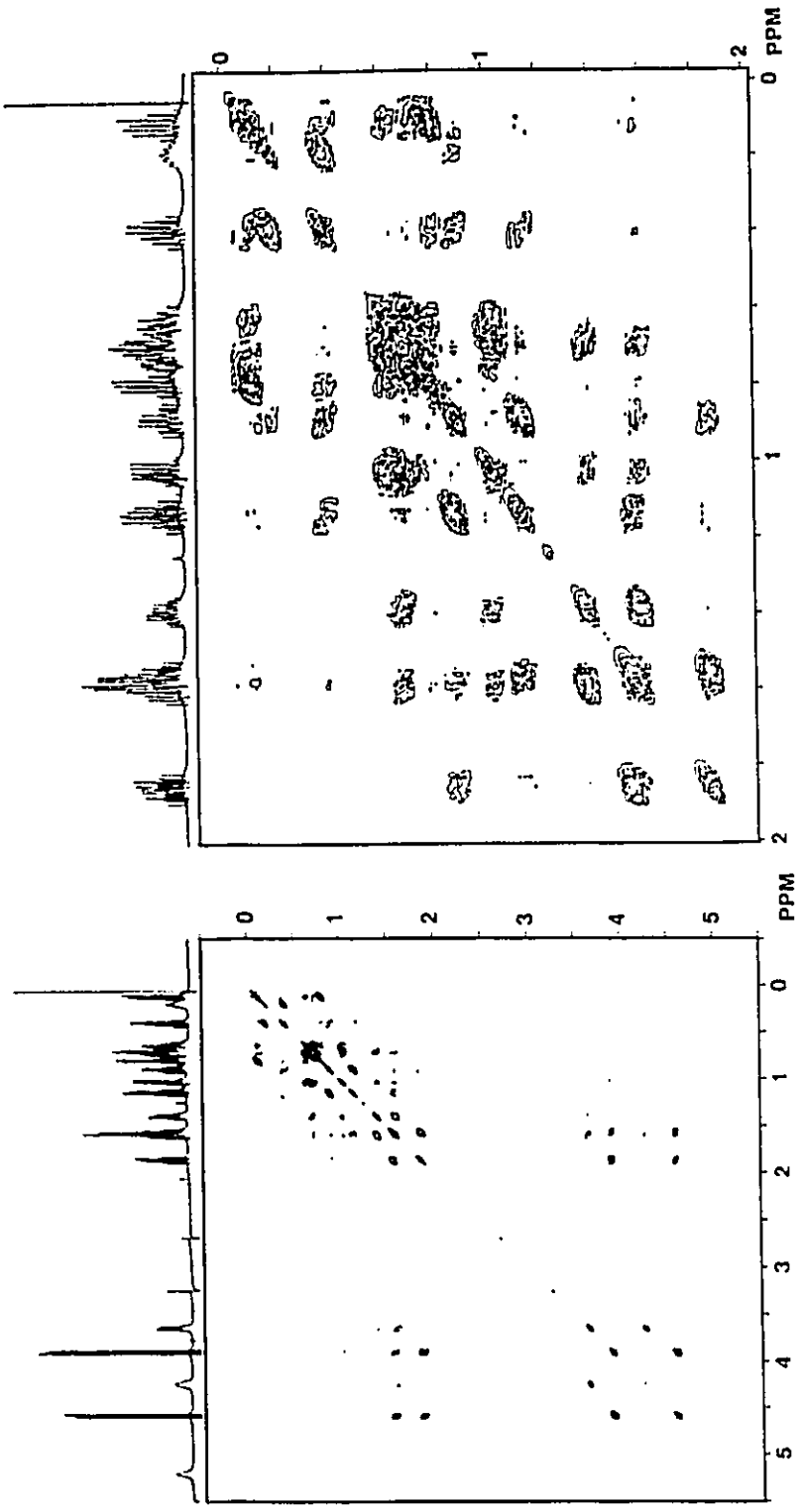

Figure 60: COSY Spectrum of [9]-(N6,9)-6-Aminopurinophane at 75°C

temperature NMR work is of little use in the study of diamagnetic anisotropy. In the fast-exchange regime, interconversion between the conformations is so rapid that the observed spectrum represents a species which is an average (with respect to chemical shifts and coupling constants) of the individual conformers. The structure of this average is a composite of two (or more) conformers and is difficult to define with respect to the relative population of each conformer present as well as their spatial positions relative to the adenine ring.

The low temperature ^{1}H-NMR spectrum of [9]-(N6,9)-6-aminopurinophane (CCl_2D_2:$CFCl_3$ solvent), on the other hand, was especially informative and showed the presence of two "frozen" conformers (see Figure 58, spectrum (c)). At -59.5°C, two species, unequal in population, were clearly evident. Most pronounced were the two sharp singlets, a set for each conformation, corresponding to H2 and H8 on the purine ring between δ 7.7 and 8.4. Signals from the aliphatic chain, at this temperature, ranged from δ 4.84 to -1.30. While the methylene hydrogens of C1′ and C9′ for each conformer were reasonably well resolved, the significant broadening seen in the high field resonances is likely a result of residual exchange of protons in very different chemical shift environments. In comparing the spectra in Figure 58, two curious features of the low temperature spectrum are worth noting. Firstly, the shift to lower field of the NH resonances as the temperature drops is quite dramatic. While all the protons did experience a chemical shift dependence with respect to temperature, the effect on the NH was most pronounced. This shift in signal to lower field is likely related to hydrogen bonding with these effects becoming more stable at lower temperatures. Secondly, the presence of a very high field signal at -1.48 ppm (at -98.9°C and shifting to lower field as the temperature increased)

is quite peculiar.

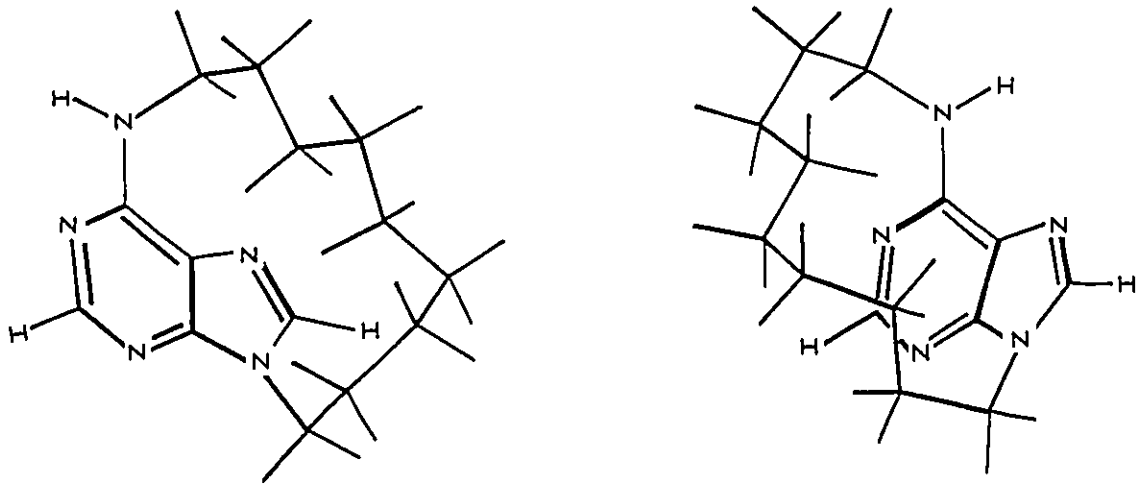

2a *anti* **2b** *syn*

Figure 61: *Anti* and *Syn* Conformations of [9]-(N6,9)-6-Aminopurinophane (bridge protons omitted for clarity)

Assignments for the two conformers observed in the low temperature spectrum of [9]-(N6,9)-6-aminopurinophane were made, again, by analysis of the 2D COSY and the 2D ^{13}C-^{1}H heteronuclear shift correlated spectra recorded at -59.5°C. Because the two conformers were of unequal population (approximately 75% of the *anti* form (**2a**) and 25% of the *syn* form (**2a**) (see Figure 61) as subsequently assigned, it was possible to use the 2D ^{13}C-^{1}H experiment (see Figure 62) to correlate each carbon in the two conformers with its attached geminal pair of diastereotopic hydrogens. The sole exception was C3′ where the correlation was too weak to be reliably distinguished from noise. The chemical shifts of C1′ and C9′ were defined by comparison with [8](N6,9)-6-aminopurinophane, (C1′ δ

Table II: ^{1}H and ^{13}C-NMR Assignments of [9]-(N6,9)-6-Aminopurinophane at -59.5°C (ppm)

	Major Conformer, **2a**			Minor Conformer, **2b**		
	^{13}C	^{1}H		^{13}C	^{1}H	
C1′	42.04	4.84	3.38	42.60	4.08	3.10
C2′	31.03	1.60	1.43	25.35	1.62	1.03
C3′	24.77	1.00	0.45	21.67	-	-
C4′	25.09	0.45	0.35	27.84	0.93	0.79
C5′	26.50	0.74	-0.09	26.64	0.70	-0.21
C6′	26.91	0.82	0.55	27.84	0.34	-1.30
C7′	22.22	1.32	0.59	25.87	1.20	0.80
C8′	25.52	1.60	1.60	30.49	1.93	1.35
C9′	45.10	4.54	3.79	44.39	4.48	4.15

43.03, C8′ δ 45.03), N6-nonyladenine (C1′ δ 40.72), and N9-nonyladenine (N9-C δ 44.48), and thence their attached pairs of protons defined. As noted above, use was then made of the 2D COSY experiment (see Figure 63) where each proton was linked with its neighbours along the chain and this procedure allowed each carbon to be assigned. Again the lack of a ^{13}C-^{1}H correlation for C3′ stopped the linking from the C1′ end of the minor conformer but it was possible to proceed uniquely from C9′ to C4′.

It should be pointed out that the 2D experiments do not permit the assignment of the *pro*-R and *pro*-S hydrogens in each diastereotopic pair. Unfortunately the severe overlaps together with the line broadening of our spectra at -59.5°C did not allow for the derivation of coupling constants of adequate accuracy for unambiguous assignments of *pro*-R and *pro*-S hydrogens via the application of the Karplus equation as described

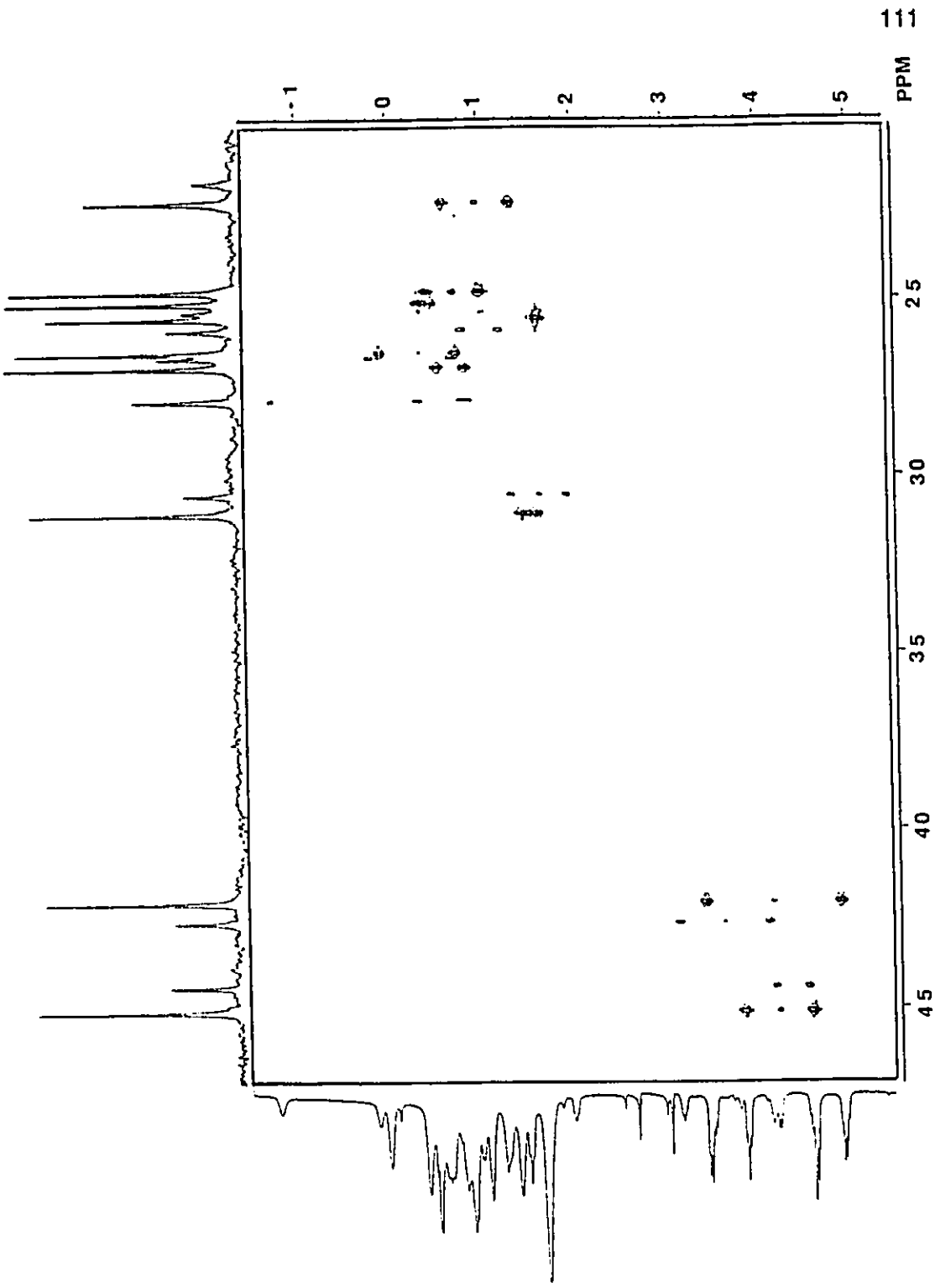

Figure 62: ^{1}H-^{13}C Shift Correlated Spectrum of [9]-(N6,9)-6-Aminopurinophane at -59.5°C

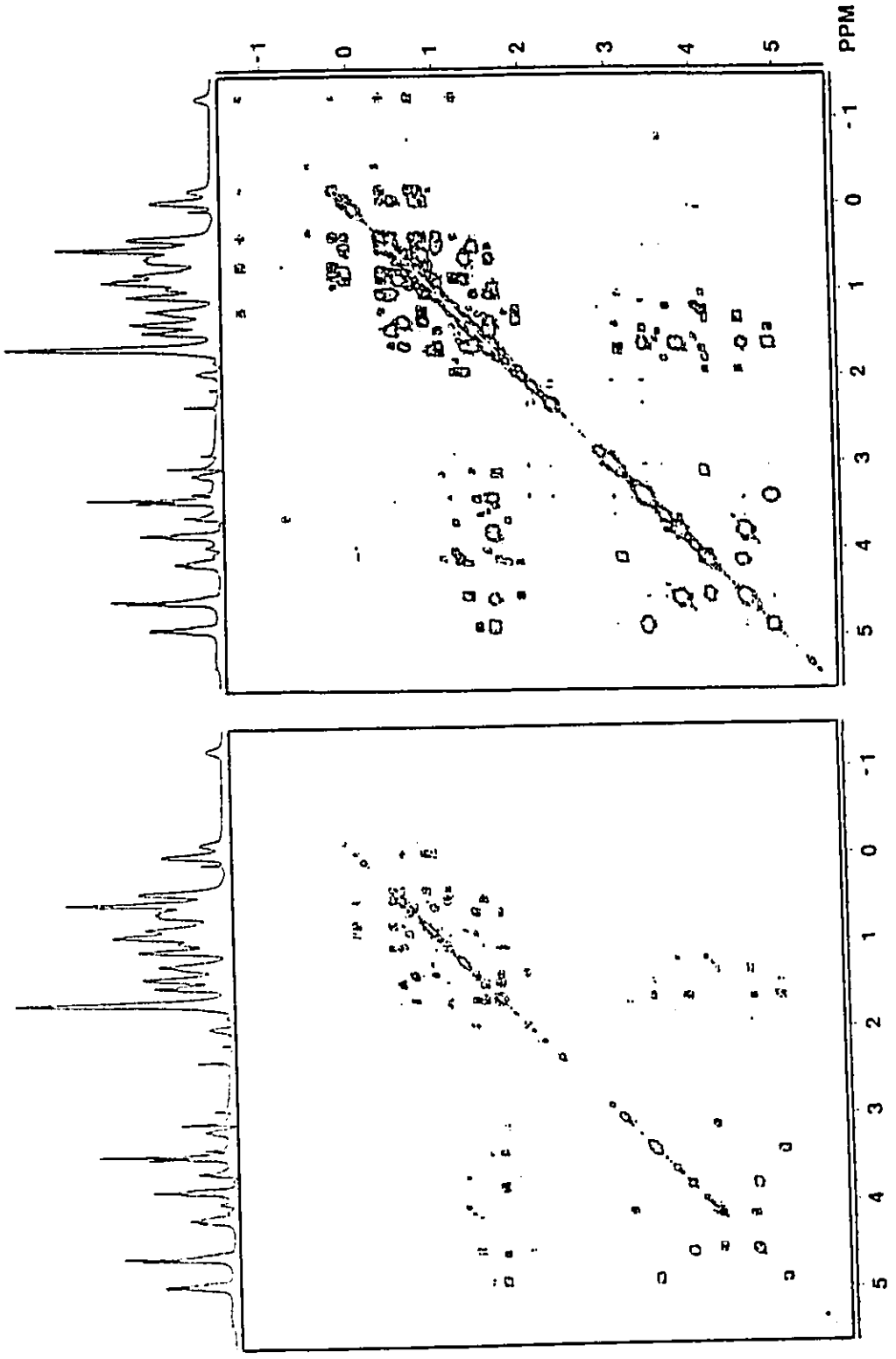

Figure 63: COSY Spectrum of [9]-(N6,9)-6-Aminopurinophane at -59.5°C

above.

To obtain the activation barrier for interconversion between the two observed conxormers, variable temperature NMR experiments were carried out over the range -98.9°C to +30°C. The H2 and H8 protons on the purine ring were the most clearly defined, well-separated singlets in the spectrum and were used for a line shape analysis.[97] Using the program DMR3[98], a series of computer-simulated spectra were matched with the actual experimental data and an exchange rate, k, was found for each temperature, T (Figure 64). The Eyring equation,

$$k=\frac{k_B T}{h} e^{\frac{(-\Delta H-T\Delta S)}{RT}} \qquad (6)$$

(where k_B=Boltzmann's constant and h is Planck's constant) was used to determine the activation parameters. A plot of ln (k/T) versus (1/T) was used to derive the enthalpy of activation, $\Delta H^{\ddagger}$, and entropy of activation, $\Delta S^{\ddagger}$, and hence the Gibbs' energy of activation, $\Delta G_T^{\ddagger}$, at any required temperature.

A linear chemical shift versus temperature change was noted for both H2 and H8 in proceeding from -98.9°C towards the coalescence temperature of these protons and this change was taken into account in calculating the activation barrier. Lineshape analysis led to a $\Delta H^{\ddagger}$=48.2 kJ/mol and a $\Delta S^{\ddagger}$=-8.0 J/mol k^{-1}. Coalescence of the signals occurred at -25°C and the $\Delta G_c^{\ddagger}$ at this temperature was determined to be 50.2 ± 2.5 kJ.mol^{-1}. Reitz

---

[97] Sandstrom, J. Dynamic NMR Spectroscopy. (London: Academic Press Ltd., 1982)

[98] Kleier, D. A. and Binsch, G. *DNMR3* (1970). Program 165. Quantum Chemistry Program Exchange, Indiana University, Bloomington, IN.

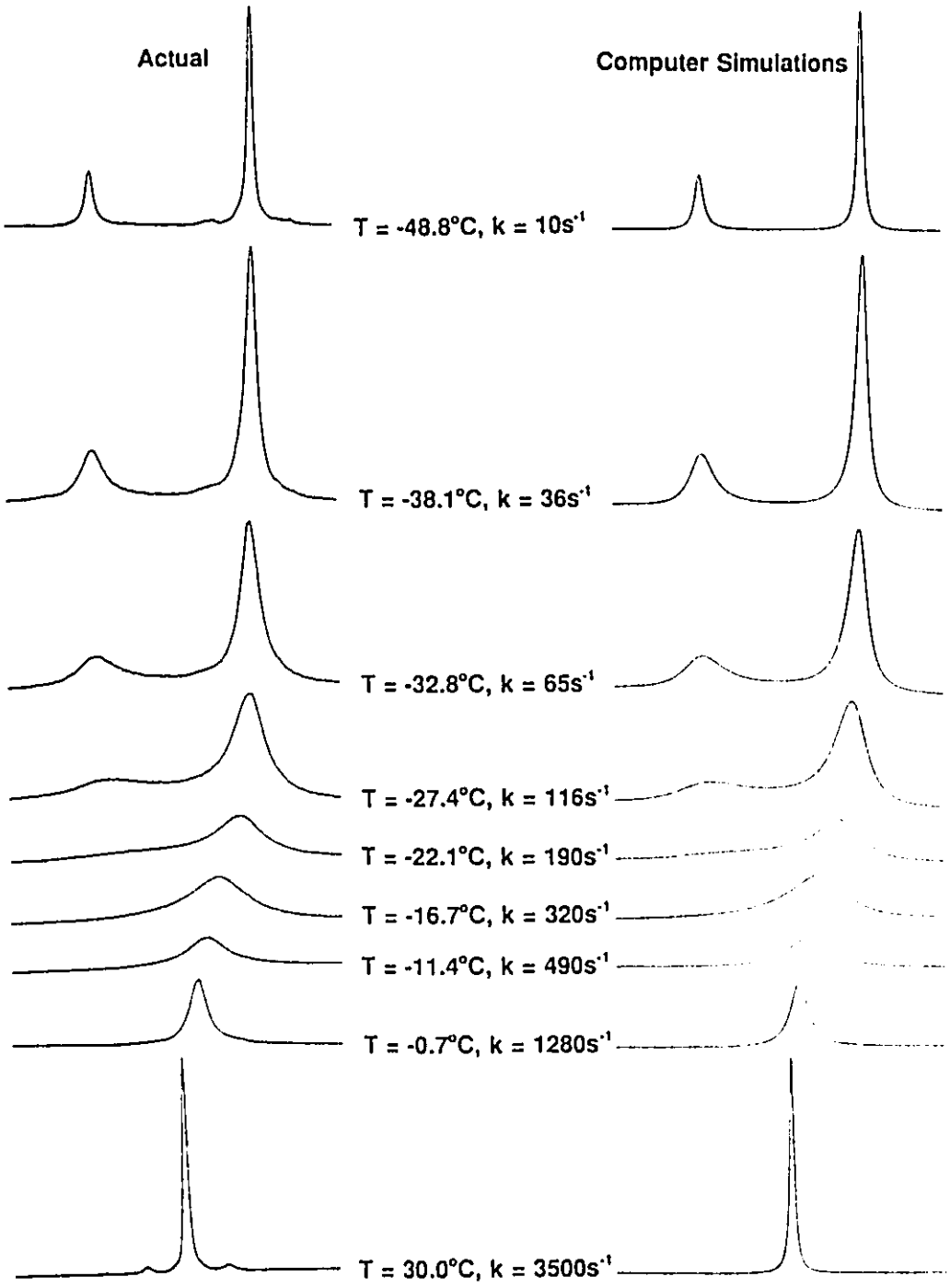

Figure 64: Variable Temperature NMR Simulations of [9]-(N6,9)-6-Aminopurinophane

et al.[62] have reported the barrier for rotation about the C6-N6 in both 9-benzyl-6-(isopropylamino)purine and 9-benzyl-6-(methylamino)purine to be 54.0 kJ.mol^{-1}. The similarity in magnitude to that obtained for [9]-(N6,9)-6-aminopurinophane strongly suggested that the two observed conformers were the result of partial rotation about the C6-N6 bond where the C1′ carbon may be *anti* (adjacent to N7) or *syn* (adjacent to N1), **2a** and **2b** respectively (see Figure 61). To further confirm this postulate, molecular mechanics calculations were performed on the two proposed conformers and the *anti* conformer was found to be 4 - 6 kJ.mol^{-1} more stable than the *syn* conformer. This relationship was consistent with that observed experimentally if the major conformer was assigned structure **2a** and the minor conformer structure **2b**. Final and convincing evidence for these assignments was obtained from the X-ray crystal structure of the nonamethylene cyclophane (*vide infra*) where it adopted the lower energy *anti* conformation. Moreover, this structure (see Figures 65 and 66) and the molecular mechanics model **2a** were found to be virtually identical, lending strong credence that the other observed conformer should be assigned *syn* structure **2b**.

It is intriguing to note that the previously reported [8]-purinophane showed only one conformation to be present in solution (the *anti* form) over a wide temperature range. The addition of one methylene unit has been sufficient to give the aliphatic bridge of the [9]-purinophane enough flexibility to permit rotation about the C6-N6 bond.

Crystallographic studies determined that the unit cell of [9](N6,9)-6-aminopurinophane contained two symmetry independent molecules (hereafter referred to as molecules A and B shown in Figures 65 and 66 with their atom labelling scheme). All crystallographic data appear in the following tables (in parentheses) located in Appendix

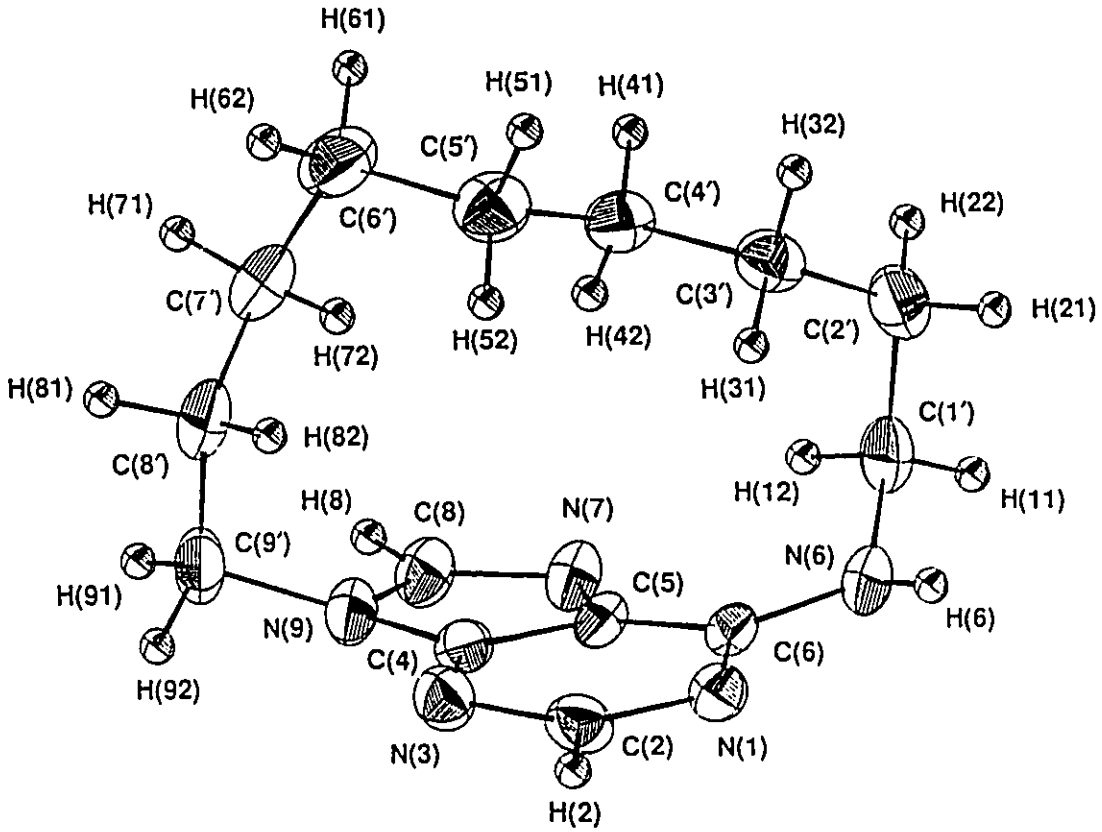

Figure 65: SNOOPI Plot of [9]-(N6,9)-6-Aminopurinophane (Molecule A)

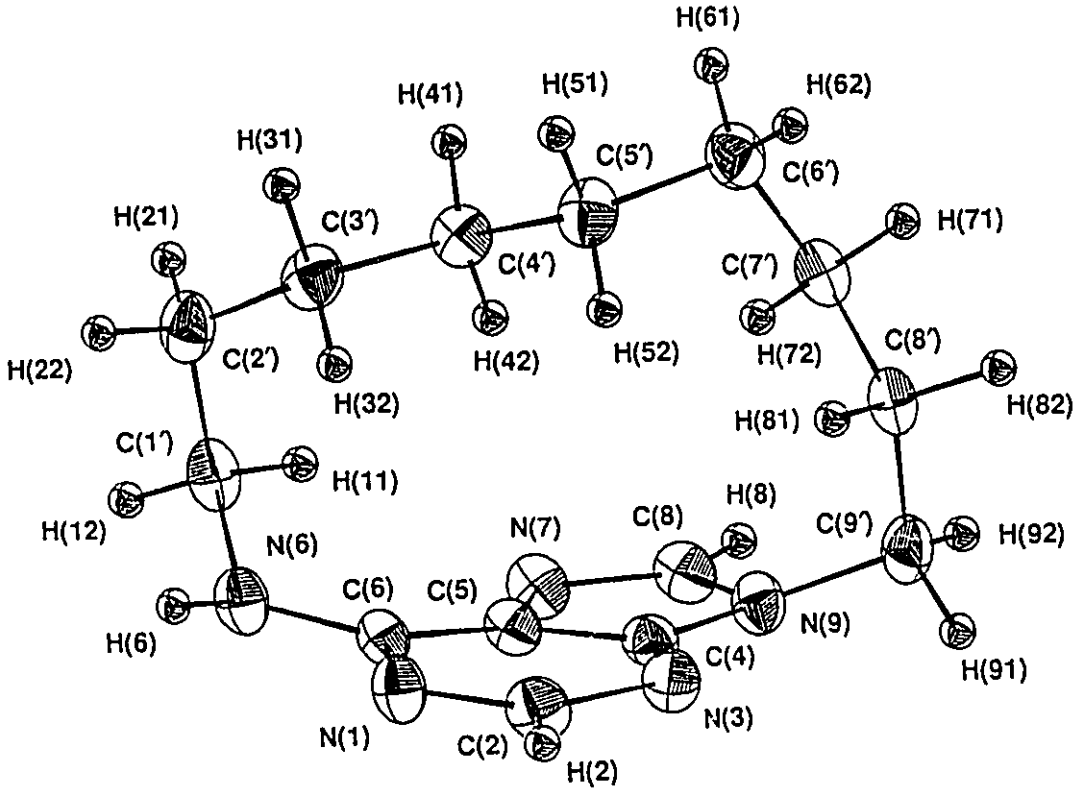

Figure 66: SNOOPI Plot of [9]-(N6,9)-6-Aminopurinophane (Molecule B)

C: crystal data and other information related to data collection (Table 1); atomic positional parameters (Table 2 and Table 3); bond lengths and angles (Table 4 and Table 5); selected dihedral and torsional angles (Table 6); least-squares mean planes (Table 7); and anisotropic temperature factors (Table 8). As may be deduced from these Tables, both molecules A and B are conformationally similar and have essentially the same geometry.

It is pertinent to compare the [9]-(N6,9)-6-aminopurinophane structural results with those obtained for [8](N6,9)-6-aminopurinophane.[35] With the addition of an extra methylene group in the aliphatic chain, one would expect the strain energy shown to be present in [8]-(N6,9)-6-aminopurinophane would be slightly less in the nonamethylene homolog; however, for both molecules A and B there are still a significant number of intramolecular non-bonding contacts less than the accepted van der Waals distances of 3.30Å, C···C; 3.20-3.25Å, C···N; 2.90-3.10Å, C···H; 2.75-3.00Å, N···H.[99] Particularly close approaches by atoms in molecule A are shown by: C(1')···C(5), 3.02; C(7')···N(9), 3.00; H(11)···C(6), 2.57; H(72)···C(8), 2.50; H(11)···N(7), 2.38; H(72)···N(9), 2.55 (all in Å); with close approaches between similar atoms in molecule B.

The bond lengths of the adenine moiety are in good agreement with [8]-(N6,9)-6-aminopurinophane and also agree well with previously published average values[100] (within 2.1σ, ($\sigma=\{\sigma_1^2+\sigma_2^2\}^{1/2}$)). Interestingly, the largest deviation found is for C(2)-N(3),

---

[99] Bondi, A. *J. Phys. Chem.* **68**, 441 (1964) and Allinger, N. L., Hirsch, J. A., Miller, M. A., Tyminski, I. J., and Van-Catledge, F. A. *J. Am. Chem. Soc.* **90**, 1199 (1968)

[100] Voet, D. and Rich, A. *Prog. Nucl. Acid Res. Mol. Biol.* **10**, 183 (1970)

2.1σ (A) and 1.6σ (B) which is consistent with that found for the octamethylene adenine cyclophane. Similarly, the bond angles are in agreement with previous adenine structures, lying within 2.9σ of the average reported values.

The adenine moiety shows the same pattern of small deviations from planarity as observed in [8]-(N6,9)-6-aminopurinophane. The dihedral angle between the mean planes through the pyrimidine and imidazole rings is 3.85(6)°, (A) and 4.47(6)°, (B) (*cf.* 5.45(9)° for the octamethylene cyclophane. This reduction in magnitude of the dihedral angle gives the impression that the twisting motion of the adenine group has been somewhat relaxed leading to a reduction in strain energy in the adenine ring system. In contrast, however, both N(6), N(6B) and C(9'), C(9'B) are displaced out of the plane of the rings to which they are attached, (in the direction of the aliphatic chain), to a greater extent than in the octamethylene homolog; (N(6), 0.325(2), N(6B), 0.362(2), C(9'), 0.577(3), C(9'B), 0.624(3), Å). If one examines the N-C-C-C and C-C-C-C torsional angles, deviations from the idealized values of 60, 120 and 180° rarely exceed 10°, (average, 9.9°, (A) and 11.0°, (B)), with the exception of one angle, C(9')-C(8')-C(7')-C(6'), (29.9°, (A) and 28.1°, (B)). It is at this position that the conformation of the aliphatic chain begins to differ from [8]-(N6,9)-6-aminopurinophane as it is being forced away from the adenine ring system. This, in turn, appears to pull C(9') further out of the mean plane. The N(1)-C(6)-N(6)-C(1') fragment adopts an *anti* conformation (as does the octamethylene adenine cyclophane) which is twisted about the N(6)-C(6) bond by approximately 35° from the plane of the purine ring. This twisting motion reduces the overlap of the nitrogen lone pair with the purine π-system. Bond lengths and angles in the aliphatic chain, (average values 1.524Å and 114.9° respectively for both (A) and (B)), are in very good agreement with average values

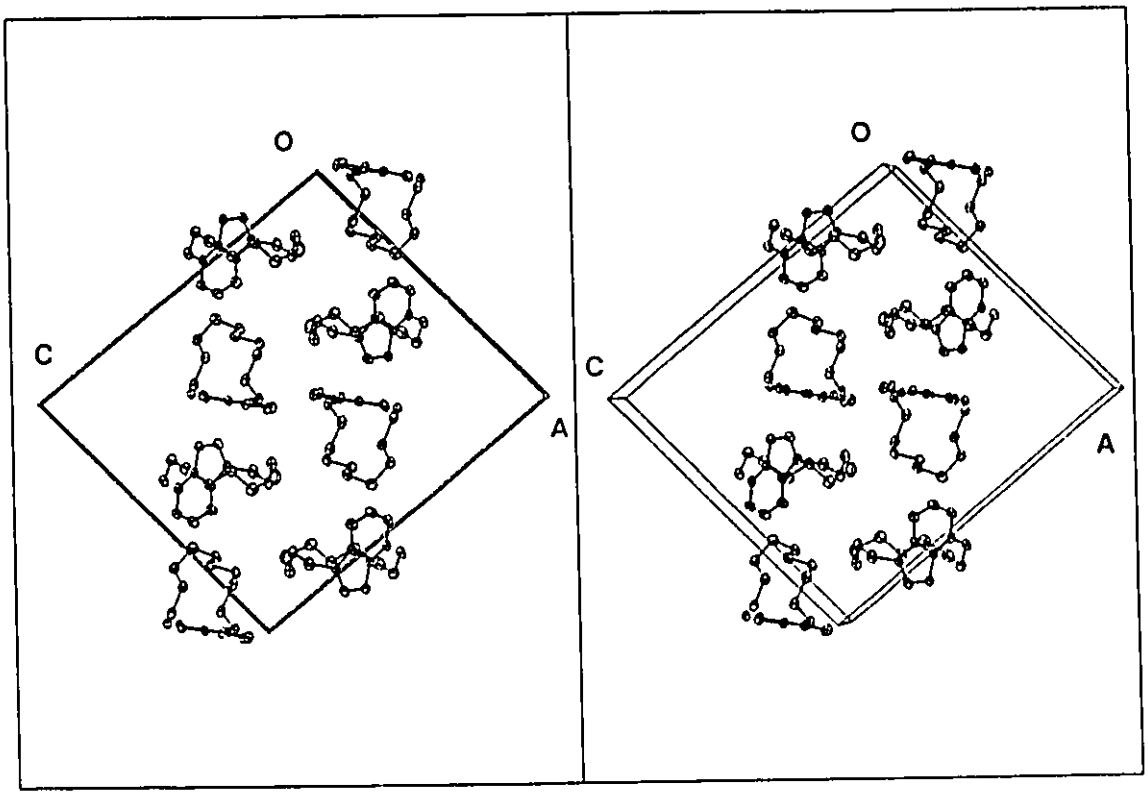

Figure 67: Stereoview of the Crystal Packing of [9]-(N6,9)-6-Aminopurinophane

reported previously.[101] A stereoview of the crystal packing is shown in Figure 67. The view is down *b*. The molecules pack in layers parallel to (-1 0 1). There are no unusual intermolecular contacts and the crystal packing appears to be dominated by van der Waals forces only.

The slightly lower barrier to rotation about C6-N6 in [9]-(N6,9)-6-aminopurinophane, when compared to the non-cyclic examples reported by Reitz *et al.*[62], warrants further scrutiny in light of the crystallographic analysis. Inspection of Dreiding models suggested the strain of the cyclophane system should increase the barrier to rotation rather than decrease it. As noted above, however, the H6-N6-C1′ fragment in the nonamethylene purinophane is twisted about the C6-N6 bond by approximately 35°, whereas, in the aliphatic examples studied by Reitz *et al.*, the ground state has this fragment essentially planar. Thus in the [9]-purinophane, the ground state energy of the system has been raised and less energy should be required to achieve rotation about the C6-N6 bond. The magnitude of the decrease is smaller (*ca* 4 kJ.mol^{-1}) than might be anticipated considering the twist is already 35° and the highest point of the barrier is presumably with a twist of 90°. However, the entire methylene chain must reorganize itself in proceeding from the *anti* to the *syn* conformation. The torsional energies associated with the reorganization contribute to the activation barrier and partially offset the increased ground state energy.

The *origin* of the barrier to rotation about the C6-N6 bond of [9]-(N6,9)-6-aminopurinophane and other N6-alkyl substituted purines has been of particular concern to chemists and the data from the crystallographic structure of the nonamethylene

---

[101] Allen, F. H., Kennard, O., Watson, D. G., Brammer, L., Orpen, G., and Taylor, R. *J. Chem. Soc. Perkin Trans.* II, S1, (1987) and Zuniga, F. J. and Chapuis, G. *Cryst. Struct. Commun.* **10**, 533 (1981)

cyclophane offer some insight into this. The barrier is generally considered to arise from destruction of the overlap of the nitrogen atom's lone pair of electrons with the electron deficient heteroaromatic ring[102] and can be depicted using the resonance picture in Figure 68.

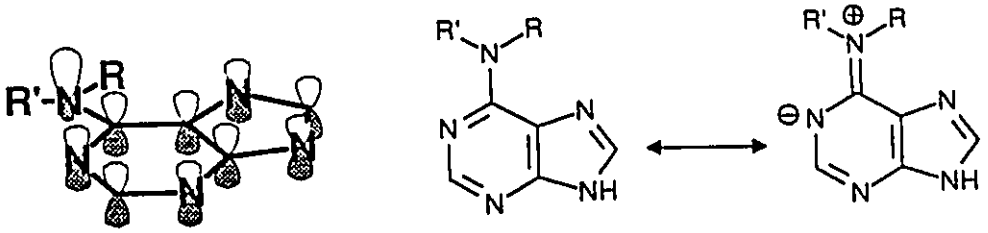

Figure 68: Resonance Structures for N6-Alkyl Adenines

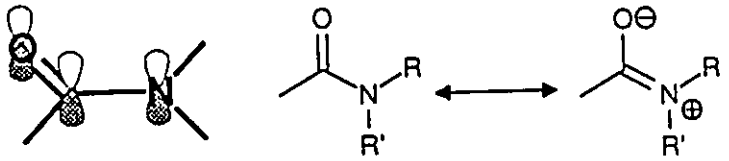

Figure 69: Resonance Structures for Amides

Similarly, the barrier to rotation in amides has been traditionally explained using resonance theory as well (Figure 69). Theoretical studies by Bader *et al.*[103] and Wiberg and Laidig[104] and experimental work by Brown *et al.*[105] have pointed out many of the

---

[102] Oki, M. Applications of Dynamic NMR Spectroscopy to Organic Chemistry. (Deerfield, FL.: VCH Publishers Inc., 1985) Chapter 2.

[103] Bader, R.F.W., Cheeseman, J.R., Laidig, K.E., Wiberg, K.B., and Breneman, C. *J. Amer. Chem. Soc.* 112, 6530-6536 (1990)

[104] Wiberg, K. B. and Laidig, K. B. *J. Amer. Chem. Soc.* 112 5935 (1987)]

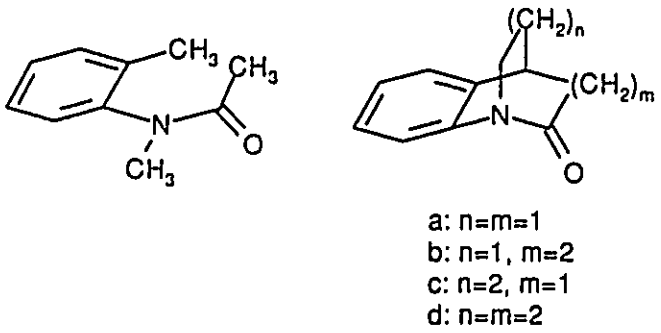

Figure 70: Anilide Series

faults with this interpretation. The resonance picture shows the lone-pair of electrons on the nitrogen donated to the carbonyl moiety. The overall result is a planar geometry for the amide as well as a shorter N-C and a longer O-C bond than structures without this conjugative ability. Interestingly, though, a review by Brown and co-workers involving the X-ray structural data for a series of anilides (see Figure 70) points out that they do not show the predicted bond changes. The anilide structures shown are unique amides in that the lone pair on nitrogen is unable to conjugate with the carbonyl moiety being twisted out of alignment with the C=O π system. In passing from monocyclic to tricyclic compounds shown (Figure 70), the N-C bond length increases only marginally while the C=O bond length is scarcely affected.

The theoretical studies by Bader and co-workers on substituted amides suggests that it is the movement apart of the two atoms about which rotation is taking place and the consequent changes in the electron-nucleus attractions and electron-electron repulsions that is the principal contributor to the activation barrier. For a planar amide, rotation about

---

[105] Bennet, A. J., Wang, Q.-P., Slebocka-Tilk, H., Somayaji, V., Brown, R. S. and Santarsiero, B. D. *J. Am. Chem. Soc.* **112**, 6383 (1990)

the C-N bond results in lengthening of this bond and pyramidalization of the N atom as the energy maximum is reached. This interpretation is consistent with Brown's experimental findings.

6-Aminopurines contain an amidine system (N1-C6-N6) and are entirely analogous to an amide. Thus, X-ray crystallographic studies of a number of N9-substituted 6-aminopurines show the average length of the C6-N6 bond to be 1.337Å[106] and show the N and H atoms of the $-NH_2$ group to be basically coplanar with the heteroaromatic ring, the N atom being only 0.01 to 0.09Å out of the C6-H61-H62 plane.[107,108,109,110,111] The N6 atom may be regarded as essentially sp^2 hybridized, as its chemical properties testify. Note that a fully pyrimadalized (or sp^3 hybridized) N, as in dimethylamine, places the N atom 0.41Å out of the basal C-C-H plane. Mono substitution of N6 with carbon groups causes small changes to this basic geometry.[112,113,114,115] The C6-N6-$C_{subst.}$ angle increases slightly to 121-123° while the average C6-N6 bond length becomes

---

106 Taylor, R. and Kennard, O. *J. Mol. Struct.* **78**, 1 (1982)

107 Bunick, G. and Voet, D. *Acta Cryst.* **B30**, 1651 (1974)

108 Lai, T. F. and Marsh, R. E. *Acta Cryst.* **B28**, 1982 (1972)

109 Sprang, S., Rohrer, D. C. and Sundaralingam, M. *Acta Cryst.* **B34**, 2803 (1978)

110 Kistenmacher, T. J. and Rossi, M. *Acta Cryst.* **B33**, 253 (1977)

111 Sheldrick, W. S. and Morr, M. *Acta Cryst.* **B36**, 2328 (1980)

112 Sternglanz, H. and Bugg, C. E. *J. Cryst. and Mol. Struct.* **8**, 263 (1978)

113 Thewalt, U. and Bugg, C. E. *Acta Cryst.* **B28**, 1767 (1972)

114 Bugg, C. E. and Thewalt, U. *Biochem. Biophys. Res. Commun.* **46**, 779 (1972)

115 McMullan, R.K. and Sundaralingam, M. *J. Am. Chem. Soc.* **93**, 7050 (1971)

1.341Å. There is no change, however, in the slight pyramidalization of the N atom as it ranges from 0.00Å[113] to 0.05Å[112] out of the plane defined by C6-H6-$C_{subst.}$ [8]-(N6,9)-6-Aminopurinophane is unique in having a 35° rotational twist enforced upon the C6-N6 bond and as such, it represents a test of the Bader-Wiberg theory for this class of compounds. From Table 4 in Appendix C, the average C6-N6 bond length for molecules A and B of [9]-(N6,9)-6-aminopurinophane is 1.347Å, a value at the upper end of the accepted average magnitude for this bond and scarcely convincing evidence for the theory. However, against this must be set the distinct pyramidalization of N6 which is 0.25Å out of the C6-H6-C1′ plane in molecule A and 0.22Å from the corresponding plane in molecule B. That is, N6 is over 50% pyrimadalized, a situation fully consistent with the Bader-Wiberg proposals.

The crystallographic data for [8]-purinophane also showed the H6-N6-C1′ fragment twisted with respect to the purine ring by 30°. Inspection of the data show the N6 atom again is pyrimadalized appreciably, being 0.23Å out of the C6-H6-C1′ plane but, as in the [9]-purinophane, the C6-N6 bond length of 1.349Å is only marginally longer than the average. Evidently, for this class of compounds rotation about the exocyclic C6-N6 bond is accompanied by strong pyramidalization but the extent of bond lengthening is much less distinctive than is observed for the amide cases.[105]

The utility of [9]-(N6,9)-6-aminopurinophane for anisotropy mapping is limited since there is no clear link between the NMR spectra and the geometry of the species giving rise to them. While there is good reason to believe that the *anti* and *syn* conformations generated by computer modelling are, in fact, the two species seen in the low temperature NMR, there is no definitive proof. This type of problem provides the impetus for the

development of a method to calculate the chemical shifts of these purinophanes. The following chapter will deal with this issue.

5.4. NMR Spectroscopy and Conformational Properties of [10]-(N6,9)-6-Aminopurinophane

The exceedingly cluttered ^{1}H-NMR spectrum of [10]-(N6,9)-6-aminopurinophane at 30°C (in $CDCl_3$) was further complicated by extensive broadening of resonances (Figure 71, spectrum (b)). This was not unexpected since conformation flexibility of the aliphatic chain should increase with each additional methylene. Within this exchange regime, attempts to assign the spectra using the regular 2D NMR experiments failed due to the lack of correlations. Note, for example, that one of C1′ protons is not seen (denoted by an arrow in Figure 71, spectrum (b)) until the sample (in $CDCl_3$) is warmed up to 90°C (see arrow in Figure 71, spectrum (a)). At this elevated temperature, the spectrum showed a marked improvement with many of the signals sharpening up and the appearance of some fine structure. Proton assignments were, once again, made possible through the application at 90°C of a HETCORR and a COSY spectrum and

Table III: ^{1}H and ^{13}C-NMR Assignments of [10]-(N6,9)-6-Aminopurinophane at 90°C (ppm)

	^{13}C	^{1}H	
C1′	42.2	3.79	4.43
C2′	31.5	1.54	1.73
C3′	29.6	1.24	1.41
C4′	29.0	0.96	1.32
C5′	28.1	0.61	0.77
C6′	28.9	1.11	1.18
C7′	28.9	0.30	0.59
C8′	25.8	1.12	1.21
C9′	29.1	1.64	2.04
C10′	44.7	3.96	4.57

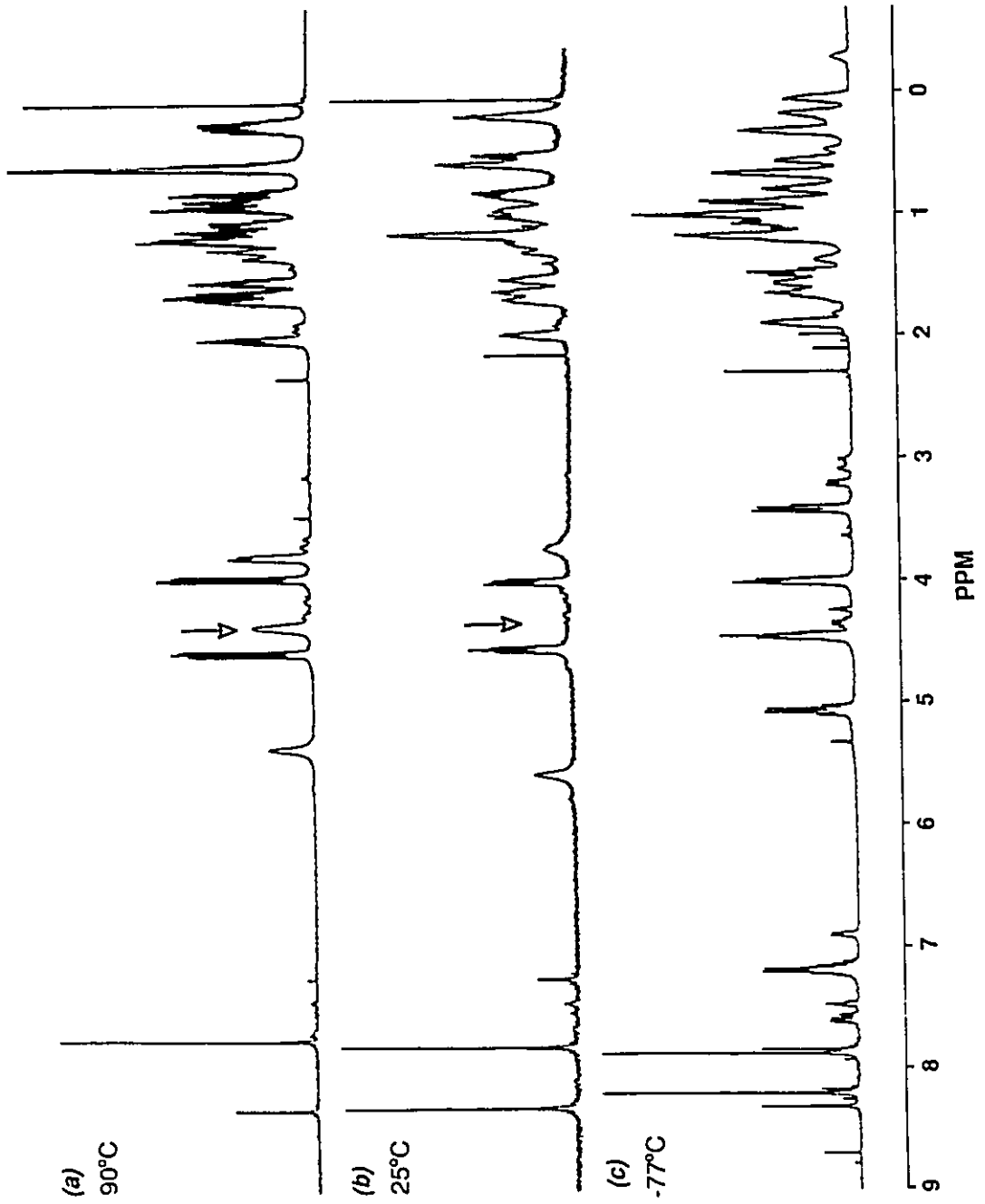

Figure 71: ^{1}H-NMR Spectra of [10]-(N6,9)-6-Aminopurinophane

appear in Table III.

The NMR work carried out at lower temperatures revealed that [10]-(N6,9)-6-aminopurinophane could adopt a number of conformations; for example, at -77°C in $CFCl_3$:CD_2Cl_2 (Figure 71, spectrum (c)), the multiple signals within the aromatic region revealed the presence of at least 4 conformations. The four major resonances at 8.29, 8.19, 7.90 and 7.88 ppm are likely due to the *anti / syn* isomerization about the N6-C6 bond (compare these signals with those seen in the low temperature [9]-(N6,9)-6-aminopurinophane NMR spectrum (Figure 58, spectrum (c)). Once again, the *anti* conformer is preferred by approximately 4:1 over the *syn* orientation. The presence of these additional conformers, some with intensities comparable to the minor *syn* isomer, made it impractical to use simply intensity techniques to assign signals.

A variable temperature NMR study was undertaken to provide the activation parameters associated with the interchange between the major conformers. The low field signals (H8) were the focus of the line shape analysis (*vide supra*) and were monitored from -77°C to 30°C. Coalescence of the lines occurred at -20°C and the $\Delta G_c^{\ddagger}$ at this temperature was determined to be 59.4 ± 5.5 $kJ.mol^{-1}$. With a number of minor conformers coalescing about the peaks of interest, the matching of simulated spectra with the actual peaks became quite difficult and is reflected in the rather large error associated with the activation parameter.

It may be recalled that Reitz *et al.*[62] had reported the barrier for rotation about the C6-N6 in their substituted adenine examples of about 54.0 $kJ.mol^{-1}$, while [9]-(N6,9)-6-aminopurinophane showed a Gibbs' energy of activation of 50.2 $kJ.mol^{-1}$. The high $\Delta G_c^{\ddagger}$ for the decamethylene cyclophane is likely due to a combination of two effects. Unlike the

H6-N6-C1′ fragment in C9 homolog which twisted about the C6-N6 bond, the longer chain length of the decamethylene cyclophane may allow this fragment to assume a more planar geometry. The barrier for rotation in [10]-(N6,9)-6-aminopurinophane, therefore, is likely to be more in keeping with the Reitz examples wherein the N6 nitrogens assume a more sp^2 type of hybridization. Secondly, the torsional energy contributions associated with the reorganization of the methylene chain in proceeding from the *anti* to the *syn* conformation will add to the activation energy of the decamethylene purinophane.

Conformational studies on the [10]-(N6,9)-6-aminopurinophane proved quite frustrating. Crystals suitable for X-ray analysis could not be obtained despite attempts to recrystallize them from a variety of solvents. Crystals grown from toluene appeared normal but did not diffract. The computer modelling exercises undertaken were not as conclusive as in the octamethylene and nonamethylene cyclophane cases. The conformational freedom conferred by the additional methylene in [10]-(N6,9)-6-aminopurinophane allowed the chain to adopt a number of geometries very similar in energy and, as a result, many conformations were obtained with different structures but similar energies.

Ultraviolet spectroscopy performed on the purinophanes and a series of substituted adenines afforded some insight into the structural characteristics of these molecules. The spectra were recorded using absolute methanol as the solvent and the results are presented in Table IV.

Note that the spectra are characterized by two transitions. Alkylation at N9 in adenine seemed to have little effect on the appearance of the spectrum with the absorptions of N9-nonyladenine effectively unchanged from those of adenine. On the

Table IV: Ultraviolet Spectra of Alkyl Adenines and [n]-(N6,9)-6-Aminopurinophanes

Compound	$\lambda_{(max)}$	
adenine	207.1 nm	260.5 nm
N9-nonyladenine	205.9 nm	261.1 nm
N6-nonyladenine	209.9 nm	268.5 nm
N6, N9-dinonyladenine	209.1 nm	268.7 nm
[8]-(N6,9)-6-aminopurinophane	217.5 nm	278.3 nm
[9]-(N6,9)-6-aminopurinophane	216.2 nm	276.2 nm
[10]-(N6,9)-6-aminopurinophane	213.0 nm	273.0 nm

other hand, substitution at N6 seemed to have a major effect on the low energy transition (268.5 nm in N6-nonyladenine compared to 260.5 in adenine) and a marginal effect on the high energy transition. The low energy transition, therefore, seemed to result from the excitation of an electron from the N6 lone pair in a non-bonding molecular orbital to an unoccupied π^* molecular orbital. The high energy transition was likely a result of a $\pi \rightarrow \pi^*$ excitation.

The cyclophane series of UV spectra were markedly different from that of the N6, N9-dinonyladenine standard. The bathochromic shift (ie. shift to longer wavelength) as the methylene chain decreased had been observed previously in the UV spectroscopy of cyclophanes.[116] The shift for the $\pi \rightarrow \pi^*$ transition in cyclophane spectra had been ascribed to the bending of the aromatic plane. The smaller the bridging chain, the greater the deformation of the purine π-system. This distortion raises of the energy of the

[116] Allinger, N. L., Sprague, J. T. and Liljefors, T. *J. Amer. Chem. Soc.* 96, 5100 (1974)

associated molecular orbital and reduces the energy difference between the π and the π^* states. The $n \rightarrow \pi^*$ transition is also a reflection of the cyclophane geometry. Studies have shown[117] that the highest energy absorption for N-substituted anilines occurs when the lone pair on the exocyclic nitrogen is conjugated with the aromatic ring (ie. the C-NH_2 atoms all lie in the same plane). Twisting the lone pair out of this orientation results in a bathochromic shift. The situation is similar for the purinophanes. The maximum transition energy is required when the N6 lone pair is aligned with the aromatic purine system. Altering the electronic character of N6 by substitution or, more dramatically, by twisting the lone pair out of conjugation, as in the cyclophane series, raises the energy of the non-bonding molecular orbital. In essence, the greater the degree of bending and twisting, the less energy is required to induce a transition.

Some of the decamethylene cyclophane structural attributes can now be deduced. The relief of strain which the C-10 chain provides enables the purine ring to flatten more so than in the C-8 and C-9 analogs as evidence by the $\pi \rightarrow \pi^*$ transition. The UV spectra also imply that the degree twisting of N6 in [10]-purinophane is less severe than in the other cases. This lends further support to the statements made in the dynamic NMR study which implicated the relative planarity of the H6-N6-C1′ fragment as a major contributor to the activation energy.

---

[117] Jaffe, H. H. and Orchin, M. Theory and Application of Ultraviolet Spectroscopy (New York: John Wiley and Sons, Inc., 1962) p.407

Chapter 6

Calculation of the Chemical Shifts in the [n]-(N6,9)-6-Aminopurinophane Series

6.1. Introduction

In addition to providing values for the spatial definition of the diamagnetic shielding anisotropy of adenine, the [n]-(N6,9)-6-aminopurinophane series can be used to assess the theoretical models that have been developed to account for the unique magnetic properties of the heterobase.[14] As seen in the Introduction, much of the theoretical work has been directed towards the determination of the factors that influence the chemical shift of stacked purine and pyrimidine protons. With adjacent bases separated by roughly 3.4 Å along the helical axis of an oligonucleotide, the results of shielding calculations are often presented as isoshielding diagrams at this distance.[13,10] In other instances, results are listed for individual protons in very specific sequences and geometries.[118,119] In either case, the reported calculations are difficult to correlate with the observed shifts seen in the adenine cyclophanes, and consequently, make appraisal of the theoretical models rather difficult.

As a result, the present chapter will deal with the development of a computer program which calculates the chemical shifts of methylene protons in the purinophane series. The program takes into account many of the features incorporated in the design

---

[118] Giessner-Prettre, C. *J. Biomol. Struct. and Dynamics.* **2**, 233-248 (1984)

[119] Giessner-Prettre, C. *J. Biomol. Struct. and Dynamics.* **4**, 99-110 (1986)

of the previous theoretical models developed for heterobase shieldings[14] and follows the same approach taken in the study of [10]-paracyclophane.[29] Ultimately, the program's ability to accurately determine the observed chemical shifts based solely on the geometry of the cyclophane will serve as the basis for an evaluation the theoretical models.

Additional impetus for the development of a program to calculate chemical shifts arose from the problems encountered with the unambiguous assignment of the nonamethylene and decamethylene purinophane proton spectra. To know *a priori* where a particular nucleus will resonate would greatly facilitate the interpretation of these spectra. Finally, the model developed would also provide the definitive link between the solution NMR spectroscopy and the solid state conformations of the purinophane molecules.

The capability to predetermine the observed chemical shifts in a spectrum has been a long-standing desire of the NMR spectroscopist. Methodologies that allow for the calculation of the chemical shifts have been developed and generally fall into two broad categories: semi-empirical and *ab initio* methodologies. Semi-empirical calculations were the first to be developed and are distinguished by their use of experimental parameters to simplify calculations. As computer technology has become more sophisticated and more powerful, *ab initio* calculations of NMR chemical shift have increased in popularity.[120] Starting from basic quantum mechanical premises, the *ab initio* calculations have surpassed their semi-empirical counterparts in their accuracy of chemical shift estimation. Unfortunately, the magnitude of the *ab initio* calculation as well as its intensive use of computational facilities has precluded its use on all but small

---

[120] Chestnut, D. B. *Annual Reports on NMR Spectroscopy.* 21, 51-97 (1989)

molecules. Owing to its relative simplicity, therefore, the approach taken in the purinophane chemical shift study is a semi-empirical one.

6.2. Theory

As seen in the Introduction (Equation 4), the total shielding, σ_{total} can be broken down into contributing effects and the early chemical shift calculations generally involved looking at these individual components of the nuclear shielding. Values for the contributions made by local diamagnetic (σ_d) and paramagnetic shielding (σ_p) as well as ring currents (σ_r), neighbouring anisotropy (σ_m), solvent (or medium) influences (σ_s) and electric field effects (σ_e) were calculated and summed together to give estimates of the σ_{total}.

Calculation of the diamagnetic term, σ_d, involves use of Lamb's equation which assumes a spherical distribution of charge about the nucleus.[121] For atoms, this formula gives the total shielding. When atoms are incorporated into molecules, however, the electron distributions are no longer spherical and other perturbing effects take on greater importance such that the Lamb formula breaks down.

The paramagnetic term, σ_p, is more complex and requires a quantum mechanical description. The Ramsey equation is employed and takes into account that the magnetic field causes a mixing of the ground state wave function with excited state wave functions.[122] Unfortunately, as a molecule becomes larger and more complex, the

---

[121] Lamb, W.E. *Phys. Rev.* 60, 817 (1941)

[122] Ramsey, N. F. *Phys. Rev.* 78, 699 (1950)

equation becomes more difficult to implement.

The difficulties encountered in applying the Lamb and Ramsey equations to chemical shift calculation can be quite stultifying and, therefore, most semi-empirical methods avoid estimations of the diamagnetic and paramagnetic terms. Equations evaluating the effects of electric fields have also been developed[123], but, as with the σ_d and σ_p calculations, estimates of the σ_e term can be quite involved.

The problems associated with these terms can be circumvented if the chemical shifts are determined relative to some appropriately chosen standard nucleus. The calculations can be set up in such a way that any change in the chemical shift from the standard value can be attributed to the effects of ring current and neighbouring magnetic anisotropy. Furthermore, if the corresponding experimental values of the chemical shifts are obtained using solvents which minimize solvent induced shifts, then the σ_s contributor to the total shielding can be ignored. Efforts have, therefore, be concentrated on the evaluation of the σ_r and σ_m terms.

Waugh and Fessenden[31,124] and Johnson and Bovey[125] have used Pauling's model[126] to calculate the ring current in benzene. Instead of approximating the σ_r effect to that of a point dipole[127], they calculated the secondary field due to a complete, classical current-loop of radius equal to the length of a carbon-carbon bond in benzene.

---

[123] Buckingham, A. D. *Can. J. Chem.* **38**, 300 (1960)

[124] Waugh, J.S., and Fessenden, R.W. . *J. Amer. Chem. Soc.* **80**, 6697 (1958)

[125] Johnson, C.E., Jr., and Bovey, F.A. *J. Chem. Phys.* **29**, 1012-1014 (1958)

[126] Pauling, L. *J. Chem. Phys.* **4**, 673 (1936)

[127] Pople, J.A. *J. Chem. Phys.* **24**, 1111 (1956)

They further made allowance for the fact that the currents do not "flow" in the molecular plane, but in loops, a distance above and below the plane (that is, they considered the actual distribution in space of the π-electron currents). The loop separation value was adjusted until the calculated ring current contribution accounted for the downfield shift seen experimentally for the benzene proton resonance.

From classical electromagnetic theory, the shielding, σ_r (ppm), provided by n electrons circulating in a loop of radius a, at a point with cylindrical co-ordinates (ρ,z) with respect to the centre of the current loop is

$$\sigma_r = \frac{ne^2}{6\pi M_e c^2} \frac{1}{[(a+\rho)^2+z^2]^{1/2}} \left[K(k) + \frac{a-\rho^2-z^2}{(a-\rho)^2+z^2} E(k) \right] \qquad (7)$$

in which

$$k = \left[\frac{4a\rho}{(a+\rho)^2+z^2} \right]^{1/2} \qquad (8)$$

and k is the modulus of the complete elliptic integrals K and E. M_0 is the mass of an electron with charge e and c is the velocity of light. This classical approach still produces similar results to those calculated quantum mechanically.[128]

The ability to break down neighbouring anisotropy effects into contributions from individual atoms was demonstrated by Barfield, Grant and Ikenberry[32] who showed that a significant part of the deshielding of protons in aromatic hydrocarbons could be ascribed

---

[128] Haigh, C.W., and Mallion, R.B. *Progress in NMR Spectroscopy*. 13, 303-344 (1980)

to cumulative anisotropic effects from each carbon atom. Pople[129] had earlier suggested that the local anisotropy effects were a large contributing factor to this deshielding phenomenon.

Mathematically, the nuclear screening constant, σ, can be expressed as a second rank tensor:

$$\sigma = \begin{pmatrix} \sigma_{11} & \sigma_{12} & \sigma_{13} \\ \sigma_{21} & \sigma_{22} & \sigma_{23} \\ \sigma_{31} & \sigma_{32} & \sigma_{33} \end{pmatrix} \qquad (9)$$

It can be shown that only the effects of the symmetric parts of the magnetic shielding tensor manifest themselves experimentally. Isotropic shielding can be described as an average of these orthogonal principal values of the shielding tensor:

$$\sigma_{isotropic} = \frac{1}{3}(\sigma_{11}+\sigma_{22}+\sigma_{33}) \qquad (10)$$

The local anisotropy of a neighbouring atom, B, can be shown to affect the shielding of a nucleus under observation, A. This contribution can be broken down to the individual contributions made by each of the principal values of the shielding tensor. Recall that σ_{11}, σ_{22} and σ_{33} have a direction association with them and, therefore, the spatial relationship between A and B is important. Effectively, a geometric factor determines the relative amount of each value of the principal shielding tensor of B which contributes to the nuclear shielding of A. Using the analogy of a current circulating in a loop of wire, the shielding component, $\sigma_{\parallel}^{A}$ is affected by the shielding component $\sigma_{\parallel}^{B}$ as

---

[129] Ferguson, A.F., and Pople, J.A. *J. Chem. Phys.* 42, 1560-1563 (1965); Pople, J.A. *J. Chem. Phys.* 41, 2559 (1964)

shown in the equation below:

$$\sigma_{ii}^{A}=\frac{a}{\pi}\frac{1}{[(a+\rho)^2+z^2]^{1/2}}\left[K(k)+\frac{a-\rho^2-z^2}{(a-\rho)^2+z^2}E(k)\right]\sigma_{ii}^{B} \qquad (11)$$

where *a* is the radius of circulation about each neighbouring atom; ρ and *z* are the cylindrical coordinates of the atom A with respect to atom B; and the complete elliptic integrals *K* and *E* are a function of the argument *k*. Performing this calculation on all of the neighbours of A in the molecule, then summing the total neighbour contributions will give the total local anisotropic contribution to the total shielding of that atom.

6.3. Calculation of the Chemical Shift

Amalgamation of the ideas presented above led to the development of an algorithm, similar to the one used for the [10]-paracyclophane study.[29] The development of the program and the refinement of the calculations centred on the octamethylene purine cyclophane whose properties were most clearly defined. As seen above, implementation of this semi-empirical model requires a knowledge of the cyclophane's molecular structure as well as the principal values and directions of the magnetic shielding tensors (σ_{11}, σ_{22}, σ_{33}) of its constituent atoms.

Generally, the values of the chemical shielding tensors may be determined experimentally using single crystal studies.[130] The proton-enhanced spectra obtained as a function of rotation angle will yield information about the shielding tensor of each

---

[130] Fyfe, C.A. Solid State NMR for Chemists. (Guelph: C.F.C. Press, 1983). pp. 156-167, 187-199

atom.[131] When related to molecular structure via an X-ray crystal structure, the principal directions are obtained. The procedure has been applied successfully to a number of molecules.[132] Alternatively, chemical shielding tensor elements have been derived from the sideband intensities in the NMR spectra of samples spinning at the magic angle.[133] This very mathematical approach, developed by Herzfeld and Berger, has been applied to the magic angle spinning (MAS) ^{13}C spectra of p-dimethoxybenzene and the ^{31}P spectra of barium diethylphosphate. The results agree well with the previous single crystal measurements.

In the case of adenine though, experimental determination of the shielding tensors is quite difficult. The quadrupole moment possessed by ^{14}N provides a highly efficient relaxation mechanism for any neighbouring ^{13}C nuclei. This effect results in significant broadening of the solid state spectra of adenine and makes application of the Herzfeld and Berger method impossible. However, the principal values of the shielding tensors for each atom in the purine and pyrimidine bases have been determined computationally by Schindler.[15] These values agree with those of Giessner-Prettre *et al.* who also used *ab initio* quantum mechanical calculations to determine the tensor quantities.[118,134]

The conformational details required were provided by the crystal structure of [8]-(N6,9)-6-aminopurinophane[35] whose positional parameters were converted to orthogonal

---

[131] Pines, A., Gibby, M.G. and Waugh, J.S. *Chem Phys. Lett.* 15, 373-376 (1972)

[132] For examples, see Pausak, S., Pines, A., and Waugh, J.S. *J. Chem. Phys.* 59, 591-595 (1973); Igner, D. and Fiat, D. *J. Mag. Res.* 46, 233-246 (1982) and Edzes, H.T. *Polymer.* 24, 1425-1428 (1983)

[133] Herzfeld, J. and Berger, A.E. *J. Chem. Phys.* 73, 6021-6030 (1980)

[134] Prado, F.R. and Giessner-Prettre, C. *J. Mag. Res.* 47, 103-117 (1982) and Giessner-Prettre, C. and Pullman, B. *J. Amer. Chem. Soc.* 104, 70-73 (1982)

angstrom coordinates. With the geometric and tensor information in hand, a BASIC program (Appendix D) was developed which incorporated contributions to the chemical shift from ring currents and local anisotropy. Aspects concerning the design of this program deserve discussion.

The program developed for the [10]-paracyclophane study approximated the geometry of the benzene with a symmetrical hexagon[29]. In the case of adenine, the 6-membered pyrimidine and 5-membered imidazole rings are distorted. The geometry is further complicated in the purinophane since the bridging methylene chain forces the aromatic ring to pucker. The torsional angles C6-C5-C4-N9 (169.2°) and N7-C5-C4-N3 (176.3°) of [8]-(N6,9)-6-aminopurinophane, determined by diffraction studies, confirm the non-planarity of the adenine moiety.[35] In an effort to simplify the calculations, the program developed assumed the pyrimidine and imidazole rings were exactly planar. It should be noted that this approximation of the true geometry is likely a source of error for the chemical shift calculation.

Two ring currents were calculated. A subroutine was designed so as to centre the axes on the pyrimidine ring, calculate the ring current experienced by a particular proton, then centre on the imidazole ring and add its contribution to the proton's shift. The number of electrons circulating in each of the current loops was varied with the best chemical shift values resulting from 6 electrons for the pyrimidine and 4 for the imidazole (*vide infra*). In this case, while the total number of electrons obeyed the 4n+2 rule for aromaticity, the 4 electrons in the imidazole leave the ring formally antiaromatic. The π-electron contribution from N6 was ignored.

Work done previously by Hunter[37] showed that introducing a loop separation into

the ring current calculation resulted in a small change in the chemical shift. Agarwal *et al.*[29] also found the best correlation between predicted and observed chemical shifts was obtained without invoking a loop separation. As a result, a zero loop separation was used in present calculation.

As seen above, the correct orientation of the principal shielding tensor values with respect to the molecule is crucial. In benzene, the σ_{11}, σ_{22}, and σ_{33} vectors centred on each carbon fall along the C-H bonds, perpendicular and parallel to the plane of the aromatic ring. The values calculated by Schindler for adenine are not so well behaved pointing off slightly into odd directions. While this was not unexpected for such an asymmetric molecule as adenine, an irregular alignment of the shielding tensor values with respect to the molecular geometry would make calculation of the local anisotropy contributions exceedingly complicated. By aligning the ring systems prior to calculation and forcing the σ_{11}, σ_{22}, and σ_{33} vectors to orient themselves as in benzene, another source of error was introduced although the calculations were simplified. Also note that only the anisotropic influences of the adenine moiety were considered in the calculation.

The radius of circulation about each atom, the *a* value, required of the local anisotropy calculation was set the same for both carbon and nitrogen. This, again, may have introduced some error into the chemical shift estimated.

Finally, the standard chemical shift chosen was based on the work of Burke and Lauterbur who determined the typical value for the methylene shifts of large cycloalkanes averaged to 1.30 ppm.[135] Any deviation from this value by a bridge methylene proton

---

[135] Burke, J. J. and Lauterbur, P. C. *J. Amer. Chem. Soc.* 86, 1870 (1964)

will be ascribed to ring current and local anisotropy effects.

With so many parameters to adjust, the temptation of "over-fitting" the theoretical predictions to the observed experimental values must be avoided. If the theoretical model is valid then reasonably accurate estimates of the chemical shifts should be obtained without having to drastically modify the individual attributes of the programs. Some fine tuning of the program is permissible; but the legitimacy of a model whose empirical parameters have been tailored to match the observed results is highly questionable.

6.4. Predicted Proton Chemical Shifts for [8](N6,9)-6-Aminopurinophane

Table V compares the observed chemical shifts of the bridging methylene protons in [8](N6,9)-6-aminopurinophane with those calculated by the BASIC program (Appendix D). The results were obtained using 6 circulating electrons in the six-membered ring, 4 electrons for the five-membered ring and a zero loop separation.

Inductively transmitted substituent effects from N6 and N9 are largely responsible for the deshielding of the protons on C1′ and C8′ and, therefore, for the purposes of comparison, these values have been ignored. It should be borne in mind that long range inductive effects may alter C2′ and C7′ proton resonances as well. If one looks at the differences in chemical shifts between the geminal protons on each methylene, the predicted values seem to follow the same general trend seen experimentally. Closer inspection of Table V reveals that, in the cases of C3′, C5′ and C6′, the predicted values are actually in greater agreement with the geminal partner. In fact, if the *pro-R* and *pro-S* labels were switched for these three pairs of geminal protons and observed chemical shifts plotted against the predicted values, one can see (Figure 72) quite a good

Table V: Observed and Predicted Chemical Shifts (ppm) for the Bridge Protons in [8]-(N6,9)-6-Aminopurinophane

atom	observed chemical shift	geminal difference	predicted chemical shift	geminal difference
H1R	3.35	1.14	2.29	0.32
H1S	4.49		2.61	
H2R	1.47	0.09	1.46	0.04
H2S	1.38		1.43	
H3R	1.03	0.85	0.34	0.62
H3S	0.18		0.96	
H4R	0.61	0.43	0.90	0.61
H4S	0.18		0.29	
H5R	-0.69	1.58	0.77	1.46
H5S	0.89		-0.76	
H6R	1.26	0.74	0.59	0.39
H6S	0.52		0.98	
H7R	1.80	0.16	1.55	0.19
H7S	1.64		1.36	
H8R	4.55	0.63	2.79	0.45
H8S	3.92		2.34	

correlation. Linear regression analysis on this plot yields a least squares correlation coefficient, *r*, of 0.9719.

Figure 73 presents a view of the octamethylene purine cyclophane which clearly shows the relationship between these six protons and the adenine ring. Note that the H3R, H5S and H6R protons are closer to the plane of the purine than their respective geminal partners. It can be demonstrated that the degree of shielding by aromatic systems increases as protons get closer to the aromatic plane. Many of the isoshielding

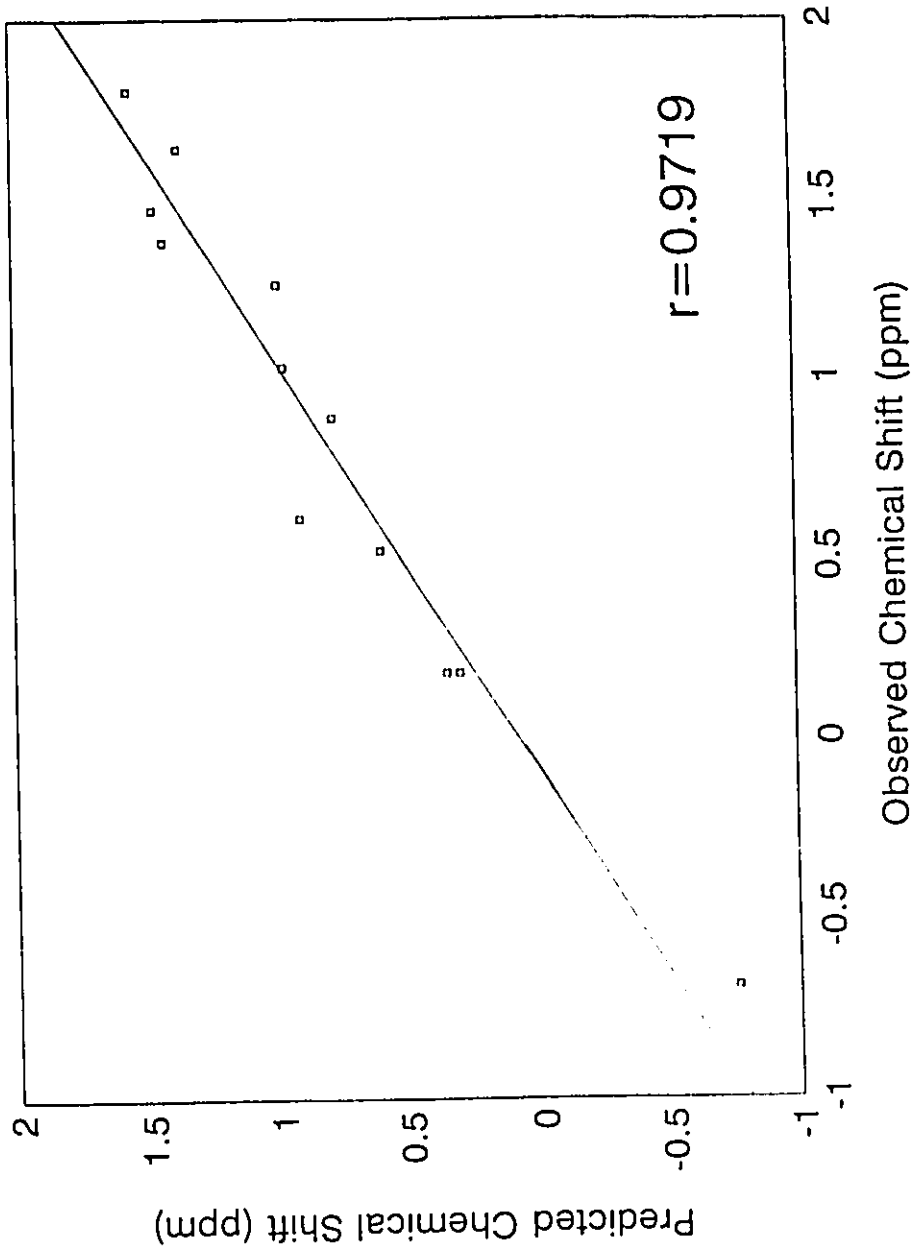

Figure 72: Plot of the Predicted vs. Observed Chemical Shifts for [8]-(N6,9)-6-Aminopurinophane

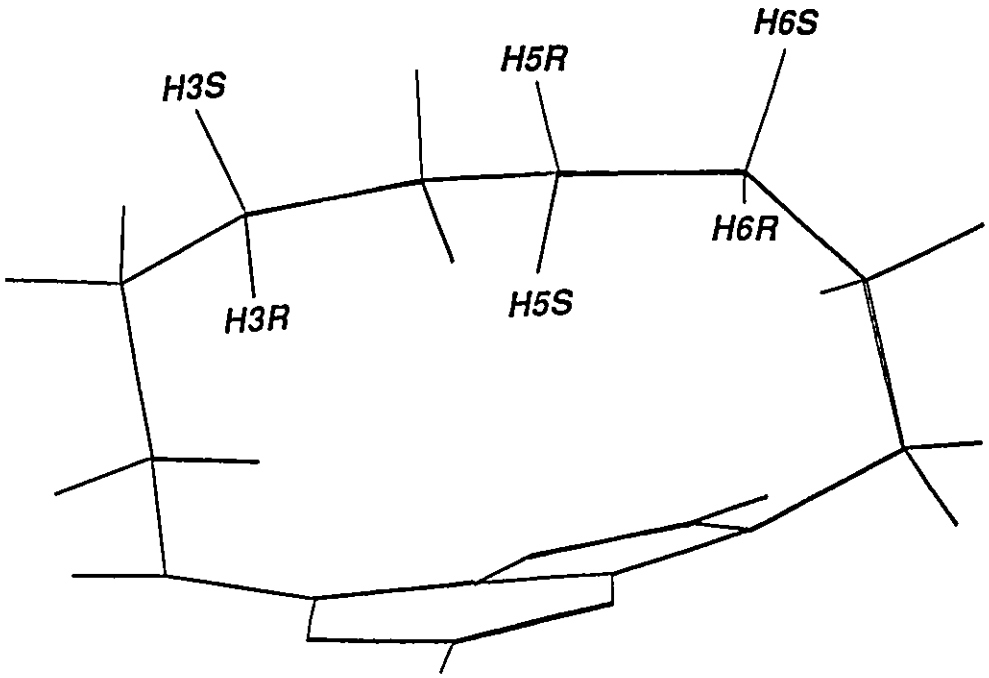

Figure 73: Geometry of Bridge Protons with respect to Adenine Ring in [8]-(N6,9)-6-Aminopurinophane (some atom labels omitted for clarity)

curves calculated graphically illustrate this effect.[10,13] Consequently, one would expect the H3R, H5S and H6R protons to be shielded and resonate at higher field than their partners. The predicted values in question correctly reflect this phenomenon and, therefore, it would seem reasonable to exchange the designations for the observed signals.

This mislabelling of geminal pairs is likely a result of the difficulties encountered in the application of the Karplus equation. As seen in Chapter 5, after having untangled all the vicinal coupling constants from each spin system application of Equation 5 permitted the determination of the dihedral angles. Inspection angles determined by X-ray crystallography then allows for *pro-R* and *pro-S* assignment. Unfortunately, as one proceeds through the aliphatic bridge, many of the dihedral angles and, hence, the

coupling constants take on very similar values. Under these conditions, the assignment of the geminal protons becomes quite complicated and errors are easily encountered.

Some fine tuning of the model was attempted by adjusting some of the parameters of the program. Hunter[37] used the CNDO/2 and MNDO methods to determine the ratio of π-electrons for each ring.[136] These studies showed that the pyrimidine and the imidazole rings should be allotted 5.275 and 4.881 electrons, respectively. These minor changes in electron distributions, though, resulted in minimal shielding changes and a very small worsening of the correlation between the predicted and observed values. Invoking a loop separation generally had a small effect on the values calculated and did not improve the correlations between the observed and the computed chemical shifts.

Overall, the computational anisotropy mapping exercise was quite successful. Although the chemical shift numbers predicted do not match exactly those seen experimentally, they do show the relative deshielding of one geminal partner over its counterpart. The geminal shift difference shown in Table V might be regarded as a better criterion for judging the calculations. This geminal difference more accurately reflects the model's ability to calculate the subtle changes in ring current and local anisotropy which distinguishes each proton's NMR signal. A comparison of the differences observed and those calculated shows a marginal correlation with an *r* value of 0.9416. Many of the sources of error cited above may have contributed to the "less than ideal" performance of the program. More likely, though, it is the high asymmetry of the adenine heterobase which makes a theoretical description of its anisotropy so complex.

---

[136] Jordan, F. and Sostman, H.D. *J. Amer. Chem. Soc.* 94, 7898 (1972)

6.5. Predicted Proton Chemical Shifts for *anti* and *syn* [9](N6,9)-6-Aminopurinophane

As seen in Chapter 5, the extensive broadening in the low temperature spectra of [9](N6,9)-6-aminopurinophane made the assignment of the *pro-R* and *pro-S* protons in the *syn* and *anti* conformations impossible. Inadequate resolution of the splitting within each spin system precluded application of the Karplus equation to distinguish prochirality. In an effort to sort out these spectra, therefore, the semi-empirical model employed in the calculation of the chemical shifts of [8](N6,9)-6-aminopurinophane (*vide supra*) was modified so as to be utilized for the assignment of the nonamethylene homolog. The program was used to determine whether a given geometry for the cyclophane was consistent with the observed chemical shifts, and if so, appropriate *pro-R* and *pro-S* assignments were made.

Using the crystal structure geometry for the *anti* conformer and the computer generated molecular model (**2b**) for the *syn* conformation, the predicted chemical shifts were calculated using the BASIC program (Appendix D) and the values presented in Table VI. Once again, the results were obtained using 6 circulating electrons in the six-membered ring, 4 electrons for the five-membered ring and a zero loop separation. The *pro-R* and *pro-S* designations were assigned by matching the lower field signal with the geminal proton predicted to resonate at lower field, leaving the higher field signal to be assigned to the proton predicted to resonate at higher field. Inspection of the Table reveals that the geometries of the cyclophanes used for the calculations are very similar to those conformations giving rise to the major and minor signals in the low temperature ^{1}H-NMR spectrum of the [9](N6,9)-6-aminopurinophane since the chemical shift values predicted using these geometries are consistent with those resonances observed.

Table VI: Observed and Predicted Chemical Shifts (ppm) for the Bridge Protons in [9]-(N6,9)-6-Aminopurinophane

Anti Conformer		
atom	predicted chemical shift	observed chemical shift
H1R	2.27	3.38
H1S	2.52	4.84
H2R	1.53	1.60
H2S	1.41	1.43
H3R	1.01	1.00
H3S	0.53	0.45
H4R	0.90	0.45
H4S	0.23	0.35
H5R	0.83	0.74
H5S	0.19	-0.09
H6R	0.98	0.55
H6S	1.06	0.82
H7R	0.48	0.59
H7S	1.12	1.32
H8R	1.58	1.60
H8S	1.34	1.60
H9R	2.18	3.79
H9S	3.03	4.54

Syn Conformer		
atom	predicted chemical shift	observed chemical shift
H1R	2.14	4.08
H1S	1.85	3.10
H2R	1.33	1.62
H2S	0.97	1.03
H3R	1.36	-
H3S	1.02	-
H4R	1.02	0.79
H4S	1.05	0.93
H5R	0.21	-0.21
H5S	0.87	0.70
H6R	0.73	0.34
H6S	-0.72	-1.30
H7R	1.05	0.80
H7S	1.08	1.20
H8R	1.46	1.93
H8S	1.05	1.35
H9R	3.01	4.48
H9S	2.19	4.15

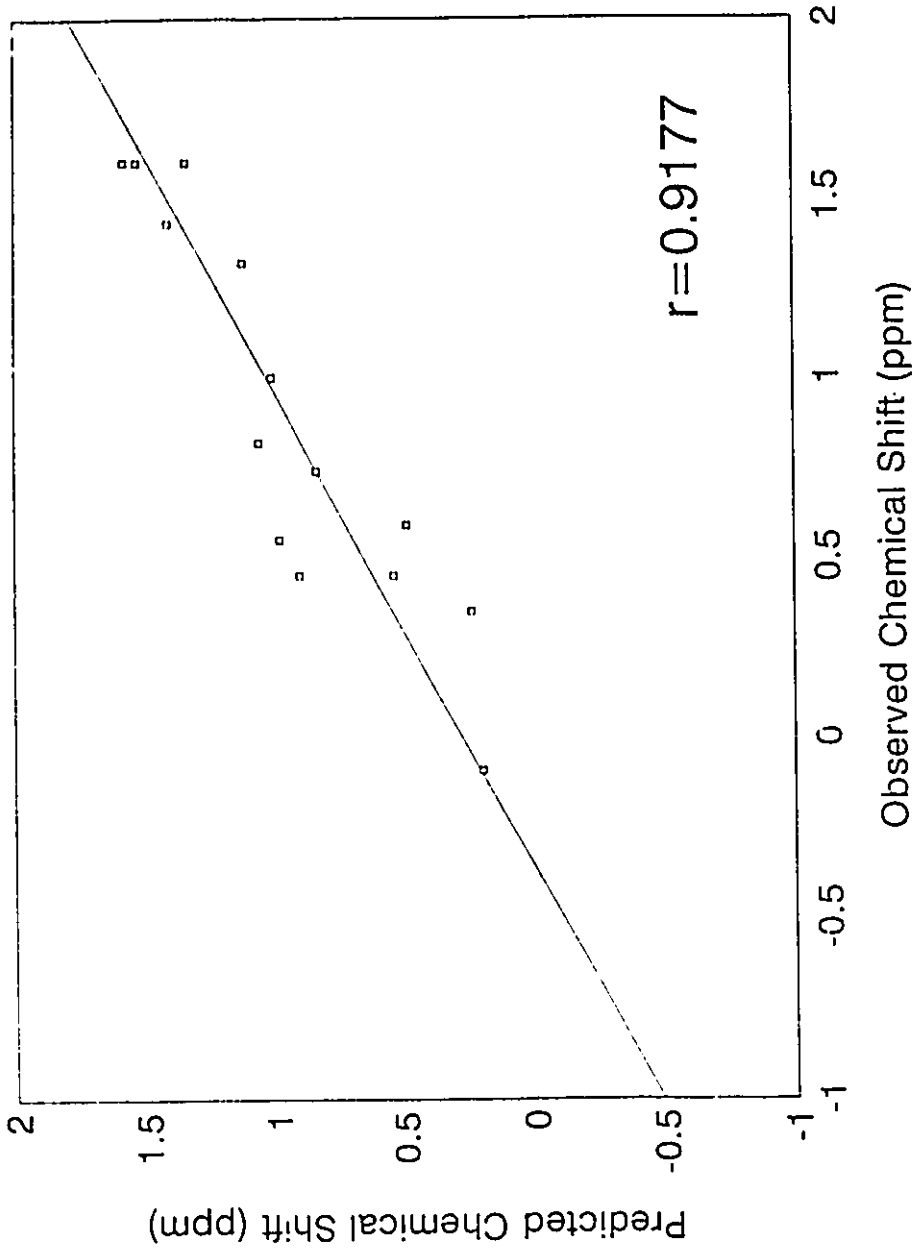

Figure 74: Plot of the Predicted vs. Observed Chemical Shifts for *anti*-[9]-(N6,9)-6-Aminopurinophane

Figure 74 presents a plot of the experimental and calculated chemical shifts for the *anti* case. Ignoring the protons on C1′ and C9′ (once again, the N6 and N9 inductive effects result in deshielding), a linear regression analysis of the data yielded a correlation coefficient of 0.9177. Interestingly, the subtle differences between the crystal structure and the molecular model generated by PC-Model (see Chapter 5) are exposed when the coordinates of the *anti* molecular model (**2a**) are used in the program. The best fit line of the experimental and predicted chemical shifts in this case possesses an *r* of 0.8403. It would seem the conformation determined crystallographically is a better reflection of the solution state geometry (as observed in the proton spectrum) than the molecular model **2a**.

On the other hand, the *syn* conformation generated by the PC-Model (**2b**) seems to have succeeded in generating a reasonable representation of the minor conformer seen in the low temperature spectrum of [9](N6,9)-6-aminopurinophane. The data for the *syn* conformation from Table VI is plotted in Figure 75. Linear regression analysis of this plot yields a least squares correlation coefficient of 0.9715.

6.6. Conclusions

In both the [8]- and [9]-(N6,9)-6-aminopurinophane cases, the BASIC program has established its usefulness by demonstrating its ability to calculate the chemical shifts of the purinophane bridge protons. Although its absolute predictive ability is limited, the program has shown that results generated using a semi-empirical model do compare relatively well with the observed ^{1}H-NMR resonances. Furthermore, the work carried out above has revealed that the ring current effects alone are insufficient to account for the

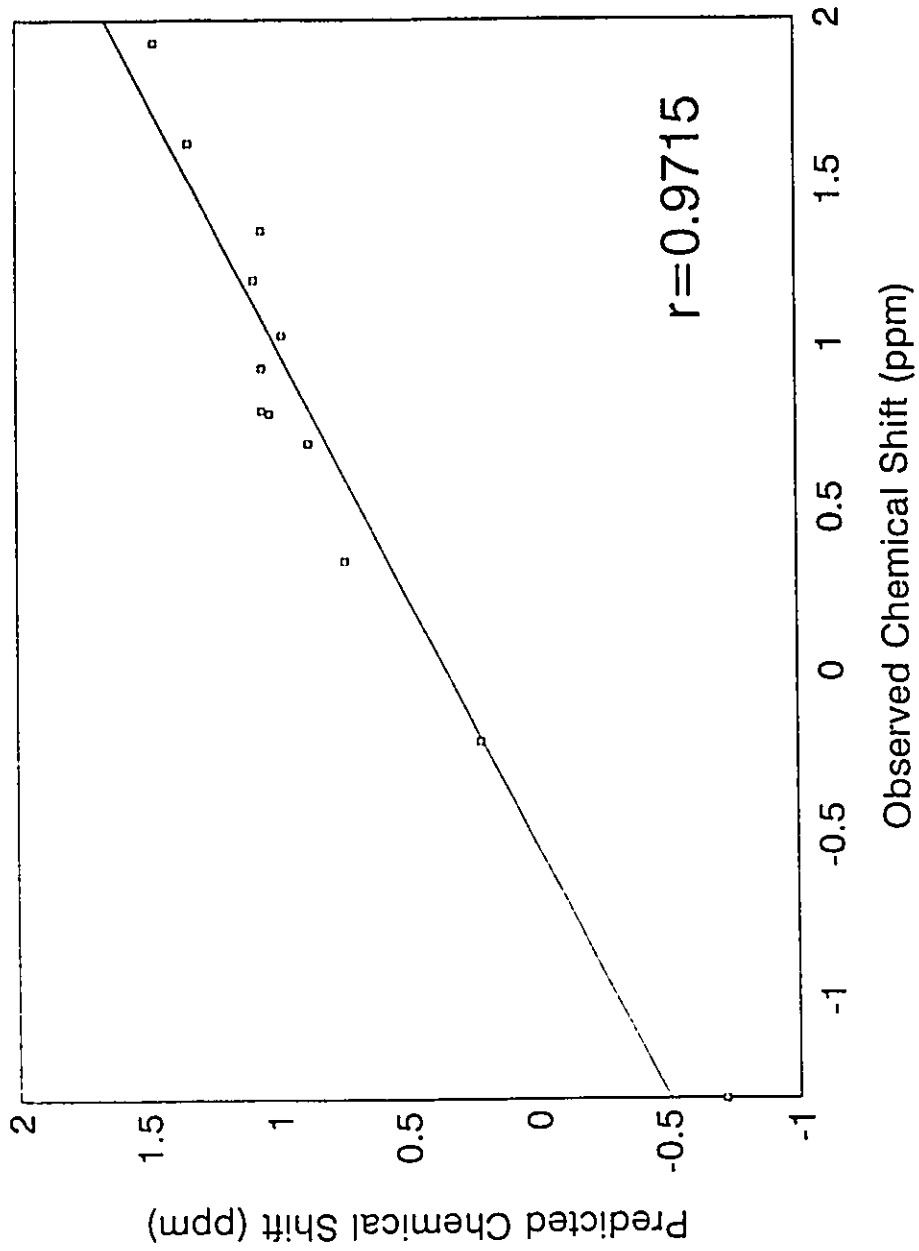

Figure 75: Plot of the Predicted vs. Observed Chemical Shifts for *syn*-[9]-(N6,9)-6-Aminopurinophane

shielding seen in the purinophane series; this is supportive of the findings of Giessner-Prettre *et al.*[14] and Agarwal *et al.*[29] who have also found it necessary to supplement the ring current with anisotropic contributions to predict the chemical shifts in their systems. Finally, the program developed has proven itself effective in providing a link between the solution NMR work and the conformational studies helping to augment the connections provided by the Karplus equation.

Any improvements that can be made to the semi-empirical model are limited since any modification will likely result in a minimal return. The next logical step in the theoretical study of these cyclophanes would be an *ab initio* approach. The individual gauges for atoms in molecules (IGAIM) approach being developed by Keith and Bader shows promise.[137] The principles behind this IGAIM strategy simplify the necessary calculations and allow the method to handle larger molecules than the conventional *ab initio* techniques. Although still in its formative stages, the purinophane series would be an ideal candidate for study using this new approach.

---

[137] Keith, T. A. and Bader, R. F. W. *Chem. Phys. Lett.* **194**, 1 (1992)

Experimental Methods

Melting points were recorded on a Gallenkamp capillary tube melting point apparatus and are uncorrected.

Proton magnetic resonance (^{1}H-NMR) spectra were recorded on a Varian EM-390 (at 90 MHz), a Bruker AC-200 (at 200.13 MHz) or a Bruker AM-500 (at 500.13 MHz) spectrometer with chloroform-d as the solvent unless otherwise noted. Unless specified, the usual internal references were tetramethylsilane (TMS) or chloroform. The abbreviations (s)=singlet, (d)=doublet, (t)=triplet, (q)=quartet, (m)=multiplet and (br)=broad are used in the description of the spin-spin splitting pattern present in the spectra. Spectra obtained on the Bruker instruments were collected in 8 scans in 16K data points over an appropriate spectral width. The free induction decay (FID) was processed using exponential multiplication (line broadening set to the Hz/point value) and was zero-filled to 32K before Fourier transformation.

The natural abundance carbon-13 magnetic resonances (^{13}C-NMR) were recorded on a AM-500 (at 125.776 MHz) or AC-200 (at 50.324 MHz) instrument using chloroform-d as the solvent and internal reference unless otherwise noted. All ^{13}C spectra were broad band decoupled and were acquired over an appropriate spectral width in 16K data points. A 35° flip angle and a 0.5 s relaxation delay were generally used. The FIDs were processed using exponential multiplication (line broadening: 4.0 Hz) and zero-filled to 32K before Fourier transformation.

Proton-proton NOE difference spectra obtained on a Bruker AM-500 and were acquired by subtraction of a control FID from an on-resonance FID. The decoupler in the control FID irradiated a position in the spectrum where there were no proton signals. The on-resonance FID was obtained with the proton of interest being selectively saturated. In both cases the same decoupler power and duration of saturation (5.0 s) were used. This saturation period also served as the relaxation delay for both the control and on-resonance FIDs. The decoupler was gated off during acquisition. Eight scans were acquired for both the control and on-resonance FIDs. This cycle of alternate acquisition of control and on-resonance FIDs was repeated 4 times for a total of 32 scans for the final difference FID. A 90° ^{1}H pulse width of 18.6 μs was used. The difference FID was processed using exponential multiplication (line broadening; 4.0 Hz) and was zero-filled to 32K before Fourier transformation. The samples were not degassed.

Proton COSY 2-D NMR spectra were recorded on the Bruker AC-200 and the AM-500 in the absolute value mode using the pulse sequence 90° - t_1 -90° - ACQ. Spectra were acquired in 16 scans for each of the 256 FIDs in F2 over an appropriate spectral width. A 1.0 s relaxation delay was employed between acquisitions. Zero-filling in F1 produced a 1K x 1K data matrix with a digital resolution of roughly 5 Hz/point in both dimensions. During 2-D Fourier transformation a sine-bell squared window function was applied to both dimensions. The transformed data were then symmetrized.

The ^{13}C - ^{1}H 2-D chemical shift correlation spectra were acquired on the Bruker AM-500 using the standard pulse sequence incorporating the BIRD pulse during the

evolution period for ^1H - ^1H decoupling in F1. The spectra in F2 were recorded over an appropriate spectral width in 4K data points. The 256 FIDs in F1 were obtained over an appropriate ^1H spectral width. Each FID was acquired in 16 scans. The fixed delays in the pulse sequence were a 1.0 s relaxation delay, BIRD pulse and polarization transfer delays of ($\frac{1}{2}$ $^1J_{CH}$) and a refocussing delay of ($\frac{1}{4}$ $^1J_{CH}$). The ^{13}C 90° pulse width was 6.4 μs while the ^1H 90° pulse width through the decoupler channel was 18.6 μs. The data were processed using exponential multiplication (line broadening: 5 Hz) in F2 and unshifted sine bell in F1.

X-Ray Crystallography

Crystals of [9](N6,9)-6-aminopurinophane were grown from chloroform/toluene (1:3) solution. The density was determined by suspension in an aqueous solution of $ZnCl_2$. Large transparent acicular crystals were examined under a polarizing microscope for homogeneity. A small irregular crystal, 0.10 x 0.20 x 0.40 mm., was cut from a larger crystal and mounted on the tip of a glass fibre with epoxy cement. The crystal was cooled by a nitrogen stream which had been passed through a liquid nitrogen cooled, heat exchanging device supplied by Molecular Structure Corporation, Texas. The unit cell parameters were determined at 173 K from a least-squares refinement of the angular positions of 25 reflections with θ in the range $39.7 \leq \theta \leq 40.0°$ recorded on a Rigaku AFC6R diffractometer with use of graphite monochromated CuKα radiation (λ=1.540598Å at 298 K). Intensity data were also recorded on a Rigaku AFC6R diffractometer at 173 K by use of ω-2θ scan for 3232 reflections, (*h.k.±l*) with $\theta \leq 50.0°$. Three standard reflections were monitored every 150 reflections and showed

no sign of instrument instability or crystal decay. Corrections were made for Lorentz-polarization effects but not for absorption. Reflections with $3\sigma_I \geq (I) \geq -3\sigma_I$ were treated by the method of French and Wilson.[138] Systematically absent data, (264 reflections), were removed and symmetry-equivalent data were averaged to give 2846 independent reflections, R_{int}=0.0249, of which 2556 were within $I \geq 2.5\sigma(I)$. The structure was solved by direct methods based on 494 reflections with $|E|>1.2$ and 30 sets of starting phases with use of the program SHELXS-86.[139] Full matrix least-squares refinement of the coordinates of the non-hydrogen atoms followed by a three-dimensional difference electron density synthesis revealed the positional parameters of all the hydrogen atoms. The temperature factors of all of the non-hydrogen atoms were made anisotropic and the hydrogen atoms were assigned a common overall isotropic temperature factor and included in refinement. Further cycles using block-matrix least-squares minimizing $\Sigma\omega(|F_o|-|F_c|)^2$, was terminated when the maximum shift/error reached 0.004. A correction for secondary extinction was made by the method in SHELX-76.[140] Final R_1=0.0364 and R_2=0.0395, S = 1.3618. Scattering factors used were those of Cromer and Mann.[141] Calculations employed

---

[138] French, S. and Wilson, K. *Acta Cryst.* **A34**, 517 (1978)

[139] Sheldrick, G.M. SHELXS-86, Program for Crystal Structure Solution. University of Göttingen, Federal Republic of Germany, 1986

[140] Sheldrick, G.M. SHELX-76, Program for Crystal Structure Determination. University of Cambridge, England. (1976)

[141] Cromer, D.T. and Mann, J.B. *Acta Cryst.* **A24**, 321 (1968)

XTAL[142], data reduction and mean planes; SHELX-76, structure refinement; MOLGEOM[143], CHEM-X[144], molecular geometry and SNOOPI[145], diagrams running on a VAX 8650 computer.

Low resolution mass spectra (MS) and high resolution mass spectra (HRMS) were obtained on either a VG Micromass 7070F or a VG ZAB-E mass spectrometer with samples being introduced through a direct inlet system. Ions were generated using electron impact (EI) or through chemical ionization (CI) with NH_3 as the reactant gas.

Infrared spectra (IR) were recorded on a Perkin Elmer 283 spectrometer. IR samples were run as neat liquids using NaCl windows. The symbols (s)=strong and (br)=broad were used in the recording of the IR data to indicate the intensity of the recorded bands.

Ultraviolet (UV) spectra were recorded on a Perkin-Elmer Lambda 9 UV/VIS/NIR spectrophotometer.

Energy-minimized structures were generated using MMX force field calculations derived from MM2. The calculations were carried out using the programs PC-Model[34] or Macromodel.[33] Restricted Hartree-Fock (RHF) calculations were carried out with AM1, Version 2.1, of the general purpose molecular orbital computational package AMPAC.[44] Optimizations were carried out with the AM1 default parameters.

---

[142] Stewart, J.M. and Hall, S.R. The XTAL System of Crystallographic Programs. Tech. Rept. TR-1364. University of Maryland, College Park, U.S.A. (1983)

[143] Stephens, J. MOLGEOM adapted from CUDLS. McMaster University, Canada. (1973)

[144] Davies, K. CHEM-X. Chemical Design Ltd., Oxford, England. (1986)

[145] Davies, K. CHEMGRAF suite: SNOOPI. Chemical Design Ltd., Oxford, England. (1983)

Tetrahydrofuran (THF) was dried by refluxing and distilling from sodium and benzophenone under dry nitrogen. THF was collected from the distillation apparatus as required. N,N-Dimethylformamide (DMF) was refluxed and subsequently distilled from BaO. Acetonitrile was distilled from P_2O_5 followed by distillation from CaH_2, discarding the first 5 and the last 10%. Dimethylsulphoxide (DMSO) was stored over NaOH pellets before being distilled at reduced pressure from BaO. All other solvents employed were of reagent grade. NMR solvents chloroform-d, methylene chloride-d_2, acetone-d_6, dimethylsulphoxide-d_6, dimethylformamide-d_7 and pyridine-d_5 were stored over molecular sieves (4Å) prior to use.

Unless specified, column chromatography was performed by the "flash" method of Still, Kahn, and Mitra.[146] The silica gel used for column chromatography (5.0% of 100 mesh up; 47.6% of 100-200 mesh and 47.4% of 200 mesh down) was purchased from Terochem. Silica gel 60 F_{254} (E. Merck Co.) plates of 0.2 mm thickness were used for analytical thin layer chromatography (tlc). Visualization was achieved using a UV lamp at 254 nm or via treatment of the tlc with either a molybdic acid spray (20 g of molybdic acid and 15 g of ceric sulphate dissolved in 1 litre of 10% sulphuric acid) or a ninhydrin spray (0.2% ninhydrin in ethanol) followed by heating.

Synthesis of 9-Azidononanol (5)

The procedure followed is similar to that described by Castro *et al.*[46] 1,9 Nonanediol (2.5 g, 15.6 mmol) was dissolved in 15 ml of dry THF under a nitrogen

---

[146] Still, W.C., Kahn, M. and Mitra, A.J. *J. Org. Chem.* **43**, 2923-2925 (1978)

atmosphere and cooled to -20°C. Carbon tetrachloride (6.0 ml, 9.6 g, 62.2 mmol) was added followed by slow dropwise addition of hexamethylphosphorus triamide (HMPT) (3.1 ml, 2.8 g, 17.1 mmol) via a syringe. The reaction mixture was then added to 100 ml of water and washed with 100 ml of diethyl ether. Potassium hexafluorophosphate (5.5 g, 30 mmol) was added to the aqueous solution which was then extracted with three 100 ml portions of chloroform. The combined organic extracts were dried over anhydrous sodium sulphate and evaporated under reduced pressure. The oily residue was dissolved in 50 ml of DMF and stirred for 12 hours in the presence of NaN_3 (5 g, 77 mmol) at 80°C. The solvent was subsequently evaporated under reduced pressure and the residue taken up into 100 ml of water followed by extraction with four 100 ml portions of ether. The ether extracts were dried over sodium sulphate and the solvent evaporated under a reduced pressure. The crude product was purified by vacuum distillation. TLC with 5% methanol in chloroform using the molybdic acid spray for visualization showed the desired product having an R_f=0.54. The yield was 87% (2.51 g, 13.6 mmol). The compound showed:

bp: 89°C @ 0.01 mm

^{1}H NMR: (200 MHz); δ 1.22 (m, 10H, $(CH_2)_5$), 1.49 (m, 4H, $C\underline{H_2}$-CH_2-OH and $C\underline{H_2}$-CH_2-N_3), 3.16 (t, 2H, J=6.8 Hz, CH_2-N_3) and 3.51 (t, 2H, J=6.6 Hz, CH_2-OH)

^{13}C NMR: (50 MHz); δ 25.57 (C3), 26.54 (C5), 28.66 (C6), 28.93 (C7), 29.17 (C4), 29.28 (C8), 32.56 (C2), 51.30 (C9), 62.64 (C1).

IR: 3360 cm^{-1} (br, OH); 2095 cm^{-1} (s, N_3)

MS [EI]: m/z (RI%); 203 $[M+18]^+$ (17), 186 $[M+1]^+$ (7), 178 (40), 158 $[M+1-N_2]^+$

(65), 70 (60), 56 (40) and 44 (100)

Synthesis of 6-Chloro-9-(1-azidononyl)purine (6)

The procedure used was similar to that of Iwakawa *et al.*[41] To a mixture of 6-chloropurine (1.59 g, 10.28 mmol), triphenylphosphine (2.7 g, 10.28 mmol) and diethyl azidocarboxylate (2.20 g, 2 ml, 12.60 mmol) in 40 ml of dry THF was added a solution of 9-azidononanol (2.00 g, 10.80 mmol) in 40 ml of THF. The solution was allowed to stir at room temperature for 48 hours at which time the reaction mixture was concentrated under reduced pressure. The residue was chromatographed on silica gel using 1% methanol in chloroform yielding a viscous yellow oil. TLC of the product with 5% methanol in chloroform gave an R_f=0.52. The yield was 23% (759 mg, 2.36 mmol). The compound showed:

^{1}H NMR: (200 MHz); δ 1.22 (m, 10H, $(CH_2)_5$), 1.56 (m, 2H, $C\underline{H_2}$-CH_2-N_3), 1.92 (m, 2H, $C\underline{H_2}$-CH_2-N9), 3.20 (t, 2H, J=6.5 Hz, CH_2-N_3), 4.27 (t, 2H, J=7.5 Hz, CH_2-N9), 8.10 (s, 1H, H8), 8.73 (s, 1H, H2).

^{13}C NMR: (50 MHz); δ 26.16 (C8′ or C5′), 26.19 (C5′ or C8′), 28.37 (C6′ or C7′), 28.45 (C7′ or C6′), 28.55 (C4′ or C3′), 28.79 (C3′ or C4′), 29.43 (C2′), 44.15 (C9′), 51.00 (C1′), 131.15 (C5), 145.06 (C8), 150.37 (C4), 151.39 (C2), 151.52 (C6).

HRMS: for $C_{14}H_{20}N_7Cl$: calculated 321.1468; observed 321.1470

MS [EI]: m/z (RI%); 321 $[M]^+$ (3), 265 $[M-CH_2N_3]^+$ (41), 209 $[M-(CH_2)_5N_3]^+$ (56), 155 (100).

Synthesis of 6-Chloro-9-(1-aminononyl)purine (7)

The procedure used was similar to that of Vaultier *et al.*[47] To 6-chloro-9-(1-azidononyl)purine (500 mg, 1.56 mmol) in 1.6 ml of THF was added triphenylphosphine (410 mg, 1.56 mmol), water (45 µl, 2.34 mmol) and a boiling chip. The evolution of N_2 began immediately. The mixture was left standing at room temperature for 18 hours. TLC of the reaction mixture showed the complete disappearance of the azide starting material and the appearance of a ninhydrin positive spot on the baseline. The solution was then concentrated, redissolved in 50 ml of chloroform and extracted with three 20 ml portions of 0.01M HCl. The combined aqueous solutions were adjusted to pH 8 with 1M NaOH and extracted with three 30 ml portions of chloroform. These combined organic solutions were dried over anhydrous sodium sulphate and evaporated under reduced pressure. The product was subjected immediately to cyclization conditions. TLC with 10% methanol in chloroform using ninhydrin spray for visualization showed the desired product with an R_f=.05. The yield was 98% (451 mg, 1.53 mmol) as demonstrated by NMR. The compound showed:

^{1}H NMR: (90 MHz) [hydrochloride salt in D_2O; internal reference: 3-(trimethylsilyl)propionic acid sodium salt]; δ 1.30 (m, 14H, $(CH_2)_7$), 3.00 (t, 2H, $C\underline{H_2}$-NH_3^+), 4.38 (t, 2H, CH_2-N9), 7.70 (s, 1H, H2) and 8.37 (s, 1H, H8).

Synthesis of [9](N6,9)-6-Aminopurinophane (2)

6-Chloro-9-(1-aminononyl)purine (100 mg, 0.338 mmol) was dissolved in 5 ml acetonitrile. Diisopropylethylamine (1 ml, 5.74 mmol) was added and the solution

diluted with an additional 45 ml of acetonitrile to give a 6.8 mM solution of the amino-purine. The reaction was left stirring at 60°C for 48 hours at which time the solution was evaporated and the resultant residue was chromatographed on silica gel using 5% methanol in chloroform. Recrystallization from toluene gave analytically pure crystals of the cyclophane. TLC of the product in 10% methanol in chloroform gave an R_f=.46. The yield was 26% (23 mg, 0.088 mmol). The compound showed:

mp: 121-123°C

^{1}H NMR: (500 MHz at 75°C; 0.2 M solution in $CDCl_3$; sealed tube); δ 0.11 (m, 1H, C5'H), 0.18 (m, 1H, C6'H), 0.39 (m, 1H, C6'H), 0.62 (m, 1H, C4'H), 0.68 (m, 1H, C3'H), 0.72 (m, 1H, C4'H), 0.79 (m, 1H, C5'H), 0.88 (m, 1H, C7'H), 1.02 (m, 1H, C3'H), 1.14 (m, 1H, C7'H), 1.38 (m, 1H, C2'H), 1.56 (m, 1H, C8'H), 1.59 (m, 1H, C2'H), 1.86 (m, 1H, C8'H), 3.64 (m, 1H, C1'H), 3.89 (m, 1H, C9'H), 4.24 (m, 1H, C1'H), 4.58 (m, 1H, C9'H), 5.21 (br, 1H, NH), 7.77 (s, 1H, H2) and 8.32 (s, 1H, H8).

^{13}C NMR: (125 MHz); δ 24.30 (C3'), 24.54 (C7'), 26.96 (C4'), 27.35 (C5'), 27.74 (C6'), 27.90 (C8'), 30.28 (C2'), 42.89 (C1'), 44.97 (C9'), 121.5 (C5), 142.39 (C8), 152.33 (C2), 158.67 (C6).

UV: λ_{max} (methanol); 276.4 nm (ε=13478), 216.2 nm (ε=15512)

HRMS: for $C_{14}H_{21}N_5$: calculated 259.1797; observed 259.1792

MS [CI]: m/z (RI%); 260 $[M+1]^+$ (18), 194 (100) and 177 (71)

Synthesis of 10-Bromo-1-decanol (8, n=10)

The procedure used was that of Kang, Kim and Moon.[43] To a solution of 1,10-

decanediol (17.4 g, 100 mmol) in benzene (200 ml) stirred in a 500 ml round bottom flask equipped with a Dean-Stark trap and a condenser was added hydrobromic acid (48%, 12.5 ml, 110 mmols). The reaction was left to stir at reflux for 28 hours during which time the water trapped was periodically drained. The mixture was washed with 6N NaOH solution (100 ml), 10% HCl (100 ml), water (2x200 ml) and saturated NaCl solution (150 ml). The organic layer was dried with anhydrous magnesium sulphate, evaporated under reduced pressure and the residue purified via distillation. The yield was 80% (18.9 g, 80 mmol). The compound showed:

bp: 110°C @ 0.2 mm (125-127°C @ 3 torr)

^{1}H NMR: (200 MHz); δ 1.23 (m, 12H, $(CH_2)_6$), 1.45 (m, 2H, $C\underline{H_2}$-CH_2-OH), 1.78 (m, 2H, $C\underline{H_2}$-CH_2-Br), 3.34 (t, 2H, J=6.8 Hz, CH_2-Br) and 3.53 (t, 2H, J=6.5 Hz, CH_2-OH)

^{13}C NMR: (50 MHz); δ 62.58, 33.90, 32.64, 32.51, 29.33, 29.23, 29.21, 28.58, 27.98, 25.58

MS[EI] m/z (RI%); 237 $[M+1]^+$ (18); 221 (63); 190 (100); 177 (44)

HRMS: for $C_{10}H_{22}BrO$ $[M+1]^+$: calculated 237.0854; observed 237.0863

Synthesis of 10-Azido-1-decanol (9, n=10)

The procedure used was that of Reeves and Bahr.[50] 10-Bromo-1-decanol (10.0 g, 42.3 mmol) was added to a stirred solution of 25% aqueous sodium azide (10.25 g in 40 ml of water). Aliquat 336 (1.62 g, 4 mmol) was added and the mixture heated to 100°C. After 30 hours, the reaction was cooled and the phases separated. The 10-azidodecanol was purified via distillation. Yield 87% (7.3 g, 36.9 mmol). The

compound showed:

bp: 103°C @ 0.3 mm

^{1}H NMR: (200 MHz); δ 1.24 (m, 12H, $(CH_2)_6$), 1.53 (m, 4H, $C\underline{H_2}$-CH_2-OH and $C\underline{H_2}$-CH_2-N_3), 3.19 (t, 2H, J=6.8 Hz, CH_2-N_3) and 3.54 (t, 2H, J=6.6 Hz, CH_2-OH)

^{13}C NMR: (50 MHz); δ 62.62, 51.29, 32.56, 29.33, 29.24, 28.96, 28.65, 26.52, 25.58

IR: 3360 cm^{-1} (br, OH); 2095 cm^{-1} (s, N_3)

Synthesis of 6-Chloro-9-(10-azidodecyl)purine (**10**)

The procedure used was similar to that of Iwakawa *et al.*[41] To a mixture of 6-chloropurine (4.77 g, 30.86 mmol), triphenylphosphine (8.09 g, 30.84 mmol) and diethyl azidocarboxylate (6.64 g, 6 ml, 30.81 mmol) in 120 ml of dry THF was added a solution of 10-azidodecanol (6.00 g, 30.15 mmol) in 40 ml of THF. The solution was allowed to stir at room temperature for 48 hours at which time the reaction mixture was concentrated under reduced pressure. The residue was chromatographed on silica gel using chloroform as the eluent yielding a viscous yellow oil. TLC of the product with 5% methanol in chloroform gave an R_f=0.62. The yield was 32% (3.31 g, 9.88 mmol). The compound showed:

^{1}H NMR: (200 MHz); δ 1.25 (m, 10H, $(CH_2)_6$), 1.57 (m, 2H, $C\underline{H_2}$-CH_2-N_3), 1.94 (m, 2H, $C\underline{H_2}$-CH_2-N9), 3.23 (t, 2H, J=6.8 Hz, CH_2-N_3), 4.27 (t, 2H, J=7.3 Hz, CH_2-N9), 8.14 (s, 1H, H2), 8.74 (s, 1H, H8)

MS [EI]: m/z (RI%); 336 $[M+1]^+$ (100); 295 (6); 265 (10); 209 (18); 115 (23)

HRMS: for $C_{15}H_{23}N_7Cl$ $[M+1]^+$: calculated 336.1703; observed 336.1714

Synthesis of 6-Chloro-9-(10-aminodecyl)purine (11)

The procedure used was similar to that of Vaultier *et al.*[47] To 6-chloro-9-(10-azidodecyl)purine (1.0 g, 2.99 mmol) in 3 ml of THF was added triphenylphosphine (783 mg, 2.99 mmol), water (80 µl, 4.50 mmol) and a boiling chip. The evolution of N_2 began immediately. The mixture was left standing at room temperature for 18 hours. TLC of the reaction mixture showed the complete disappearance of the azide starting material and the appearance of a ninhydrin positive spot on the baseline. The solution was then concentrated, redissolved in 50 ml of chloroform and extracted with three 20 ml portions of 0.01M HCl. The combined aqueous solutions were adjusted to pH 8 with 1M NaOH and extracted with three 30 ml portions of chloroform. These combined organic solutions were dried over anhydrous sodium sulphate and evaporated under reduced pressure. The product was subjected immediately to cyclization conditions.

Synthesis of [10](N6,9)-6-Aminopurinophane (3)

6-Chloro-9-(10-aminodecyl)purine (700 mg, 2.27 mmol) was dissolved in 50 ml acetonitrile. Diisopropylethylamine (2 ml, 11.48 mmol) was added and the solution diluted with an additional 450 ml of acetonitrile. The reaction was left stirring at 60°C for 48 hours at which time the solution was evaporated and the resultant residue was chromatographed on silica gel using 5% methanol in chloroform. TLC of the product in 10% methanol in chloroform gave an R_f=0.50. The yield was 37% (229 mg, 0.84 mmol). The compound showed:

^{1}H NMR: (500 MHz at 90°C; 0.2 M solution in $CDCl_3$; sealed tube); δ 0.30 (m, 1H, C7'H), 0.59 (m, 1H, C7'H), 0.61 (m, 1H, C5'H), 0.77 (m, 1H, C5'H), 0.96 (m, 1H, C4'H), 1.11 (m, 1H, C6'H), 1.12 (m, 1H, C8'H), 1.18 (m, 1H, C6'H), 1.21 (m, 1H, C8'H), 1.24 (m, 1H, C3'H), 1.32 (m, 1H, C4'H), 1.41 (m, 1H, C3'H), 1.54 (m, 1H, C2'H), 1.64 (m, 1H, C9'H), 1.73 (m, 1H, C2'H), 2.04 (m, 1H, C9'H), 3.79 (m, 1H, C1'H), 3.96 (m, 1H, C10'H), 4.34 (m, 1H, C1'H), 4.57 (m, 1H, C10'H), 5.3 (br, 1H, NH), 7.8 (s, 1H, H2) and 8.2 (s, 1H, H8).

^{13}C NMR: (125 MHz); δ 25.8 (C8'), 28.1 (C5'), 28.9 (C7'), 28.9 (C6'), 29.0 (C4'), 29.1 (C9'), 29.6 (C3'), 31.5 (C2'), 42.2 (C1'), 44.7 (C10'), 124.1 (C5), 146.9 (C8), 155.3 (C2), 159.7 (C6).

MS [EI]: m/z (RI%); 273 $[M]^+$ (100), 244 (7), 230 (23), 216 (12), 176 (15), 148 (29), 120 (13), 84 (38)

HRMS: for $C_{15}H_{23}N_5$: calculated 273.1953; observed 273.1945

UV: λ_{max} (methanol); 273.0 nm (ε=13823), 213.0 nm (ε=16150)

Synthesis of 7-Azidoheptanol

The procedure followed is similar to that described by Castro *et al.*[46] 1,7-Heptanediol (2.06 g, 15.6 mmol) was dissolved in 15 ml of dry THF under a nitrogen atmosphere and cooled to -20°C. Carbon tetrachloride (6.0 ml, 9.6 g, 62.2 mmol) was added followed by slow dropwise addition of hexamethylphosphorus triamide (HMPT) (3.1 ml, 2.8 g, 17.1 mmol) via a syringe. The reaction mixture was then added to 100 ml of water and washed with 100 ml of diethyl ether. Potassium hexafluorophosphate

(5.5 g, 30 mmol) was added to the aqueous solution which was then extracted with three 100 ml portions of chloroform. The combined organic extracts were dried over anhydrous sodium sulphate and evaporated under reduced pressure. The oily residue was dissolved in 50 ml of DMF and stirred for 12 hours in the presence of NaN_3 (5 g, 77 mmol) at 80°C. The solvent was subsequently evaporated under reduced pressure and the residue taken up into 100 ml of water followed by extraction with four 100 ml portions of ether. The ether extracts were dried over sodium sulphate and the solvent evaporated under a reduced pressure. The compound was purified by column chromatography on silica gel using 1% methanol in chloroform. TLC with 5% methanol in chloroform using the molybdic acid spray reagent for visualization showed the desired product with an R_f=0.50. The yield was 76% (1.86 g, 11.9 mmol). The compound showed:

^{1}H NMR: (500 MHz); δ 1.34 (m, 6H, $(CH_2)_3$), 1.56 (m, 4H, $C\underline{H_2}$-CH_2-N_3 and $C\underline{H_2}$-CH_2-OH), 3.23 (t, 2H, J=6.7 Hz, CH_2-N_3) and 3.61 (t, 2H, J=6.5 Hz, CH_2-OH)

MS [CI]: m/z (RI%); 175 $[M+18]^+$ (6), 158 $[M+1]^+$ (6), 130 $[M+1-N_2]^+$ (100), 91 (26) and 74 (87)

IR: 3360 cm^{-1} (br, OH), 2095 cm^{-1} (s, N_3)

Synthesis of 6-Chloro-9(7-azidoheptyl) purine

The procedure used was similar to that of Iwakawa *et al.*[41] To a mixture of 6-chloropurine (1.59 g, 10.28 mmol), triphenylphosphine (2.7 g, 10.28 mmol) and diethyl azidocarboxylate (2.20 g, 2 ml, 12.60 mmol) in 40 ml of dry THF was added a solution

of 7-azidoheptanol (1.70 g, 10.80 mmol) in 40 ml of THF. The solution was allowed to stir at room temperature for 48 hours at which time the reaction mixture was concentrated under reduced pressure. The compound was purified by column chromatography on silica gel using 1% methanol in dichloromethane. TLC with 5% methanol in dichloromethane showed the desired product with R_f=0.44. The yield was 20% (632 mg, 2.16 mmol). The compound showed:

^{1}H NMR: (500 MHz); δ 1.29 (m, 6H, $(CH_2)_3$), 1.49 (m, 2H, $C\underline{H_2}$-CH_2-N_3), 1.86 (m, 2H, $C\underline{H_2}$-CH_2-N9), 3.16 (t, 2H, J=6.8 Hz, $C\underline{H_2}$-N_3), 4.21 (t, 2H, J=7.3 Hz, $C\underline{H_2}$-N9), 8.04 (s, 1H, H2) and 8.67 (s, 1H, H8)

MS [EI]: m/z (RI%); 294 $[M+1]^+$ (100), 251 $[M-N_3]^+$ (19), 237 $[M-CH_2N_3]^+$ (20), 223 $[M-(CH_2)_2N_3]^+$ (14), 209 $[M-(CH_2)_3N_3]^+$ (34), 195 $[M-(CH_2)_4N_3]^+$ (39), 181 $[M-(CH_2)_5N_3]^+$ (26), 167 $[M-(CH_2)_6N_3]^+$ (46), 155 $[M-(CH_2)_7N_3]^+$ (57) and 119 (19)

Synthesis of 6-Chloro-9(7-aminoheptyl) purine

The procedure used was similar to that of Vaultier *et al.*[47] To 6-chloro-9-(7-azidoheptyl)purine (457 mg, 1.56 mmol) in 1.6 ml of THF was added triphenylphosphine (410 mg, 1.56 mmol), water (45 µl, 2.34 mmol) and a boiling chip. The evolution of N_2 began immediately. The mixture was left standing at room temperature for 18 hours. TLC of the reaction mixture showed the complete disappearance of the azide starting material and the appearance of a ninhydrin positive spot on the baseline. The solution was then concentrated, redissolved in 50 ml of chloroform and extracted with three 20 ml portions of 0.01M HCl. The combined

aqueous solutions were adjusted to pH 8 with 1M NaOH and extracted with three 30 ml portions of chloroform. These combined organic solutions were dried over anhydrous sodium sulphate and evaporated under reduced pressure. The product was subjected immediately to cyclization conditions. TLC with 10% methanol in chloroform using ninhydrin spray for visualization showed the desired product with an R_f=0.05. The compound showed:

^{1}H NMR: (500 MHz); δ 1.32 (m, 6H, $(CH_2)_3$), 1.70 (m, 2H, $C\underline{H_2}$-CH_2-NH_2), 1.87 (m, 2H, $C\underline{H_2}$-CH_2-N9), 2.93 (br, 2H, CH_2-NH_2), 4.24 (t, 2H, J=7.3 Hz, CH_2-N9), 8.25 (br, 2H, NH_2), 8.27 (s, 1H, H2) and 8.69 (s, 1H, H8)

MS [CI]: m/z (RI%); 268 $[M+1]^+$ (100), 234 $[M+1-35]^+$ (22), 203 (6) and 132 (18).

Attempted Synthesis of [7](N6,9)-6-Aminopurinophane

The procedure employed in the synthesis of [9]-(N6,9)-6-aminopurinophane was used with 267 mg (1.00 mmol) of 6-chloro-9(7-aminoheptyl) purine and diisopropylethylamine (1 ml, 5.74 mmol) stirred in 1 litre of refluxing acetonitrile for 48 hours. The solvent was evaporated under a reduced pressure and the reaction products chromatographed on silica gel using 5% methanol in chloroform. Analysis of the fractions collected showed the presence of mostly unreacted starting material and no evidence of cyclophane. Repeating the reaction in the presence of one equivalent of silver tetrafluoroborate produced essentially the same results.

Synthesis of N6-Nonyladenine (12)

6-Chloropurine (1 g, 6.47 mmol) was dissolved in a solution of 1-nonylamine

(2.78 g, 3.56 ml, 19.41 mmol) in 25 ml of acetonitrile and allowed to stir at room temperature for 48 hours. The solution was concentrated under reduced pressure and chromatographed on silica gel using 5% methanol in chloroform as the eluent. The alkylated purine was recrystallized from toluene. TLC using 10% methanol in chloroform showed the desired product with an R_f=0.36. The yield was 83% (1.40 g, 5.37 mmol). The compound showed:

m.p.: 162-164°C

^{1}H NMR: (500 MHz); δ 0.86 (t, 3H, J=6.7 Hz, CH_3), 1.25 (m, 8H, CH_3-(CH_2)$_4$), 1.34 (m, 2H, NH-(CH_2)$_3$-CH_2), 1.43 (m, 2H, NH-(CH_2)$_2$-CH_2), 1.71 (m, 2H, NH-CH_2-CH_2), 3.66 (br, 2H, NH-CH_2), 6.16 (br, 1H, NH), 7.97 (s, 1H, H2), 8.43 (s, 1H, H8)

^{13}C NMR: (125 MHz); δ 14.04 (CH_3), 22.61 (CH_2-CH_3), 26.91, 29.21, 29.33, 29.48, 29.68, 31.82, 40.85 (NH-CH_2), 137.94 (C8), 152.24 (C2)

MS [EI]: m/z (RI%); 261 [M]$^+$ (47), 246 (6), 232 (12), 218 (20), 204 (43), 190 (70), 176 (36), 162 (39), 149 (100), 135 (88), 108 (27), 94 (7), 79 (7), 67 (13), 55 (27)

HRMS: for $C_{14}H_{23}N_5$: calculated 261.1953; observed 261.1963

UV: λ_{max} (methanol); 209.9 nm , 268.5 nm

Synthesis of 6-Chloro-9-nonyl purine (**13**)

The procedure used was similar to that of Iwakawa *et al.*[41] To a mixture of 6-chloropurine (4.77 g, 30.86 mmol), triphenylphosphine (8.09 g, 30.84 mmol) and diethyl azidocarboxylate (6.64 g, 6 ml, 30.81 mmol) in 120 ml of dry THF, was added a

solution of 1-nonanol (4.35 g, 5.26 ml, 30.15 mmol) in 40 ml of THF. The solution was allowed to stir at room temperature for 48 hours, at which time the reaction mixture was concentrated under reduced pressure. The residue was chromatographed on silica gel using chloroform as the eluent. TLC of the product with 5% methanol in chloroform gave an R_f=0.75. The yield was 80% (6.75 g, 24.12 mmol). The compound showed:

^{1}H NMR: (200 MHz); δ 0.85 (t, 3H, J=6.7 Hz, CH_3), 1.23 (m, 12H, $(C\underline{H}_2)_6$-CH_3), 1.90 (m, 2H, N9-CH_2-$C\underline{H}_2$), 4.24 (t, 2H, J=7.3 Hz, N9-CH_2), 8.12 (s, 1H, H2), 8.72 (s, 1H, H8)

Synthesis of N6, N9-Dinonyladenine (14)

6-Chloro-9-nonyl-purine (1 g, 3.57 mmol) was dissolved in a solution of 1-nonyl amine (1.53 g, 2 ml, 10.71 mmol) in 25 ml of acetonitrile and allowed to stir at room temperature for 48 hours. The solution was concentrated under reduced pressure and chromatographed on silica gel using ethyl acetate as the eluent. TLC using ethyl acetate showed the desired product with an R_f=0.73. The yield was 62% (857 mg, 2.21 mmol). The compound showed:

^{1}H NMR: (500 MHz); δ 0.76 (t, 6H, J=6.8 Hz, 2xCH_3), 1.14 (m, 16H), 1.21 (m, 4H), 1.29 (m, 2H), 1.56 (m, 2H), 1.78 (m, 2H), 3.54 (br, 2H, NH-$C\underline{H}_2$), 4.07 (t, 2H, J=7.3 Hz, N9-CH_2), 6.14 (s, 1H, NH), 7.63 (s, 1H, H2), 8.30 (s, 1H, H8)

^{13}C NMR: (125 MHz); δ 13.80, 22.41, 26.48, 26.77, 28.88, 28.96, 29.06, 29.12, 29.12, 29.33, 29.62, 29.95, 31.60, 31.66, 40.57, 43.66, 119.99 (C5),

139.25 (C8), 148.77 (C4), 152.97 (C2), 154.90 (C6)

MS [EI]: m/z (RI%); 387 $[M]^+$ (100), 371 (73), 358 (58), 344 (44), 330 (60), 316 (96), 302 (39), 288 (95)

HRMS: for $C_{23}H_{41}N_5$: calculated 387.3362; observed 387.3370

UV: λ_{max} (methanol); 209.1 nm , 268.7 nm

Synthesis of 9-Nonyladenine (15)

6-Chloro-9-nonyl-purine (1 g, 3.57 mmol) was dissolved in 50 ml of saturated methanolic ammonia and left to stir for 30 days. The solvent was removed under reduced pressure and the residue chromatographed on silica gel using 5% methanol in chloroform as the eluent. The alkylated purine was recrystallized from toluene. TLC using 10% methanol in chloroform showed the desired product having an R_f=0.44. The yield was 25% (232 mg, 0.89 mmol). The compound showed:

m.p.: 121-126°C

^{1}H NMR: (500 MHz); δ 0.84 (t, 3H, J=6.8 Hz, CH_3), 1.22 (m, 8H, CH_3-($C\underline{H}_2$)$_4$), 1.30 (m, 4H, N9-CH_2-CH_2-($C\underline{H}_2$)$_2$), 1.87 (m, 2H, N9-CH_2-$C\underline{H}_2$), 4.16 (t, 2H, J=7.3 Hz, N9-CH_2), 5.90 (s, 2H, NH_2), 7.77 (s, 1H, H2), 8.35 (s, 1H, H8)

^{13}C NMR: (125 MHz); δ 14.02 (CH_3), 22.58 (CH_3-$\underline{C}H_2$), 26.58, 26.63, 29.01, 29.11, 29.33, 30.06, 31.75, 43.95 (N9-CH_2), 119.71 (C5), 140.43 (C8), 152.85 (C2), 155.47 (C6)

MS [EI]: m/z (RI%); 261 $[M]^+$ (10), 245 (6), 190 (10), 177 (10), 162 (26), 148 (100), 135 (82), 119 (19), 93 (8), 55 (11)

HRMS: for $C_{14}H_{23}N_5$: calculated 261.1953; observed 261.1958

UV: λ_{max} (methanol); 205.9 nm , 261.1 nm

Synthesis of 1-Azido-9-bromononane (16)

The procedure used was that of Olah *et al.*[56] Chlorotrimethylsilane (3.2 ml, 2.7 g, 25 mmol) was added to a solution of lithium bromide (1.74 g, 20 mmol) in 20 ml of dry acetonitrile under a nitrogen atmosphere. 9-Azidononanol (925 mg, 5 mmol) was then added and the reaction mixture heated under reflux for 24 hours. The solution was taken up into 50 ml of diethyl ether and then washed successively with two 25 ml portions of water, 50 ml of 10% sodium bicarbonate solution and 50 ml of saturated sodium chloride. The organic layer is then dried with anhydrous sodium sulphate and evaporated to a syrup. The product was then purified by chromatography on silica gel using hexanes as the eluent. TLC with CCl_4 using molybdic acid spray for visualization showed the desired product with an R_f=.63. The isolated yield was 90% (1.1 g, 4.5 mmol). The compound showed:

^{1}H NMR: (200 MHz); δ 1.29 (m, 10H, $(CH_2)_5$), 1.57 (m, 2H, $C\underline{H_2}$-CH_2-N_3), 1.79 (m, 2H, $C\underline{H_2}$-CH_2-Br), 3.24 (t, 2H, J=6.8 Hz, CH_2-N_3) and 3.37 (t, 2H, J=6.8 Hz, CH_2-Br).

MS [CI]: m/z (RI%); 222 $[M-2-N_2]^+$ (99), 185 $[M+18-HBr]^+$ (100), 140 (23), 123 (10), 84 (12) and 70 (48).

Synthesis of N4-Acetylcytosine (17)

Cytosine (1 g, 9.00 mmol) was suspended in 50 ml of 10% pyridine in acetic anhydride, heated to 70°C and allowed to stir for 4 hours. The solvent is then

evaporated under a reduced pressure affording pure product. Yield, as determined by NMR, was quantitative. The compound showed:

^{1}H NMR: (200 MHz in DMSO-d_6); δ 2.07 (s, 3H, CH_3), 7.07(d, 1H, J=7.0 Hz, H5) and 7.81 (d, 1H, J=7.0 Hz, H6).

MS [EI]: m/z (RI%); 153 $[M]^+$ (71) and 110 $[M\text{-}COCH_3]^+$ (100)

Synthesis of 1-(9-Azidononyl) cytosine (18)

The procedure used is similar to that employed by Browne *et al.*[54] N4-Acetylcytosine (237 mg, 1.55 mmol) was dissolved, with heating, in 35 ml of dry dimethylsulphoxide. After allowing the solution to cool to room temperature, 1-azido-9-bromononane (384 mg, 1.55 mmol) and anhydrous potassium carbonate (235 mg, 1.70 mmol) were added and the mixture left to stir at room temperature for 48 hours. The reaction mixture was then filtered and the solvent evaporated under reduced pressure. The remaining pale yellow oil was taken up into 50 ml of water and extracted with four 50 ml portions of chloroform. The chloroform extracts were then dried with anhydrous sodium sulphate and evaporated under a reduced pressure. The resultant syrup was dissolved in 25 ml of methanolic ammonia (presaturated at room temperature) and allowed to stand at ambient temperature overnight. The solvent was then evaporated and the crude product chromatographed on silica gel with 7.5% methanol in chloroform. TLC with 10% methanol in chloroform showed the desired product having an R_f=0.16. The yield was 26% (112 mg, 0.40 mmol). The compound showed:

^{1}H NMR: (200 MHz in DMSO-d_6); δ 1.24 (m, 10H, $(CH_2)_5$), 1.51 (m, 4H, $C\underline{H_2}$-CH_2-N_3 and $C\underline{H_2}$-CH_2-N1), 3.29 (t, 2H, J=6.8 Hz, CH_2-N_3), 3.58 (t, 2H, J=7.1

Hz, CH_2-N1), 5.60 (d, 1H, J=7.1 Hz, H5), 6.98 (br, 2H, NH_2) and 7.54 (d, 1H, J=7.1 Hz, H6).

Synthesis of 1-(9-Azidononyl)-4-N-tosylcytosine (19)

p-Toluenesulfonyl chloride (130 mg, 0.684 mmol) was dissolved in 2 ml of dry pyridine under a nitrogen atmosphere. To this solution was added 1-(9-azidononyl)-cytosine (95 mg, 0.342 mmol) in 3 ml of dry pyridine. The solution was stirred at 60°C for 16 hours. The reaction mixture was then taken up into 50 ml of chloroform and washed with three 50 ml portions of water. The chloroform layer was then dried with anhydrous sodium sulphate and evaporated under reduced pressure. The resultant syrup was chromatographed on silica gel using 2% methanol in dichloromethane. TLC in 5% methanol in dichloromethane showed the desired product with R_f=0.50. The yield was 79% (116 mg, 0.270 mmol). The compound showed:

^{1}H NMR: (200 MHz) δ 1.29 (m, 10H, $(CH_2)_5$), 1.60 (m, 4H, $C\underline{H}_2$-CH_2-N_3 and $C\underline{H}_2$-CH_2-N1), 2.41 (s, 3H, CH_3), 3.25 (t, 2H, J=6.8 Hz, CH_2-N_3), 3.72 (t, 2H, J=7.1 Hz, CH_2-N1), 7.22 (d, 2H, J=8.3 Hz, meta-H's on tosylate), 7.26 (d, 1H, J=7.1 Hz, H5), 7.31 (d, 1H, J=7.1 Hz, H6) and 7.82 (d, 2H, J=8.3 Hz, ortho-H's on tosylate).

MS [CI] m/z (RI%); 433 $[M+1]^+$ (100), 279 [M+1-tosylate]$^+$ (32), 222 [M+1-tosylate-CH_2N_3]$^+$ (6), 174 (27) and 139 (24)

Synthesis of 1-(9-Aminononyl)-4-N-tosylcytosine (20)

The procedure used was similar to that of Vaultier *et al.*[47] To 1-(9-azidononyl)-

4-N-tosylcytosine (1.29 g, 2.99 mmol) in 3 ml of THF was added triphenylphosphine (783 mg, 2.99 mmol), water (80 µl, 4.50 mmol) and a boiling chip. The evolution of N_2 began immediately. The mixture was left standing at room temperature for 18 hours. The disappearance of the spot attributed to the azide coincided with the appearance of a new spot on the baseline which was shown to be an amine via the ninhydrin spray. The solution was then concentrated, redissolved in 50 ml of chloroform and extracted with three 20 ml portions of 0.01M HCl. The combined aqueous solutions were adjusted to pH 8 with 1M NaOH and extracted with three 30 ml portions of chloroform. These combined organic solutions were dried over anhydrous sodium sulphate and evaporated under reduced pressure. The amine was subjected immediately to cyclization conditions.

Attempted Synthesis of [9](1,N4)-4-Amino-2-one-pyrimidinophane via 1-(9-Aminononyl)-4-tosylcytosine

1-(9-Aminononyl)-4-tosylcytosine (100 mg, 0.246 mmol) was dissolved in 50 ml of dry pyridine, heated to 60°C and stirred for 5 days. The solvent was evaporated under a reduced pressure and the reaction products chromatographed on silica gel using 5% methanol in chloroform. Analysis of the fractions collected showed the presence of mostly unreacted starting material and no evidence of cyclophane formation.

Synthesis of 1-Octyluracil (21)

The procedure used was a modification of that employed by Browne *et al.*[54] To

a solution of uracil (10 g, 0.089 mmol) in 650 ml of dry dimethylsulphoxide were added 8-bromooctane (19.3 g, 13.3 ml, 0.100 mol) and anhydrous potassium carbonate (13.8 g, 0.100 mol). The suspension was left to stir at room temperature for 48 hours at which time the reaction mixture was filtered and the solvent evaporated under reduced pressure. The remaining pale yellow oil was taken up into 1 litre of water and extracted with six 500 ml portions of chloroform. The chloroform extracts were then dried with anhydrous sodium sulphate and evaporated under a reduced pressure. The resultant yellow syrup was dissolved in 25 ml of absolute ethanol and then treated with 50 ml of water. Evaporation of the ethanol allowed for the precipitation of the product in the remaining water. The product was filtered and the ethanol-water precipitation repeated twice more. TLC using 5% methanol in chloroform showed the desired product with R_f=0.37. The yield was 33% (6.57 g, 0.029 mmol). The compound showed:

^{1}H NMR: (200 MHz) δ 0.88 (t, 3H, J=6.7 Hz, CH_3), 1.28 (m, 10H, $(CH_2)_5$), 1.70 (m, 2H, $C\underline{H_2}$-CH_2-N1), 3.72 (t, 2H, J=7.2 Hz, CH_2-N1), 5.71 (d, 1H, J=7.8 Hz, H5), 7.17 (d, 1H, J=7.8 Hz, H6) and 9.01 (br, 1H, NH)

MS [EI]: m/z (RI%); 2224 $[M]^+$ (40), 209 $[M\text{-}CH_3]^+$ (6), 195 $[M\text{-}CH_2CH_3]^+$ (22), 181 $[M\text{-}(CH_2)_2CH_3]^+$ (26), 167 $[M\text{-}(CH_2)_3CH_3]^+$ (55), 153 $[M\text{-}(CH_2)_4CH_3]^+$ (85), 139 $[M\text{-}(CH_2)_5CH_3]^+$ (13), 126 (34), 125 (27), 112 (93), 96 (21), 82 (100) and 69 (31).

Synthesis of 1-Octyl-4-chloro-pyrimidin-2-one (**22**)

The procedures developed were similar to those used by Zemlicka and Sorm.[60]

Method A: *Catalytic generation of Vilsmeier's reagent (chloromethylene dimethyl ammonium chloride) "in situ"*

1-Octyl-uracil (900 mg, 4 mmol) was dissolved in 20 ml of chloroform. To this solution, thionyl chloride (3.2 ml, 0.02 mole) and dimethylformamide (0.2 ml) were added and the mixture refluxed for 6 hours. At this time, the solution was allowed to cool and carried on to the following step. The yield, as determined by ^{1}H-NMR, was 98%.

Method B: *Addition of one equivalent of Vilsmeier's reagent*

1-Octyl-uracil (900 mg, 4 mmol) was dissolved in 20 ml of chloroform. To this solution, chloromethylene dimethyl ammonium chloride (Vilsmeier's reagent as prepared by Hepburn and Hudson[61] (525 mg, 4.1 mmol) was added and the mixture refluxed for 3 H. At this time, the solution was allowed to cool and carried on to the following step. The yield, as determined by ^{1}H-NMR, was 95%. The compound showed:

^{1}H NMR: (500 MHz); δ 0.80 (t, 3H, J=6.7 Hz, CH_3), 1.20 (m, 12H, $(CH_2)_6$), 1.70 (m, 2H,$C\underline{H}_2$-CH_2-N1), 3.82 (t, 2H, J=7.5 Hz, CH_2-N1), 6.30 (d, 1H, J=6.8 Hz, H5), 7.59 (d, 1H, J=6.8 Hz, H6)

MS[EI]: m/z (RI%); 243 $[M+1]^+$ (48); 207 $[M-Cl]^+$ (23); 185 (30); 171 (20); 158 (23); 144 (100); 131 (82)

Synthesis of 1-Octyl-4-N-butyl cytosine via 1-Octyl-4-chloro-pyrimidin-2-one (**23**)

1-Octyl-4-chloro pyrimidin-2-one (100 mg, 0.40 mmol) was freshly prepared in 2 ml of chloroform (as above). The mixture was added to 10 ml of *n*-butyl amine and the

solution stirred for 1 hour at room temperature. Evaporation under reduced pressure gave a pale yellow oil which was purified using column chromatography on silica gel eluting with 5% methanol in chloroform. Yield 95% (106 mg, 0.38 mmol). The compound showed:

^{1}H-NMR: (200 MHz in acetone-d_6); δ 0.89 (m, 6H, 2 x CH_3), 1.29 (m, 12H, $(CH_2)_5$ + CH_2), 1.53 (m, 2H, $C\underline{H_2}$-CH_2-N1), 1.64 (m, 2H, $C\underline{H_2}$-CH_2-N4), 3.35 (m, 2H, CH_2-N4), 3.68 (t, 2H, J=7.0 Hz, CH_2-N1), 5.71 (d, 1H, J=7.1 Hz, H5), 7.42 (d, 1H, J=7.1 Hz, H6)

MS[EI]: m/z (RI%); 279 $[M]^+$ (70); 264 $[M-CH_3]^+$ (14); 250 $[M-CH_2-CH_3]^+$ (66); 236 $[M-(CH_2)_2-CH_3]^+$ (74); 222 $[M-(CH_2)_3-CH_3]^+$ (76); 208 $[M-(CH_2)_4-CH_3]^+$ (50); 194 $[M-(CH_2)_5-CH_3]^+$ (51); 181 (100); 167 (38)

HRMS: for $C_{16}H_{29}N_3O$: calculated 279.2311; observed 279.2301

Synthesis of 1-(9-Azidononyl)-uracil (**24**)

Method A:

The procedure used was a modification of that employed by Browne *et al.*[54] To a solution of uracil (10 g, 89 mmol) in 650 ml of dry dimethylsulphoxide were added 1-azido-9-bromononane (24.8 g, 100 mmol) and anhydrous potassium carbonate (13.8 g, 100 mmol). The suspension was left to stir at room temperature for 48 hours at which time the reaction mixture was then filtered and the solvent evaporated under reduced pressure. The remaining pale yellow oil was taken up into 1 litre of water and extracted with six 500 ml portions of chloroform. The chloroform extracts were then dried with anhydrous sodium sulphate and evaporated under a reduced pressure. The

crude product was purified by column chromatography on silica gel using chloroform as the eluent. TLC using 5% methanol in chloroform showed the desired product with an R_f=0.50. The yield was 34% (3.4 g, 30 mmol).

Method B:

The procedure used was similar to that of Iwakawa *et al.*[41] To a mixture of uracil (1.44 g, 12.86 mmol), triphenylphosphine (3.37 g, 12.86 mmol) and diethyl azidocarboxylate (2.24 g, 2.03 ml, 12.86 mmol) in 50 ml of dry THF was added a solution of 9-azidononanol (2.32 g, 12.56 mmol) in 15 ml of THF. The solution was allowed to stir at room temperature for 48 hours at which time the reaction mixture was concentrated under reduced pressure. The product was purified as described above. Yield (not optimized) 7% (246 mg, 0.88 mmol).

Method C:

The procedure used was that described by Signh, Aggarwal and Kumar.[58] To a solution of 2,4-bis(trimethylsiloxy)pyrimidine (1.12 g, 10 mmol)(as prepared by Aoyama[59]) in 1,2 dichloroethane (20 ml) was added 1-azido-9-bromononane (2.96 g, 12 mmol) and iodine (20 mg). The solution was heated to reflux and allowed to stir for 48 hours. At this time, the reaction mixture was cooled and treated with 1M $Na_2S_2O_3$ (3 x 50 ml). The organic layer was dried with magnesium sulphate, evaporated under reduced pressure and chromatographed on silica gel as described above. Yield (not optimized) 29% (809 mg, 2.9 mmol). The compound showed:

mp: 41-43°C

^{1}H NMR: (500 MHz); δ 1.21 (m, 10H, $(CH_2)_5$), 1.49 (m, 2H,C$\underline{H_2}$-CH_2-N1), 1.58 (m, 2H,C$\underline{H_2}$-CH_2-N_3), 3.16 (t, 2H, J=6.9 Hz, CH_2-N_3), 3.63 (t, 2H, J=7.3 Hz,

CH_2-N1), 5.61 (d, 1H, J=7.8 Hz, H5), 7.11 (d, 1H, J=7.8 Hz, H6) and 10.20 (s, 1H, H3)

^{13}C NMR: (125 MHz); δ 26.04, 26.33, 28.50, 28.71, 28.93, 48.54 (C1'), 51.13 (C9'), 101.75 (C5), 144.43 (C6), 150.94 (C2), 164.27 (C4)

MS[EI]: m/z (RI%); 280 $[M+1]^+$ (17); 237 $[M-N_3]^+$ (10); 223 $[M-CH_2-N_3]^+$ (26); 209 $[M-(CH_2)_2-N_3]^+$ (37); 195 $[M-(CH_2)_3-N_3]^+$ (10); 181 $[M-(CH_2)_4-N_3]^+$ (21); 167 $[M-(CH_2)_5-N_3]^+$ (26); 153 $[M-(CH_2)_6-N_3]^+$ (28); 140 (35); 126(79); 113 (100)

HRMS: for $C_{13}H_{21}N_5O_2$ $[M+1]^+$: calculated 280.1774; observed 280.1777

IR: 2075 cm^{-1} (s, N_3); 1680 cm^{-1} (br, CONH)

Synthesis of 1-(9-Azidononyl)-4-chloro-pyrimidin-2-one (25)

The procedures developed in the synthesis of 1-(octyl)-4-chloro pyrimidin-2-one were followed with 1-(9-azidononyl)-uracil (1.12g, 4mmol) substituted for the 1-octyl-uracil. The yield, as determined by ^1H-NMR, was 95%.

^1H NMR: (200 MHz); δ 1.23 (m, 10H, $(CH_2)_5$), 1.50 (m, 2H, $C\underline{H_2}$-CH_2-N_3), 1.70 (m, 2H, $C\underline{H_2}$-CH_2-N1), 3.17 (t, 2H, J=6.8 Hz, CH_2-N_3), 3.80 (t, 2H, J=7.2 Hz, CH_2-N1), 6.30 (d, 1H, J=6.8 Hz, H5), 7.62 (d, 1H, J=6.8 Hz, H6)

Reduction of 1-(9-Azidononyl)-4-chloro-pyrimidin-2-one (26) and Attempted Synthesis of [9](1,N4)-4-Amino-2-one-pyrimidinophane

The procedure used was that of Vaultier *et al.*[47] Freshly prepared 1-(9-azidononyl)-4-chloro-pyrimidin-2-one (163 mg, 0.55 mmol) (as above) was evaporated to a residue and redissolved in dry tetrahydrofuran (0.5 ml). To this solution was

added triphenylphosphine (145 mg, 0.55 mmol), H_2O (15 µl, 0.825 mmol) and a boiling chip. Evolution of N_2 began immediately. The mixture was left standing at room temperature for 18h. TLC of the reaction mixture showed the appearance of a ninhydrin positive spot on the baseline. The mixture was then added to 500 ml of dry acetonitrile treated with diisopropylethylamine (1 ml, 5.74 mmol) and left to stir at 60°C for 48 hours. At this time the solution was evaporated under reduced pressure and the resultant residue chromatographed on silica gel. Analysis of the fractions collected showed no evidence of the cyclophane but mostly 1-(9-aminononyl)-uracil.

Synthesis of 1-(9-Aminononyl)-uracil (**27**)

The procedure used was that of Corey *et al.*[63] 1-(9-Azidononyl)-uracil (250 mg, 0.89 mmol) in ethanol (10 ml) was stirred with Lindlar's catalyst (80 mg) under 1 atmosphere of H_2. The reduction was complete in 6 hours at which time the mixture was filtered through celite and the ethanol evaporated under reduced pressure. Yield 89% (200 mg, 0.79 mmol). The compound showed:

^{1}H NMR: (200 MHz); δ 1.27 (m, 10H, $(CH_2)_5$), 1.45 (m, 2H, $C\underline{H_2}$-CH_2-N1), 1.65 (m, 2H, $C\underline{H_2}$-CH_2-NH_2), 2.67 (m, 2H, CH_2-NH_2), 3.69 (t, 2H, J=7.1 Hz, CH_2-N1), 4.20 (m, 2H, NH_2), 5.66 (d, 1H, J=7.8 Hz, H5), 7.12 (d, 1H, J=7.8 Hz, H6)

MS[CI]: m/z (RI%); 254 $[M+1]^+$ (100)

Synthesis of 1-(9-Aminononyl)-4-chloro-pyrimidin-2-one Hydrochloride (28) and Attempted Synthesis of [9](1,N4)-4-Amino-2-one-pyrimidinophane

1-(9-Aminononyl)-uracil (450 mg, 2 mmol) was dissolved in 10 ml of dimethylforamide and HCl gas was bubbled through the solution for 10 minutes. Chloromethylene dimethyl ammonium chloride (Vilsmeier's reagent) (260 mg, 2.1 mmol), prepared as above, was then added and the solution refluxed for 6 hours. The mixture was then added to 500 ml of dry acetonitrile, treated with diisopropylethylamine (1 ml, 5.74 mmol) and left to stir at 60°C for 48 hours. The solution was evaporated under reduced pressure and the resultant residue chromatographed on silica gel. Analysis of the fractions collected showed no evidence of the cyclophane with mostly 1-(9-aminononyl)-uracil being recovered.

Synthesis of 1-(9-Azidononyl)-4-thiophenyl-pyrimidin-2-one (29)

1-(9-Azidononyl)-4-chloro pyrimidin-2-one (119 mg, 0.40 mmol) was freshly prepared (as described above) and added to a flask containing 5 ml of thiophenol. The mixture was allowed to stir at room temperature for 6 hours at which time the thiophenol was removed by distillation. The residue was dissolved in a small amount of chloroform, treated with toluene, and crystallized over 18 hours at 0°C. TLC with 5% methanol in chloroform showed the desired product with an R_f=0.50. Yield 85% (126 mg, 0.34 mmol). The compound showed:

^{1}H NMR: (500 MHz); δ 1.27 (m, 10H, $(CH_2)_5$), 1.50 (m, 2H, $C\underline{H_2}$-CH_2-N_3), 1.69 (m, 2H, $C\underline{H_2}$-CH_2-N1), 3.21 (t, 2H, J=6.9 Hz, CH_2-N_3), 3.77 (t, 2H, J=7.1 Hz, CH_2-N1), 5.80 (d, 1H, J=6.4 Hz, H5), 7.29 (d, 1H, J=6.4 Hz, H6), 7.44 (m, 3H, meta- and para-H's), 7.56 (m, 2H, ortho-H's)

MS[CI]: m/z (RI%); 388 (5); 372 $[M+1]^+$ (100); 345 (20); 317 (15); 280 [M-

thiophenyl+18] (14)

Synthesis of 1-(Octyl)-4-thiophenyl-pyrimidin-2-one (**30**)

1-Octyl-4-chloro pyrimidin-2-one (100 mg, 0.40 mmol) was freshly prepared (as described above) and added to a flask containing 5 ml of thiophenol. The mixture was allowed to stir at room temperature for 6 hours at which time the thiophenol was removed by distillation. The residue was dissolved in a small amount of chloroform, treated with toluene, and crystallized over 18 hours at 0°C. TLC with 5% methanol in chloroform showed the desired product with an R_f=.48. Yield 83% (104 mg, 0.33 mmol). The compound showed:

^{1}H NMR: (200 MHz); δ 0.88 (t, 3H, J=6.7 Hz, CH_3), 1.24 (m, 10H, $(CH_2)_5$), 1.66 (m, 2H, $C\underline{H_2}$-CH_2-N1), 3.74 (t, 2H, J=7.1 Hz, CH_2-N1), 5.78 (d, 1H, J=6.5 Hz, H5), 7.27 (d, 1H, J=6.5 Hz, H6), 7.49 (m, 5H, phenyl)

MS[CI]: m/z (RI%); 337 (6); 317 $[M+1]^+$ (92); 241 (28); 225 (49); 209 (100)

Oxidation of 1-(Octyl)-4-thiophenyl pyrimidin-2-one (**31**)

The preparation of tetra-*n*-butylammonium oxone and the oxidation procedure employed was that of Trost and Braslau.[65] To a solution of Oxone (10.86 g, 18 mmol) in 45 ml of water was added tetrabutylammonium bisulphate (30.0g, 88 mmol). After stirring at room temperature for half an hour, the reaction mixture was extracted with dichloromethane (3 x 70 ml). The combined organic extracts were dried over $MgSO_4$ and the solvent removed by evaporation under reduced pressure yielding 25.64 g of the oxidizing agent. The tetra-*n*-butylammonium oxone (360 mg, 1.00 mmol) was then

added to a solution of 1-(octyl)-4-thiophenyl pyrimidin-2-one (100 mg, 0.32 mmol) in 1.5 ml of methylene chloride. The reaction was stirred for 24 hours at room temperature. NMR and IR spectroscopy indicated the presence of greater than 95% of the starting material with small amounts of the desired oxidized substrate. The addition of *n*-butyl amine was followed by workup and chromatography yielded less than 5% of 1-octyl-4-chloro-pyrimidin-2-one (4 mg, 0.014 mmol).

Synthesis of 1-Octyl-4-O-(2,4,6-triisopropylbenzenesulphonyl)-pyrimidin-2-one (**32**)

The preparation employed is similar to that of Bischofberger.[67] 1-Octyl uracil (1.045 g, 5.0 mmol) was added to a suspension of NaH (1.250 g, 50 mmol) in tetrahydrofuran (100 ml) and the mixture allowed to stir at room temperature under an argon atmosphere for 30 minutes. At this time, 2,4,6-triisopropylbenzenesulphonyl chloride (2.725 g, 9mmol) was added and the mixture stirred for an additional 16 hours. The reaction was quenched at 0°C with saturated NH_4Cl solution and extracted with chloroform. The organic layer was dried with magnesium sulphate, evaporated under reduced pressure and chromatographed on silica gel using 20% ethyl acetate in hexanes. Yield 70% (1.720 g, 3.5 mmol). The compound showed:

^{1}H-NMR: (200 MHz); δ 0.84 (t, 3H, J=6.8 Hz, $(CH_2)_7$-C$\underline{H}_3$); 1.24 (m, 28H, CH(C$\underline{H}_3$)$_2$ and $(CH_2)_5$); 1.68 (m, 2H, C$\underline{H}_2$-CH_2-N1); 2.88 (m, 1H, para-C$\underline{H}$(CH$_3$)$_2$); 3.77 (t, 2H, J=7.2 Hz, CH_2-N1); 4.22 (m, 2H, ortho-C$\underline{H}$(CH$_3$)$_2$); 6.03 (d, 1H, J=7.0 Hz, H5); 7.18 (s, 2H, meta-H's); 7.60 (d, 1H, J=7.0 Hz, H6).

HRMS: for $C_{27}H_{43}O_4N_2S$: calculated 491.2944; observed 491.2933

Synthesis of 1-Octyl-4-N-butyl cytosine (**23**) via 1-octyl-4-O-(2,4,6-triisopropylbenzenesulphonyl)-pyrimidin-2-one

1-Octyl-4-O-(2,4,6-triisopropylbenzenesulphonyl)-pyrimidin-2-one (196 mg, 0.40 mmol) in 2 ml of chloroform was added to 10 ml of *n*-butyl amine and the solution stirred for 1 hour at room temperature. Evaporation under reduced pressure gave a pale yellow oil which was purified using column chromatography on silica gel eluting with 5% methanol in chloroform. Yield 83% (92 mg, 0.33 mmol). The physical characteristics of the product are listed above.

Synthesis of 1-(9-Azidononyl)-4-O-(triisopropylbenzenesulphonyl) pyrimidin-2-one (**33**)

The procedure developed in the synthesis of 1-octyl-4-O-(2,4,6-triisopropylbenzenesulphonyl)-pyrimidin-2-one was employed using 1.395 g (5 mmol) of 1-(9-azidononyl)-uracil, 1.250 g (50 mmol) of NaH and 2.725 g (9mmol) of 2,4,6-triisopropylbenzenesulphonyl chloride. Yield 67% (1.84 g, 3.35 mmol). The compound showed:

^{1}H-NMR: (200 MHz); δ 1.26 (m, 28H, $CH(C\underline{H}_3)_2$ and $(CH_2)_5$); 1.56 (m, 2H, $C\underline{H}_2$-CH_2-N_3), 1.68 (m, 2H, $C\underline{H}_2$-CH_2-N1); 2.88 (m, 1H, para-$C\underline{H}(CH_3)_2$); 3.22 (t, 2H, J=6.8 Hz, CH_2-N_3), 3.77 (t, 2H, J=7.1 Hz, CH_2-N1); 4.22 (m, 2H, ortho-$C\underline{H}(CH_3)_2$); 6.03 (d, 1H, J=7.0 Hz, H5); 7.18 (s, 2H, meta-H's); 7.59 (d, 1H, J=7.0 Hz, H6).

MS[CI]: m/z (RI%); 568 $[M+18]^+$ (31); 546 $[M+1]^+$ (100); 297 (23); 280 [M-TPS+18]$^+$ (98)

Reduction of 1-(9-Azidononyl)-4-O-(triisopropylbenzenesulphonyl) pyrimidin-2-one (**34**) and Attempted Synthesis of [9](1,N4)-4-Amino-2-one-pyrimidinophane

The procedure used for the reduction of the azide was that of Vaultier *et al.*[47] To 1-(9-Azidononyl)-4-O-(triisopropylbenzenesulphonyl)-pyrimidin-2-one (300 mg, 0.55 mmol) dissolved in 0.5 ml tetrahydrofuran was added triphenylphosphine (145 mg, 0.55 mmol), H_2O (15 µl, 0.825 mmol) and a boiling chip. Evolution of N_2 began immediately. The mixture was left standing at room temperature for 18 hours. TLC of the reaction mixture showed the complete disappearance of the azide and the appearance of a ninhydrin positive spot on the baseline. The mixture was then added to 500 ml of dry acetonitrile treated with diisopropylethylamine (1 ml, 5.74 mmol) and left to stir at 60°C for 48 hours. At this time the solution was evaporated under reduced pressure and the resultant residue chromatographed on silica gel. Analysis of the fractions collected showed no evidence of the cyclophane with the mostly starting material being recovered. Substantial amounts degradative material was isolated when the reaction times were increased.

Synthesis of 1-(3-Bromopropyl)-uracil (**35**)

The procedure employed was a modification of that outlined by Browne, Eisinger and Leonard.[54] 2,4-Bis(trimethylsilyloxy)pyrimidine was prepared by refluxing uracil (17.5 g, 0.156 mol), hexamethyldisilazane (31.5 g, 41 ml, 0.195 mol) and trimethylchlorosilane (1.2 g, 1 ml, 0.008 mol) under a nitrogen atmosphere for 2 hours, as outlined by Aoyama.[59] The bis(trimethylsilyloxy)pyrimidine could then be purified by distillation (71°C @ 0.5 mm) or the remainder of the preparation could be carried out

on the crude reaction mixture. 1,3-Dibromopropane (497 g, 250 ml, 2.463 mol) was added to the bis(trimethylsilyl)pyrimidine and the solution allowed to stir at room temperature for 7 days. At this time, the reaction mixture was poured into 1 litre of water and extracted with 4 x 500 ml of chloroform. The extracts were then dried with sodium sulphate and concentrated by evaporation under reduced pressure to give a solution of the product in 1,3-dibromopropane. Application of this solution to a silica gel column packed in chloroform, followed by chromatography using 2% methanol in chloroform yielded the product as a pale yellow solid. Recrystallization from isopropyl alcohol yielded analytically pure crystals. TLC in 5% methanol in ethyl acetate showed the desired product with an R_f=0.67. The yield was 30% (10.8 g, 46.8 mmol). The compound showed:

m.p.: 87-96°C (lit. 87-96°C)

^{1}H NMR: (200 MHz); δ 2.24 (m, 2H, Br-CH_2-$C\underline{H}_2$), 3.41 (t, 2H, J=6.1 Hz, Br-CH_2), 3.89 (t, 2H, J=6.6 Hz, N1-CH_2), 5.70 (d, 1H, J=7.9 Hz, H5), 7.24 (d, 1H, J=7.9 Hz, H6), 9.95 (s, 1H, H3)

^{13}C NMR: (50 MHz): δ 29.76 (N1-CH_2-$\underline{C}H_2$), 30.93 (Br-CH_2), 47.41 (N1-CH_2), 102.30 (C5), 144.76 (C6), 151.00 (C2), 164.04 (C4)

MS [EI]: m/z (RI%); 234 $[M+2]^+$ (14), 232 $[M]^+$ (15), 155 $[M-Br]^+$ (66), 139 (5), 125 (21), 110 (10), 96 (10), 82 (100), 55 (8), 41 (31)

HRMS: for $C_7H_9O_2N_2Br$: calculated 231.9847; observed 231.9856

Synthesis of 1-(4-Pentynyl)-uracil (**36**)

Using a dry-ice condenser, ammonia (50 ml) was condensed into a cooled 3-

necked flask equipped with a stir-bar. A wide-bore tube was used to introduce acetylene into the reaction vessel. While maintaining a constant stream of acetylene, small chunks of sodium (1.8 g, 0.08 mol in total) were introduced to the stirred ammonia. Care was taken so as to not allow the solution to turn blue. Once all the sodium was added, the acetylene bubbling was discontinued, and 1-(3-bromopropyl)-uracil (1.00 g, 4.3 mmol), in 20 ml of dry THF was added dropwise over 60 minutes by means of a motor-driven syringe. The mixture was allowed to stir for 18 hours and the ammonia permitted to evaporate. Ice water (250 ml) was added carefully to decompose the excess $NaNH_2$. The solution was then treated with 6N HCl until the pH was slightly acidic. The product was extracted with 4 x 100 ml of chloroform and dried with sodium sulphate. The chloroform was evaporated under reduced pressure and the pale yellow powder was recrystallized from isopropanol to give the pure compound. The yield was 87% (0.66 g, 3.7 mmol). TLC using 5% methanol in ethyl acetate showed the desired product with an R_f=0.68. The compound showed:

m.p.: 122-125°C

^{1}H NMR: (500 MHz); δ 1.90 (m, 2H, N1-CH_2-$C\underline{H}_2$), 2.02 (t, 1H, J=2.5 Hz, C≡C-H), 2.24 (dt, 2H, J=2.5 and 6.6 Hz, $C\underline{H}_2$-C≡C-H), 3.85 (t, 2H, J=6.8 Hz, N1-CH_2), 5.68 (d, 1H, J=7.9 Hz, H5), 7.21 (d, 1H, J=7.9 Hz, H6), 9.63 (s, 1H, H3)

^{13}C NMR: (125 MHz); δ 15.38 ($\underline{C}H_2$-C≡C-H), 27.03 (N1-CH_2-$\underline{C}H_2$), 47.73 (N1-CH_2), 70.12 (C≡$\underline{C}$-H), 82.24 ($\underline{C}$≡C-H), 102.10 (C5), 144.72 (C6), 150.96 (C2), 163.93 (C4)

MS [EI]: m/z (RI%); 178 $[M]^+$ (25), 150 (32), 133 (100), 125 (75)

HRMS: for $C_9H_{10}O_2N_2$: calculated 178.0742; observed 178.0740

Coupling of 1-(4-Pentynyl)-uracil (37)

The procedure described is that of Eglington and McCrae.[72] 1-(4-Pentynyl)-uracil (500 mg, 2.81 mmol) in 3 ml of pyridine is added to a solution of $Cu(OAc)_2$ (1.05 g, 5.78 mmol) in 15 ml of pyridine and 15 ml of methanol. The mixture is refluxed for 4 hours, cooled, then added to 200 ml of 3N HCl. The product is extracted into chloroform (3 x 100 ml), dried with sodium sulphate and evaporated to dryness under a reduced pressure. The yield was 83% (414 mg, 1.17 mmol) as determined by NMR. The compound showed:

m.p.: 167-171°C

^{1}H NMR: (200 MHz in pyridine-d_5); δ 2.00 (m, 2H, N1-CH_2-C$\underline{H_2}$), 2.43 (t, 2H, J=6.4 Hz, N1-CH_2-CH_2-C$\underline{H_2}$), 3.93 (t, 2H, J=6.5 Hz, N1-CH_2), 5.77 (d, 1H, J=7.9 Hz, H5), 7.37 (d, 1H, J=7.9 Hz, H6), 13.26 (br, 1H, NH)

MS [CI]: m/z (RI%); 335 $[M+1]^+$ (25), 210 (90), 168 (100)

HRMS: for $C_{18}H_{18}O_4N_4$: calculated 354.1328; observed 354.1311

Synthesis of 1-(4-Pentynyl)-4-N-butyl-cytosine (38)

1-(4-pentynyl)-uracil (712 mg, 4 mmol) was dissolved in 20 ml of chloroform. To this solution, chloromethylene dimethyl ammonium chloride (525 mg, 4.1 mmol) was added and the mixture refluxed for 3 hours. The solution was then cooled and added dropwise to a stirred solution of *n*-butyl amine (1.48 g, 2 ml, 20 mmol) in 5 ml of chloroform. The mixture was then concentrated and chromatographed on silica gel

using 10% methanol in ethyl acetate. TLC using 10% methanol in ethyl acetate showed the desired product with an R_f=0.53. The yield was 95% (885 mg, 3.8 mmol). The compound showed:

m.p. 124-126°C

^{1}H NMR: (200 MHz); δ 0.88 (t, 3H, J=6.7 Hz, CH_3), 1.33 (m, 2H, NH-CH_2-CH_2-CH_2), 1.52 (m, 2H, NH-CH_2-CH_2), 1.91 (m, 2H, N1-CH_2-CH_2), 1.98 (t, 1H, J=2.5 Hz, C≡C-H), 2.19 (dt, 2H, J=2.5 and 6.6 Hz, CH_2-C≡C-H), 3.42 (m, 2H, NH-CH_2), 3.84 (t, 2H, J=7.1 Hz, N1-CH_2), 5.63 (d, 1H, J=7.0 Hz, H5), 7.14 (d, 1H, J=7.0 Hz, H6)

^{13}C NMR: (50 MHz); δ 13.70 (CH_3), 15.31 (N1-CH_2-CH_2-CH_2), 20.00 (NH-CH_2-CH_2-CH_2), 27.11 (N1-CH_2-CH_2), 31.17 (NH-CH_2-CH_2), 40.48 (NH-CH_2), 48.65 (N1-CH_2), 69.59 (C≡CH), 82.84 (C≡CH), 95.10 (C5), 143.91 (C6), 159.25 (C2), 164.04 (C4)

MS [CI]: m/z (RI%); 234 $[M+1]^+$ (100)

HRMS: for $C_{13}H_{19}N_3O$: calculated 233.1528; observed 233.1522

Coupling of 1-(4-Pentynyl)-4-N-butyl cytosine (39)

1-(4-Pentynyl)-4-N-butyl-cytosine (100 mg, 0.216 mmol) was dissolved into 1 ml of dry pyridine and added to a solution of $Cu(OAC)_2$ (150 mg, 0.825 mmol) in 2 ml of pyridine, 2 ml of methanol and 1 ml of diisopropylethylamine. The mixture was left stirring under nitrogen at room temperature for 2 days, at which time it was added to 50 ml of concentrated NH_4OH and extracted with 3 x 25 ml of methylene chloride. The organic extracts were then dried with sodium sulphate and evaporated under a

reduced pressure. The residue was chromatographed on silica gel using 10% methanol in chloroform. TLC using 10% methanol in chloroform showed the desired product with an R_f=0.42. The yield was 40% (20 mg, 0.043 mmol). The compound showed:

^{1}H NMR: (200 MHz); δ 0.86 (t, 3H, J= 6.7Hz, CH_3), 1.32 (m, 2H, NH-CH_2-CH_2-$\underline{CH_2}$), 1.53 (m, 2H, NH-CH_2-$\underline{CH_2}$), 1.90 (m, 2H, N1-CH_2-$\underline{CH_2}$), 2.28 (t, 2H, J=6.5 Hz, $\underline{CH_2}$-C≡C), 3.49 (m, 2H, NH-$\underline{CH_2}$), 3.80 (t, 2H, J=6.9 Hz, N1-CH_2), 5.82 (d, 1H, J=7.1 Hz, H5), 7.10 (d, 1H, J=7.1 Hz, H6)

^{13}C NMR: (50 MHz); δ 13.79 (CH_3), 16.34 (N1-CH_2-CH_2-$\underline{C}H_2$), 20.11 (NH-CH_2-CH_2-$\underline{C}H_2$), 27.17 (N1-CH_2-$\underline{C}H_2$), 31.20 (NH-CH_2-$\underline{C}H_2$), 40.56 (NH-CH_2), 48.93 (N1-CH_2), 66.29 (CH_2-C≡$\underline{C}$), 91.00 (CH_2-$\underline{C}$≡C), 95.50 (C5), 143.77 (C6), 157.13 (C2), 164.10 (C4)

MS [EI]: m/z (RI%); 464 $[M]^+$ (10), 446 (14), 435 (48), 422 (16), 364 (8), 297 (100), 284 (86)

HRMS: for $C_{26}H_{36}N_6O_2$: calculated 464.2900; observed 464.2887

Synthesis of 5-Amino-1-pentyne (40)

The procedure used was a modification of that employed by Lindgren, Svensson and Dahlbom.[78] Sodium azide (15 g, 0.231 mol) was added to a solution of 5-chloro-1-pentyne (10 g, 0.097 mol) in 280 ml of dimethylformamide. The mixture was stirred at 50°C for 15 hours and then added to 1000 ml of water. The azido-alkyne was extracted with 4 x 100 ml of ether, dried over K_2CO_3 and concentrated to roughly 50 ml. This solution was then added, with stirring, to a slurry of lithium

aluminum hydride (LAH, 3.68 g, 0.097 mol) in 100 ml of dry ether. After refluxing for 2 hours, the reaction mixture was cooled and the excess LAH was destroyed via the cautious addition of water. The resultant suspension was refluxed for an additional hour, filtered through celite and dried with K_2CO_3. The ether was evaporated under reduced pressure and the residue purified by fractional distillation. The yield was 30% (2.4 g, 0.029 mol). The compound showed:

b.p.: 122-123°C

^{1}H NMR: (200 MHz); δ 1.07 (br, 2H, NH_2), 1.57 (m, 2H, NH_2-CH_2-$C\underline{H_2}$), 1.87 (t, 1H, J=2.7 Hz, C≡C-H), 2.17 (dt, 2H, J=2.7 and 7.0 Hz, CH_2-C≡C), 2.71 (t, 2H, J=6.8 Hz, NH_2-CH_2)

^{13}C NMR: (50 MHz); δ 15.68 (NH_2-CH_2-CH_2-$\underline{C}H_2$), 32.00 (NH_2-CH_2-$\underline{C}H_2$), 40.91 (NH_2-$\underline{C}H_2$), 68.38 (C≡$\underline{C}$-H), 83.83 ($\underline{C}$≡C-H)

IR: 3400 (s, N-H), 3300 (s,≡CH), 2150 (m, C≡C), 1600 (m, N-H)

Synthesis of 1-(4-Pentynyl)-4-N-(4-pentynyl)-cytosine (41)

1-(4-Pentynyl)-uracil (712 mg, 4 mmol) was dissolved in 20 ml of chloroform. To this solution, chloromethylene dimethyl ammonium chloride (Vilsmeier's reagent) (525 mg, 4.1 mmol) was added and the mixture refluxed for 3 hours. At this time, the solution was cooled under a nitrogen atmosphere and added to a solution of 5-amino-1-pentyne (415 mg, 5 mmol) and diisopropylethylamine (3.5 ml, 2.6 g, 20 mmol) dissolved in 5 ml of chloroform. The solution was allowed to stir at room temperature for one hour, at which time the chloroform was evaporated under reduced pressure and the residue chromatographed on silica gel using 5% methanol in ethyl acetate.

The product was recrystallized from ethyl acetate. TLC using 5% methanol in ethyl acetate showed the desired product with an R_f=0.45. The yield was 77% (748 mg, 3.08 mmol). The compound showed:

m.p.: 94-95°C

^{1}H NMR: (500 MHz); δ 1.81 (m, 2H, NH-CH_2-C$\underline{H_2}$), 1.93 (m, 2H, N1-CH_2-C$\underline{H_2}$), 1.96 (br, 1H, NH-CH_2-CH_2-CH_2-C≡C-$\underline{H}$), 1.99 (t, 1H, J=2.6 Hz, N1-CH_2-CH_2-CH_2-C≡C-$\underline{H}$), 2.21 (dt, 2H, J=2.6 and 7.0 Hz, N1-CH_2-CH_2-C$\underline{H_2}$), 2.25 (dt, 2H, J=2.6 and 6.8 Hz, N4-CH_2-CH_2-C$\underline{H_2}$), 3.38 and 3.57 (br, 2H, NH-C$\underline{H_2}$ exchanging), 3.86 (t, 2H, J=6.9 Hz, N1-CH_2), 5.59 (br, 1H, H5 exchanging), 7.19 (br, 1H, H6 exchanging)

^{13}C NMR: (125 MHz); δ 15.27 (N1-CH_2-CH_2-$\underline{C}H_2$), 15.96 (NH-CH_2-CH_2-$\underline{C}H_2$), 27.04 (N1-CH_2-$\underline{C}H_2$), 27.61 (NH-CH_2-$\underline{C}H_2$), 39.64 (NH-$\underline{C}H_2$), 48.62 (N1-$\underline{C}H_2$), 68.79 (NH-CH_2-CH_2-CH_2-C≡$\underline{C}$-H), 69.63 (N1-CH_2-CH_2-CH_2-C≡$\underline{C}$-H), 82.77 (N1-CH_2-CH_2-CH_2-$\underline{C}$≡C-H), 83.66 (NH-CH_2-CH_2-CH_2-$\underline{C}$≡CH), 95.41 (C5), 143.84 (C6), 157.10 (C2), 164.18 (C4)

MS [EI]: m/z (RI%); 242 $[M]^+$ (30), 215 (76), 191 (66), 176 (51), 161 (24), 149 (15), 124 (23), 107 (10), 95 (19), 81 (74), 67 (33), 54 (18)

HRMS: for $C_{14}H_{16}N_3O$: calculated 242.1293; observed 242.1291

Attempted Synthesis of Cytosine Cyclophane Via Copper Coupling of 1-(4-Pentynyl)-4-N-(4-pentynyl)-cytosine

Method A

The procedure described is a "high dilution" version of the one employed for the

coupling of 1-(4-pentynyl)-uracil. 1-(4-Pentynyl)-4-N-(4-pentynyl)-cytosine (50 mg, 0.207 mmol) was dissolved in 10 ml of dry pyridine and added dropwise over one hour via a motor-driven syringe to a solution of $Cu(OAc)_2$ (3.0 g, 16.5 mmol) in 40 ml of pyridine and 40 ml of methanol. The mixture was allowed to reflux for 2 days. The reaction mixture was then concentrated by evaporation under a reduced pressure, added to 150 ml of concentrated NH_4OH and extracted with 3 x 100 ml of methylene chloride. The organic extracts were collected, dried with sodium sulphate and evaporated under a reduced pressure. The residue was chromatographed on silica gel using 10% methanol in chloroform. Analysis of the crude mixture and the chromatographed fractions by NMR, MS and TLC failed to provide any evidence for the presence of the desired product. Mostly material resulting from the decomposition of the pyrimidine ring was recovered. Attempts involving reaction times of 7 days and 30 days met with similar results.

Method B

The procedure described is a "high dilution" version of the one employed for the coupling of 1-(4-pentynyl)-4-N-butyl cytosine. 1-(4-Pentynyl)-4-N-(4-pentynyl)-cytosine (50 mg, 0.207 mmol) was dissolved in 10 ml of dry pyridine and added dropwise over one hour via a motor-driven syringe to a solution of $Cu(OAc)_2$ (3.0 g, 16.5 mmol) in 40 ml of pyridine, 40 ml of methanol and 20 ml of diisopropylethylamine. The mixture was left stirring under nitrogen at room temperature for 2 days. The reaction mixture was then concentrated by evaporation under a reduced pressure, added to 150 ml of concentrated NH_4OH and extracted with 3 x 100 ml of methylene chloride. The

organic extracts were collected, dried with sodium sulphate and evaporated under a reduced pressure. The residue was chromatographed on silica gel using 10% methanol in chloroform. Analysis of the crude mixture and the chromatographed fractions by NMR, MS and TLC failed to provide any evidence for the presence of the desired product. Mostly material resulting from the decomposition of the pyrimidine ring was recovered. Attempts involving reaction times of 7 days and 30 days met with similar results.

Method C

The procedure described is a modification of that described by Ojima, Shiroishi, Wada and Sondheimer.[73] 1-(4-Pentynyl)-4-N-(4-pentynyl)-cytosine (363 mg, 1.5 mmol) was dissolved in 10 ml of pyridine and added dropwise over one hour via a motor-driven syringe to a solution of $Cu(OAc)_2$ (1.95 g, 10.7 mmol) in 100 ml pyridine at 50°C. After the addition of the bis-alkyne was complete, the reaction mixture was stirred for an additional 30 minutes. The reaction mixture was then cooled, concentrated by evaporation under reduced pressure, added to 200 ml of concentrated NH_4OH and extracted with 3 x 100 ml of methylene chloride. The organic extracts were collected, dried with sodium sulphate and evaporated under a reduced pressure. The residue was chromatographed on silica gel using 10% methanol in chloroform. Analysis of the crude mixture and the chromatographed fractions by NMR, MS and TLC failed to provide any evidence for the presence of the desired product. Mostly material resulting from the decomposition of the pyrimidine ring was recovered. Attempts involving reaction times of 3 hours, 24 hours and 3 days met with similar

results.

Method D

The procedure employed is that described by O'Krongly, Denmead, Chiang and Breslow.[74] 1-(4-Pentynyl)-4-N-(4-pentynyl)-cytosine (298 mg, 1.23 mmol) in 10 ml of "O_2-free" pyridine was added dropwise over one hour via a motor-driven syringe to a solution of anhydrous CuCl (12.1 g, 123 mmol), and anhydrous $CuCl_2$ (2.0 g, 15 mmol) in 1230 ml of "O_2-free" pyridine at 0°C. After addition of the bis-alkyne, the solution was blanketed with argon and left for 48 hours at 5°C. The reaction mixture was then concentrated, added to 200 ml of concentrated NH_4OH and extracted with 3 x 100 ml of methylene chloride. The organic extracts were then washed with 100 ml of concentrated NH_4OH, dried with sodium sulphate and evaporated under a reduced pressure. The residue was chromatographed on silica gel using 10% methanol in chloroform. Analysis of the crude mixture and the chromatographed fractions by NMR, MS, and TLC failed to provide any evidence for the presence of the desired product. Mostly material resulting from the decomposition of the pyrimidine ring was recovered.

Method E

The procedure described is that used by Dietrich-Buchecker, Khemiss and Sauvage.[75] 1-(4-Pentynyl)-4-N-(4-pentynyl)-cytosine (63 mg, 0.26 mmol) was dissolved in 10 ml of dimethyl formamide and added dropwise over one hour via a motor-driven syringe to a solution of CuCl (3.46 g, 35 mmol) and $CuCl_2$ (834 mg, 6.2 mmol) in 30 ml of dimethylformamide. The solution was stirred at room temperature for 3 days in the

presence of air. The reaction mixture was concentrated, added to 200 ml of concentrated NH_4OH and extracted with 3 x 100 ml of methylene chloride. The organic extracts were then washed with 100 ml of concentrated NH_4OH, dried with sodium sulphate and evaporated under a reduced pressure. The residue was chromatographed on silica gel using 10% methanol in chloroform. Analysis of the crude mixture and the chromatographed fractions by NMR, MS and TLC failed to provide any evidence for the presence of the desired product. Attempts involving reaction times of 7 days and 30 days met with similar results. Mostly material resulting from the decomposition of the pyrimidine ring was recovered.

Synthesis of 5-Azido-1-pentanol (42)

The procedures described by Kang *et al.*[49] and Reeves *et al.*[50] were used. To a solution of 1,5-pentanediol (10.4 g, 100 mmol) in 200 ml of benzene, stirred in a round bottom flask equipped with a Dean-Stark trap, was added hydrobromic acid (48%, 12.5 ml, 110 mmol). The reaction was allowed to reflux for 28 hours with the trap emptied periodically. The mixture was washed successively with 100 ml of 6N NaOH, 100 ml of 10% HCl, 2 x 200 ml of water and 150 ml of saturated NaCl solution. The organic layer was dried with sodium sulphate and evaporated under reduced pressure. The bromo-alcohol was carried through to the next step without additional purification.

1-Bromo-5-pentanol was added to a stirred solution of 25% aqueous sodium azide (10.25 g in 40 ml of water). Aliquat 336 (1.6 g, 4 mmol) was added and the mixture is heated to 100°C. After 30 hours, the reaction was cooled and the phases separated. The 5-azido-1-pentanol was purified via distillation. Overall yield was 72%

(9.3 g, 72 mmol). The compound showed:

b.p. 63-65°C @ 0.3 mm

^{1}H NMR: (200 MHz); δ 1.38-1.58 (m, 6H, $(CH_2)_3$), 2.86 (br, 1H, OH), 3.20 (t, 2H, J=6.8 Hz, CH_2-N_3), 3.52 (t, 2H, J=6.6 Hz, CH_2-OH)

^{13}C NMR: (50 MHz); δ 22.75 (N_3-CH_2-CH_2-$\underline{C}H_2$), 28.78 (N_3-CH_2-$\underline{C}H_2$) 31.83 (HO-CH_2-$\underline{C}H_2$), 51.13 (N_3-CH_2), 61.99 (HO-CH_2)

Synthesis of 1-Bromo-5-azido-pentane (**43**)

The procedure developed by Olah *et al.* was used.[56] Chlorotrimethylsilane (32 ml, 27 g, 250 mmol) was added to a solution of lithium bromide (17.4 g, 200 mmol) in 200 ml of dry acetonitrile. 5-Azido-1-pentanol (6.45 g, 50 mmol) was then added and the reaction mixture heated under reflux for 24 hours. The solution was cooled, taken up into 500 ml of ether and washed with 2 x 25 ml of water, 500 ml of 10% sodium bicarbonate solution and 500 ml of saturated sodium chloride solution. The organic layer was then dried with anhydrous sodium sulphate and evaporated under a reduced pressure. Further purification was not deemed necessary and the product was carried through to the next step. The yield was 80% (7.68 g, 40 mmol). The compound showed:

^{1}H NMR: (200 MHz); δ 1.57 (m, 4H, N_3-CH_2-$C\underline{H}_2$-$C\underline{H}_2$), 1.87 (m, 2H, Br-CH_2-$C\underline{H}_2$), 3.27 (t, 2H, J=6.8 Hz, N_3-CH_2), 3.62 (t, 2H, J=6.8 Hz, Br-CH_2)

^{13}C NMR: (50 MHz); δ 25.07 (N_3-CH_2-CH_2-$\underline{C}H_2$), 28.40 (N_3-CH_2-$\underline{C}H_2$), 32.00 (Br-CH_2-$\underline{C}H_2$), 33.16 (Br-CH_2), 50.76 (N_3-CH_2)

Synthesis of 7-Azido-1-heptyne (44)

Using a dry-ice condenser, ammonia (50 ml) was condensed into a cooled 3-necked flask equipped with a stir bar. A wide-bore tube was used to introduce acetylene into the reaction vessel. While maintaining a constant stream of acetylene, small chunks of sodium (1.8 g, 0.08 mol) were introduced into stirred ammonia. Care was taken so as to not allow the solution to turn blue. Once all the sodium had been added, the acetylene bubbling was discontinued, and 1-bromo-5-azido pentane (826 mg, 4.3 mmol) in 20 ml of dry THF was added dropwise over one hour by means of a motor-driven syringe. The mixture was allowed to stir for 18 hours and the ammonia permitted to evaporate. Ice water (250 ml) was added carefully to decompose the excess $NaNH_2$. The solution was then treated with 6N HCl until the pH was slightly acidic. The product was extracted with 4 x 100 ml of chloroform and dried with sodium sulphate. The chloroform was evaporated under reduced pressure, leaving the 7-azido-1-heptyne. The yield was 78% (370 mg, 3.4 mmol). The compound showed:

^{1}H NMR: (500 MHz); δ 1.46 (m, 2H, N_3-CH_2-CH_2-$C\underline{H_2}$), 1.51 (m, 2H, $C\underline{H_2}$-CH_2-N_3 or $C\underline{H_2}$-CH_2-C≡C-H), 1.58 (m, 2H, $C\underline{H_2}$-CH_2-C≡CH or $C\underline{H_2}$-CH_2-N_3), 1.92 (t, 1H, J=2.7 Hz, C≡C-H), 2.17 (dt, 2H, J=2.7 and 6.8 Hz, $C\underline{H_2}$-C≡C-H), 3.24 (t, 2H, J=6.8 Hz, CH_2-N_3)

^{13}C NMR: (125 MHz); δ 18.16 ($\underline{C}H_2$-CH_2-C≡CH), 25.72 ($\underline{C}H_2$-CH_2-CH_2-N_3), 27.84 ($\underline{C}H_2$-CH_2-C≡CH), 28.28 ($\underline{C}H_2$-CH_2-N_3), 51.20 ($\underline{C}H_2$-N_3), 68.42 (C≡$\underline{C}$H), 83.87 ($\underline{C}$≡CH)

Synthesis of 7-Amino-1-heptyne (45)

The reduction was performed according to the method described by Vaultier *et al.*[47] 1-Azido-1-heptyne (170 mg, 1.56 mmol) was dissolved in 1.6 ml of THF and treated with triphenylphosphine (410 mg, 1.56 mmol) and water (45 µl, 2.34 mmol). A boiling chip was added and the evolution of nitrogen began immediately. The mixture was left standing at room temperature for 18 hours. The solution was then concentrated, redissolved in 25 ml of methylene chloride and extracted with 3 x 20 ml portions of 0.01 M HCl. These combined aqueous solutions were adjusted to pH 8 with 1M NaOH and extracted with 3 x 30 ml of methylene chloride. The combined organic extracts were dried over anhydrous sodium sulphate and evaporated under a reduced pressure. The yield was 73% (126 mg, 1.14 mmol). The compound showed:

^{1}H NMR: (500 MHz); δ 1.07 (br, 2H, NH_2), 1.18 (m, 4H), 1.28 (m, 2H), 1.71 (t, 1H, J=2.7 Hz, C≡C-H), 1.92 (dt, 2H, J=2.7 and 7.0 Hz, $C\underline{H}_2$-C≡C-H), 2.42 (t, 2H, J=6.1 Hz, $C\underline{H}_2$-NH_2)

^{13}C NMR: (125 MHz); δ 17.77 ($\underline{C}H_2$-CH_2-C≡CH), 25.42 ($\underline{C}H_2$-CH_2-CH_2-NH_2), 27.73 ($\underline{C}H_2$-C≡CH), 32.65 ($\underline{C}H_2$-CH_2-NH_2), 41.46 (CH_2-NH_2), 67.85 (C≡$\underline{C}$H), 83.83 (C≡$\underline{C}$H)

MS [CI]: m/z (RI%); 112 $[M+1]^+$ (100), 104 (22)

Synthesis of 1-(4-pentynyl)-4-N-(6-heptynyl)-cytosine (46)

The procedure used was a modification of that used by Zemlicka and Sorm.[60] 1-(4-Pentynyl)-uracil (712 mg, 4 mmol) was dissolved in 20 ml of chloroform. To this solution, chloromethylene dimethyl ammonium chloride (525 mg, 4.1 mmol) was added and the mixture refluxed for 3 hours. At this time, the reaction mixture was cooled and

added to a solution of 7-amino-1-heptyne (555 mg, 5 mmol) and diisopropylethylamine (3.5 ml, 2.6 g, 20 mmol) dissolved in 5 ml of chloroform. The solution was allowed to stir at room temperature for one hour, at which time the chloroform was evaporated under reduced pressure and the residue chromatographed on silica gel using 5% methanol in ethyl acetate. TLC using 10% methanol in ethyl acetate showed the desired product with an R_f= 0.64. The yield was 62% (670 mg, 2.48 mmol). The compound showed:

m.p. 72-80°C

^{1}H NMR: (500 MHz in DMF-d_7); δ 1.43 (m, 2H), 1.48 (m, 2H), 1.55 (m, 2H), 1.85 (m, 2H), 2.18 (dt, 2H, J=2.6 and 7.0 Hz, C$\underline{H_2}$-C≡C-H), 2.21 (dt, 2H, J=2.6 and 7.2 Hz, C$\underline{H_2}$-C≡C-H), 2.67 (t, 1H, J=2.6 Hz, C≡CH), 2.74 (t, 1H, J=2.6 Hz, C≡CH), 3.33 (m, 2H, NH-CH_2), 3.78 (t, 2H, J=7.1 Hz, N1-CH_2), 5.78 (d, 1H, J=7.2 Hz, H5), 7.54 (d, 1H, J=7.2 Hz, H6), 7.58 (br, 1H, NH)

^{13}C NMR: (125 MHz in DMF-d_7); δ 15.89, 18.46, 26.65, 28.60, 28.86, 29.13, 40.58 (NH-CH_2), 48.91 (N1-CH_2), 70.67 (C≡$\underline{C}$H), 71.26 (C≡$\underline{C}$H), 83.91 ($\underline{C}$≡CH), 84.90 ($\underline{C}$≡CH), 94.69 (C5), 145.43 (C6), 156.82 (C2), 164.98 (C4)

MS [CI]: m/z (RI%); 272 $[M+1]^+$ (100)

HRMS: for $C_{16}H_{21}N_3O$: calculated 271.1685; observed 271.1672

Attempted Synthesis of a Cytosine Cyclophane via Copper Coupling of 1-(4-Pentynyl)-4-N-(6-heptynyl)-cytosine

The methods (A,B,C,D,E) employed in the attempted cyclization of 1-(4-

pentynyl)-4-N-(4-pentynyl)-cytosine were used. The reactions were carried out on the same scale as described above. Analysis of the crude reaction mixtures, as well as the chromatographed fractions from each attempt by TLC, NMR and MS failed to provide any evidence for the presence of the desired product. Products from degradative processes were isolated in all cases.

Synthesis of Dodec-5-en-7-yne (47)

The procedure employed was that of Ratovelomana and Linstrumelle.[85] 1-Bromo-1-hexene (381 mg, 2.34 mmol) was added to a stirred solution of tetrakis(triphenylphosphine)palladium (60 mg, 0.05 mmol) in benzene. After stirring the mixture for one hour under nitrogen, a solution of 1-hexyne (96 mg, 1.17 mmol) in *n*-butyl amine (1.2 ml, 12 mmol), followed by copper iodide (35 mg, 0.191 mmol) were added. The mixture was left stirring for 10 hours at room temperature, at which time 10 ml of ether were added and the mixture poured into 20 ml of aqueous saturated ammonium chloride. The product was extracted with 3 x 10 ml ether, washed with aqueous ammonium chloride and the ether extracts dried with sodium sulphate. Careful distillation of the ether allowed for isolation of the enyne. The yield was 70% (134 mg, 0.82 mmol). The compound showed:

^{1}H NMR: (200 MHz); δ 0.91 (m, 6H, 2 x CH_3), 1.25-1.51 (m, 8H, 2 x CH_3-CH_2-CH_2), 2.01 (m, 2H, CH_2-CH=CH), 2.27 (t, 2H, J=6.8 Hz, CH_2-C≡C), 5.43 (d, 1H, J=16.0 Hz, CH=CH-C≡C), 6.02 (dt, 1H, J=7.0 and 16.0 Hz, CH=CH-C≡C)

^{13}C NMR: (50 MHz); δ 13.72 (CH_3), 13.79 (CH_3), 19.00 (CH_2-C≡C), 21.96(CH_2-

CH_3), 22.11 ($\underline{C}H_2$-CH_3), 30.97 ($\underline{C}H_2$-CH_2-CH_3), 30.70 ($\underline{C}H_2$-CH_2-CH_3), 32.58 ($\underline{C}H_2$-CH=CH), 79.16 (C≡$\underline{C}$-CH=CH), 88.55 ($\underline{C}$≡C-CH=CH), 109.85 (C≡C-$\underline{C}$H=CH), 143.16 (C≡C-CH=$\underline{C}$H)

Synthesis of 1-(Undec-4-yn-6-enyl)-uracil (48)

The procedure used was a modification of that described by Hobbs.[84] 1-Bromo-1-hexene (326 mg, 2.00 mmol) was added to a stirred solution of tetrakis(triphenylphosphine)palladium (231 mg, 0.20 mmol) in 5 ml of dimethylformamide. After stirring for an hour, a solution of 1-(4-pentynyl)-uracil (356 mg, 2.00 mmol) in 5 ml of dimethylformamide and triethylamine (405 mg, 558 µl, 4 mmol) was added. Following the addition of copper (I) iodide (76 mg, 0.40 mmol), the mixture was stirred under nitrogen for 4 hours. The reaction mixture was then poured into 100 ml of chloroform and treated with 2 x 75 ml of saturated aqueous NH_4Cl and 2 x 75 ml 10% HCl. The organic layer was dried using sodium sulphate and the chloroform evaporated under reduced pressure. The residue was chromatographed on silica gel using ethyl acetate in hexanes (1:1) as the eluent and the desired enyne isolated. TLC using 1% methanol, 50% ethyl acetate and 49% hexanes showed the desired product with an R_f=0.26. The yield was 73% (380 mg, 1.46 mmol). The compound showed:

^{1}H NMR: (500 MHz); δ 0.88 (t, 3H, J=6.6 Hz, CH_3), 1.34 (m, 4H, $C\underline{H}_2$-$C\underline{H}_2$-CH_3), 1.89 (m, 2H, N1-CH_2-$C\underline{H}_2$), 2.06 (m, 2H, CH=CH-$C\underline{H}_2$), 2.36 (t, 2H, J=6.5 Hz, $C\underline{H}_2$-C≡C), 3.85 (t, 2H, J=6.8 Hz, N1-CH_2), 5.42 (d, 1H, J=15.7 Hz, C≡C-$C\underline{H}$=CH), 5.67 (d, 1H, J=7.9 Hz, H5), 6.06 (dt, 1H, J=7.0 and 15.7

Hz, C≡C-CH=C<u>H</u>), 7.21 (d, 1H, J=7.9 Hz, H6), 8.97 (s, 1H, H3)

^{13}C NMR: (125 MHz); δ 13.82 (CH_3), 16.35 ($\underline{C}H_2$-C≡C), 22.19 ($\underline{C}H_2$-CH_3), 27.39 (N1-CH_2-$\underline{C}H_2$), 30.84 ($\underline{C}H_2$-CH_2-CH_3), 32.63 ($\underline{C}H_2$-CH=CH), 47.99 (N1-CH_2), 81.09 (C≡$\underline{C}$-CH=CH), 85.81 ($\underline{C}$≡C-CH=CH), 101.99 (C5), 109.18 (C≡C-$\underline{C}$H=CH), 144.52 (C≡C-CH=$\underline{C}$H), 144.80 (C6), 150.77 (C2), 163.60 (C4)

MS [CI]: m/z (RI%); 278 $[M+18]^+$ (52), 261 $[M+1]^+$ (100)

HRMS: for $C_{15}H_{20}O_2N_2$: calculated 260.1525; observed 260.1518

<u>Synthesis of 4-Pentynyl-t-butyldimethylsilyl ether</u> (49)

The procedure used was that of Nicolaou *et al.*[80] To a solution of 4-pentyn-1-ol (8.41 g, 9.3 ml, 100 mmol) in 100 ml of dry dichloromethane cooled to 0°C was added 26 ml of dry 2,6-lutidine (distilled from CaH_2) and <u>tert</u>-butyldimethylsilyl triflate (34.5 ml, 150 mmol) dropwise over 20 minutes. The solution was stirred for additional hour at room temperature. The reaction mixture was diluted with 500 ml of diethyl ether and poured into 100 ml of ice water. The organic layer was separated and washed successively with 100 ml 10% HCl and 100 ml of saturated NaCl. The ether layer was then dried using sodium sulphate and fractionally distilled to give the desired TBDMS-ether. The yield was 91% (18.02 g, 91 mmol). The compound showed:

b.p.: 34-36°C @ 0.6 mm.

^{1}H NMR: (200 MHz); δ 0.02 (6H, s, Si-$(CH_3)_2$), 0.87 (9H, s, $(CH_3)_3$-C), 1.73 (m, 2H, O-CH_2-$\underline{CH_2}$), 1.90 (t, 1H, J=2.7 Hz, C≡C-H), 2.25 (dt, 2H, J=2.7 and 7.0 Hz, $\underline{CH_2}$-C≡C-H), 3.67 (t, 2H, J=6.0 Hz, O-CH_2)

^{13}C NMR: (50 MHz); δ -5.38 ($(CH_3)_2Si$), 14.81 (O-CH_2-CH_2-$\underline{C}H_2$), 18.29 ((CH_3)$_3$$\underline{C}$-Si), 25.90 ($(\underline{C}H_3)_3C$-Si), 31.50 (O-$CH_2$-$\underline{C}H_2$), 61.39 (O-$CH_2$), 68.21 (C≡$\underline{C}$-H), 84.20 ($\underline{C}$≡CH)

Synthesis of 1-Bromo-1-penten-5-ol (50)

The preparation employed was that of Nicolaou *et al.*[80] 4-Pentynyl-TBDMS ether (17.0 g, 85.9 mmol) was added to tributyltin hydride (37.5 g, 35 ml, 128.8 mmol) and azobisisobutyronitrile (AIBN, 250 mg). The stirred solution was heated at 130°C for 2.5 hours. The reaction was then cooled to -20°C (CCl_4 and CO_2 slush bath) and Br_2 913.7 g, 4.5 ml, 86 mmol) in 95 ml of CCl_4 was added dropwise to the vinylstannane intermediate via a motor-driven syringe over one hour.

After evaporation of the CCl_4 under a reduced pressure, the TBDMS group was removed by adding the reaction mixture to 50 g of NH_4F dissolved in 500 ml of methanol.[67] The solution was heated to 60°C for 3 hours at which time the methanol was evaporated under reduced pressure. The residue was then dissolved into 500 ml of chloroform and washed with 3 x 500 ml of water. The chloroform layer was dried with sodium sulphate and concentration to a small volume permitted precipitation of the tributyltin fluoride which was removed by filtration. The remaining solution was then fractionally distilled under a reduced pressure to allow for isolation of the desired vinyl-bromo-alcohol. The yield was 82% (11.6 g, 70.7 mmol). The compound showed:

b.p.: 60°C @ 0.7 mm

^1H NMR: (200 MHz); δ 1.63 (m, 2H, $C\underline{H}_2$-CH_2-OH), 2.10 (m, 2H, $C\underline{H}_2$-CH=CH-Br), 2.33 (s, 1H, OH), 3.58 (t, 2H, J=6.7 Hz, $C\underline{H}_2$-OH), 6.12 (m, 2H, mixture

of *cis* and *trans* CH=CH-Br)

^{13}C NMR: (50 MHz); δ 29.12 ($\underline{C}H_2$-CH=CH-Br), 31.23 ($\underline{C}H_2$-CH_2-OH), 61.55 (CH_2-OH), 104.65 (CH=$\underline{C}$H-Br), 137.23 ($\underline{C}$H=CH-Br)

MS [CI]: m/z (RI%); 184 $[M+2+18]^+$ (16), 182 $[M+18]^+$ (17), 165 $[M+2]^+$ (14), 163 $[M]^+$ (15), 148 $[M+2-18]^+$ (10), 146 $[M-18]^+$ (11), 84 $[M-Br]^+$ (100), 67 (24), 56 (20)

Synthesis of 1-Bromo-1-pentenyl-5-toluenesulphonate (51)

1-Bromo-1-penten-5-ol (1.0 g, 6.1 mmol) was dissolved in 2 ml of dry pyridine and cooled to 0°C. p-Toluenesulphonyl chloride (1.30 g, 6.8 mmol) was added in small portions so as to not allow the temperature to rise significantly. The solution was allowed to stir under a nitrogen atmosphere at this temperature for 2.5 hours. Cold water (50 ml) was added and the solution extracted into 50 ml of ether. Washing with 3 x 25 ml of 10% HCl and 3 x 25 ml 10% Na_2CO_3 was followed by drying of the ether layer with sodium sulphate and evaporation of the solvent under reduced pressure. The product was a clear oil. The yield was 88% (1.7 g, 5.4 mmol). The compound showed:

^{1}H NMR: (200 MHz); δ 1.71 (m, 2H, $C\underline{H}_2$-CH_2-O), 2.06 (m, 2H, $C\underline{H}_2$-CH=CH-Br), 2.41 (s, 3H, CH_3), 3.97 (t, 2H, J=6.0 Hz, CH_2-O), 5.97 (m, 2H, mixture of *cis* and *trans* CH=CH-Br), 7.32 (d, 2H, J=8.3 Hz, meta-H's), 7.74 (d, 2H, J=8.3 Hz, ortho-H's)

^{13}C NMR: (50 MHz); δ 21.50 (CH_3), 27.20 ($\underline{C}H_2$-CH=CH-Br), 28.49 ($\underline{C}H_2$-CH_2-O), 68.95 (CH_2-O), 105.67 (CH=$\underline{C}$H-Br), 127.70 (meta C's), 129.80 (ortho

C's), 132.66 (para C's), 135.65 (CH=CH-Br), 144.82 (C-SO_3)

MS [EI]: m/z (RI%); 320 $[M+2]^+$ (2), 318 $[M]^+$ (2), 148 [M+2-OTs] (45), 146 [M-OTs] (46), 91 (48), 67 (100)

Synthesis of 1-Bromo-5-azido-1-pentene (**52**)

To a stirred suspension of NaN_3 (2.1 g, 32.3 mmol) in 25 ml of dimethylformamide, was added 1-bromo-1-pentenyl-5-toluenesulphonate (1.9 g, 6.1 mmol). After 24 hours at room temperature, 25 ml of water were added and the mixture extracted with 6 x 50 ml of hexanes. The organic layer was dried with sodium sulphate and hexanes removed by evaporation under reduced pressure. The yield was 87% (1.0 g, 5.3 mmol). The compound showed:

^{1}H-NMR: (200 MHz); δ 1.69 (m, 2H, CH_2-CH=CH), 2.12 (m, 2H, N_3-CH_2-CH_2), 3.38 (m, 2H, J=6.7 Hz, N_3-CH_2), 6.11 (m, 2H, mixture of *cis* and *trans* CH=CH-Br)

^{13}C-NMR: (50 MHz); δ 27.74 (CH_2-CH=CH-Br), 29.90 (CH_2-CH_2-N_3), 50.37 (CH_2-N_3), 105.49 (CH=CH-Br), 136.28 (CH=CH-Br)

MS [CI]: m/z (RI%); 110 $[M-Br]^+$ (7), 91 (55), 82 (13), 74 (100), 53 (12)

Synthesis of 1-Bromo-5-amino-1-pentene (**53**)

Reduction of 1-bromo-5-azido-1-pentene was achieved using the method of Vaultier *et al.*[47] To 1-bromo-5-azido-1-pentene (570 mg, 3.0 mmol) in 3 ml of THF was added triphenylphosphine (783 mg, 3.0 mmol), water (80 µl, 4.50 mmol), and a boiling chip. The evolution of N_2 began immediately. The mixture is left standing at room

temperature for 18 hours, at which time the solution is concentrated, redissolved in 50 ml of $CHCl_3$ and extracted with 3 x 20 ml of 0.01 M HCl. The combined aqueous solutions were adjusted to pH 9 with 1 M NaOH and extracted with 3 x 30 ml of chloroform. These combined organic solutions were dried over anhydrous sodium sulphate and evaporated under reduced pressure. The yield was 81% (391 mg, 2.4 mmol). The compound showed:

^{1}H NMR: (500 MHz); δ 1.47 (m, 2H, $C\underline{H}_2$-CH=CH-Br), 2.01 (m, 2H, $C\underline{H}_2$-CH_2-NH_2), 2.34 (s, 2H, NH_2), 2.62 (m, 2H, $C\underline{H}_2$-NH_2), 6.04 (m, 2H, mixture of *cis* and *trans* CH=CH-Br).

^{13}C NMR: (50 MHz); δ 30.03 ($\underline{C}H_2$-CH=CH-Br), 31.65 ($\underline{C}H_2$-CH_2-NH_2), 40.83 (CH_2-NH_2), 104.40 (CH=$\underline{C}$H-Br), 137.22 ($\underline{C}$H=CH-Br)

MS [EI]: m/z (RI%); 164 $[M+1]^+$ (3), 148 (19), 146 (20), 121 (9), 119 (10), 84 (100), 67 (62), 56 (86)

Synthesis of 1-(4-Pentynyl)-4-N-(5-bromo-4-pentenyl)-cytosine (54)

A stirred solution of 1-(4-pentynyl)-uracil (207 mg, 1.16 mmol) and chloromethylene dimethyl ammonium chloride (164 mg, 1.28 mmol) in 5 ml of chloroform was refluxed under a nitrogen atmosphere for 3 hours. The reaction was then cooled to room temperature and added dropwise to a solution containing 1-bromo-5-amino-1-pentene (190 mg, 1.16 mmol) and diisopropylethylamine (646 mg, 870 µl, 5 mmol) in 2 ml of chloroform. The solution was allowed to stir for one hour, concentrated and chromatographed on silica gel using 10% methanol in ethyl acetate. The pure compound was obtained after recrystallization from ethyl acetate. TLC with

10% methanol in chloroform showed the desired product with an R_f=0.52. The yield was 43% (163 mg, 0.50 mmol). The compound showed:

m.p. 96-98°C

^{1}H NMR: (500 MHz in DMF-d_7); δ 1.66 (m, 2H, C<u>H</u>$_2$-CH=CH-Br), 1.85 (m, 2H, N1-CH$_2$-C<u>H</u>$_2$), 2.13 (m, 2H, NH-CH$_2$-C<u>H</u>$_2$), 2.22 (dt, 2H, J=2.6 and 7.3 Hz, C<u>H</u>$_2$-C≡CH), 2.74 (t, 1H, J=2.6 Hz, C≡C-H), 3.34 (m, 2H, CH$_2$-NH), 3.79 (t, 2H, J=6.9 Hz, CH$_2$-N1), 5.77 (d, 1H, J=7.3 Hz, H5), 6.26 (dt, 1H, J=13.4 and 7.1 Hz, C<u>H</u>=CH-Br), 6.35 (d, 1H, J=13.4 Hz, CH=C<u>H</u>-Br), 7.55 (d, 1H, J=7.3 Hz, H6), 7.62 (br, 1H, NH)

^{13}C NMR: (125 MHz in DMF-d_7); δ 15.90 (N1-CH$_2$-CH$_2$-<u>C</u>H$_2$), 28.61 (N1-CH$_2$-<u>C</u>H$_2$ and NH-CH$_2$-<u>C</u>H$_2$), 30.61 (<u>C</u>H$_2$-CH=CH-Br), 39.97 (NH-<u>C</u>H$_2$), 48.94 (N1-CH$_2$), 71.28 (C≡<u>C</u>H), 83.90 (<u>C</u>≡CH), 94.70 (C5), 105.66 (CH=<u>C</u>H-Br), 138.52 (<u>C</u>H=CH-Br), 145.54 (C6), 156.90 (C2), 165.04 (C4)

MS [CI]: m/z (RI%); 325 $[M+2]^+$ (99), 323 $[M]^+$ (100), 244 $[M-Br]^+$ (23)

HRMS: for $C_{14}H_{18}ON_3Br$: calculated 323.0633; observed 323.0616

<u>Attempted Synthesis of the Cytosine Cyclophane via Palladium Coupling of 1-(4-Pentynyl)-4-N-(5-bromo-4-pentynyl)-cytosine</u>

The procedure used was a modification of that described by Hobbs.[84] To a solution of 1-(4-Pentynyl)-4-N-(5-bromo-4-pentynyl)-cytosine (65 mg, 0.2 mmol) in 10 ml of dimethylformamide, tetrakis(triphenylphosphine)palladium (231 mg, 0.20 mmol) was added. After stirring for one hour, the solution was diluted with 90 ml of dimethylformamide and treated with CuI (76 mg, 0.4 mmol) in 6 ml of Et_3N. The

reaction was stirred for 2 days at room temperature under a nitrogen atmosphere. The reaction mixture was then poured into 500 ml of chloroform and treated with 2 x 200 ml of saturated aqueous NH_4Cl. The organic layer was dried using sodium sulphate and the chloroform evaporated under reduced pressure. The residue was chromatographed on silica gel using 10% methanol in chloroform. Analysis of the crude reaction mixture and the chromatographed fractions by NMR, MS and TLC failed to provide any evidence for the presence of the desired product. The final reaction mixture contained starting material and products resulting from the decomposition of the pyrimidine ring. Attempts involving reaction times of 7 days and 30 days met with similar results.

Appendix A

AMPAC Calculations

Table 1 Coefficients of Atomic Orbitals Contributing to the Highest Occupied Molecular Orbital of Purine Anions.

atom	*orbital*	*adenine*	*6-aminomethyladenine*	*6-chloropurine*
N1	s	-.00553	-.02698	-.00001
	p_x	-.00388	.02774	-.00010
	p_y	-.00385	.00880	.00004
	p_z	.05233	.25869	-.05027
C2	s	.00233	.01319	-.00016
	p_x	.00871	-.02540	.00014
	p_y	-.00509	.00515	.00068
	p_z	-.37038	-.28426	-.40489
N3	s	.00166	-.00022	.00015
	p_x	-.00297	-.03600	-.00005
	p_y	-.00575	-.01745	.00008
	p_z	-.20048	-.36591	-.13542
C4	s	.00099	.00819	-.00002
	p_x	.00166	.02554	.00003
	p_y	.00409	.02225	.00002
	p_z	.41377	.28933	.43361
C5	s	-.00325	.00685	-.00009
	p_x	-.00425	-.01513	-.00008

	p_y	-.01030	-.00466	-.00016
	p_z	.31093	.08582	.26966
C6	s	.00952	.01034	-.00003
	p_x	.00354	.05572	.00015
	p_y	.01533	.08558	-.00050
	p_z	.32627	.24417	.36267
N7	s	-.00215	-.00379	.00004
	p_x	-.00541	.00274	.00014
	p_y	.00030	-.02847	.00004
	p_z	-.42954	-.47276	-.46033
C8	s	-.00050	-.00527	-.00006
	p_x	.00159	.00890	-.00004
	p_y	.00040	.00132	.00007
	p_z	-.36979	-.15614	-.37373
N9	s	.00186	.01041	.00002
	p_x	-.00397	-.00926	.00004
	p_y	-.00692	-.02455	-.00001
	p_z	.20526	.45450	.20407

Appendix A

Table 2 Charges Calculated on Atoms of Purine Anions

atom	adenine	6-aminomethylpurine	6-chloropurine
N1	-.2878	-.3355	-.2287
C2	-.0727	-.0504	-.0929
N3	-.1735	-.1742	-.1522
C4	-.0519	-.0284	-.0566
C5	-.2284	-.2326	-.1783
C6	.1216	.1846	.0461
N7	-.2369	-.2542	-.2163
C8	-.1524	-.1285	-.1361
N9	-.2318	-.2905	-.2273
N6	-.3112	-.2917	

Appendix B

Table 1 Cartesian Coordinates and Chemical Shifts for Atoms in [8]-(N6,9)-6-Aminopurinophane

Atom	*Cartesian Coordinates*			*Chemical Shift (ppm)*
	x	*y*	*z*	
N1	0.00000	0.00000	0.00000	
C2	1.33900	0.00000	0.00000	152.3
N3	2.19233	1.02319	0.00000	
C4	1.51097	2.17470	0.14339	154.1
C5	0.15316	2.33354	0.29427	121.2
C6	-0.63103	1.19503	0.06499	159.9
N7	-0.17322	3.67078	0.49820	
C8	0.97188	4.27726	0.40217	143.0
N9	2.03956	3.44274	0.16810	
N6	-1.96522	1.20758	-0.13089	
C1′	-2.63870	2.35002	-0.76687	43.0
C2′	-2.62395	2.28116	-2.29491	30.9
C3′	-1.25097	2.13500	-2.95522	25.2
C4′	-0.34872	3.36413	-2.85403	26.1
C5′	1.12343	3.03640	-3.02497	31.3
C6′	2.11803	4.15341	-2.68419	23.1
C7′	3.36069	3.67466	-1.92526	28.7
C8′	3.32249	3.85443	-0.41446	45.0
H2	1.72697	-0.87765	-0.03087	7.76

H8	1.09767	5.23798	0.48459	8.21
H6	-2.33936	0.41533	-0.37692	5.40
H1r	-3.58086	2.33150	-0.45054	3.35
H1s	-2.21291	3.22658	-0.44915	4.49
H2r	-3.19490	1.53303	-2.56846	1.47
H2s	-3.03473	3.16524	-2.65615	1.38
H3r	-0.78418	1.31347	-2.50226	1.03
H3s	-1.41733	1.92378	-3.91286	0.18
H4r	-0.66208	4.03915	-3.53921	0.61
H4s	-0.47681	3.81015	-1.99964	0.18
H5r	1.27204	2.70838	-3.90092	-0.69
H5s	1.28295	2.23456	-2.43369	0.89
H6r	1.62700	4.84154	-2.17886	1.26
H6s	2.40251	4.57373	-3.56640	0.52
H7r	4.17369	4.19371	-2.22889	1.80
H7s	3.55363	2.71371	-2.13129	1.64
H8r	3.46239	4.74010	-0.16010	4.55
H8s	4.05174	3.27280	0.05452	3.92

Appendix C

Tables of Crystallographic Information for [9](N6,9)-6-Aminopurinophane

Table 1. Full Crystal Data for [9](N6,9)-6-aminopurinophane

Formula	$C_{14}H_{21}N_5$
Crystal Size, mm	0.10x0.20x0.40
Formula Weight	259.35
System	Monoclinic
Space Group	$P2_1/n$ (No. 14)
a, Å	16.941(3)
b, Å	8.512(2)
c, Å	19.300(2)
β, °	95.90(1)
V, Å^3	2769(1)
Z	8
D_c, g cm^{-3}	1.24 ± 0.04
D_m, g cm^{-3}	1.27
F(000)	1120
Diffractometer	Rigaku AFC6R
Temperature	173K
Radiation	CuKα (λ=1.5418 Å)
μ(Cu K_α), cm^{-1}	5.84
No. of reflections used in cell dtn.	25 ($39.7 \leq \Theta \leq 40.0°$)
Standard reflections (esd %)	3,1,1 (1.5)
	2,1,3 (4.3)
	3,1,0 (1.1)

Table 1. - cont'd.

Data collected	$h,k,\pm l$
2θ max.	100°
Reflections collected	3232
Independent reflections, used	2846
R_{int}[a]	0.0249
Final Shift / error max. (avg.)	0.004 , (0.001)
No. of variables	238
Final R_1, R_2[b,d]	0.0364, 0.0395
Weighting scheme	$(\sigma^2 F+0.0005F^2)^{-1}$
Error in observation of unit weight[c]	1.3618
Secondary Extinction, x[e]	0.00991
Highest peak, eÅ^{-3}; location	0.16; 0.812, 0.538, 0.187
Lowest peak, eÅ^{-3}	-0.16

[a] $R_{int}=[\Sigma(N\Sigma(\omega(\langle F\rangle-F^2))/\Sigma(N-1)\Sigma\omega F_o^2]^{1/2}$

[b] $R_1=\Sigma \; |F_o - F_c| / \Sigma \; F_o \quad R_2=[\Sigma\omega(F_o - F_c)^2/\Sigma\omega F_o^2]^{1/2}$

[c] $S=[\Sigma\omega(F_o - F_c)^2/(m-n)]^{1/2}$

m=number of reflections, n=number of variables

[d] R_1, R_2 = 0.0319, 0.0365 for 2556 reflections with $I \geq 2.5\sigma(I)$.

[e] $F' = F(1-0.0001xF^2 / \sin\theta)$

* In the block diagonal refinement, each molecule was refined independantly in separate cycles.

Table 2. Positional parameters ($x10^4$) and U_{eq}($Å^2$)($x10^3$) for the non-hydrogen atoms of [9](N6,9)-6-aminopurinophane with standard errors in parentheses.

Molecule A

Atom	*x*	*y*	*z*	U_{eq}
N(1)	9737(1)	3284(2)	528(1)	28
C(2)	9664(1)	1740(2)	635(1)	31
N(3)	9125(1)	975(2)	961(1)	29
C(4)	8663(1)	2002(2)	1259(1)	25
C(5)	8702(1)	3634(2)	1244(1)	24
C(6)	9220(1)	4274(2)	799(1)	24
N(7)	8133(1)	4290(2)	1629(1)	29
C(8)	7759(1)	3060(2)	1840(1)	29
N(9)	8045(1)	1645(2)	1639(1)	27
N(6)	9247(1)	5802(2)	611(1)	27
C(1′)	8530(1)	6768(2)	508(1)	29
C(2′)	8145(1)	6708(2)	-236(1)	33
C(3′)	7923(1)	5074(2)	-521(1)	32
C(4′)	7269(1)	4223(2)	-181(1)	30
C(5′)	7179(1)	2516(2)	-410(1)	32
C(6′)	6483(1)	1643(2)	-143(1)	34
C(7′)	6589(1)	1244(2)	632(1)	30
C(8′)	7201(1)	-22(2)	845(1)	29
C(9′)	7603(1)	163(2)	1583(1)	31

Table 2. - cont'd.

Molecule B

Atom	*x*	*y*	*z*	U_{eq}
N(1)	5320(1)	6521(2)	-545(1)	30
C(2)	5854(1)	7584(2)	-697(1)	34
N(3)	5948(1)	8277(2)	-1299(1)	34
C(4)	5345(1)	7892(2)	-1775(1)	28
C(5)	4713(1)	6918(2)	-1688(1)	25
C(6)	4757(1)	6075(2)	-1057(1)	26
N(7)	4185(1)	6894(2)	-2289(1)	31
C(8)	4525(1)	7794(2)	-2720(1)	34
N(9)	5230(1)	8430(2)	-2451(1)	31
N(6)	4291(1)	4862(2)	-923(1)	33
C(1′)	3943(1)	3814(2)	-1472(1)	36
C(2′)	4460(1)	2379(2)	-1570(1)	40
C(3′)	5302(1)	2740(2)	-1723(1)	37
C(4′)	5419(1)	3442(3)	-2433(1)	36
C(5′)	6271(1)	3975(3)	-2476(1)	43
C(6′)	6457(1)	4639(3)	-3172(1)	50
C(7′)	6070(1)	6226(3)	-3361(1)	44
C(8′)	6438(1)	7616(2)	-2938(1)	40
C(9′)	5869(1)	8959(2)	-2852(1)	38

where $U_{eq}=⅓(U_{11}+U_{22}+U_{33}+2\cos\beta U_{13})$

Table 3. Hydrogen positional parameters ($x10^3$) for [9](N6,9)-6-aminopurinophane with standard errors in parentheses

Molecule A

Atom	*x*	*y*	*z*
H(2)	1003(1)	111(2)	43(1)
H(6)	958(1)	599(2)	29(1)
H(8)	732(1)	308(2)	209(1)
H(11)	815(1)	640(2)	83(1)
H(12)	869(1)	782(2)	62(1)
H(21)	773(1)	735(2)	-25(1)
H(22)	849(1)	715(2)	-54(1)
H(31)	773(1)	513(2)	-103(1)
H(32)	842(1)	437(2)	-46(1)
H(41)	677(1)	474(2)	-32(1)
H(42)	740(1)	425(2)	32(1)
H(51)	708(1)	247(2)	-93(1)
H(52)	770(1)	193(2)	-28(1)
H(61)	598(1)	236(2)	-23(1)
H(62)	642(1)	76(2)	-39(1)
H(71)	608(1)	89(2)	77(1)
H(72)	674(1)	218(2)	89(1)
H(81)	760(1)	2(2)	54(1)
H(82)	693(1)	111(2)	80(1)
H(91)	799(1)	-72(2)	171(1)
H(92)	721(1)	21(2)	191(1)

Table 3.- cont'd.

Molecule B

Atom	*x*	*y*	*z*
H(2)	624(1)	789(2)	-32(1)
H(6)	445(1)	441(2)	-52(1)
H(8)	435(1)	795(2)	-320(1)
H(11)	344(1)	350(2)	-135(1)
H(12)	382(1)	445(2)	-191(1)
H(21)	447(1)	177(2)	-112(1)
H(22)	422(1)	175(2)	-195(1)
H(31)	556(1)	347(2)	-136(1)
H(32)	563(1)	177(2)	-170(1)
H(41)	523(1)	271(2)	-281(1)
H(42)	509(1)	431(2)	-255(1)
H(51)	661(1)	305(2)	-236(1)
H(52)	642(1)	473(2)	-210(1)
H(61)	631(1)	385(2)	-352(1)
H(62)	708(1)	483(2)	-316(1)
H(71)	612(1)	642(2)	-386(1)
H(72)	549(1)	613(2)	-330(1)
H(81)	690(1)	806(2)	-315(1)
H(82)	662(1)	724(2)	-247(1)
H(91)	561(1)	942(2)	-331(1)
H(92)	613(1)	982(2)	-261(1)

Table 4. Bond lengths (Å) and bond angles (°) for non-hydrogen atoms of [9](N6,9)-6-amino-purinophane with estimated standard deviations in parentheses.

Molecule A

N(1)-C(2)	1.338(2)	C(2)-N(3)	1.332(2)	N(3)-C(4)	1.342(2)
C(4)-C(5)	1.392(2)	C(5)-C(6)	1.401(2)	C(6)-N(1)	1.358(2)
C(5)-N(7)	1.392(2)	N(7)-C(8)	1.311(2)	C(8)-N(9)	1.369(2)
N(9)-C(4)	1.372(2)	C(6)-N(6)	1.352(2)	N(6)-C(1′)	1.463(2)
C(1′)-C(2′)	1.515(3)	C(2′)-C(3′)	1.528(3)	C(3′)-C(4′)	1.528(3)
C(4′)-C(5′)	1.522(3)	C(5′)-C(6′)	1.527(3)	C(6′)-C(7′)	1.526(3)
C(7′)-C(8′)	1.523(3)	C(8′)-C(9′)	1.523(3)	C(9′)-N(9)	1.465(2)
C(6)-N(1)-C(2)	118.4(2)	N(1)-C(2)-N(3)	129.2(2)	C(2)-N(3)-C(4)	110.1(1)
N(3)-C(4)-C(5)	127.6(2)	C(4)-C(5)-C(6)	115.8(2)	C(5)-C(6)-N(1)	117.7(2)
N(3)-C(4)-N(9)	126.6(2)	C(5)-C(4)-N(9)	105.8(1)	C(4)-N(9)-C(8)	105.5(1)
N(9)-C(8)-N(7)	114.7(2)	C(8)-N(7)-C(5)	103.2(1)	N(7)-C(5)-C(6)	133.1(2)
N(7)-C(5)-C(4)	110.6(1)	C(5)-C(6)-N(6)	125.3(2)	N(1)-C(6)-N(6)	117.0(2)
C(6)-N(6)-C(1′)	121.8(1)	N(6)-C(1′)-C(2′)	112.3(2)	C(1′)-C(2′)-C(3′)	116.0(2)
C(2′)-C(3′)-C(4′)	116.1(2)	C(3′)-C(4′)-C(5′)	112.5(2)	C(4′)-C(5′)-C(6′)	115.0(2)
C(5′)-C(6′)-C(7′)	115.0(2)	C(6′)-C(7′)-C(8′)	115.5(2)	C(7′)-C(8′)-C(9′)	114.0(2)
C(8′)-C(9′)-N(9)	109.5(1)	C(9′)-N(9)-C(4)	124.3(1)	C(9′)-N(9)-C(8)	125.8(2)

Table 4. - cont'd.

Molecule B

N(1)-C(2)	1.333(2)	C(2)-N(3)	1.328(2)	N(3)-C(4)	1.343(2)
C(4)-C(5)	1.379(3)	C(5)-C(6)	1.409(2)	C(6)-N(1)	1.355(2)
C(5)-N(7)	1.389(2)	N(7)-C(8)	1.307(3)	C(8)-N(9)	1.366(3)
N(9)-C(4)	1.378(3)	C(6)-N(6)	1.341(2)	N(6)-C(1′)	1.462(2)
C(1′)-C(2′)	1.526(3)	C(2′)-C(3′)	1.518(3)	C(3′)-C(4′)	1.527(3)
C(4′)-C(5′)	1.523(3)	C(5′)-C(6′)	1.519(3)	C(6′)-C(7′)	1.530(3)
C(7′)-C(8′)	1.533(3)	C(8′)-C(9′)	1.516(3)	C(9′)-N(9)	1.464(3)

C(6)-N(1)-C(2)	118.2(2)	N(1)-C(2)-N(3)	129.7(2)	C(2)-N(3)-C(4)	109.8(2)
N(3)-C(4)-C(5)	127.6(2)	C(4)-C(5)-C(6)	116.0(1)	C(5)-C(6)-N(1)	117.3(2)
N(3)-C(4)-N(9)	126.2(2)	C(5)-C(4)-N(9)	106.2(1)	C(4)-N(9)-C(8)	105.1(1)
N(9)-C(8)-N(7)	114.5(2)	C(8)-N(7)-C(5)	103.6(1)	N(7)-C(5)-C(6)	133.4(2)
N(7)-C(5)-C(4)	110.4(1)	C(5)-C(6)-N(6)	125.3(2)	N(1)-C(6)-N(6)	117.4(1)
C(6)-N(6)-C(1′)	122.2(2)	N(6)-C(1′)-C(2′)	112.6(2)	C(1′)-C(2′)-C(3′)	115.2(2)
C(2′)-C(3′)-C(4′)	117.7(2)	C(3′)-C(4′)-C(5′)	112.1(2)	C(4′)-C(5′)-C(6′)	116.2(2)
C(5′)-C(6′)-C(7′)	114.7(2)	C(6′)-C(7′)-C(8′)	114.4(2)	C(7′)-C(8′)-C(9′)	114.3(2)
C(8′)-C(9′)-N(9)	109.8(2)	C(9′)-N(9)-C(4)	124.2(1)	C(9′)-N(9)-C(8)	125.9(2)

Table 5. Bond lengths (Å) and angles (°) involving hydrogen atoms.

Molecule A

C(2)-H(2)	0.94(2)	C(8)-H(8)	0.93(2)	N(6)-H(6)	0.90(2)
C(1')-H(11)	0.99(2)	C(1')-H(12)	0.95(2)	C(2')-H(21)	0.89(2)
C(2')-H(22)	0.96(2)	C(3')-H(31)	1.00(2)	C(3')-H(32)	1.03(2)
C(4')-H(41)	0.96(2)	C(4')-H(42)	0.97(2)	C(5')-H(51)	1.00(2)
C(5')-H(52)	1.02(2)	C(6')-H(61)	1.05(2)	C(6')-H(62)	0.89(2)
C(7')-H(71)	0.98(2)	C(7')-H(72)	0.96(2)	C(8')-H(81)	0.94(2)
C(8')-H(82)	1.04(2)	C(9')-H(91)	1.01(2)	C(9')-H(92)	0.95(2)

N(1)-C(2)-H(2)	115(1)	N(3)-C(2)-H(2)	116(1)	N(7)-C(8)-H(8)	126(1)
N(9)-C(8)-H(8)	119(1)	C(6)-N(6)-H(6)	114(1)	C(1')-N(6)-H(6)	112(1)
N(6)-C(1')-H(11)	109(1)	N(6)-C(1')-H(12)	107(1)	C(2')-C(1')-H(11)	109(1)
C(2')-C(1')-H(12)	109(1)	H(11)-C(1')-H(12)	110(1)	C(1')-C(2')-H(21)	105(1)
C(1')-C(2')-H(22)	110(1)	C(3')-C(2')-H(21)	113(1)	C(3')-C(2')-H(22)	106(1)
H(21)-C(2')-H(22)	106(2)	C(2')-C(3')-H(31)	111(1)	C(2')-C(3')-H(32)	109(1)
C(4')-C(3')-H(31)	105(1)	C(4')-C(3')-H(32)	107(1)	H(31)-C(3')-H(32)	109(1)
C(3')-C(4')-H(41)	109(1)	C(3')-C(4')-H(42)	108(1)	C(5')-C(4')-H(41)	107(1)
C(5')-C(4')-H(42)	109(1)	H(41)-C(4')-H(42)	111(1)	C(4')-C(5')-H(51)	109(1)
C(4')-C(5')-H(52)	110(1)	C(6')-C(5')-H(51)	105(1)	C(6')-C(5')-H(52)	111(1)
H(51)-C(5')-H(52)	107(1)	C(5')-C(6')-H(61)	108(1)	C(5')-C(6')-H(62)	107(1)
C(7')-C(6')-H(61)	107(1)	C(7')-C(6')-H(62)	110(1)	H(61)-C(6')-H(62)	111(1)
C(6')-C(7')-H(71)	109(1)	C(6')-C(7')-H(72)	109(1)	C(8')-C(7')-H(71)	108(1)
C(8')-C(7')-H(72)	108(1)	H(71)-C(7')-H(72)	108(1)	C(7')-C(8')-H(81)	108(1)
C(7')-C(8')-H(82)	109(1)	C(9')-C(8')-H(81)	108(1)	C(9')-C(8')-H(82)	109(1)
H(81)-C(8')-H(82)	109(1)	C(8')-C(9')-H(91)	112(1)	C(8')-C(9')-H(92)	110(1)
N(9)-C(9')-H(91)	108(1)	N(9)-C(9')-H(92)	108(1)	H(91)-C(9')-H(92)	110(1)

Table 5. - cont'd.

Molecule B

C(2)-H(2)	0.96(2)	C(8)-H(8)	0.95(2)	N(6)-H(6)	0.88(2)
C(1')-H(11)	0.94(2)	C(1')-H(12)	1.01(2)	C(2')-H(21)	1.02(2)
C(2')-H(22)	0.97(2)	C(3')-H(31)	1.00(2)	C(3')-H(32)	0.99(2)
C(4')-H(41)	0.98(2)	C(4')-H(42)	0.94(2)	C(5')-H(51)	0.99(2)
C(5')-H(52)	0.99(2)	C(6')-H(61)	0.96(2)	C(6')-H(62)	1.06(2)
C(7')-H(71)	1.00(2)	C(7')-H(72)	1.00(2)	C(8')-H(81)	0.99(2)
C(8')-H(82)	0.98(2)	C(9')-H(91)	1.02(2)	C(9')-H(92)	0.96(2)

N(1)-C(2)-H(2)	116(1)	N(3)-C(2)-H(2)	114(1)	N(7)-C(8)-H(8)	126(1)
N(9)-C(8)-H(8)	120(1)	C(6)-N(6)-H(6)	112(1)	C(1')-N(6)-H(6)	116(1)
N(6)-C(1')-H(11)	108(1)	N(6)-C(1')-H(12)	108(1)	C(2')-C(1')-H(11)	110(1)
C(2')-C(1')-H(12)	114(1)	H(11)-C(1')-H(12)	104(2)	C(1')-C(2')-H(21)	105(1)
C(1')-C(2')-H(22)	110(1)	C(3')-C(2')-H(21)	110(1)	C(3')-C(2')-H(22)	107(1)
H(21)-C(2')-H(22)	110(2)	C(2')-C(3')-H(31)	110(1)	C(2')-C(3')-H(32)	110(1)
C(4')-C(3')-H(31)	107(1)	C(4')-C(3')-H(32)	105(1)	H(31)-C(3')-H(32)	106(2)
C(3')-C(4')-H(41)	110(1)	C(3')-C(4')-H(42)	113(1)	C(5')-C(4')-H(41)	113(1)
C(5')-C(4')-H(42)	108(1)	H(41)-C(4')-H(42)	100(2)	C(4')-C(5')-H(51)	107(1)
C(4')-C(5')-H(52)	109(1)	C(6')-C(5')-H(51)	109(1)	C(6')-C(5')-H(52)	111(1)
H(51)-C(5')-H(52)	105(2)	C(5')-C(6')-H(61)	107(1)	C(5')-C(6')-H(62)	109(1)
C(7')-C(6')-H(61)	112(1)	C(7')-C(6')-H(62)	106(1)	H(61)-C(6')-H(62)	108(2)
C(6')-C(7')-H(71)	108(1)	C(6')-C(7')-H(72)	107(1)	C(8')-C(7')-H(71)	108(1)
C(8')-C(7')-H(72)	111(1)	H(71)-C(7')-H(72)	108(1)	C(7')-C(8')-H(81)	111(1)
C(7')-C(8')-H(82)	108(1)	C(9')-C(8')-H(81)	107(1)	C(9')-C(8')-H(82)	107(1)
H(81)-C(8')-H(82)	109(2)	C(8')-C(9')-H(91)	115(1)	C(8')-C(9')-H(92)	111(1)
N(9)-C(9')-H(91)	107(1)	N(9)-C(9')-H(92)	108(1)	H(91)-C(9')-H(92)	105(2)

Table 6. Selected Dihedral and Torsional Angles (°)

Molecule A

N(3)-C(4)-C(5)-N(7)	-178.6(2)	C(6)-C(5)-C(4)-N(9)	-171.2(2)
C(5)-C(4)-N(9)-C(9′)	156.7(2)	N(3)-C(4)-N(9)-C(9′)	-22.7(2)
N(7)-C(8)-N(9)-C(9′)	-157.5(2)	C(4)-N(9)-C(9′)-C(8′)	-61.5(2)
C(8)-N(9)-C(9′)-C(8′)	91.9(2)	N(9)-C(9′)-C(8′)-C(7′)	-62.5(2)
C(9′)-C(8′)-C(7′)-C(6′)	150.1(2)	C(8′)-C(7′)-C(6′)-C(5′)	-70.5(2)
C(7′)-C(6′)-C(5′)-C(4′)	-72.3(2)	C(6′)-C(5′)-C(4′)-C(3′)	-174.5(2)
C(5′)-C(4′)-C(3′)-C(2′)	-170.6(2)	C(4′)-C(3′)-C(2′)-C(1′)	66.4(2)
C(3′)-C(2′)-C(1′)-N(6)	56.6(2)	C(2′)-C(1′)-N(6)-C(6)	-89.8(2)
C(1′)-N(6)-C(6)-N(1)	144.5(2)	C(1′)-N(6)-C(6)-C(5)	-35.1(2)
N(6)-C(6)-N(1)-C(2)	-172.1(2)	N(6)-C(6)-C(5)-C(4)	167.7(2)
N(6)-C(6)-C(5)-N(9)	156.5(2)		

Molecule B

N(3)-C(4)-C(5)-N(7)	176.1(2)	C(6)-C(5)-C(4)-N(9)	172.4(2)
C(5)-C(4)-N(9)-C(9′)	-154.7(2)	N(3)-C(4)-N(9)-C(9′)	26.5(2)
N(7)-C(8)-N(9)-C(9′)	155.4(2)	C(4)-N(9)-C(9′)-C(8′)	61.9(2)
C(8)-N(9)-C(9′)-C(8′)	-90.2(2)	N(9)-C(9′)-C(8′)-C(7′)	63.8(2)
C(9′)-C(8′)-C(7′)-C(6′)	-151.9(2)	C(8′)-C(7′)-C(6′)-C(5′)	72.7(2)
C(7′)-C(6′)-C(5′)-C(4′)	68.9(2)	C(6′)-C(5′)-C(4′)-C(3′)	177.9(2)
C(5′)-C(4′)-C(3′)-C(2′)	171.2(2)	C(4′)-C(3′)-C(2′)-C(1′)	-70.2(2)
C(3′)-C(2′)-C(1′)-N(6)	-56.4(2)	C(2′)-C(1′)-N(6)-C(6)	92.4(2)
C(1′)-N(6)-C(6)-N(1)	-150.8(2)	C(1′)-N(6)-C(6)-C(5)	28.7(2)
N(6)-C(6)-N(1)-C(2)	171.4(2)	N(6)-C(6)-C(5)-C(4)	-166.6(2)
N(6)-C(6)-C(5)-N(9)	-156.7(2)		

Table 7. Least-squares mean planes (Å)

Molecule A

*Distance of atom from the plane (* atoms are used to define the plane).*

Plane 1.

N(1)*, -0.003(2); C(2)*, 0.062(2); N(3)*, 0.005(2); C(4)*, 0.004(2); C(5)*, 0.041(2); C(6)*, -0.097(2); N(7)*, 0.059(2); C(8)*, -0.012(2); N(9)*, -0.048(2); N(6), -0.325(2); C(9'), -0.577(3); C(8'), -2.047(2); C(1'), -1.159(3); C(2'), -2.618(3).

Plane 2.

N(1)*, 0.011(2); C(2)*, 0.047(2); N(3)*, -0.026(2); C(4)*, -0.009(2); C(5)*, 0.058(2); C(6)*, -0.066(2); N(6), -0.264(2); N(7), 0.088(3); N(9), -0.070(2); C(9'), -0.627(3); C(1'), -1.081(3).

Plane 3.

C(4)*, 0.011(2); C(5)*, -0.012(2); N(7)*, 0.008(2); C(8)*, -0.005(2); N(9)*, -0.003(2); N(3), 0.029(3); C(6), -0.197(3); C(9'), -0.468(3); C(1'), -1.336(4).

Equations of best planes (in Å, orthogonal axes)

Plane 1. 0.6546x+0.0153y+0.7558z=10.2747

Plane 2. 0.6552x+0.0374y+0.7545z=10.3333

Plane 3. 0.6397x-0.0265y+0.7682z=9.9905

Dihedral angles

Plane 1 - Plane 2 1.27(5)

Plane 1 - Plane 3 2.64(6)

Plane 2 - Plane 3 3.85(6)

Table 7. - cont'd.

Molecule B

*Distance of atom from the plane (* atoms are used to define the plane).*

Plane 1.

N(1)*, 0.013(2); C(2)*, 0.084(2); N(3)*, 0.006(2); C(4)*, -0.018(2); C(5)*, 0.014(2); C(6)*, -0.114(2); N(7)*, 0.062(2); C(8)*, 0.009(2); N(9)*, -0.053(2); N(6), -0.362(2); C(9'), -0.609(3); C(8'), -2.085(3); C(1'), -1.111(3); C(2'), -2.605(3).

Plane 2.

N(1)*, 0.016(2); C(2)*, 0.051(2); N(3)*, -0.031(2); C(4)*, -0.013(2); C(5)*, 0.060(2); C(6)*, -0.070(2); N(6), -0.282(3); N(7), 0.143(3); N(9), -0.038(3); C(9'), -0.624(3); C(1'), -0.991(3).

Plane 3.

C(4)*, 0.016(2); C(5)*, -0.014(2); N(7)*, 0.006(2); C(8)*, -0.001(2); N(9)*, -0.006(2); N(3), 0.081(3); C(6), -0.165(3); C(9'), -0.506(3); C(1'), -1.261(4).

Equations of best planes (in Å, orthogonal axes).

Plane 1.	-0.5251x+0.7625y+0.3780z=-1.2363
Plane 2.	-0.5537x+0.7466y+0.3687z=-1.5653
Plane 3.	-0.4884x+0.7891y+0.3725z=-0.7368

Dihedral angles

Plane 1 - Plane 2	1.95(5)
Plane 1 - Plane 3	2.62(6)
Plane 2 - Plane 3	4.47(6)

Table 8. Anisotropic temperature factors ($x10^4$) for the non-hydrogen atoms of [9](N6,9)-6-aminopurinophane with standard errors in parentheses.

Molecule A

Atom	U_{11}	U_{22}	U_{33}	U_{23}	U_{13}	U_{12}
N(1)	288(9)	249(9)	320(8)	-16(6)	88(6)	-12(6)
C(2)	245(11)	331(13)	358(11)	-25(9)	55(9)	33(10)
N(3)	257(8)	277(9)	334(9)	6(6)	52(6)	29(8)
C(4)	217(10)	305(12)	218(10)	11(8)	-1(8)	-12(9)
C(5)	220(10)	293(11)	222(9)	-27(8)	33(9)	-13(8)
C(6)	234(10)	237(11)	238(9)	-26(8)	5(8)	-30(9)
N(7)	299(8)	330(9)	245(8)	-52(6)	55(6)	-25(8)
C(8)	265(11)	392(13)	220(10)	-34(9)	55(9)	-29(10)
N(9)	298(9)	283(9)	234(8)	2(6)	43(6)	-38(6)
N(6)	263(9)	276(10)	314(9)	-18(6)	100(6)	-16(6)
C(1')	296(11)	223(11)	385(12)	-27(9)	109(9)	-11(9)
C(2')	308(12)	312(12)	391(12)	57(9)	110(10)	13(9)
C(3')	343(11)	372(12)	243(11)	34(9)	50(9)	3(10)
C(4')	308(11)	311(11)	292(11)	-5(9)	12(9)	5(9)
C(5')	414(12)	304(11)	245(11)	-12(9)	31(9)	-22(10)
C(6')	392(12)	276(11)	343(12)	-43(9)	-24(10)	-51(10)
C(7')	285(11)	286(11)	342(11)	-20(9)	50(9)	-60(9)
C(8')	299(11)	234(11)	345(11)	9(9)	50(9)	-55(9)
C(9')	301(11)	297(11)	340(11)	69(9)	93(9)	-12(10)

Table 8. - cont'd.

Molecule B

N(1)	365(9)	297(9)	244(9)	1(6)	13(8)	4(8)
C(2)	430(13)	285(11)	296(12)	-34(10)	-41(10)	-18(10)
N(3)	398(10)	324(9)	308(10)	1(8)	-6(8)	-53(8)
C(4)	351(12)	257(10)	244(11)	-3(8)	26(9)	38(9)
C(5)	239(10)	304(10)	216(11)	5(8)	50(8)	30(9)
C(6)	279(10)	267(11)	261(11)	1(9)	95(9)	31(9)
N(7)	275(9)	396(9)	264(9)	86(8)	35(8)	19(6)
C(8)	345(12)	410(12)	261(11)	60(10)	11(10)	26(10)
N(9)	319(10)	334(9)	279(9)	63(6)	44(6)	-11(8)
N(6)	366(9)	378(10)	245(9)	78(8)	51(8)	-23(8)
C(1')	311(12)	418(13)	366(12)	67(10)	23(10)	100(10)
C(2')	490(13)	348(12)	365(12)	46(10)	-30(10)	-80(11)
C(3')	432(13)	316(11)	356(12)	-11(10)	-36(10)	44(10)
C(4')	375(13)	359(12)	342(12)	-21(10)	-4(10)	48(10)
C(5')	377(13)	453(13)	465(13)	-6(11)	13(10)	83(11)
C(6')	453(13)	581(15)	496(13)	-108(12)	152(11)	9(12)
C(7')	432(13)	585(15)	329(12)	6(11)	125(10)	1(11)
C(8')	364(12)	526(13)	340(12)	71(10)	98(10)	-86(11)
C(9')	420(13)	389(13)	357(12)	93(10)	73(10)	-96(11)

Anisotropic temperature factors are of the form:

$\exp[-2\pi^2(h^2\, a^*\, 2U_{11} + k^2\, b^*\, 2U_{22} + l^2\, c^*\, 2U_{33} + 2\, h\, k\, a^*\, b^*\, U_{12} + 2\, h\, l\, a^*\, c^*\, U_{13} + 2\, k\, l\, b^*\, c^*\, U_{23})]$

where a^*, b^* and c^* are the reciprocal lattice vectors.

Appendix D

QuickBASIC (Version 4.0) Program Used to Calculate the Chemical Shifts in the [n]-(N6,9)-Aminopurinophane Series

The complete program for the calculation of chemical shifts in [8](N6,9)-6-aminopurinophane is shown below:

```
REM                    LOCAL ANISOTROPY AND RING CURRENT
REM          CONTRIBUTION TO CHEMICAL SHIFT OF BRIDGE PROTONS IN
REM                              PURINE CYCLOPHANES
REM *** INITIALIZE THE DIMENSION OF ARRAYS AND GENERATE CONSTANTS ***
DIM MF(60)
DIM RNUMBER(20), RLABEL$(20), RX(20), RY(20), RZ(20)
DIM SIG1(20), SIG2(20), SIG3(20)
DIM HNUMBER(20), HLABEL$(20), HX(20), HY(20), HZ(20)
DIM CHX(20), CHY(20), CHZ(20)
DIM CRX(20), CRY(20), CRZ(20)
DIM RHO(3), ZED(3)
DIM B(3)
DIM FA(60): DIM FB(60)
DIM LOCANI(20), RC(20)
DIM I(20), NH$(20), X(20), Y(20), Z(20)
EC = 1 * EXP(-39): PI = 3.14159265#
REM *** PROGRAM TITLE SCREEN ***
CLS 0
FOR P = 1 TO 12
PRINT
NEXT P
PRINT "                    LOCAL ANISOTROPY AND RING CURRENT"
PRINT "          CONTRIBUTION TO CHEMICAL SHIFT OF BRIDGE PROTONS IN"
PRINT "                    OCTAMETHYLENEPURINE CYCLOPHANE"
FOR P = 1 TO 12
PRINT
NEXT P
```

```
INPUT " Please give a name to the output file: ", FILENAME$
REM *** SETUP FILE FOR OUTPUT ***
OPEN FILENAME$ FOR OUTPUT AS #1
REM *** INPUT NECESSARY DATA ***
CLS
FOR P = 1 TO 12
PRINT
NEXT P
PRINT "Do you want to have a loop separation for the ring current?"
PRINT "Hit <ENTER> for zero loop separation, otherwise input the value"
PRINT
INPUT "Loop Separation= ", LL
PRINT "Unless otherwise requested, a 6 electron pi current is assumed "
PRINT "for both rings: Hit RETURN or input the number of electrons."
PRINT
PRINT "HOW MANY PI ELECTRONS ARE IN THE SIX-MEMBERED RING?": INPUT CA
IF CA = 0 THEN CA = 6
PRINT "HOW MANY PI ELECTRONS ARE IN THE FIVE-MEMBERED RING?": INPUT CB
IF CB = 0 THEN CB = 6
CLS 0
PRINT "LOOP SEPARATION IS", LL
PRINT "PI ELECTRONS ARE IN THE SIX-MEMBERED RING= ", CA
PRINT "PI ELECTRONS ARE IN THE FIVE-MEMBERED RING= ", CB
PRINT
WRITE #1, "LOOP SEPARATION IS", LL
WRITE #1, "PI ELECTRONS ARE IN THE SIX-MEMBERED RING= ", CA
WRITE #1, "PI ELECTRONS ARE IN THE FIVE-MEMBERED RING= ", CB
WRITE #1,
REM *** GENERATE CONSTANTS FOR ELLIPTICAL INTEGRALS ***
AA = 1: BB = 1
FOR MF = 1 TO 57 STEP 2
AA = MF / (MF + 1)
BB = BB * AA
FA(MF) = BB ^ 2
FB(MF) = BB ^ 2 / MF
NEXT MF
REM *** SET ARRAYS FOR RING ATOMS ***
FOR I = 1 TO 10
READ RNUMBER(I), RLABEL$(I), RX(I), RY(I), RZ(I), SIG1(I), SIG2(I),
```

```
SIG3(I)
NEXT I
REM *** READ IN HYDROGENS ***
FOR H = 1 TO 16
READ HNUMBER(H), HLABEL$(H), HX(H), HY(H), HZ(H)
REM *** CENTRE ON EITHER 6-MEMBERED OR 5-MEMBERED RING ***
FOR R = 1 TO 10
IF R = 1 THEN CHX(H) = HX(H) + 3.52763: CHY(H) = HY(H) + 4.58916:
            CHZ(H) = HZ(H) - 11.00188
IF R = 8 THEN CHX(H) = HX(H) + 3.52763: CHY(H) = HY(H) + 2.51601:
            CHZ(H) = HZ(H) - 11.00188
IF R <= 7 THEN GOTO CEN6
IF R >= 8 THEN GOTO CEN5
CEN6:
      CRX(R) = RX(R) + 3.52763
      CRY(R) = RY(R) + 4.58916
      CRZ(R) = RZ(R) - 11.00188
      GOTO CC
CEN5:
      CRX(R) = RX(R) + 3.52763
      CRY(R) = RY(R) + 2.51601
      CRZ(R) = RZ(R) - 11.00188
      GOTO CC
REM *** CYLINDRICAL COORDINATE CONVERSION ***
CC:
        DELTAX = ABS(CHX(H) - CRX(R))
        DELTAY = ABS(CHY(H) - CRY(R))
        DELTAZ = ABS(CHZ(H) - CRZ(R))
        RHO(1) = SQR(DELTAX ^ 2 + DELTAZ ^ 2)
        RHO(2) = SQR(DELTAX ^ 2 + DELTAY ^ 2)
        RHO(3) = SQR(DELTAY ^ 2 + DELTAZ ^ 2)
        ZED(1) = DELTAY
        ZED(2) = DELTAZ
        ZED(3) = DELTAX
REM *** LOCAL ANISOTROPY ***
A = .47: CST = A / PI
FOR L = 1 TO 3
W = (A + RHO(L)) ^ 2 + ZED(L) ^ 2
RR = 4 * A * RHO(L) / W
```

```
G = 1: EA = 1: V = 1
        FOR MF = 1 TO 57 STEP 2
        G = G + (FA(MF) * RR ^ V)
        EB = FB(MF) * (RR ^ V)
        IF EB < EC THEN GOTO LA
        EA = EA - EB
        V = V + 1
        NEXT MF
LA:
        C = PI * G / 2: E = PI * EA / 2
        S = A ^ 2 - RHO(L) ^ 2 - ZED(L) ^ 2
        T = (A - RHO(L)) ^ 2 + ZED(L) ^ 2
        B(L) = (CST / SQR(W)) * (C + S * E / T)
NEXT L
SIGMA = 0
SIGA = B(1) * SIG1(R): SIGB = B(2) * SIG2(R): SIGC = B(3) * SIG3(R)
SIGMA = SIGMA + (SIGA / 3) + (SIGB / 3) + (SIGC / 3)
TLA = TLA + SIGMA
NEXT R
LOCANI(H) = -TLA
TLA = 0
NEXT H
DATA 1, N1, -4.21099, -5.76335, 10.99488, 253.9, -94.5, -147.6
DATA 2, C2, -2.87887, -5.66778, 11.07580, 136.6, 24.7, -81.3
DATA 3, N3, -2.09204, -4.59271, 11.01592, 280.7, -81.9, -148.3
DATA 4, C4, -2.84906, -3.48509, 10.99160, 145.9, 17.6, -55.6
DATA 5, C5, -4.21926, -3.40887, 11.04199, 161.6, 54.5, 36.8
DATA 6, C6, -4.91553, -4.61717, 10.89107, 148.1, -12.1, -51.6
DATA 7, N6, -6.23099, -4.72036, 10.61468, 242.8, 191.9, 122.8
DATA 8, N7, -4.63831, -2.08551, 11.07899, 264.0, -73.0, -247.4
DATA 9, C8, -3.52973, -1.41264, 10.98684, 132.0, 69.0, -48.5
DATA 10, N9, -2.40177, -2.18795, 10.90997, 176.4, 116.6, 30.2
DATA 1, H1R, -6.57945, -2.77002, 10.06395
DATA 2, H1S, -7.88594, -3.75497, 10.07740
DATA 3, H2R, -7.31684, -4.73936,  8.08583
DATA 4, H2S, -7.25096, -3.11925,  7.83072
DATA 5, H3R, -4.90946, -4.77799,  8.32114
DATA 6, H3S, -5.48541, -4.36513,  6.81651
DATA 7, H4R, -4.78767, -2.22910,  8.56658
```

```
DATA 8, H4S, -4.88658, -2.17564,  7.00253
DATA 9, H5R, -2.91330, -3.71034,  8.41379
DATA 10, H5S, -2.85827, -3.39425,  6.90541
DATA 11, H6R, -2.74573, -1.07531,  8.40352
DATA 12, H6S, -1.86842, -1.42985,  7.10254
DATA 13, H7R, -0.70288, -3.04185,  8.79892
DATA 14, H7S, -0.16954, -1.54084,  8.57834
DATA 15, H8R, -0.38228, -2.22458, 10.93735
DATA 16, H8S, -1.04383, -0.83466, 10.52893
FOR I = 1 TO 16
READ I, NH$(I), X(I), Y(I), Z(I)
FOR QQQ = 1 TO 2
IF QQQ = 1 THEN X = X(I) - 1.95936: Y = Y(I) + 10.93229:
      Z = Z(I) - 3.45958
IF QQQ = 2 THEN X = X(I) - 1.95936: Y = Y(I) + 10.93229:
      Z = Z(I) - 1.3912
IF QQQ = 1 THEN A = 1.349: CONS = 8.97: ZZZ = 0
IF QQQ = 2 THEN A = 1.154: CONS = 8.97: ZZZ = 0
Y = Y + (LL / 2)
COLOR (10), 0
FOR PP = 1 TO 2
P = SQR(X ^ 2 + Z ^ 2): PZ = ABS(Y)
W = (A + P) ^ 2 + PZ ^ 2
R = 4 * A * P / W
G = 1: EA = 1: V = 1
FOR MF = 1 TO 57 STEP 2
G = G + (FA(MF) * (R ^ V))
EB = FB(MF) * (R ^ V)
V = V + 1
IF EB < EC THEN GOTO RC
EA = EA - EB
NEXT MF
RC:
C = PI * G / 2
E = PI * EA / 2
S = A ^ 2 - P ^ 2 - PZ ^ 2
T = (A - P) ^ 2 + PZ ^ 2
IF QQQ = 1 THEN B(LL) = (CA * CONS) / (6 * SQR(W)) * (C + S * E / T)
IF QQQ = 2 THEN B(LL) = (CB * CONS) / (6 * SQR(W)) * (C + S * E / T)
```

```
ZZZ = ZZZ + B(LL)
IF QQQ = 1 THEN RCSIX = ZZZ
IF QQQ = 2 THEN RCFIVE = ZZZ
Y = Y - LL
NEXT PP
NEXT QQQ
RC(I) = -(RCSIX + RCFIVE) / 2
NEXT I
FOR F = 1 TO 16
NEXT F
FOR G = 1 TO 16
PRINT "Predicted shift for "; HLABEL$(G); " is ";1.3 + LOCANI(G) + RC(G)
WRITE #1, HLABEL$(G), " at ", 1.3 + LOCANI(G) + RC(G)
NEXT G
CLOSE #1
END
DATA 1, H1R, 6.29942,-9.93378,2.68179
DATA 2, H1S, 4.99320,-9.94065,1.68252
DATA 3, H2R, 5.63755,-7.70001,2.03703
DATA 4, H2S, 5.70493,-7.95101,3.64466
DATA 5, H3R, 3.30935,-8.23241,3.66749
DATA 6, H3S, 3.87428,-6.70883,3.25607
DATA 7, H4R, 3.27455,-6.90338,1.06697
DATA 8, H4S, 3.18861,-8.47665,1.11355
DATA 9, H5R, 1.25490,-6.84107,2.25085
DATA 10, H5S, 1.32226,-8.34969,2.57492
DATA 11, H6R, 1.15359,-8.34454,-0.06297
DATA 12, H6S, 0.27069,-7.06061,0.29048
DATA 13, H7R, -0.87201,-8.77519,1.88269
DATA 14, H7S, -1.40701,-7.56083,0.37694
DATA 15, H8R, -0.51876,-10.49113,-0.31306
DATA 16, H8S, -1.17943,-10.91684,1.06789
```

In order to calculate the chemical shifts in [9](N6,9)-6-aminopurinophane (*anti* conformation), the following sections were substituted into the above program:

```
REM *** CENTRE ON EITHER 6-MEMBERED OR 5-MEMBERED RING ***
        FOR R = 1 TO 10
        IF R = 1 THEN CHX(H) = HX(H): CHY(H) = HY(H): CHZ(H) = HZ(H)
        IF R = 8 THEN CHX(H) = HX(H): CHY(H) = HY(H) - 2.07776:
                      CHZ(H) = HZ(H)
        IF R <= 7 THEN GOTO CEN6
        IF R >= 8 THEN GOTO CEN5
CEN6:
        CRX(R) = RX(R): CRY(R) = RY(R): CRZ(R) = RZ(R)
        GOTO CC
CEN5:
        CRX(R) = RX(R): CRY(R) = RY(R) - 2.07776: CRZ(R) = RZ(R)
        GOTO CC

DATA 1, N1, -0.66940, -1.17626, -0.01532, 253.9, -94.5, -147.6
DATA 2, C2, 0.65217, -1.07558, 0.12272, 136.6, 24.7, -81.3
DATA 3, N3, 1.43060, -0.00072, 0.08107, 280.7, -81.9, -148.3
DATA 4, C4, 0.67404, 1.10671, 0.01574, 145.9, 17.6, -55.6
DATA 5, C5, -0.70226, 1.18410, -0.02195, 161.6, 54.5, 36.8
DATA 6, C6, -1.38515, -0.03826, -0.18226, 148.1, -12.1, -51.6
DATA 7, N6, -2.68238, -0.16618, -0.49616, 242.8, 191.9, 122.8
DATA 8, N7, -1.11338, 2.51034, 0.00163, 264.0, -73.0, -247.4
DATA 9, C8, 0.00883, 3.18133, 0.00366, 132.0, 69.0, -48.5
DATA 10, N9, 1.13277, 2.40634, 0.00090, 176.4, 116.6, 30.2

DATA 1, H1R, -4.28401, 0.87337, -0.96904
DATA 2, H1S, -3.01526, 1.74316, -1.05621
DATA 3, H2R, -3.90441, -0.33807, -2.87835
DATA 4, H2S, -3.82185, 1.23503, -3.26442
DATA 5, H3R, -2.06522, 0.01161, -4.30971
DATA 6, H3S, -1.46364, -0.30523, -2.86905
DATA 7, H4R, -1.56278, 2.27350, -4.10883
DATA 8, H4S, -1.08016, 2.11412, -2.72054
DATA 9, H5R, 0.22991, 0.76862,-4.78185
DATA 10, H5S, 0.67773, 0.65020, -3.28845
```

```
DATA 11, H6R, 0.81216, 3.04187, -4.79833
DATA 12, H6S, 2.14496, 2.11357, -4.55930
DATA 13, H7R, 0.75375, 3.42773, -2.38664
DATA 14, H7S, 2.03051, 4.07525, -3.14353
DATA 15, H8R, 3.52221, 2.63351, -2.21932
DATA 16, H8S, 2.40218, 1.50569, -2.05163
DATA 17, H9R, 2.57047, 3.79278, -0.26973
DATA 18, H9S, 3.11443, 2.34959, 0.03510

REM *** RE-ORIENT MOLECULE FOR RING CURRENT CALCULATION ***
FOR I = 1 TO 18
READ II, NH$(I), X(I), Y(I), Z(I)
FOR QQQ = 1 TO 2
IF QQQ = 1 THEN X = X(I): Y = Y(I): Z = Z(I)
IF QQQ = 2 THEN X = X(I): Y = Y(I): Z = Z(I) - 2.07776
IF QQQ = 1 THEN A = 1.349: CONS = 8.97: ZZZ = 0
IF QQQ = 2 THEN A = 1.154: CONS = 8.97: ZZZ = 0

DATA 1, H1R, -4.28401, -0.96904, 0.87337
DATA 2, H1S, -3.01526, -1.05621, 1.74316
DATA 3, H2R, -3.90441, -2.87835, -0.33807
DATA 4, H2S, -3.82185, -3.26442, 1.23503
DATA 5, H3R, -2.06522, -4.30971, 0.01161
DATA 6, H3S, -1.46364, -2.86905, -0.30523
DATA 7, H4R, -1.56278, -4.10883, 2.27350
DATA 8, H4S, -1.08016, -2.72054, 2.11412
DATA 9, H5R, 0.22991, -4.78185, 0.76862
DATA 10, H5S, 0.67773, -3.28845, 0.65020
DATA 11, H6R, 0.81216, -4.79833, 3.04187
DATA 12, H6S, 2.14496, -4.55930, 2.11357
DATA 13, H7R, 0.75375, -2.38664, 3.42773
DATA 14, H7S, 2.03051, -3.14353, 4.07525
DATA 15, H8R, 3.52221, -2.21932, 2.63351
DATA 16, H8S, 2.40218, -2.05163, 1.50569
DATA 17, H9R, 2.57047, -0.26973, 3.79278
DATA 18, H9S, 3.11443, 0.03510, 2.34959
```

In order to calculate the chemical shifts in [9](N6,9)-6-aminopurinophane (*syn* conformation), the following sections were substituted into the above program:

```
REM *** CENTRE ON EITHER 6-MEMBERED OR 5-MEMBERED RING ***
        FOR R = 1 TO 10
        IF R = 1 THEN CHX(H) = HX(H): CHY(H) = HY(H): CHZ(H) = HZ(H)
        IF R = 8 THEN CHX(H) = HX(H): CHY(H) = HY(H) - 2.01797:
                      CHZ(H) = HZ(H)
        IF R <= 7 THEN GOTO CEN6
        IF R >= 8 THEN GOTO CEN5
CEN6:
        CRX(R) = RX(R): CRY(R) = RY(R): CRZ(R) = RZ(R)
        GOTO CC
CEN5:
        CRX(R) = RX(R): CRY(R) = RY(R) - 2.01797: CRZ(R) = RZ(R)
        GOTO CC

DATA 1, N1, -0.63711, -1.09005, 0.00770, 253.9, -94.5, -147.6
DATA 2, C2, 0.63873, -1.10937, 0.00737, 136.6, 24.7, -81.3
DATA 3, N3, 1.30770, -0.02347, 0.02590, 280.7, -81.9, -148.3
DATA 4, C4, 0.67156, 1.07649, 0.00823, 145.9, 17.6, -55.6
DATA 5, C5, -0.66246, 1.15655, -0.04241, 161.6, 54.5, 36.8
DATA 6, C6, -1.31842, -0.01015, -0.00680, 148.1, -12.1, -51.6
DATA 7, N6, -2.67725, -0.04900, 0.09072, 242.8, 191.9, 122.8
DATA 8, N7, -1.06749, 2.36975, -0.06490, 264.0, -73.0, -247.4
DATA 9, C8, -0.03671, 3.12457, -0.00186, 132.0, 69.0, -48.5
DATA 10, N9, 1.09510, 2.36248, 0.10095, 176.4, 116.6, 30.2
DATA 1, H1R, -4.38736, -0.64049, 1.14022
DATA 2, H1S, -3.33445, -1.98522, 0.57913
DATA 3, H2R, -3.18671, -1.69344, 3.08127
DATA 4, H2S, -1.61752, -1.41308, 2.30558
DATA 5, H3R, -2.27599, 1.18133, 2.35248
DATA 6, H3S, -3.59410, 0.66276, 3.42299
DATA 7, H4R, -1.82123, 1.36536, 4.88919
DATA 8, H4S, -1.81154, -0.42008, 4.94244
DATA 9, H5R, 0.15096, -0.36731, 3.25155
DATA 10, H5S, 0.49104, 0.30923, 4.87128
DATA 11, H6R, 0.16798, 2.64695, 4.00788
```

```
DATA 12, H6S, -0.19244, 1.99873, 2.39488
DATA 13, H7R, 2.19747, 0.86304, 2.47131
DATA 14, H7S, 2.44430, 1.80882, 3.95953
DATA 15, H8R, 3.41306, 3.27126, 2.43754
DATA 16, H8S, 1.74606, 3.90293, 2.39456
DATA 17, H9R, 3.15412, 2.03461, 0.34295
DATA 18, H9S, 2.67150, 3.74132, 0.09641

REM *** RE-ORIENT MOLECULE FOR RING CURRENT CALCULATION ***
FOR I = 1 TO 18
READ II, NH$(I), X(I), Y(I), Z(I)
FOR QQQ = 1 TO 2
IF QQQ = 1 THEN X = X(I): Y = Y(I): Z = Z(I)
IF QQQ = 2 THEN X = X(I): Y = Y(I): Z = Z(I) - 2.01797
IF QQQ = 1 THEN A = 1.349: CONS = 8.97: ZZZ = 0
IF QQQ = 2 THEN A = 1.154: CONS = 8.97: ZZZ = 0

DATA 1, H1R, -4.38736, 1.14022, -0.64049
DATA 2, H1S, -3.33445, 0.57913, -1.98522
DATA 3, H2R, -3.18671, 3.08127, -1.69344
DATA 4, H2S, -1.61752, 2.30558, -1.41308
DATA 5, H3R, -2.27599, 2.35248, 1.18133
DATA 6, H3S, -3.59410, 3.42299, 0.66276
DATA 7, H4R, -1.82123, 4.88919, 1.36536
DATA 8, H4S, -1.81154, 4.94244, -0.42008
DATA 9, H5R, 0.15096, 3.25155, -0.36731
DATA 10, H5S, 0.49104, 4.87128, 0.30923
DATA 11, H6R, 0.16798, 4.00788, 2.64695
DATA 12, H6S, -0.19244, 2.39488, 1.99873
DATA 13, H7R, 2.19747, 2.47131, 0.86304
DATA 14, H7S, 2.44430, 3.95953, 1.80882
DATA 15, H8R, 3.41306, 2.43754, 3.27126
DATA 16, H8S, 1.74606, 2.39456, 3.90293
DATA 17, H9R, 3.15412, 0.34295, 2.03461
DATA 18, H9S, 2.67150, 0.09641, 3.74132
```

Also note that the appropriate "*FOR..NEXT*" loops were changed in the nonamethylene programs to include the additional protons.

References Cited

1. Majumdar, A. and Hosur, R. V. *Prog. NMR Spec.* **24**, 109 (1992); Wemmer, D. E. *Curr. Opin. Struct. Bio.* **1**, 452 (1991); Hosur, R.V., Govil, G., and Miles, H.T. *Magn. Res. Chem.* **26**, 927-944 (1988); Van de Ven, F.J., and Hilbers, C.W. *Eur. J. Biochem.* **178**, 1-38 (1988)

2. Bovey, F.A. Nuclear Magnetic Resonance Spectroscopy. (New York: Academic Press, 1988); Harris, R. K. Nuclear Magnetic Resonance Spectroscopy. (Essex: Longman Scientific and Technical, 1986); Gunther, H. NMR Spectroscopy. (New York: John Wiley and Sons, 1980)

3. Carrington, A. and McLachlan, A. D. Introduction to Magnetic Resonance. (New York: Harper and Row, 1967)

4. Lee, C.-H., Ezra, F.S., Kondo, N.S., Sarma, R. H. and Danyluk, S. S. *Biochemistry.* **15**, 3627 (1976)

5. Ezra, F.S., Lee, C.-H., Kondo, N.S., Danyluk, S.S., and Sarma, R. H. *Biochemistry.* **16**, 1977 (1977); Bell, R.A., Everett, J.R., Hughes, D.W., Coddington, J.M., Alkema, D., Hader, P.A. and Neilson, T. *J. Biomol. Struct. and Dynamics.* **2**, 693-707 (1985)

6. Basic Principles in Nucleic Acid Chemistry, Volumes I and II, P.O.P. Ts'O, editor. (New York: Academic Press, 1974)

7. Saenger, W. Principles of Nucleic Acid Structure (New York: Springer-Verlag, 1984)

8. Robillard, G. T. and Reid, B. R. in Biological Applications of Magnetic Resonance, R. G. Shulman, editor. (New York: Academic Press, 1979)

9. Giessner-Prettre, C., Pullman, B., Borer, P.N., Kan, L-S, and Ts'o, P.O.P. *Biolpolymers.* **15**, 2277-2286 (1976)

10. Giessner-Prettre, C. and Pullman, B. *Biochem. Biophys. Res. Comms.* **70**, 578-581 (1976)

11. Giessner-Prettre, C., Pullman, B. and Caillet, J. *Nuc. Acids Res.* **4**, 99-116 (1977)

12. Giessner-Prettre, C. and Pullman, B. *J. Theor. Biol.* **65**, 171-188 and 189-201 (1977)

13. Giessner-Prettre, C. and Pullman, B. *J. Theor. Biol.* **27**, 87-95 (1970)

14. Giessner-Prettre, C. and Pullman, B. *Quarterly Rev. of Biophys.* **20**, 113-172 (1987)

15. Schindler, M. *J. Amer. Chem. Soc.* **110**, 6623-6630 (1988)

16. Cram, D.J., and Steinberg, H. *J. Amer. Chem. Soc.* **73**, 5691 (1951)

17. Cyclophanes, Vol. I and II, Keehn, P. M. and Rosenfeld, S. M., eds. (New York, Academic Press, 1983); F. Diederich, Cyclophanes (Cambridge: Royal Society of Chemistry, 1991)

18. Bickelhaupt, F. *Pure & Appl. Chem.* **62**, 373-382 (1990)

19. Zipplies, M.F., and Staab, H.A. *Tet. Lett.* **25**, 1035 (1984) and Zipplies, M.F., Krieger, C., and Staab, H.A. *Tet. Lett.* **24**, 1925 (1983)

20. Baldwin, J.E., and Perlmutter, P. *Top. Curr. Chem.* **121**, 181 (1984)

21. Sakamoto, T., Nishimura, S., Kondo, Y. and Yamanaka, H. *Heterocycles.* **27**, 475-478 (1988)

22. Kinoshita, T., Tanaka, H., and Furukawa, S. *Chem. Pharm. Bull.* **34**, 1809-1813 (1986)

23. Kinoshita, T., Odawara, S., Fukumura, K., and Furukawa, S. *J. Heterocyclic Chem.* **22**, 1573-1576 (1985)

24. Brown, D.J., and Ienaga, K. *J. Chem. Soc., Perkins I*, 2182-2185 (1975) and Brown, D.J., and Ienaga, K. *Aust. J. Chem.* **28**, 119-127 (1975)

25. Krieger, C., and Neugebauer, F.A. *Chem. Ber.* **123**, 1885-1889 (1990)

26. Seyama, F., Akahori, K., Sakata, Y., Misumi, S., Aida, M. and Nagata, C. *J. Amer. Chem. Soc.* **110**, 2192-2201 (1988)

27. Sakata, Y., Higuchi, H., Doyama, K., Higashii, T., Mitsuoka, M., and Misumi, S. *Bull. Chem. Soc. Jpn.* **62**, 3155-3160 (1989)

28. Higuchi, H., Mitsuoka, M., Sakata, Y., and Misumi, S. *Tetrahedron Lett.* **26**, 3849 (1985)

29. Agarwal, A., Barnes, J.A., Fletcher, J.L., McGlinchey, M.J. and Sayer, B.G. *Can J. Chem.* **55**, 2575-2581 (1977)

30. Nozaki, H., Koyama, T. and Mori, T. *Tetrahedron.* **25**, 5357 (1969)

31. Waugh, J. S., and Fessenden, R. W. *J. Amer. Chem. Soc.* **79**, 846 (1957)

32. Barfield, M., Grant, D.M., and Ikenberry, D. *J. Amer. Chem. Soc.* **97**, 6956-6961 (1975)

33. Macromodel Computer Program. Version 1.5. W. C. Still (1987), Columbia University

34. PC-Model. Version 4.0. Serena Software, (1991)

35. Bell, R. A., Hunter, H. N., Lock, C. J. L. and Fagiani, R. *Can. J. Chem.* **70**, 186 (1992)

36. Bell, R.A. and Hunter, H.N. *Tetrahedron Lett.* **28**, 147-150 (1987)

37. Hunter, H.N. PhD. Thesis. McMaster University, 1988

38. Sutherland, M. and Christensen, B.E. *J. Amer. Chem. Soc.* **79**, 2251-2252 (1957)

39. Osterman, R. M., McKittrick, B. A., and Chan, T.-M. *Tet. Lett.* **33**, 4867 (1992) and Carraway, K.L., Haung, P.C., and Scott, T.G. in Synthetic Procedures in Nucleic Acid Chemistry, Zorbach, W.W. and Tipson, R.S., eds. New York: John Wiley and Sons, Inc. (1968). Vol. I, p. 3-5

40. Mitsunobu, O. *Synthesis*, 1-28 (1981)

41. Iwakawa, M., Pinto, B.M. and Szarek, W.A. *Can. J. Chem.* **56**, 326-335 (1978)

42. Mitsunobu, O. and Iguchi, M. *Bull. Chem. Soc. Jpn.* **44**, 2327 (1971)

43. Cucinella, S., Dozzi, G., Mazzei, A. and Salvatori, T. *J. Organomet. Chem.* **90**, 257 (1975); Cucinella, S., Salvatori, T., Busetto, G., Perego, G. and Mazzei, A. *J. Organomet. Chem.* **78**, 185 (1974)

44. Dewar Research Group and J. J. P. Stewart. *QCPE Bull.* **6**, 2 (1986)

45. Ho, T.-L. *Tetrahedron*, **41** 1 (1985)

46. Boigegrain, R., Castro, B., and Selve, C. *Tetrahedron Lett.* No. 30, 2529-2530 (1975) and Castro, B. *Organic Reactions.* Vol.29, Chpt.1.; Castro, B., and Selve, C. *Bull. Soc. Chim. France.* **12**, 3009-3014 (1974)

47. Knouzi, N., Vaultier, M. and Carrie, R. *Bulletin de la Société Chimique de France.*

No. 5, 815-819 (1985); Vaultier, M., Knouzi, N. and Carrie, R. *Tetrahedron Lett.* **24**, 763-764 (1983)

48. Staudinger, H and Meyer, J. *Helv. Chim. Acta.* **2**, 635 (1919)

49. Kang, S.-K., Kim, W.-S., and Moon, B.-H. *Synthesis.* 1161-1162 (Dec. 1985)

50. Reeves, W. P. and Bahr, M. L. *Synthesis.* 823 (1976)

51. *Top. Curr. Chem.* **102**, 147 (1982)

52. Long, J. R. *Aldrich Chimica Acta*, **14** 63 (1981)

53. Allinger, N.L., Walter, T.J. and Newton, M.G. *J. Amer. Chem. Soc.* **96**, 4588-4597 (1974)

54. Browne, D.T., Eisinger, J. and Leonard, N.J. *J. Amer. Chem. Soc.* **90**, 7302-7323 (1968)

55. Markiewicz, W.T., Kierzek, R. and Hernes, B. *Nucleosides and Nucleotides.* **6**, 269-272 (1987)

56. Olah, G.A., Balaram Gupta, B.G., Malhorta, R., Narang, S.C. *J. Org. Chem.* **45**, 1638-1639 (1980)

57. Handbook of Biochemistry and Molecular Biology, Third Edition. G.E. Fasman, ed. (Cleveland: Chemical Rubber Company Press, Inc., 1976)

58. Singh, H., Aggarwal, P., and Kumar, S. *Synthesis.*, 520-522 (June 1990)

59. Aoyama, H. *Bull. Chem. Soc. Jap.* **60**, 2076 (1987)

60. Hrebabecky, H. and Beranek, J. *Coll. Czech. Chem. Comm.* **49**, 2689-2697 (1984) and Zemlicka, J. and Sorm, F. *Coll. Czech. Chem. Comm.* **30**, 2052-2066 (1965)

61. Hepburn, D. R. and Hudson, H. R. *J. Chem. Soc., Perkins I.* 754-757 (1976)

62. Reitz, A.B., Graden, D.W., Jordan, A.D., and Maryanoff, B.E., *J. Org. Chem.* **55**, 5761-5766 (1990)

63. Corey, E.J., Nicolaou, K.C., Balanson, R.D., and Machida, Y. *Synthesis.* 590-591 (Sept. 1975)

64. Brown, D.J. and Ford, P.W. *J. Chem. Soc. (C).* 568-572 (1967)

65. Trost, B.M., and Braslau, R. *J. Org. Chem.* **53**, 532-537 (1988)

66. Trost, B.M., and Curran, D.P. *Tetrahedron. Lett.* **22**, 1287-1290 (1981)

67. Bischofberger, N. *Tetrahedron Lett.* **28**, 2821-2824 (1987)

68. Galli, C., Illuminati, G. and Mandolini, L. *J. Org. Chem.* **45**, 311 (1980)

69. Illuminati, G., Mandolini, L. and Galli, C., *J. Amer. Chem. Soc.* **99**, 6308 (1977)

70. Dietrich-Buchecker, C.O. and Sauvage, J-P. *Chem. Rev.* **87**, 795 (1987)

71. Glaser, C. *Ann.* **154**, 137 (1870) and Glaser, C. *Ber.* **2**, 422 (1869)

72. Eglinton, G. and McCrae, W. in Advances in Organic Chemistry: Methods and Results, Volume 4. (New York: John Wiley and Sons, Inc.) p.225 (1963)

73. Ojima, J., Shiroishi, Y., Wada, K., and Sondheimer, F. *J. Org. Chem.* **45**, 3564-3570 (1980)

74. O'Krongly, D., Denmead, S.R., Chiang, M.Y., and Breslow, R. *J. Amer. Chem. Soc.* **107**, 5544-5545 (1985)

75. Dietrich-Buchecker, C.O., Khemiss, A., and Sauvage, J.P. *J. Chem. Soc., Chem. Commun.*, 1376-1378 (1986)

76. Kleblansky, A. L., Grachev, I. V., and Kuznetsova, J. *J. Gen. Chem. U.S.S.R.* **27**, 3008 (1957)

77. Matsuoka, T., Negi, T., Oysubo, T., Sakata, Y. and Misumi, S. *Bulletin of the Chemical Society of Japan*, **45**, 1825-1833 (1972)

78. Lindgren, S., Svensson, U., and Dahlbom, R. *Acta Pharm. Succ.* **12**, 503-506 (1975)

79. Tsuji, J. Organic Synthesis with Palladium Compounds. (New York: Springer-Verlag, 1980)

80. Nicolaou, K.C., Veale, C.A., Webber, S.E. and Katerinopoulos, H. *J. Amer. Chem. Soc.* **107**, 7515-7518 (1985)

81. Trost, B.M., Chan, C., and Ruhter, G. *J. Amer. Chem. Soc.* **109**, 3486-3487 (1987)

82. Takahashi, S., Kuroyama, Y., Sonogashira, K., and Hagihara, N. *Synthesis*, 627 (1980)

83. Heck, R. F. Palladium Reagents in Organic Syntheses. (London: Academic Press, Inc., 1985) p. 299

84. Hobbs, F.W. *J. Org. Chem.* 54, 3420-3422 (1989)

85. Ratovelomana, V., and Linstrumelle, G. *Synthetic Comm.* 11, 917-923 (1981)

86. Corey, E.J., Cho, H., Rucker, C., and Hua, D.H. *Tetrahedron. Lett.* 22, 3455-3458 (1981)

87. Zhang, W., and Robins, M.J. *Tetrahedron. Lett.* 33, 1177-1180 (1992)

88. Cotton, F.A. and Wilkinson, G. Advanced Inorganic Chemistry. (New York: John Wiley and Sons, 1980). pp. 950-966

89. Otsubo, T. and Misumi, S. *Synth. Commun.* 8, 285 (1978)

90. Vogtle, F. and Rossa, L. *Angew. Chem. Int. Ed. Eng.*, 18 515 (1979)

91. Derome, A. E. Modern NMR Techniques for Chemistry Research. (Oxford: Pergamon Press, 1988) and Sanders J. K. M. and Hunter, B. K. Modern NMR Spectroscopy: A Guide for Chemists. (Oxford: Oxford University Press, 1988)

92. Bain, A.D., Hughes, D.W. and Hunter, H.N. *Mag. Res. Chem.* 26, 1058-1061 (1988)

93. Bax, A. and Freeman, R. *J. Mag. Res.*, 44 542 (1981)

94. Lowry, T. H. and Richardson, K. S. Mechanism and Theory in Organic Chemistry. (New York: Harper and Row, 1987). p.133

95. Bothner-By, A. A. *Adv. Magn. Res.*, 1 195 (1965); Karplus, M. *J. Amer. Chem. Soc.* 85, 2870 (1963) and Karplus, M. *J. Chem. Phys.* 30, 11 (1959)

96. Parameter Adjustment in NMR by Iterative Calculation (PANIC.81) Program. Bruker Spectrospin, 1981.

97. Sandstrom, J. Dynamic NMR Spectroscopy. (London: Academic Press Ltd., 1982)

98. Kleier, D. A. and Binsch, G. *DNMR3* (1970). Program 165. Quantum Chemistry Program Exchange, Indiana University, Bloomington, IN.

99. Bondi, A. *J. Phys. Chem.* 68, 441 (1964) and Allinger, N. L., Hirsch, J. A., Miller, M. A., Tyminski, I. J., and Van-Catledge, F. A. *J. Am. Chem. Soc.* 90, 1199 (1968)

100. Voet, D. and Rich, A. *Prog. Nucl. Acid Res. Mol. Biol.* **10**, 183 (1970)

101. Allen, F. H., Kennard, O., Watson, D. G., Brammer, L., Orpen, G., and Taylor, R. *J. Chem. Soc. Perkin Trans.* II. S1, (1987) and Zuniga, F. J. and Chapuis, G. *Cryst. Struct. Commun.* **10**, 533 (1981)

102. Oki, M. Applications of Dynamic NMR Spectroscopy to Organic Chemistry. (Deerfield, FL.: VCH Publishers Inc., 1985) Chapter 2.

103. Bader, R.F.W., Cheeseman, J.R., Laidig, K.E., Wiberg, K.B., and Breneman, C. *J. Amer. Chem. Soc.* **112**, 6530-6536 (1990)

104. Wiberg, K. B. and Laidig, K. B. *J. Amer. Chem. Soc.* **112** 5935 (1987)

105. Bennet, A. J., Wang, Q.-P., Slebocka-Tilk, H., Somayaji, V., Brown, R. S. and Santarsiero, B. D. *J. Am. Chem. Soc.* **112**, 6383 (1990)

106. Taylor, R. and Kennard, O. *J. Mol. Struct.* **78**, 1 (1982)

107. Bunick, G. and Voet, D. *Acta Cryst.* **B30**, 1651 (1974)

108. Lai, T. F. and Marsh, R. E. *Acta Cryst.* **B28**, 1982 (1972)

109. Sprang, S., Rohrer, D. C. and Sundaralingam, M. *Acta Cryst.* **B34**, 2803 (1978)

110. Kistenmacher, T. J. and Rossi, M. *Acta Cryst.* **B33**, 253 (1977)

111. Sheldrick, W. S. and Morr M. *Acta Cryst.* **B36**, 2328 (1980)

112. Sternglanz, H. and Bugg, C. E. *J. Cryst. and Mol. Struct.* **8**, 263 (1978)

113. Thewalt, U. and Bugg, C. E. *Acta Cryst.* **B28**, 1767 (1972)

114. Bugg, C. E. and Thewalt, U. *Biochem. Biophys. Res. Commun.* **46**, 779 (1972)

115. McMullan, R.K. and Sundaralingam, M. *J. Am. Chem. Soc.* **93**, 7050 (1971)

116. Allinger, N. L., Sprague, J. T. and Liljefors, T. *J. Amer. Chem. Soc.* **96**, 5100 (1974)

117. Jaffe, H. H. and Orchin, M. Theory and Application of Ultraviolet Spectroscopy (New York: John Wiley and Sons, Inc., 1962) p.407

118. Giessner-Prettre, C. *J. Biomol. Struct. and Dynamics.* **2**, 233-248 (1984)

119. Giessner-Prettre, C. *J. Biomol. Struc. Dyn.* **4**, 99-110 (1986)

120. Chestnut, D. B. *Annual Reports on NMR Spectroscopy.* **21**, 51-97 (1989)

121. Lamb, W.E. *Phys. Rev.* **60**, 817 (1941)

122. Ramsey, N. F. *Phys. Rev.* **78**, 699 (1950)

123. Buckingham, A. D. *Can. J. Chem.* **38**, 300 (1960)

124. Waugh, J.S., and Fessenden, R.W. . *J. Amer. Chem. Soc.* **80**, 6697 (1958)

125. Johnson, C.E., Jr., and Bovey, F.A. *J. Chem. Phys.* **29**, 1012-1014 (1958)

126. Pauling, L. *J. Chem. Phys.* **4**, 673 (1936)

127. Pople, J.A. *J. Chem. Phys.* **24**, 1111 (1956)

128. Haigh, C.W., and Mallion, R.B. *Progress in NMR Spectroscopy.* **13**, 303-344 (1980)

129. Ferguson, A.F., and Pople, J.A. *J. Chem. Phys.* **42**, 1560-1563 (1965); Pople, J.A. *J. Chem. Phys.* **41**, 2559 (1964)

130. Fyfe, C.A. Solid State NMR for Chemists. (Guelph: C.F.C. Press, 1983). pp. 156-167, 187-199

131. Pines, A., Gibby, M.G. and Waugh, J.S. *Chem Phys. Lett.* **15**, 373-376 (1972)

132. For examples, see Pausak, S., Pines, A., and Waugh, J.S. *J. Chem. Phys.* **59**, 591-595 (1973); Igner, D. and Fiat, D. *J. Mag. Res.* **46**, 233-246 (1982) and Edzes, H.T. *Polymer.* **24**, 1425-1428 (1983)

133. Herzfeld, J. and Berger, A.E. *J. Chem. Phys.* **73**, 6021-6030 (1980)

134. Prado, F.R. and Giessner-Prettre, C. *J. Mag. Res.* **47**, 103-117 (1982) and Giessner-Prettre, C. and Pullman, B. *J. Amer. Chem. Soc.* **104**, 70-73 (1982)

135. Burke, J. J. and Lauterbur, P. C. *J. Amer. Chem. Soc.* **86**, 1870 (1964)

136. Jordan, F. and Sostman, H.D. *J. Amer. Chem. Soc.* **94**, 7898 (1972)

137. Keith, T. A. and Bader, R. F. W. *Chem. Phys. Lett.* **194**, 1 (1992)

138. French, S. and Wilson, K. Acta Cryst. **A34**, 517 (1978)

139. Sheldrick, G.M. SHELXS-86, Program for Crystal Structure Solution. University of Göttingen, Federal Republic of Germany, 1986)

140. Sheldrick, G.M. SHELX-76, Program for Crystal Structure Determination. University of Cambridge, England. (1976)

141. Cromer, D.T. and Mann, J.B. *Acta Cryst.* **A24**, 321 (1968)

142. Stewart, J.M. and Hall, S.R. The XTAL System of Crystallographic Programs. Tech. Rept. TR-1364. University of Maryland, College Park, U.S.A. (1983)

143. Stephens, J. MOLGEOM adapted from CUDLS. McMaster University, Canada. (1973)

144. Davies, K. CHEM-X. Chemical Design Ltd., Oxford, England. (1986)

145. Davies, K. CHEMGRAF suite: SNOOPI. Chemical Design Ltd., Oxford, England. (1983)

146. Still, W.C., Kahn, M. and Mitra, A.J. *J. Org. Chem.* **43**, 2923-2925 (1978)